eCAM Evidence-Based Complementary and Alternative Medicine

Application of Complementary and Alternative Medicine on Neurodegenerative Disorders 2013

Guest Editors: Paul Siu-Po Ip, Karl Wah-Keung Tsim, Kelvin Chan, and Rudolf Bauer

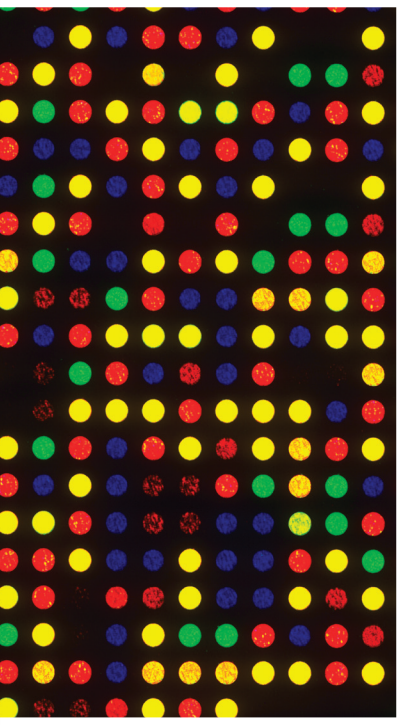

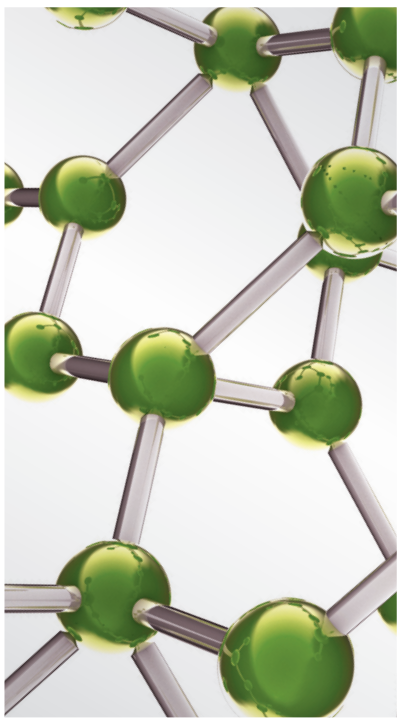


Application of Complementary and Alternative Medicine on Neurodegenerative Disorders 2013

Evidence-Based Complementary and Alternative Medicine

Application of Complementary and Alternative Medicine on Neurodegenerative Disorders 2013

Guest Editors: Paul Siu-Po Ip, Karl Wah-Keung Tsim, Kelvin Chan, and Rudolf Bauer

Editorial Board

Contents

Hindawi Publishing Corporation
Evidence-Based Complementary and Alternative Medicine
Volume 2014, Article ID 463929, 2 pages
http://dx.doi.org/10.1155/2014/463929

Editorial

Application of Complementary and Alternative Medicine on Neurodegenerative Disorders 2013

Paul Siu-Po Ip,[1] Karl Wah-Keung Tsim,[2] Kelvin Chan,[3,4] and Rudolf Bauer[5]

[1] *School of Chinese Medicine, The Chinese University of Hong Kong, Shatin, New Territories, Hong Kong*
[2] *Division of Life Science, The Hong Kong University of Science and Technology, Clear Water Bay, Kowloon, Hong Kong*
[3] *Faculty of Pharmacy, The University of Sydney, NSW 2006, Australia*
[4] *Centre for Complementary Medicine Research, University of Western Sydney, NSW 2560, Australia*
[5] *Department of Pharmacognosy, Institute of Pharmaceutical Sciences, University of Graz, 8010 Graz, Austria*

Correspondence should be addressed to Paul Siu-Po Ip; paulip@cuhk.edu.hk

Received 28 November 2013; Accepted 28 November 2013; Published 22 January 2014

Neurodegenerative disorders such as Alzheimer's disease and Parkinson's disease are characterized by progressive loss of neurons in sensory, motor, and cognitive systems. Based on limited knowledge on the pathogenic mechanisms of the diseases, some drugs have been developed. For example, acetylcholinesterase inhibitors and N-methyl-D-aspartate receptor antagonist have been widely used for treating Alzheimer's disease. However, these drugs have not shown promising results and tolerance may be developed after a short period of treatment. The etiopathology of neurodegenerative diseases is extremely complex and has not been fully revealed. It is reasonable to expect that drugs acting on multiple targets can provide better treatment results than those acting on a single target for these diseases. Some herbal remedies have been used traditionally for improving cognitive function and treating mental diseases for many years. These drugs contain a number of active ingredients and can be the potential candidates for the treatment of neurodegenerative disorders.

In the special issue of "Application of Complementary and Alternative Medicine on Neurodegenerative Disorders" published last year, we have collected papers on the application of complementary and alternative medicine for treating Alzheimer's disease, Parkinson's disease, and depression. In this year, Alzheimer's disease is still a hot topic of investigation. Alzheimer's disease is a well-known neurodegenerative disease characterized by a progressive deterioration of cognitive function and memory. Although the pathological mechanism of the disease is not fully understood, the deposition of beta-amyloid and the generation of reactive oxygen species are believed to play important roles in the pathogenesis of the disease. Therefore, neurotoxicity induced by beta-amyloid or oxidants has been commonly used as a cellular model of Alzheimer's disease. In this issue, C.-F. Ng et al. reported that a decoction of Gastrodiae Rhizoma (rhizome of *Gastrodia elata* Bl.) was able to protect against *in vivo* and *in vitro* neurotoxicity induced by beta-amyloid through the inhibition of apoptosis and oxidative damage. A similar study by M. Maiwulanjiang et al. showed that Song Bu Li decoction, a herbal remedy prepared by boiling with Nardostachyos Radix et Rhizoma, protected against cellular toxicity induced by tert-butyl hydroperoxide in cultured PC12 cells. They suggested that the protective effect of the herbal drug was mediated by activating the transcriptional activity of antioxidant response element.

Previous studies by Y.-F. Xian et al. have identified an active ingredient (isorhynchophylline) from Uncariae Ramulus cum Uncis by bioassay-guided fractionation which

is effective in inhibiting neurotoxicity induced by beta-amyloid. In this special issue, the authors suggested that the protective effect of isorhynchophylline against beta-amyloid-induced cytotoxicity in PC12 cells was associated with the enhancement of p-CREB expression via PI3K/Akt/GSK-3β signaling pathway.

Apart from bioassay-guided isolation, high-throughput screening is another commonly used method to search for novel drugs. In recent years, a new method of drug discovery (*in silico* virtual screening) has been adopted by many researchers. By modelling the laboratory processes such as the binding of molecules to a receptor via computer algorithms, potential drugs can be identified and then confirmed by biological testing. This approach will greatly reduce laboratory works in high-throughput screening. In this special issue, Y. Wang et al. have identified twelve phytochemicals as acetylcholinesterase inhibitors by using *in silico* screening method. Subsequent biological tests conducted by the research team showed that acetylshikonin was the most effective compound among these acetylcholinesterase inhibitors in preventing apoptosis induced by hydrogen peroxide in neuronal SH-SY5Y and PC12 cells.

Parkinson's disease is the second most common neurodegenerative disorder which is characterized by the loss of dopaminergic neurons in the substantia nigra of ventral midbrain area. Tremor, rigidity, bradykinesia, and postural instability are the typical symptoms observed in patients suffering from the disease. 6-Hydroxydopamine is a neurotoxin which can selectively destroy dopamine-generating neurons in the brain. Therefore, neurotoxicity induced by 6-hydroxydopamine is commonly used as a model of Parkinson's disease. By using this model, X.-B. Meng et al. demonstrated that notoginsenoside R2, a triterpenoid isolated from Notoginseng Radix et Rhizoma (root and rhizome of *Panax notoginseng*), protected against neurotoxicity through the enhancement of phase II detoxifying enzymes which were triggered by the activation of MEK1/2-ERK1/2 pathways. Besides, a literature review by S.-V. More et al. indicated that a lot of chemical ingredients isolated from herbal medicine could be the potential drugs for treating Parkinson's disease.

The prevention of illness by maintaining homeostasis and enhancing body's defense is a major goal of herbal medicine. K.-Y. Zhu et al. showed that Kai-Xin-San, a herbal formula prescribed traditionally to treat stress-related psychiatric diseases, was able to stimulate the expression and secretion of neurotrophic factors in cultured astrocytes. These neurotrophic factors are playing important roles in maintaining the survival, growth, and differentiation of neurons. The depletion of neurotrophic factors can lead to neuronal death which contributes to the pathogenesis of neurodegenerative disorders. By using similar techniques, S.-L. Xu et al. demonstrated that a lot of flavonoids isolated from herbal materials were able to induce the synthesis and secretion of neurotrophic factors, including nerve growth factor, glial-derived neurotrophic factor, and brain-derived neurotrophic factor.

In the last special issue, we have mentioned that clinical trial is needed to provide supporting evidence for the application of herbal medicine on neurodegenerative disorders. In this issue, a clinical report by W. Pan et al. showed that Jiawei Sijunzi decoction, a six-herb herbal formula, delayed the development of amyotrophic lateral sclerosis in some patients. We still hope that large-scale, double-blind, placebo-controlled trial can be collected in the coming issues.

Acknowledgments

We thank the authors of this special issue for their contributions. We are grateful to all the scientific colleagues for providing their valuable comment for these manuscripts.

Paul Siu-Po Ip
Karl Wah-Keung Tsim
Kelvin Chan
Rudolf Bauer

Hindawi Publishing Corporation
Evidence-Based Complementary and Alternative Medicine
Volume 2013, Article ID 163057, 8 pages
http://dx.doi.org/10.1155/2013/163057

Research Article

Isorhynchophylline Protects PC12 Cells Against Beta-Amyloid-Induced Apoptosis via PI3K/Akt Signaling Pathway

Yan-Fang Xian,[1] Zhi-Xiu Lin,[1] Qing-Qiu Mao,[1] Jian-Nan Chen,[2] Zi-Ren Su,[2] Xiao-Ping Lai,[2] and Paul Siu-Po Ip[1]

[1] *School of Chinese Medicine, Faculty of Medicine, The Chinese University of Hong Kong, Shatin, Hong Kong*
[2] *College of Chinese Medicines, Guangzhou University of Chinese Medicine, 510006 Guangzhou, China*

Correspondence should be addressed to Zhi-Xiu Lin; linzx@cuhk.edu.hk and Paul Siu-Po Ip; paulip@cuhk.edu.hk

Received 3 June 2013; Revised 12 September 2013; Accepted 23 September 2013

Academic Editor: Karl Wah-Keung Tsim

The neurotoxicity of amyloid-β (Aβ) has been implicated as a critical cause of Alzheimer's disease. Isorhynchophylline (IRN), an oxindole alkaloid isolated from *Uncaria rhynchophylla,* exerts neuroprotective effect against Aβ_{25-35}-induced neurotoxicity *in vitro*. However, the exact mechanism for its neuroprotective effect is not well understood. The present study aimed to investigate the molecular mechanisms underlying the protective action of IRN against Aβ_{25-35}-induced neurotoxicity in cultured rat pheochromocytoma (PC12) cells. Pretreatment with IRN significantly increased the cell viability, inhibited the release of lactate dehydrogenase and the extent of DNA fragmentation in Aβ_{25-35}-treated cells. IRN treatment was able to enhance the protein levels of phosphorylated Akt (p-Akt) and glycogen synthase kinase-3β (p-GSK-3β). Lithium chloride blocked Aβ_{25-35}-induced cellular apoptosis in a similar manner as IRN, suggesting that GSK-3β inhibition was involved in neuroprotective action of IRN. Pretreatment with LY294002 completely abolished the protective effects of IRN. Furthermore, IRN reversed Aβ_{25-35}-induced attenuation in the level of phosphorylated cyclic AMP response element binding protein (p-CREB) and the effect of IRN could be blocked by the PI3K inhibitor. These experimental findings unambiguously suggested that the protective effect of IRN against Aβ_{25-35}-induced apoptosis in PC12 cells was associated with the enhancement of p-CREB expression via PI3K/Akt/GSK-3β signaling pathway.

1. Introduction

Alzheimer's disease (AD) is the most common form of neurodegenerative disorders of the brain and affects an estimated 26.6 million people across the globe in 2006 [1]. The neuropathological hallmarks of AD include massive accumulation of beta-amyloid (Aβ) in senile plaques, abnormal tau filaments in neurofibrillary tangles, and extensive neuronal loss [2, 3]. Aβ is a 39- to 43-amino acid peptide fragment derived from sequential proteolysis of amyloid precursor protein (APP) through cleavage by β-secretase and γ-secretase [4]. Recent studies have suggested that Aβ plays an important role in the pathogenesis of AD [5]. Aβ accumulation has been causatively implicated in the neuronal dysfunction and neuronal loss that underlie the clinical manifestations of AD [6]. A correlation among memory deficits, Aβ elevation, and amyloid plaques on transgenic has been reported in previous studies [7, 8]. Therefore, inhibition of Aβ-induced neuronal degeneration may provide clinical benefits to AD patients.

Isorhynchophylline (IRN, Figure 1), an oxindole alkaloid, has been identified as the main active ingredient responsible for the biological activities of *Uncaria rhynchophylla* [9, 10]. IRN has also been reported to protect against the ischemia- and glutamate-induced neuronal damage or death [9, 11], and inhibition of 5-HT receptor [12, 13]. Previous studies in our laboratory has demonstrated that IRN protected rat pheochromocytoma (PC12) cells against the Aβ_{25-35}-induced oxidative stress, mitochondrial dysfunction, apoptosis, calcium influx, and tau protein hyperphosphorylation

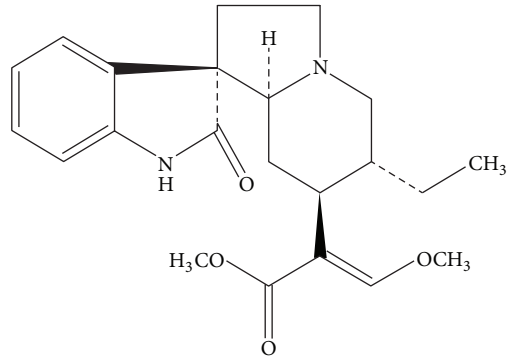

Figure 1: Chemical structure of isorhynchophylline (IRN).

[14, 15]. However, the molecular mechanisms underlying the protective effect of IRN against the neurotoxicity induced by $A\beta_{25-35}$ have not been fully understood. In this study, we aimed to elucidate the molecular signaling pathway involved in the neuroprotective effect of IRN.

2. Materials and Methods

2.1. Chemicals and Reagents. Isorhynchophylline (IRN, purity ⩾ 98%) was purchased from Chengdu Mansite Pharmaceutical Co. Ltd. (Chengdu, Sichuan, China). Its identity was confirmed by comparing its H^1 NMR spectra with the published data [16]. Nerve growth factor (NGF), LY294002 (LY), lithium chloride (LiCl), and β-amyloid peptide ($A\beta_{25-35}$) were purchased from Sigma-Aldrich (St. Louis, MO, USA). Dulbecco's modified Eagle medium (DMEM), fetal bovine serum (FBS), penicillin, and streptomycin were obtained from Gibco (Grand Island, NY, USA). Unless otherwise indicated, all other reagents were of analytical grade and were obtained from Sigma-Aldrich.

2.2. Peptide Preparation. $A\beta_{25-35}$, which is the most toxic peptide fragment derived from amyloid precursor protein, was dissolved in deionized distilled water at the concentration of 1 mM. The stock solution was diluted to desired concentrations immediately before use and added to cell culture medium.

2.3. Cell Culture and Drug Treatment. The PC12 cells were obtained from the American Type Culture Collection (Rockville, MD, USA). They were maintained in DMEM medium supplemented with penicillin (100 U/mL), streptomycin (100 μg/mL), 6% FBS, and 6% horse serum at 37°C in a humidified atmosphere of 95% air and 5% CO_2. Unless otherwise specified, the cells were seeded onto 24-well culture plate at a density of 8×10^4 cells/well. PC12 cells were differentiated with 50 ng/mL NGF in serum-free DMEM for 3 days [15]. IRN and all inhibitors were dissolved in DMSO and diluted with culture medium. The final concentration of DMSO in the test solutions was less than 0.1%. The cells were incubated with different concentrations of IRN (final concentrations: 1, 10, and 50 μM) for 2 h. $A\beta_{25-35}$ at a final concentration of 20 μM was then added to the culture for an additional 24 h. In experiments involving kinase inhibitors, the inhibitors LY294002 (50 μM) or LiCl (10 mM) were added 1 h prior to IRN (50 μM) and/or $A\beta_{25-35}$ (20 μM) treatment.

2.4. Cell Viability Assay. Cell viability was measured using a CellTiter 96 AQ_{ueous} One Solution Cell Proliferation Assay (Promega, Madison, WI, USA). In brief, PC12 cells were seeded onto a 96-well culture plate at a density of 2×10^4 cells/well. Cells were washed with D-Hanks solution after drug treatment. Then, 100 μL of serum-free medium and 20 μL of CellTiter 96 AQ_{ueous} One Solution were added into each well. The cells were incubated at 37°C for 2 h. The quantity of formazan product, which is directly proportional to the number of living cells, was measured using a FLUOstar OPTIMA microplate reader (BMG Labtech, Offenbury, Germany) at 490 nm. Cell viability was expressed as percentage of nontreated control.

2.5. Lactate Dehydrogenase (LDH) Activity Assay. LDH activity was measured using a LDH diagnostic kit (STANBIO Laboratory, Boerne, TX, USA) according to the manufacturer's protocol. Briefly, PC12 cells were seeded onto 24-well culture plates at a density of 1×10^5 cells/well. At the end of the drug treatment, the medium was collected. Subsequently, 100 μL of the medium was added to a polystyrene cuvette containing 1 mL of LDH reagent. The cuvette was placed immediately into a spectrophotometer and maintained at 30°C. After stabilization for 1 min, the absorbance at 340 nm was recorded at 1 min intervals for 3 min. The enzyme activity was expressed in unit per liter. To determine intracellular LDH activity, the cells were washed with D-Hanks solution and then scraped from the plates into 500 μL of ice-cold PBS (0.1 M, containing 0.05 mM of EDTA) and homogenized. The homogenate was centrifuged (4000 ×g) at 4°C for 30 min. The resulting supernatant was collected for the LDH assay. The total LDH activity was computed by summing the activities in the cell lysate and medium. Cellular toxicity was indicted by the percentage of LDH released from the cell.

2.6. Quantification of DNA Fragmentation. Quantification of DNA fragmentation was determined by Cell Death Detection $ELISA^{Plus}$ kit (Roche Applied Sciences, Basel, Switzerland) according to the manufacturer's protocol. In brief, the cells were washed with HBSS after drug treatment. Then, the cells were incubated with 200 μL of lysis buffer for 30 min at room temperature. The plate was centrifuged at 200 ×g for 10 min at 4°C. An aliquot (20 μL) of the supernatant from each well was transferred into a streptavidin-coated microplate and incubated with a mixture of anti-histone biotin and anti-DNA peroxidase. The apoptotic nucleosomes were captured via their histone component by the anti-histone-biotin antibody which was bound to the streptavidin-coated microplate. Simultaneously, anti-DNA peroxidase was bound to the DNA part of the nucleosomes. After removing the unbound antibodies, the amount of peroxidase retained in the immunocomplex was quantified by adding 2,2′-azinobis (3-ethylbenzthiazoline-6-sulphonic acid) (ABTS) as

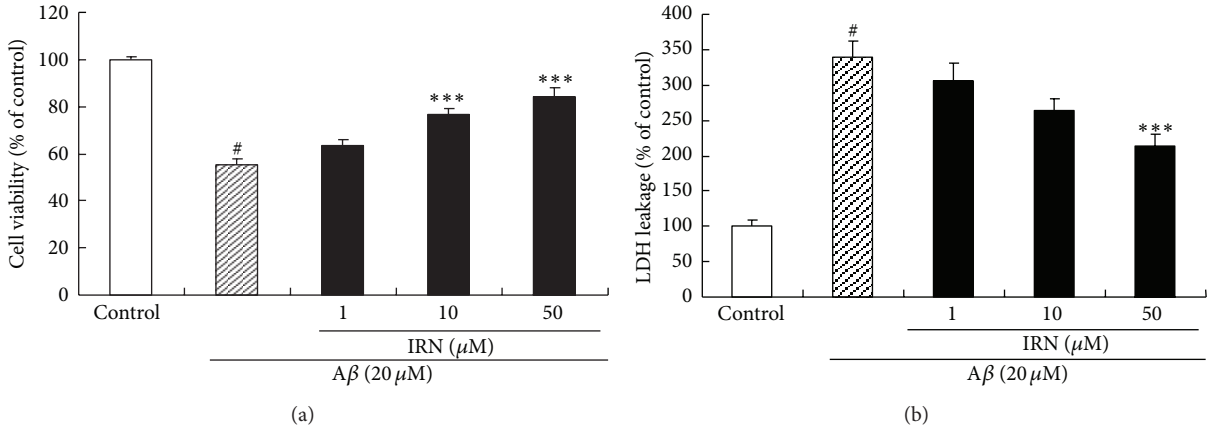

Figure 2: Effects of IRN on the $A\beta_{25-35}$-induced neurotoxicity in PC12 cells. Cell viability was measured by MTS assay (a) and LDH assay (b). Values given are the mean ± SEM ($n = 6$). $^{\#}P < 0.001$ compared with the control group; $^{***}P < 0.001$ compared with the $A\beta_{25-35}$-treated control.

the substrate, and the absorbance of the reaction mixture was measured at 405 nm using a microplate reader. The absorbance is directly proportional to the number of apoptotic nucleosomes. The extent of DNA fragmentation was expressed as percentage of the control.

2.7. Western Blot Analysis. PC12 cells were seeded onto 100 mm^2 dish at 5×10^6 cells/dish. The cells were washed twice with D-Hanks solution after drug treatment. The cells were harvested and lysed with protein lysis buffer (50 mM Tris-HCl, pH 7.5, 100 mM NaCl, 1% NP-40, 0.5% sodium deoxycholate, 0.1% SDS, 1 mM EDTA, 1 mM sodium orthovanadate, 10 mM sodium fluoride, and 100 mg/mL PMSF). Protein concentration in the supernatants was determined with the BCA protein assay. Protein samples were electrophoresed by SDS-PAGE for 2 h at 80 V. The separated proteins were transferred to polyvinylidene fluoride (PVDF) membranes using a transblotting apparatus (Bio-Rad Laboratories, Hercules, CA, USA) for 30 min at 15 V. The membranes were blocked with 5% (w/v) nonfat milk in TBS-T (Tris-buffer saline containing 0.1% Tween-20) at room temperature for 2 h and subsequently incubated at 4°C overnight with appropriate amount of primary antibodies against p-Akt (Ser 473), Akt, phosphorylation of glycogen synthase kinase-3β (p-GSK-3β, Ser9), GSK-3β, phosphorylation cyclic AMP response element binding protein (p-CREB, Ser133), CREB (Cell Signaling Technology, Beverly, MA), and β-actin (Santa Cruz Biotechnology Inc., USA) at 4°C overnight. Next, the membrane was washed with TBS-T three times and probed with horseradish peroxidase conjugated secondary antibody at room temperature for 1 h. To verify equal loading of samples, the membranes were incubated with monoclonal antibody β-actin, followed by a horseradish peroxidase conjugated goat anti-mouse IgG. The membrane again was washed with TBS-T for three times, and finally the protein bands were visualized by the ECL western blotting detection reagents (Amersham Biosciences, Buckinghamshire, UK). The intensity of each band was analyzed using Image J software (NIH Image, Bethesda, MD, USA).

2.8. Statistical Analysis. Data were expressed as mean ± SEM. Multiple group comparisons were performed using one-way analysis of variance (ANOVA) followed by Tukey's test in order to detect intergroup differences. GraphPad Prism software (Version 4.0; GraphPad Software, Inc., San Diego, CA) was used to perform the statistical analysis. A difference was considered statistically significant if the P value was less than 0.05.

3. Results

3.1. Effects of IRN on $A\beta_{25-35}$-Induced Cytotoxicity in PC12 Cells. The effect of IRN on cell viability of $A\beta_{25-35}$-treated PC12 cells was shown in Figure 2(a). Treating the cells with $A\beta_{25-35}$ at 20 μM for 24 h could significantly decrease cell viability, as compared to the control group ($P < 0.001$). Pretreatment with IRN (10 and 50 μM) in the presence of 20 μM $A\beta_{25-35}$ for 24 h was able to significantly increase the cell viability as compared with the $A\beta_{25-35}$-treated control ($P < 0.001$ for both concentrations).

To investigate the protective effect of IRN, a LDH assay was performed. As shown in Figure 2(b), when PC12 cells were incubated with 20 μM of $A\beta_{25-35}$ for 24 h, the percentage of LDH leakage was conspicuously increased ($P < 0.001$). When the cells were pretreated with IRN (50 μM) in the presence of 20 μM of $A\beta_{25-35}$ for 24 h, the percentage of LDH leakage was significantly reduced as compared with the $A\beta_{25-35}$-treated control ($P < 0.001$).

3.2. Effect of IRN on $A\beta_{25-35}$-Induced Activation of GSK-3β in PC12 Cells. To investigate the effect of IRN on the activation of GSK-3β in $A\beta_{25-35}$-treated PC12 cells, the protein levels of GSK-3β and p-GSK-3β (Ser9) were determined. As shown in Figure 3(a), the level of p-GSK-3β was significantly decreased ($P < 0.001$) after treatment with 20 μM of $A\beta_{25-35}$. Interestingly, pretreatment with IRN (1, 10 and 50 μM) markedly elevated the level of p-GSK-3β ($P < 0.00$, $P < 0.01$ and $P < 0.001$, resp.) when compared to the $A\beta_{25-35}$-treated control, indicating that IRN suppressed the activation

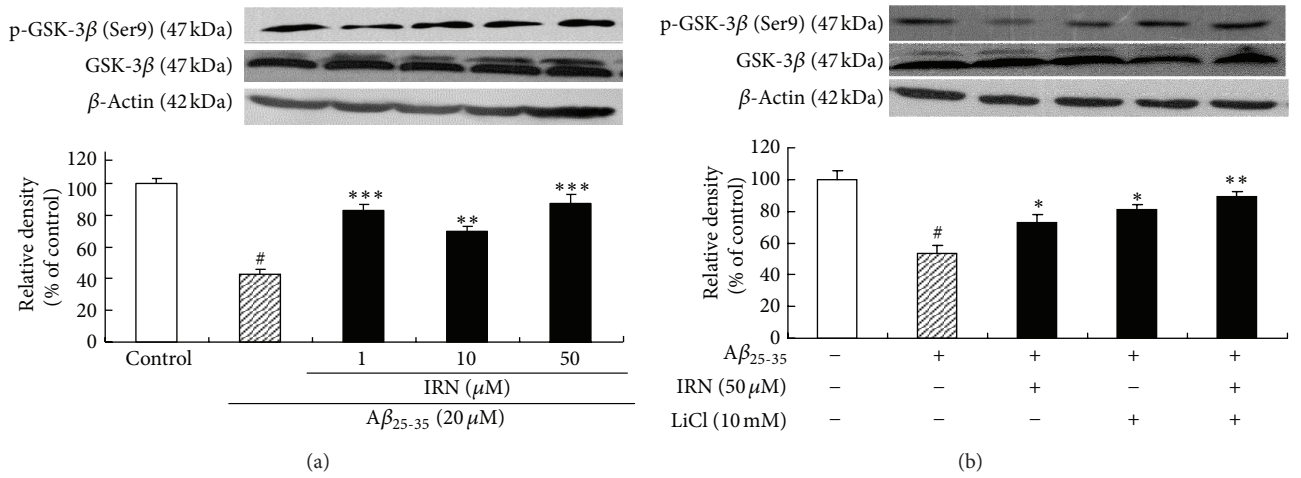

Figure 3: Effects of IRN on the $A\beta_{25-35}$-induced activation of GSK-3β in PC12 cells. Values given are the mean ± SEM ($n = 3$). $^{\#}P < 0.001$ compared with the control group; $^{*}P < 0.05$, $^{**}P < 0.01$, and $^{***}P < 0.001$ compared with the $A\beta_{25-35}$-treated control.

of GSK-3β induced by $A\beta_{25-35}$. To show the correlation between p-GSK-3β and cell viability, LiCl, a potent GSK-3β inhibitor, was used. Results showed that pretreatment with LiCl (10 mM) could significantly accentuate cell viability ($P < 0.01$, Figure 6(a)) and the protein level of p-GSK-3β ($P < 0.05$, Figure 3(b)). The treatment also attenuated LDH leakage ($P < 0.001$, Figure 6(b)) and DNA fragmentation ($P < 0.001$, Figure 6(c)) in $A\beta_{25-35}$-treated cells.

3.3. Effect of IRN on $A\beta_{25-35}$-Induced Inactivation of PI3K/Akt Pathway. As shown in Figure 4(a), treatment with 20 μM of $A\beta_{25-35}$ for 24 h significantly decreased the protein level of p-Akt (Ser473). However, pretreatment with IRN (50 μM) markedly increased the protein level of p-Akt ($P < 0.001$), indicating that IRN was able to activate PI3K/Akt signaling pathway in the $A\beta_{25-35}$-treated cells. LY294002, a potent PI3K/Akt signaling pathway inhibitor [17, 18], thoroughly abolished the effects of IRN on p-Akt and p-GSK-3β (Figures 4(b) and 4(c)). In these experiments, total protein levels of Akt and GSK-3β did not change in all groups.

3.4. Effect of IRN on the Phosphor-CREB through PI3K Activation. As shown in Figure 5, treating the cells with 20 μM of $A\beta_{25-35}$ for 24 h significantly decreased protein level of p-CREB (Ser133), while pretreatment with IRN (10 and 50 μM) markedly elevated protein level of p-CREB ($P < 0.05$ and $P < 0.001$, resp.), as compared with the $A\beta_{25-35}$-treated control. The effect of IRN was completely blocked by LY294002, indicating the involvement of PI3K signal transduction.

4. Discussion

Previous studies in our laboratory demonstrated that IRN could significantly reduce the neurotoxicity induced by $A\beta_{25-35}$ via inhibiting oxidative stress, calcium influx, tau protein hyperphosphorylation, and suppressing cellular apoptosis in PC12 cells [14, 15]. The present study revealed that IRN could protect PC12 cells against the $A\beta_{25-35}$-induced neurotoxicity via PI3K/Akt/GSK-3β signaling pathway.

Recent studies suggest that GSK-3β plays an important role in AD neuropathology [19] and its activity accounts for many pathological hallmarks of the disease in both sporadic and familial AD cases. Hyperactivation of GSK-3β has been reported to induce neuronal cell death [20] and abnormal tau protein hyperphosphorylation [21, 22], both of which are the cardinal pathogenesis of AD. GSK-3β genes have been identified as potential candidate susceptibility genes for dementia [23]. In addition, GSK-3β expression is elevated in APP transgenic cultures which is coincided with the development of neuronal injury in brains of AD patients [24, 25]. Unlike most protein kinases, phosphorylation of GSK-3β at Ser9 leads to the inactivation of the enzyme [26]. Therefore, upregulation of p-GSK-3β (Ser9) may confer a protective effect. Our findings showed that Aβ significantly reduced the protein level of p-GSK-3β (Ser9), while pretreatment with IRN variably elevated the protein level of p-GSK-3β (Ser9). Treating the cells with LiCl, an inhibitor of GSK-3β, produces similar effects as IRN on $A\beta_{25-35}$-induced cytotoxicity (Figure 6). However, synergistic effect was not observed between IRN and LiCl. Our previous studies demonstrated that IRN was able to reverse cellular apoptosis and tau protein hyperphosphorylation in Aβ-treated PC12 cells [14, 15]. These results suggest that the protective effect of IRN against $A\beta_{25-35}$-induced apoptosis and tau protein hyperphosphorylation may be mediated by the suppression of GSK-3β activation.

Akt is a well-known prosurvival kinase and is activated by the phosphorylation at the Ser473 via PI3K pathway [27, 28]. PI3K/Akt signaling pathway has been suggested to play a pivotal role in GSK-3β-mediated tau protein hyperphosphorylation and neuronal survival. Inhibition of PI3K/Akt signaling pathway increases GSK-3β activity, resulting in tau protein hyperphosphorylation [29]. PI3K enhances neuroprotection through regulating phosphorylation level and activation of the Akt. Akt activity can be modulated by

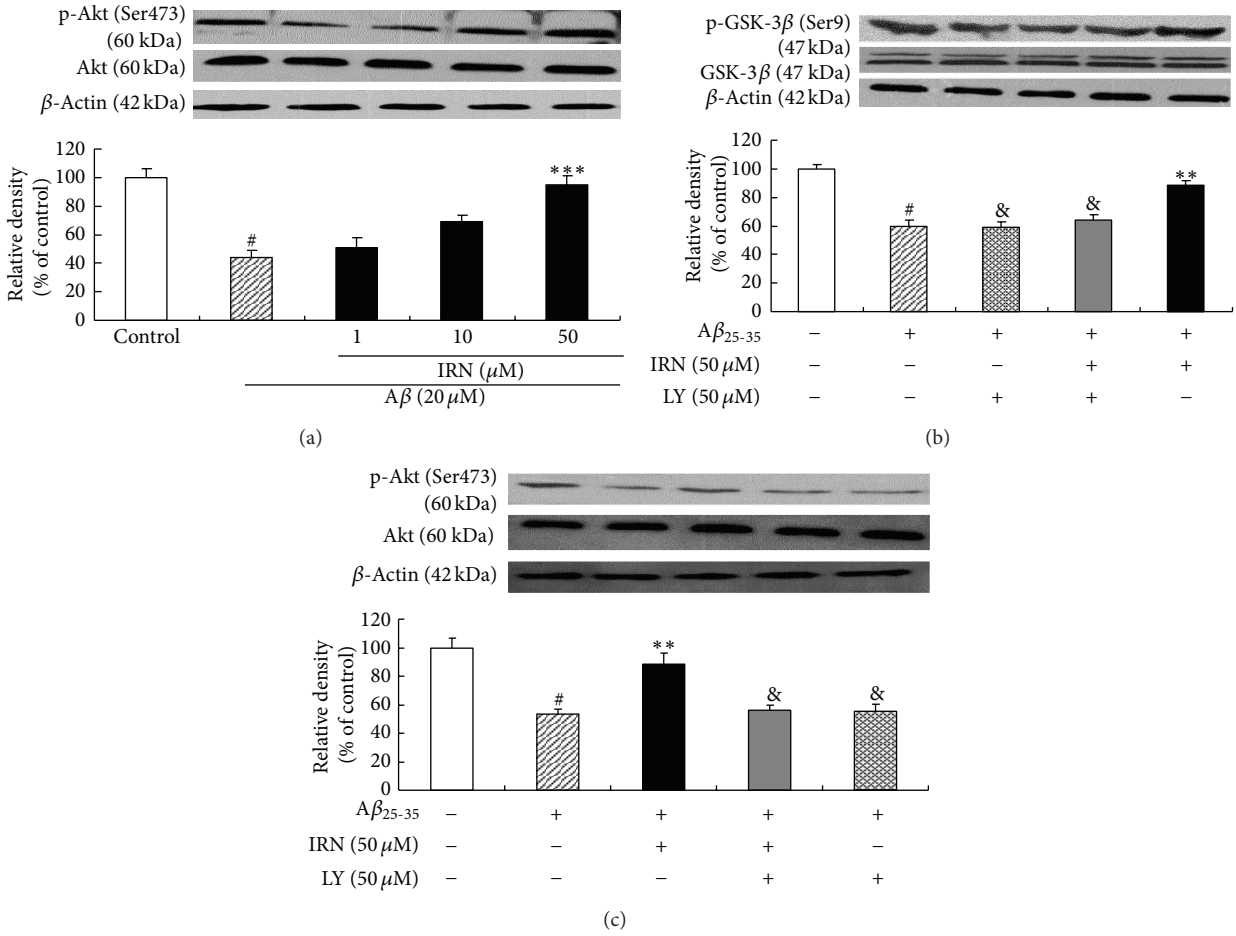

FIGURE 4: Effect of IRN on $A\beta_{25-35}$-induced inactivation of PI3K/Akt pathway. Values given are the mean ± SEM ($n = 3$). $^{\#}P < 0.001$ compared with the control group; $^{**}P < 0.01$ and $^{***}P < 0.001$ compared with the $A\beta_{25-35}$-treated control; $^{\&}P < 0.05$ compared with the group treated with $A\beta_{25-35}$ and IRN (50 μM).

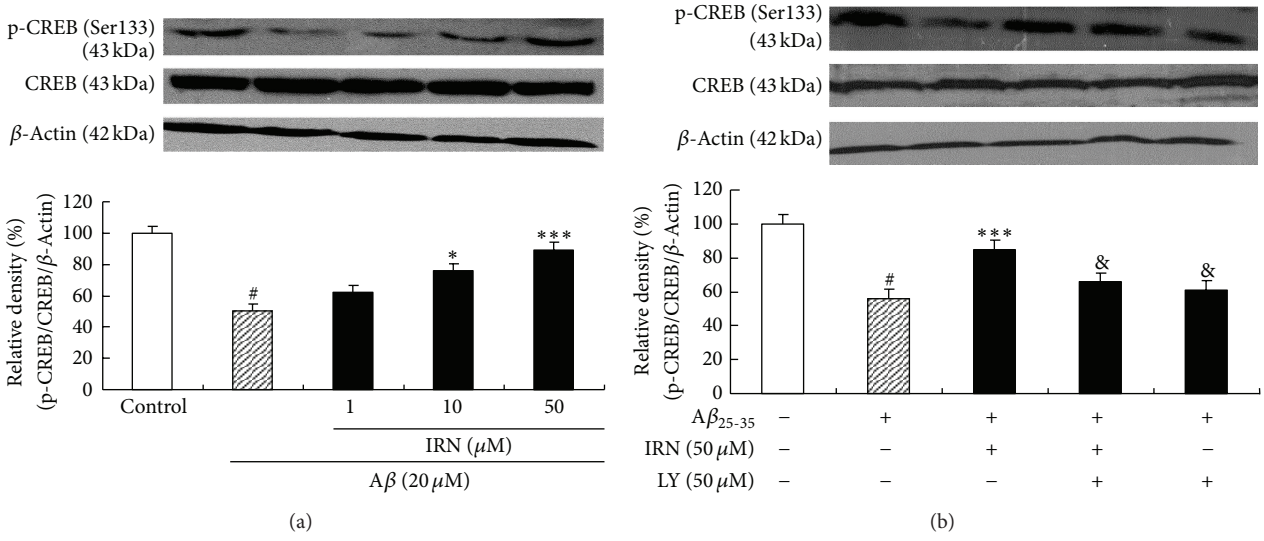

FIGURE 5: Effect of IRN on the p-CREB through PI3K activation. Values given are the mean ± SEM ($n = 3$). $^{\#}P < 0.001$ compared with the control group; $^{*}P < 0.05$ and $^{***}P < 0.001$ compared with the $A\beta_{25-35}$-treated control; $^{\&}P < 0.05$ compared with the group treated with $A\beta_{25-35}$ and IRN (50 μM).

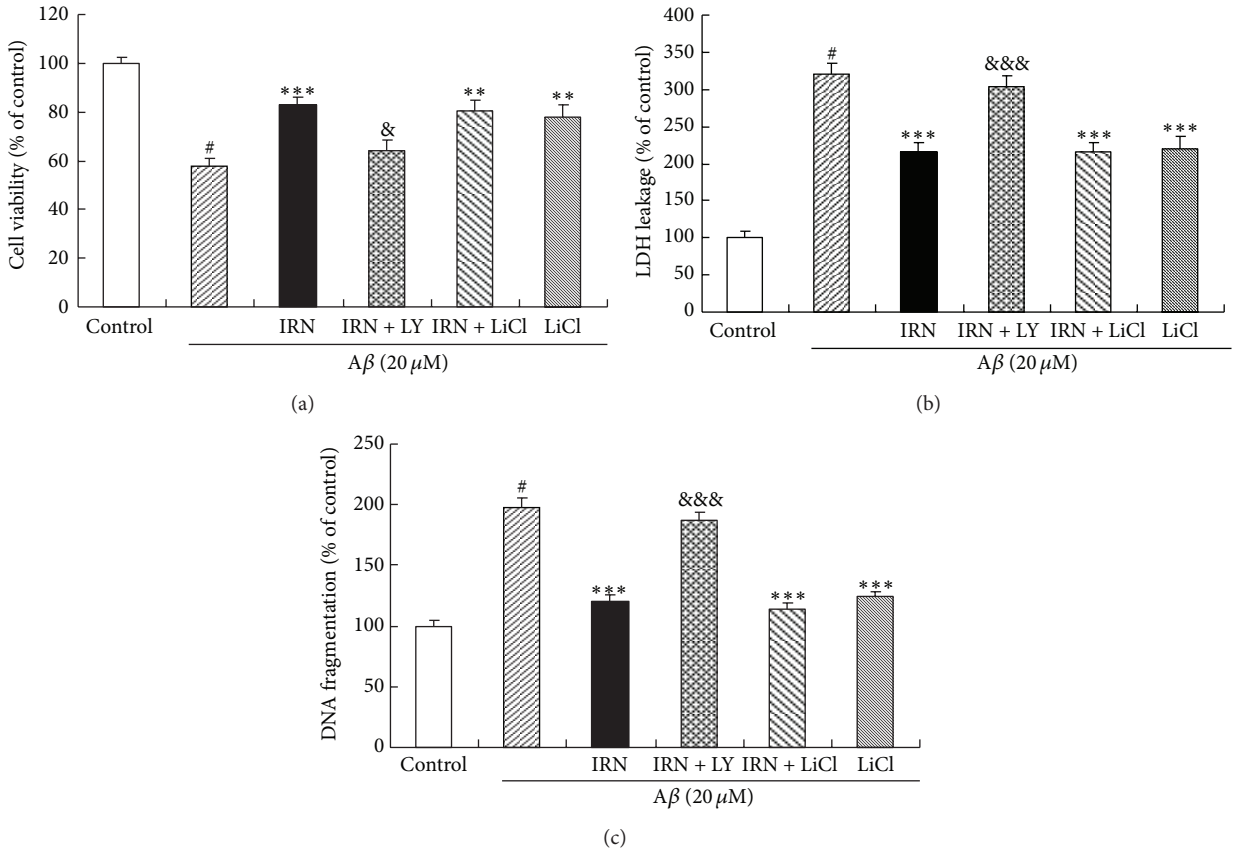

Figure 6: Effect of kinase inhibitors on neuroprotection of IRN against $A\beta_{25-35}$-induced neurotoxicity. $A\beta_{25-35}$-induced neurotoxicity was indicated by cell viability (a), LDH leakage (b), and the production of DNA fragmentation (c), respectively. Values given are the mean ± SEM ($n = 6$). $^{\#}P < 0.001$ compared with the control group; $^{**}P < 0.01$ and $^{***}P < 0.001$ compared with the $A\beta_{25-35}$-treated control; $^{\&}P < 0.05$ and $^{\&\&\&}P < 0.001$ compared with the group treated with $A\beta_{25-35}$ and IRN (50 μM).

phosphorylation either on the residue Thr308 or Ser473 [30, 31]. The activation of Akt can lead to the suppression of GSK-3β activity [32]. Our results showed that Aβ treatment significantly decreased the protein level of p-Akt (Ser473) in PC12 cells. Pretreatment with IRN could significantly reverse the effect of Aβ on p-Akt which accounted for the protective mechanism of IRN against Aβ-induced neurotoxicity. Cotreatment with LY294002, a specific inhibitor of PI3K, completely abolished the effect of IRN on p-Akt and p-GSK-3β (Figure 4). Consistent results were obtained for the interaction of LY294002 and IRN on Aβ-induced cytotoxicity and DNA fragmentation (Figure 6). These findings strongly suggested that the protective effect of IRN against the $A\beta_{25-35}$-induced neurotoxicity in PC12 cells was medicated via PI3K/Akt signaling pathway.

In addition to robustly phosphorylated tau protein, GSK-3β also acts as a key regulator of a broad array of transcriptional factors, that is, β-catenin, activator protein-1, nuclear factor kappa B (NFκB), p53, CREB, heat shock factor (HSF-1), and CCAAT/enhancer binding protein [33]. Among these factors, CREB is the most important element in regulating cell survival and death. P-CREB (Ser133) is a downstream protein of the PI3K/Akt pathway [34] and acts as a substrate for GSK-3β [35]. It participates in many vital processes, including cell survival [36]. Our data showed that treatment with $A\beta_{25-35}$ markedly inhibited the content of p-CREB, while pretreatment with IRN significantly increased the content of p-CREB via PI3K activation. Recent studies revealed that Akt and CREB could promote cell survival by upregulating the expression of antiapoptotic proteins such as Bcl-2 [37, 38]. Interestingly, our previous study indicated that pretreatment with IRN could significantly enhance the expression of Bcl-2 [14]. Furthermore, our results showed that PI3K inhibitor, LY294002, could abolish the accentuating effect of IRN on the protein expression of p-CREB, suggesting that p-CREB was involved in the neuroprotective mechanism of IRN.

In summary, our results demonstrated that IRN could protect against the $A\beta_{25-35}$-induced apoptosis in PC12 cells. The protective effect of IRN was associated with the enhancement of p-CREB expression via PI3K/Akt/GSK-3β signaling pathway. The results from the present study advance our knowledge regarding the neuroprotective mechanism of IRN. More importantly, this study has laid a foundation for future clinical studies to evaluate the potential benefits of IRN on AD patients.

Acknowledgment

This study was supported by a Direct Grant of The Chinese University of Hong Kong.

References

[1] R. Brookmeyer, E. Johnson, K. Ziegler-Graham, and H. M. Arrighi, "Forecasting the global burden of Alzheimer's disease," *Alzheimer's and Dementia*, vol. 3, no. 3, pp. 186–191, 2007.

[2] H. L. Weiner, C. A. Lemere, R. Maron et al., "Nasal administration of amyloid-beta peptide decreases cerebral amyloid burden in a mouse model of Alzheimer's disease," *Annals of Neurology*, vol. 48, no. 4, pp. 567–579, 2000.

[3] M. Bothwell and E. Giniger, "Alzheimer's disease: neurodevelopment converges with neurodegeneration," *Cell*, vol. 102, no. 3, pp. 271–273, 2000.

[4] D. J. Selkoe, "Alzheimer's disease: genotypes, phenotype, and treatments," *Science*, vol. 275, no. 5300, pp. 630–631, 1997.

[5] E. Hellström-Lindahl, M. Viitanen, and A. Marutle, "Comparison of Aβ levels in the brain of familial and sporadic Alzheimer's disease," *Neurochemistry International*, vol. 55, no. 4, pp. 243–252, 2009.

[6] M. R. Basha, M. Murali, H. K. Siddiqi et al., "Lead (Pb) exposure and its effect on APP proteolysis and Aβ aggregation," *FASEB Journal*, vol. 19, no. 14, pp. 2083–2084, 2005.

[7] Y. Hashimoto, T. Niikura, T. Chiba et al., "The cytoplasmic domain of Alzheimer's amyloid-β protein precursor causes sustained apoptosis signal-regulating kinase 1/c-Jun NH 2-terminal kinase-mediated neurotoxic signal via dimerization," *Journal of Pharmacology and Experimental Therapeutics*, vol. 306, no. 3, pp. 889–902, 2003.

[8] D. L. McPhie, R. Coopersmith, A. Hines-Peralta et al., "DNA synthesis and neuronal apoptosis caused by familial Alzheimer disease mutants of the amyloid precursor protein are mediated by the p21 activated kinase PAK3," *Journal of Neuroscience*, vol. 23, no. 17, pp. 6914–6927, 2003.

[9] T. H. Kang, Y. Murakami, H. Takayama et al., "Protective effect of rhynchophylline and isorhynchophylline on in vitro ischemia-induced neuronal damage in the hippocampus: putative neurotransmitter receptors involved in their action," *Life Sciences*, vol. 76, no. 3, pp. 331–343, 2004.

[10] D. Yuan, B. Ma, J. Y. Yang et al., "Anti-inflammatory effects of rhynchophylline and isorhynchophylline in mouse N9 microglial cells and the molecular mechanism," *International Immunopharmacology*, vol. 9, no. 13-14, pp. 1549–1554, 2009.

[11] Y. Shimada, H. Goto, T. Itoh et al., "Evaluation of the protective effects of alkaloids isolated from the hooks and stems of Uncaria sinensis on glutamate-induced neuronal death in cultured cerebellar granule cells from rats," *Journal of Pharmacy and Pharmacology*, vol. 51, no. 6, pp. 715–722, 1999.

[12] H. Kanatani, H. Kohda, and K. Yamasaki, "The active principles of the branchlet and hood of Uncaria sinensis Oliv. examined with a 5-hydroxytryptamine receptor binding assay," *Journal of Pharmacy and Pharmacology*, vol. 37, no. 6, pp. 401–404, 1985.

[13] K. Matsumoto, R. Morishige, Y. Murakami et al., "Suppressive effects of isorhynchophylline on 5-HT2A receptor function in the brain: behavioural and electrophysiological studies," *European Journal of Pharmacology*, vol. 517, no. 3, pp. 191–199, 2005.

[14] Y. F. Xian, Z. X. Lin, Q. Q. Mao, S. P. Ip, Z. R. Su, and X. P. Lai, "Protective effect of isorhynchophylline against β-amyloid-induced neurotoxicity in PC12 cells," *Cellular and Molecular Neurobiology*, vol. 32, no. 3, pp. 353–360, 2012.

[15] Y. F. Xian, Z. X. Lin, Q. Q. Mao, M. Zhao, Z. Hu, and S. P. Ip, "Bioassay-guided isolation of neuroprotective compounds from uncaria rhynchophylla against beta-amyloid-induced neurotoxicity in PC12 cells," *Evidence-Based Complementary and Alternative Medicine*, vol. 2012, Article ID 802625, 8 pages, 2012.

[16] J. Haginiwa, S. Sakai, and N. Aimi, "Studies of plants containing indole alkaloids. (II). The alkaloids of Uncaria rhynchophylla Miq," *Yakugaku Zasshi*, vol. 93, no. 4, pp. 448–452, 1973.

[17] K. W. Zeng, H. Ko, H. O. Yang, and X. M. Wang, "Icariin attenuates β-amyloid-induced neurotoxicity by inhibition of tau protein hyperphosphorylation in PC12 cells," *Neuropharmacology*, vol. 59, no. 6, pp. 542–550, 2010.

[18] Z. Zhang, R. Zhao, J. Qi, S. Wen, Y. Tang, and D. Wang, "Inhibition of glycogen synthase kinase-3β by Angelica sinensis extract decreases β-amyloid-induced neurotoxicity and tau phosphorylation in cultured cortical neurons," *Journal of Neuroscience Research*, vol. 89, no. 3, pp. 437–447, 2011.

[19] L. Sun, C. Guo, D. Liu et al., "Protective effects of bone morphogenetic protein 7 against amyloid-beta induced neurotoxicity in PC12 cells," *Neuroscience*, vol. 184, pp. 151–163, 2011.

[20] M. Pap and G. M. Cooper, "Role of glycogen synthase kinase-3 in the phosphatidylinositol 3- kinase/Akt cell survival pathway," *Journal of Biological Chemistry*, vol. 273, no. 32, pp. 19929–19932, 1998.

[21] G. Alvarez, J. R. Muñoz-Montaño, J. Satrústegui, J. Avila, E. Bogónez, and J. Díaz-Nido, "Regulation of tau phosphorylation and protection against beta-amyloid-induced neurodegeneration by lithium. Possible implications for Alzheimer's disease," *Bipolar Disorders*, vol. 4, no. 3, pp. 153–165, 2002.

[22] F. Plattner, M. Angelo, and K. P. Giese, "The roles of cyclin-dependent kinase 5 and glycogen synthase kinase 3 in tau hyperphosphorylation," *Journal of Biological Chemistry*, vol. 281, no. 35, pp. 25457–25465, 2006.

[23] D. H. Geschwind and B. L. Miller, "Molecular approaches to cerebral laterality: development and neurodegeneration," *American Journal of Medical Genetics*, vol. 101, no. 4, pp. 370–381, 2001.

[24] C. Tackenberg and R. Brandt, "Divergent pathways mediate spine alterations and cell death induced by amyloid-β, wild-type tau, and R406W tau," *Journal of Neuroscience*, vol. 29, no. 46, pp. 14439–14450, 2009.

[25] J. J. Pei, E. Braak, H. Braak et al., "Distribution of active glycogen synthase kinase 3β (GSK-3β) in brains staged for Alzheimer disease neurofibrillary changes," *Journal of Neuropathology and Experimental Neurology*, vol. 58, no. 9, pp. 1010–1019, 1999.

[26] M. D. Kaytor and H. T. Orr, "The GSK3β signaling cascade and neurodegenerative disease," *Current Opinion in Neurobiology*, vol. 12, no. 3, pp. 275–278, 2002.

[27] I. Tato, R. Bartrons, F. Ventura, and J. L. Rosa, "Amino acids activate mammalian target of rapamycin complex 2 (mTORC2) via PI3K/Akt signaling," *Journal of Biological Chemistry*, vol. 286, no. 8, pp. 6128–6142, 2011.

[28] R. Zhao, Z. Zhang, Y. Song, D. Wang, J. Qi, and S. Wen, "Implication of phosphatidylinositol-3 kinase/Akt/glycogen synthase kinase-3β pathway in ginsenoside Rb1's attenuation of beta-amyloid-induced neurotoxicity and tau phosphorylation," *Journal of Ethnopharmacology*, vol. 133, no. 3, pp. 1109–1116, 2011.

[29] L. Baki, J. Shioi, P. Wen et al., "PS1 activates PI3K thus inhibiting GSK-3 activity and tau overphosphorylation: effects of FAD mutations," *EMBO Journal*, vol. 23, no. 13, pp. 2586–2596, 2004.

[30] S. F. Moore, R. W. Hunter, and I. Hers, "mTORC2 protein-mediated protein kinase B (Akt) serine 473 phosphorylation is not required for Akt1 activity in human platelets," *Journal of Biological Chemistry*, vol. 286, no. 28, pp. 24553–24560, 2011.

[31] H. Koide, T. Asai, K. Furuya et al., "Inhibition of Akt (ser473) phosphorylation and rapamycin-resistant cell growth by knock-down of mammalian target of rapamycin with small interfering RNA in vascular endothelial growth factor receptor-1-targeting vector," *Biological and Pharmaceutical Bulletin*, vol. 34, no. 5, pp. 602–608, 2011.

[32] J. M. Beaulieu, R. R. Gainetdinov, and M. G. Caron, "Akt/GSK3 signaling in the action of psychotropic drugs," *Annual Review of Pharmacology and Toxicology*, vol. 49, pp. 327–347, 2009.

[33] C. A. Grimes and R. S. Jope, "The multifaceted roles of glycogen synthase kinase 3β in cellular signaling," *Progress in Neurobiology*, vol. 65, no. 4, pp. 391–426, 2001.

[34] K. Du and M. Montminy, "CREB is a regulatory target for the protein kinase Akt/PKB," *Journal of Biological Chemistry*, vol. 273, no. 49, pp. 32377–32379, 1998.

[35] T. R. Salas, S. A. Reddy, J. L. Clifford et al., "Alleviating the suppression of glycogen synthase kinase-3β by Akt leads to the phosphorylation of cAMP-response element-binding protein and its transactivation in intact cell nuclei," *Journal of Biological Chemistry*, vol. 278, no. 42, pp. 41338–41346, 2003.

[36] D. W. Kim, J. H. Lee, S. K. Park et al., "Astrocytic expressions of phosphorylated Akt, GSK3β and CREB following an excitotoxic lesion in the mouse hippocampus," *Neurochemical Research*, vol. 32, no. 9, pp. 1460–1468, 2007.

[37] L. Ji, E. Mochon, M. Arcinas, and L. M. Boxer, "CREB proteins function as positive regulators of the translocated bcl-2 allele in t(14;18) lymphomas," *Journal of Biological Chemistry*, vol. 271, no. 37, pp. 22687–22691, 1996.

[38] Y. Takada-Takatori, T. Kume, M. Sugimoto, H. Katsuki, H. Sugimoto, and A. Akaike, "Acetylcholinesterase inhibitors used in treatment of Alzheimer's disease prevent glutamate neurotoxicity via nicotinic acetylcholine receptors and phosphatidylinositol 3-kinase cascade," *Neuropharmacology*, vol. 51, no. 3, pp. 474–486, 2006.

Hindawi Publishing Corporation
Evidence-Based Complementary and Alternative Medicine
Volume 2013, Article ID 937370, 11 pages
http://dx.doi.org/10.1155/2013/937370

Research Article

Acetylshikonin, a Novel AChE Inhibitor, Inhibits Apoptosis via Upregulation of Heme Oxygenase-1 Expression in SH-SY5Y Cells

Yan Wang, Wen-Liang Pan, Wei-Cheng Liang, Wai-Kit Law, Denis Tsz-Ming Ip, Tzi-Bun Ng, Mary Miu-Yee Waye, and David Chi-Cheong Wan

School of Biomedical Sciences, The Chinese University of Hong Kong, Shatin, New Territories, Hong Kong

Correspondence should be addressed to David Chi-Cheong Wan; chicheongwan@cuhk.edu.hk

Received 14 June 2013; Revised 10 September 2013; Accepted 11 September 2013

Academic Editor: Karl Wah-Keung Tsim

Acetylcholinesterase inhibitors are prominent alternative in current clinical treatment for AD patients. Therefore, there is a continued need to search for novel AChEIs with good clinical efficacy and less side effects. By using our in-house natural product database and AutoDock Vina as a tool in docking study, we have identified twelve phytochemicals (emodin, aloe-emodin, chrysophanol, and rhein in Rhei Radix Et Rhizoma; xanthotoxin, phellopterin, alloisoimperatorin, and imperatorin in Angelicae dahuricae Radix; shikonin, acetylshikonin, isovalerylshikonin, and β,β-dimethylacrylshikonin in Arnebiae Radix) as candidates of AChEIs that were not previously reported in the literature. In addition to AChEI activity, a series of cell-based experiments were conducted for the investigation of their neuroprotective activities. We found that acetylshikonin and its derivatives prevented apoptotic cell death induced by hydrogen peroxide in human and rat neuronal SH-SY5Y and PC12 cells at 10 μM. We showed that acetylshikonin exhibited the most potent antiapoptosis activity through the inhibition of the generation of reactive oxygen species as well as protection of the loss of mitochondria membrane potential. Furthermore, we identified for the first time that the upregulation of heme oxygenase 1 by acetylshikonin is a key step mediating its antiapoptotic activity from oxidative stress in SH-SY5Y cells.

1. Introduction

Alzheimer's disease (AD) is one of the most devastating neurodegeneration diseases characterized by progressive memory loss and cognitive dysfunction in the aging population. Although beta-amyloid aggregation and fibrillar tau-tangles have been identified as the major pathogenesis markers in AD patients and they are now promising targets for drug development, there is still no available drug against these targets (reviewed in [1–3]). Therefore, acetylcholinesterase inhibitors (AChEIs) are alternative option in current clinical treatment, and there is a continued need to search for novel AChEIs with less side effect to treat AD [4].

Synthetic compounds are now a central focus when searching any AChEIs. Many of these AChEIs potently inhibited the enzyme at the nanomolar level [5–7]. However, not much information regarding the potency and efficacy of these AChEIs in animal study or clinical trials can be gathered, due to the fact that the potency of AChEIs inhibition may not correlate with their neuroprotection efficacy due to their increases in cellular toxicity. It is supported by the recent study that the role of AChEIs against AD might be far beyond its AChE inhibition that enhances neuronal transmission acetylcholine [8]. Abundant evidence from *in vitro* and *in vivo* studies has demonstrated that AChEIs exhibited remarkably neuroprotective effects through attenuation of oxidative stress and enhancement of antioxidant status [9, 10]. Therefore, both anti-AChE activity and antioxidative stress should be considered when searching novel AChEIs as drugs to treat AD.

In recent years, *in silico* virtual drug screening became a preferred approach to screen novel compounds given that the structures of molecular targets (enzymes or receptors) are determined. The high-throughput docking screen can provide possible candidates for further biomedical validation so as to reduce the time and cost of research and development in drug discovery (reviewed in [11]). The availability of the structure of AChEs has provided the opportunity of

widespread *in silico* screening of novel AChEIs [12–18]. The objective of the present study is to compile a comprehensive database from natural herbs in which the key constituents have been chemically characterized. It was inspired by the fact that the natural AChEI, galantamine, the FDA approved drug to treat mild-to-moderate AD, is a natural alkaloid that has only mild AChEI activity but strong neuroprotective efficacy [19]. Using this database, we have successfully identified some groups of phytochemicals that have mild AChEI activity but showed very promising neuroprotection in neuronal cell cultures induced by oxidative damages.

2. Materials and Methods

2.1. Molecular Docking Screening. For ligands library establishment, approximately 8,000 phytochemicals were compiled based on selected reference books. The SMILE format of phytochemicals was compiled from Pubchem (http://pubchem.ncbi.nlm.nih.gov/) or Scifinder (https://www.cas.org/products/scifinder/). The SMILES format of compounds was converted to PDB format by CORINA online service (http://www.molecular-networks.com/online_demos/corina_demo/). The PDB format of compounds was then converted to PDBQT format by AutoDock Tools 1.5.6 (The Scripps Research Institute, CA, USA). For receptor preparation, the crystal structure of human AChE was obtained from the Protein Data Bank (PDB 1B41). Both ligands and water molecules in 1B41 were removed by Chimera 1.7mac (UCSF Resource for Biocomputing, Visualization, and Informatics, CA, USA). The modified 1B41 was converted to PDBQT format by AutoDock Tools 1.5.6 (The Scripps Research Institute, CA, USA) for docking screening. The docking parameters were set as previous study with default values, and the size of grid box was set as 20 Å × 20 Å × 20 Å for encompassing catalytic site. The molecular docking screening was performed by AutoDock Vina v.1.0.2 (The Scripps Research Institute, CA, USA).

2.2. Reagents and Antibodies. 2′,7′-Dichlorodihydrofluorescein diacetate (H_2DCF-DA), pentahydrate (bis-benzimide) (Hoechst 33258), and 3,6-diamino-9-(2-(methoxycarbonyl) phenyl, chloride (Rhodamine 123) were obtained from Invitrogen (Carlsbad, CA, USA). Acetylthiocholine iodide (ATCI), 5′,5-dithio-bis-(2-nitrobenzoate) (DTNB), zinc protoporphyrin IX (ZnPP), H_2O_2, and all other chemicals used in this study were purchased from Sigma (St. Louis, MO, USA). All cell culture reagents were obtained from Invitrogen (Carlsbad, CA, USA). Antibodies against p53, Bax, Bcl-2, caspase-3, and beta-actin were purchased from Cell Signaling Technology (Danvers, MA, USA). Antibody against HO-1 was obtained from Santa Cruz Biotechnology (Santa Cruz, CA, USA). Shikonin, acetylshikonin, beta, beta-dimethylacrylshikonin, isovalerylshikonin, xanthotoxin, phellopterin, imperatorin, and alloisoimperatorin were obtained from Apin Chemicals Ltd (Oxfordshire, UK). Emodin, aloe-emodin, rhein. and chrysophanol were obtained from National Institutes for Food and Drug Control (Beijing, China). The test chemicals were dissolved in distilled water and dimethyl sulfoxide (DMSO); the final concentration of DMSO was less than 0.1%.

2.3. AChE Assay. Candidate phytochemicals dissolved in DMSO were tested for AChE inhibitory activity by the Ellman assay with minor modifications [20]. Ten μL of human recombinant AChE (prepared in-house [20]) and 1 μL of drug were added into 190 μL of PBS buffer (100 mM, pH 7.4) and incubated in a 96-well plate at 37°C for 10 min. Then 25 μL of 12.5 mM ATCI and 25 μL of 10 mM DTNB were premixed and added into each well. After 10 min incubation with the substrate, the optical densities were measured in a 96-well plate reader at 412 nm. The optical density was inversely proportional to the inhibitory activity. By contrast, a blank control without the tested compound was also performed in parallel; the normal hydrolytic rate of the enzyme can be represented by the blank control. Each assay was performed in triplicate.

The percentage inhibitory activities of the various compounds were calculated by comparison with the positive control and the blank control. The formula was shown as follows: percent of inhibitory activity of the compound = (1 − absorbance of sample/absorbance of blank control)/(1 − absorbance of positive control/absorbance of blank control) × 100%. Data analysis was performed with Prism software. Inhibitory effects were expressed as IC_{50} value calculated by regression analysis.

2.4. Cell Cultures. Human neuroblastoma SH-SY5Y cells were from ATCC (Manassas, VA, usa) and maintained in DMEM/F-12 containing 10% FBS and maintained at 37°C with 95% humidified air and 5% CO_2. Rat adrenal medulla pheochromocytoma PC12 cells were from ATCC (Manassas, VA, USA) and maintained in DMEM containing 10% FBS at 37°C with 95% humidified air and 5% CO_2.

2.5. Cell Viability Assay. MTT colorimetric assay was performed to determine the cell viability. Cells were seeded in 96-well plates at a density of 5×10^3 cells/well and treated with test chemicals at desired concentration at 37°C for 12 hours. Subsequently, cells were stimulated with H_2O_2 (500 μM) for 4 hours. After the exposure period, the cells were incubated with 20 μL MTT (5 mg/mL) for 4 h. The cells were eluted with DMSO and quantified with a spectrophotometer (Ultramark Microplate Reader, Bio-Rad) at a wavelength of 590 nm.

2.6. Nuclear Staining with Hoechst 33258. SH-SY5Y cells and PC12 cells (1×10^4 cells/well) in 24-well plates were preincubated with or without test chemicals for 12 hours and subsequently stimulated with H_2O_2 for the 4 hours. The nuclear morphology of apoptotic cells was measured by Hoechst 33258 nuclear staining according to the manufacturer's instructions. The nuclear morphological change was observed under a fluorescence microscope (Nikon Live Cell Imaging System Ti-E, Japan) using excitation/emission of 360/460 nm.

Table 1: Summary of ranking list of molecular docking screen.

Chemical name	Binding affinity	Binding residues (H-bond)	Binding residues (π-π)
Huperzine A	−10.4	Ser125, 203	Trp86, Tyr337
Galantamine	−8.4	Trp86, Tyr337, 124	Trp86, Tyr337
Tacrine	−8.4	Tyr337	Trp86
Emodin	−8	Tyr133, 337, Glu202	Trp86
Aloe-emodin	−8.2	Trp86, Ser125	Tyr337
Chrysophanol	−8		Trp86
Rhein	−7.4	Asp74, Tyr337	Trp86
Xanthotoxin	−8.5	Ser125	Trp86, Tyr337
Phellopterin	−8.5	Tyr337, 124, Ser125	Trp86
Alloisoimperatorin	−9.4	Tyr133, Asn87, Ser125	Trp86
Imperatorin	−8.2	Tyr337, 341, 124, Asp74	Trp86
Shikonin	−9.2	Glu202, Tyr337	Trp86
Acetylshikonin	−8.6	Ser203, Gly121, 122, 126	Trp86, Tyr124
Isovalerylshikonin	−8.1	Gly120, 126, Tyr337, Ser203	Trp86
β,β-Dimethylacrylshikonin	−8.5	Tyr337, Ser203, Gly120, 121, 122	Trp86

2.7. Intracellular Reactive Oxygen Species (ROS) Measurement. The cells were treated with desired concentration of acetylshikonin for 12 hours, and then the cells were stained with H_2DCF-DA (10 μM) for 30 min. After 30 min staining, cells were stimulated with H_2O_2 (500 μM) for 2 h, and the fluorescence intensity of H_2DCF-DA was measured/detected by a fluorescence spectrophotometer (M1000, TECAN, Austria GmbH, Austria) using excitation/emission of 485/530 nm and a fluorescence microscope (Nikon Live Cell Imaging System Ti-E, Japan) using excitation/emission of 490/530 nm, respectively. Fluorescence intensity of each group was normalized to the control group.

2.8. Measurement of Mitochondrial Membrane Potential. The cells were treated with desired concentration of acetylshikonin for 12 hours, and then the cells were stimulated with H_2O_2 (500 μM) for 2 h. Rhodamine 123 (2 μM) was added to cells after the treatment for 30 min at 37°C. Fluorescence intensity of Rhodamine 123 was measured/detected by a fluorescence spectrophotometer (M1000, TECAN, Austria GmbH, Austria) using excitation/emission of 485/530 nm and a fluorescence microscope (Nikon Live Cell Imaging System Ti-E, Japan) and using excitation/emission of 490/530 nm, respectively. Fluorescence intensity of each group was normalized to the control group.

2.9. Western Blot Assay. Proteins in the total cell lysate were separated by 10% SDS polyacrylamide gel electrophoresis and electrotransferred to a polyvinylidene difluoride membrane (Immobilon-P membrane; Millipore, Bedford, MA, USA). After the blot was blocked in a solution of 5% bovine serum albumin, membrane was incubated overnight with primary antibodies against Bcl-2, Bax, Caspase-3, p53, HO-1, or beta-actin followed by incubation with horseradish peroxidase-conjugated secondary antibodies for 1 h. Specific bands were detected with ECL-plus western blotting detection reagent (GE Healthcare Bio-Sciences) and photographed with Fuji-Film LAS-3000 (Fujifilm, Tokyo, Japan).

2.10. Statistics. Statistical significance was determined using the One-Way ANOVA (GraphPad Software, CA, USA). The results are presented as the means ± SEM. The significance was accepted when P value was < 0.05.

3. Results

3.1. Potential AChE Inhibitors from Natural Products Were Identified by Molecular Docking Screen. Using the natural product database and AutoDock vina for screening, we have identified 12 phytochemicals reportedly (emodin, aloe-emodin, chrysophanol, and rhein from anthraquinone fraction in RHEI RADIX ET RHIZOMA; xanthotoxin, phellopterin, alloisoimperatorin, and imperatorin from furanocoumarin fraction in ANGELICAE DAHURICAE RADIX; shikonin, acetylshikonin, isovalerylshikonin, and β,β-dimethylacrylshikonin from naphthoquinone fraction in ARNEBIAE RADIX) which can act as AChEIs. Huperzine A, the positive control, exhibited the highest docking score in the ranking list. It is noted that Trp86 is the key residue interacting with all AChEIs through π-π interaction in docking simulation, which is consistent with the key role of Trp86 in the catalytic pocket of AChE (Table 1) [21]. *In vitro* validation demonstrated that anthraquinones from RHEI RADIX ET RHIZOMA were the strongest AChEIs (Table 2). The inhibition of emodin, aloe-emodin, chrysophanol, and rhein on human AChE showed different degrees of concentration-dependent inhibition. Among these, emodin and aloe-emodin were more potent with IC_{50} 21.80 μM and 26.76 μM, respectively. The other anthraquinones exhibited relatively weak inhibitory effects on AChE activity. Alloisoimperatorin is most potent anti-AChE chemicals with IC_{50} 20.7 μM in furanocoumarin fraction in ANGELICAE DAHURICAE RADIX. In addition, acetylshikonin is the most potent anti-AChE chemicals with IC_{50} 34.6 μM in naphthoquinone fraction in ARNEBIAE RADIX.

3.2. The Effects of H_2O_2 or AChE Inhibitors from Natural Products on Cell Viability in SH-SY5Y or PC12 Cells. H_2O_2-induced cytotoxicity in both SH-SY5Y and PC12 cells was

Table 2: Summary of potential AChE inhibitors from molecular docking screen.

Plant	Classification	Chemical name	Core structure	R1	R2	IC_{50} [μM]
Rhei Radix Et Rhizoma	Anthraquinone	Emodin	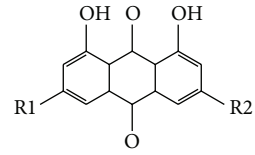	CH_3	OH	21.8
		Aloe-emodin		CH_2OH	H	26.8
		Chrysophanol		H	OH	75.8
		Rhein		COOH	OH	236.6
Angelicae Dahuricae Radix	Furanocoumarin	Xanthotoxin	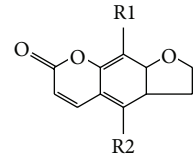	OCH_3	H	132.7
		Phellopterin		$OCH_2CHC(CH_3)_2$	OCH_3	177.4
		Alloisoimperatorin		$CH_2CHC(CH_3)_2$	OH	20.7
		Imperatorin		$OCH_2CHC(CH_3)_2$	H	Undetected
Arnebiae Radix	Naphthoquinone	Shikonin	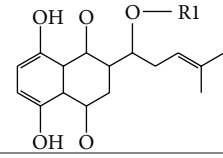	H	—	71.8
		Acetylshikonin		$C(O)CH_3$	—	34.6
		Isovalerylshikonin		$C(O)CH_2CH(CH_3)_2$	—	82.4
		β,β-Dimethylacrylshikonin		$C(O)CHC(CH_3)_2$	—	62.4

treated with various concentrations of H_2O_2 (50–500 μM) for 4 hours, and the subsequent cell viability was measured by MTT assay. As shown in Figures 1(a) and 1(b), H_2O_2 at concentration of 500 μM led to approximately half-maximal cell death (60% cell death in SH-SY5Y cells and 40% cell death in PC12 cells). Therefore, this concentration was selected to evaluate the potential protective effects of AChE inhibitors from natural products on H_2O_2-stimulation oxidative stress and apoptosis in SH-SY5Y and PC12 cells. After pretreatment with test chemicals, the cells were exposed to H_2O_2 for 4 hours and applied to MTT assay. Results showed that H_2O_2-induced cell death was statistically attenuated by seven test chemicals at 10 μM in SH-SY5Y cells (Figure 1(c)). In PC12 cells, five chemicals rescued H_2O_2-induced cell death (Figure 1(d)). Notably, acetylshikonin-treated cells exhibited the highest viability during H_2O_2 stimulation, indicating that acetylshikonin might be the strongest neuroprotective candidate among these potential AChE inhibitors. Thus, study in the latter part will be focused on neuroprotective effects of acetylshikonin on H_2O_2-induced cell apoptosis in both SH-SY5Y and PC12 cells.

3.3. Acetylshikonin Attenuated H_2O_2-Induced Cell Death with Dose-Dependent Manner in SH-SY5Y and PC 12 Cells. H_2O_2 was a strong peroxide and it significantly induced cell death ($P < 0.05$) and caused morphology change, which were dose dependently attenuated by acetylshikonin (1–10 μM) in both SH-SY5Y (Figures 2(a) and 2(c)) and PC12 (Figures 2(b) and 2(d)) cells. Meanwhile, the cytotoxic potential of acetylshikonin was also tested at 10 μM. Cytotoxicity of acetylshikonin was not observed at used dosage in MTT assay and no morphological change was found. To evaluate the protective effects of acetylshikonin on H_2O_2-induced apoptosis, the nuclear morphological observation was measured by Hoechst 33258 staining. As shown in Figures 2(e) and 2(f), H_2O_2 stimulation resulted in cell shrinkage and nuclear condensation, which were indicated by red arrows. However, this morphological change was dramatically ameliorated by acetylshikonin in both SH-SY5Y and PC12 cells.

3.4. Acetylshikonin Attenuated H_2O_2-Induced ROS Generation and Mitochondrial Membrane Potential Loss with Dose-Dependent Manner in SH-SY5Y and PC 12 Cells. As shown in Figures 3(a) and 3(b), H_2O_2-treated cells exhibited bright green fluorescence while the fluorescence did not appear in the control cells, indicating that total intracellular ROS was significantly increased after H_2O_2 stimulation. In contrast, acetylshikonin reduced H_2O_2-induced bright green fluorescence at 5 and 10 μM, representing that the ROS generation was also diminished. The quantitative analysis was consistent with microscopic observation; H_2O_2-induced ROS generation was statistically declined by pretreatment with acetylshikonin in a dose-dependent manner (Figures 3(c) and 3(d)).

Mitochondrial depolarization is the critical event in oxidant-induced apoptosis as stated before [22], and the effect of acetylshikonin on H_2O_2-induced mitochondrial membrane potential (MMPs) loss was detected by Rhodamine 123 staining. As shown in Figures 3(e) and 3(f) of representative pictures, the control cells exhibited bright green fluorescence, whereas stimulation of H_2O_2 cells only showed blank background, reflecting the loss of mitochondrial membrane potentials. Notably, pretreatment with acetylshikonin significantly attenuated the H_2O_2-induced MMPs loss. For quantitative analysis, the MMPs were further detected by fluorescence spectrometer. As shown in Figures 3(g) and 3(h), H_2O_2 stimulation statistically reduced MMPs, which was rescued by acetylshikonin in a dose-dependent manner in both SH-SY5Y and PC12 cells.

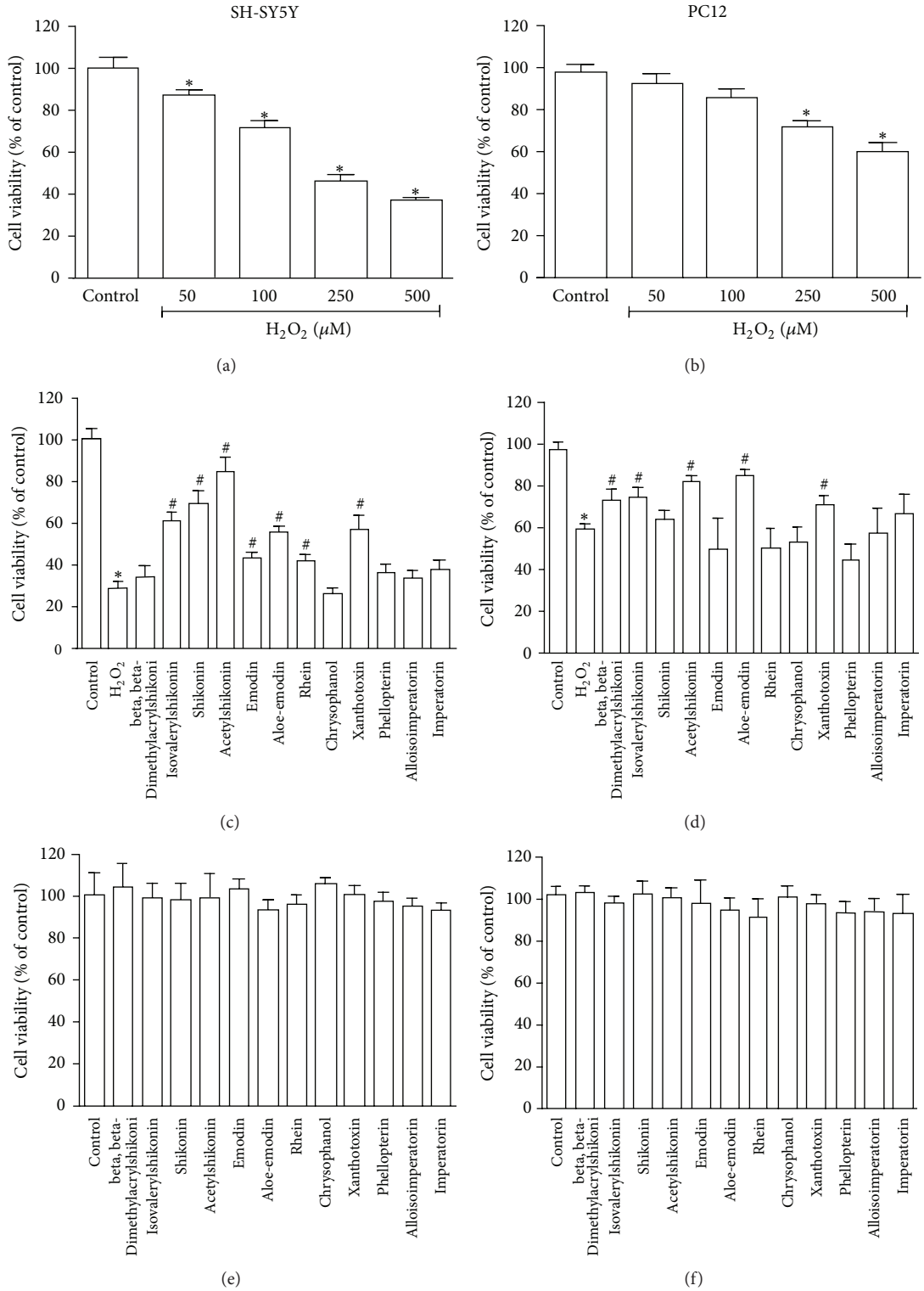

Figure 1: Potential AChE inhibitors of natural products attenuated H_2O_2-induced cell death in both SH-SY5Y and PC12 cells. SH-SY5Y (a) or PC12 (b) cells were cultured with desired concentration of H_2O_2 for 4 hours; the cell viability was detected by MTT. Data shown are means ± SEM of results from independent experiments in triplicate. $^*P < 0.05$ compared with control cells. SH-SY5Y (c) or PC12 (d) cells were incubated with different potential AChE inhibitors (10 μM) for 12 hours and then stimulated with H_2O_2 (500 μM) for 4 hours, and the viability was detected by MTT. Data shown are means ± SEM of results from independent experiments in triplicate. $^*P < 0.05$ compared with control cells; $^\#P < 0.05$ compared with H_2O_2-stimulated cells. For cytotoxicity test, SH-SY5Y (e) or PC12 (f) cells were incubated with different potential AChE inhibitors (10 μM) for 12 hours, and the viability was detected by MTT. Data shown are means ± SEM of results from independent experiments in triplicate. $^*P < 0.05$ compared with control cells.

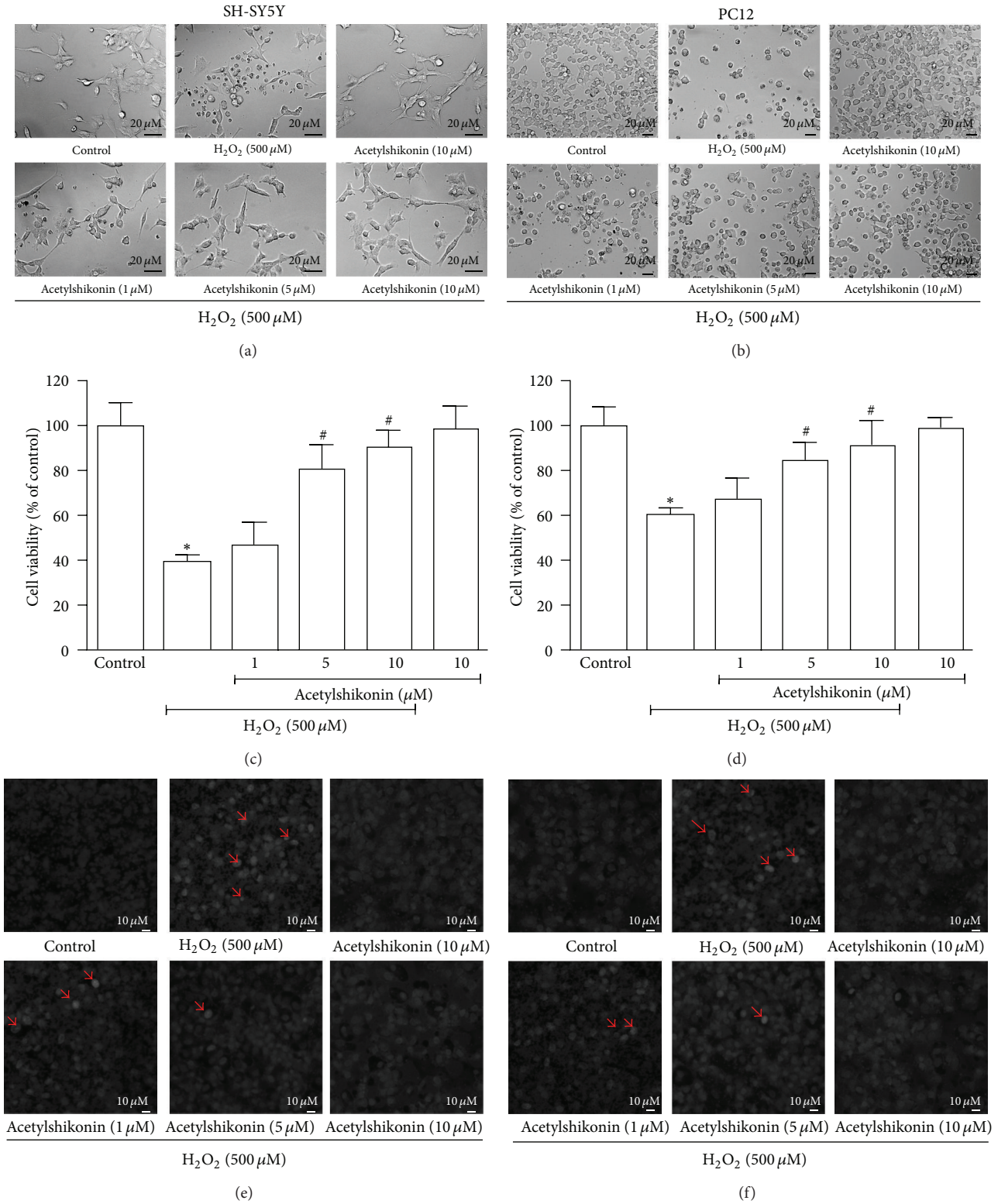

FIGURE 2: Acetylshikonin attenuated H_2O_2-induced cell death and apoptosis in both SH-SY5Y and PC12 cells with dose-dependent manner. SH-SY5Y or PC12 cells were incubated with desired concentration of acetylshikonin for 12 hours and then stimulated with H_2O_2 (500 μM) for 4 hours, and the change of cell morphology ((a) SH-SY5Y; (b) PC12), cell viability ((c) SH-SY5Y; (d) PC12), and change of nuclear morphology ((e), SH-SY5Y; (f), PC12) were measured, respectively. Data shown are means ± SEM of results from independent experiments in triplicate. $^{*}P < 0.05$ compared with control cells; $^{\#}P < 0.05$ compared with H_2O_2-stimulated cells.

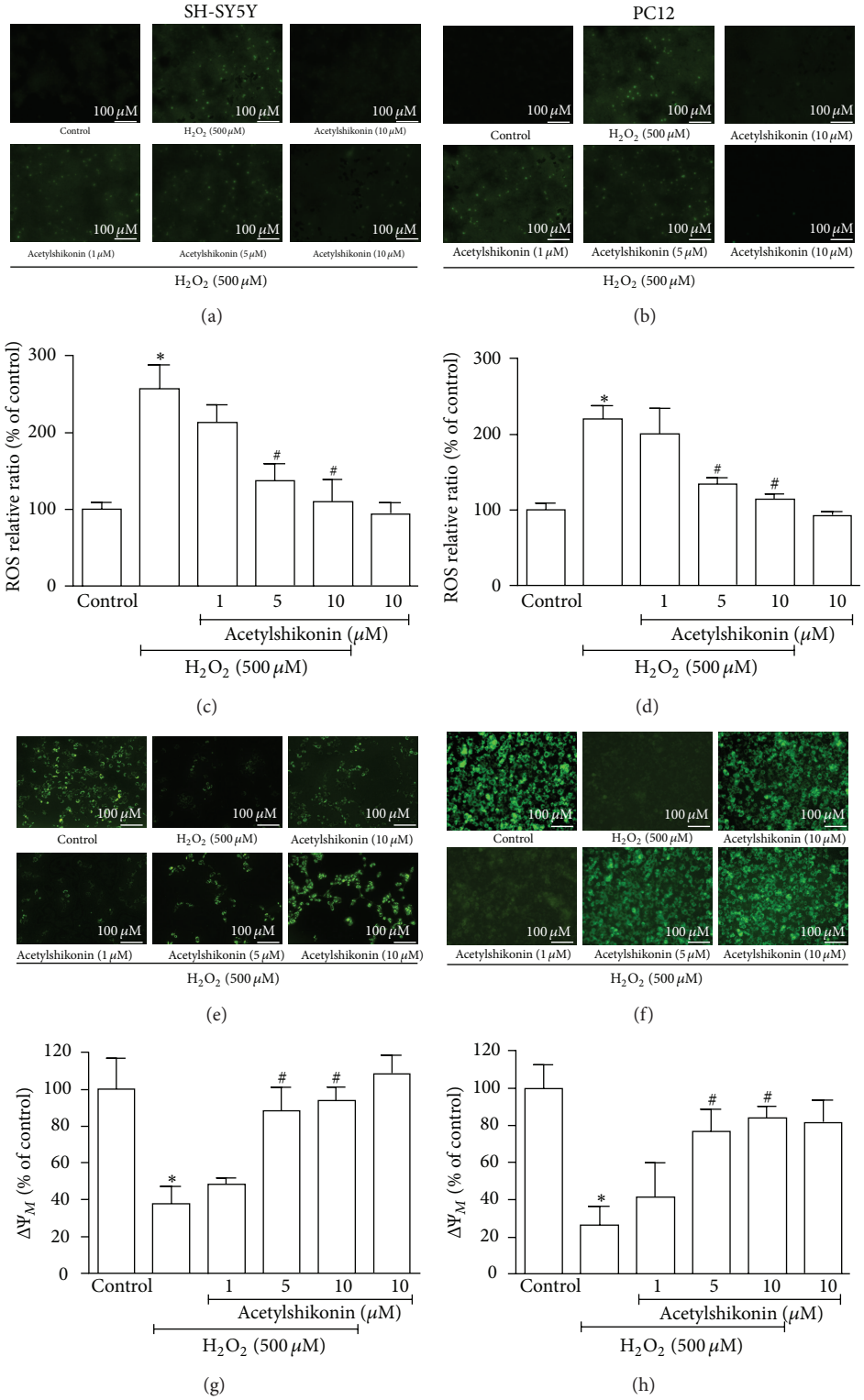

FIGURE 3: Acetylshikonin attenuated H_2O_2-induced ROS generation and mitochondrial membrane potential loss in both SH-SY5Y and PC12 cells with dose-dependent manner. The cells were treated with desired concentration of acetylshikonin for 12 hours and then stimulated with H_2O_2 (500 μM) for 2 hours, and the ROS generation and mitochondrial membrane potential loss were detected by H_2DCF-DA and Rhodamine 123 staining, respectively. Representative photograph of ROS generation in SH-SY5Y (a) or PC12 (b) cells was taken by fluorescence microscope; the quantitative analysis of ROS generation in SH-SY5Y (c) or PC12 (d) cells was measured by fluorescence spectrophotometer. Representative photograph of mitochondrial membrane potential loss in SH-SY5Y (e) or PC12 (f) cells was taken by fluorescence microscope; the quantitative analysis of mitochondrial membrane potential loss in SH-SY5Y (g) or PC12 (h) cells was measured by fluorescence spectrophotometer. Data shown are means ± SEM of results from independent experiments in triplicate. $^*P < 0.05$ compared with control cells; $^\#P < 0.05$ compared with H_2O_2-stimulated cells.

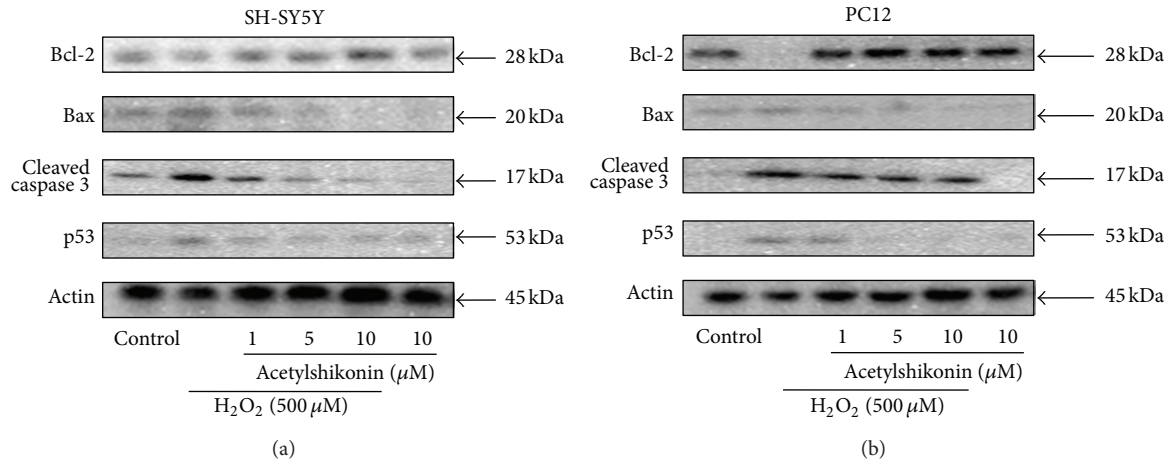

Figure 4: Acetylshikonin modulated H_2O_2-induced apoptosis-related protein expression in both SH-SY5Y (a) and PC12 (b) cells. The cells were treated with desired concentration of acetylshikonin for 12 hours and then stimulated with H_2O_2 (500 μM) for 1 hour, and the apoptosis-related protein expression was detected by western blot.

3.5. Acetylshikonin Modulated H_2O_2-Induced Apoptosis-Related Protein Expression in Both SH-SY5Y and PC12 Cells. To further explore the detailed neuroprotective mechanisms of acetylshikonin on H_2O_2-induced apoptosis, the possible related proteins were measured by western blot. As shown in Figures 4(a) and 4(b), H_2O_2-stimulation decreased Bcl-2 expression level, while it increased Bax and p53 expression level. In contrast, acetylshikonin concentration dependently led to increased expression of Bcl-2 as well as decreased Bax and p53 expression in H_2O_2-induced SH-SY5Y and PC12 cells. Caspase cascade has been identified as the critical executor for apoptosis. In H_2O_2-induced cells, the decreased caspase-3 and the increased cleaved caspase-3 were observed, which was rescued by acetylshikonin in a dose-dependent manner.

3.6. Upregulation of Heme Oxygenase-1 (HO-1) by Acetylshikonin Played a Key Role of Its Antiapoptotic Activity in H_2O_2-Induced SH-SY5Y Cells. It has been widely accepted that upregulation of Heme oxygenase 1 (HO-1) expression protects cells against the oxidative-stress cellular injury [23]. Western blot results showed that HO-1 expression was increased after acetylshikonin treatment in SH-SY5Y cells. However, acetylshikonin treatment has no impact on the level of HO-1 expression in PC12 cells (Figure 5(a)). To further confirm the role of HO-1 in antiapoptotic effects of acetylshikonin, we cotreated acetylshikonin with ZnPP (HO-1 inhibitors, 10 μM) in H_2O_2-induced cells. Cell viability results demonstrated that ZnPP reversed the protective effects of acetylshikonin on H_2O_2-induced cell death in SH-SY5Y cells (Figure 5(b), right panel). However, these reversed effects of ZnPP were not observed in PC12 cells (Figure 5(b), left panel), and they were consistent with Western blot results. Therefore, HO-1 induction by acetylshikonin was critical against the oxidative-stress induced cell apoptosis in SH-SY5Y cells. In contrast, acetylshikonin was not able to upregulate HO-1 expression in PC12 cells, indicating that antiapoptotic activity of acetylshikonin in oxidative stress condition might be mediated through other antioxidant pathway in PC12 cells.

4. Discussion

With the rapid advances in personal computing power, virtual drug screening is popular and prominent. While there are numerous databases for synthetic compounds, there are only a few natural product databases that are specifically for *in silico* docking study. To facilitate virtual docking on natural compounds, we have established our in-house natural products database, which contains approximately 8,000 naturally occurring chemicals so far. Based on docking screening, top chemicals in ranking list were selected for the following analysis. The classic analysis, which has been widely accepted in most synthesis chemical virtual screen, is to rank the binding affinity and then choose the high ranking chemicals for further *in vitro* validation. Natural products, unlike synthesis chemicals, come from natural sources, such as plants, fungus, animals, and minerals. This characteristic might lead to a possibility that the high ranking chemicals have derivatives in the same species or genus. The collection of this kind of derivatives has been identified as bioactive fraction in complementary medicine. Therefore, we selected these top ranking derivatives for further validation. Here we identified three bioactive fractions as AChEIs, including anthraquinone fraction in RHEI RADIX ET RHIZOMA, furanocoumarin fraction in ANGELICAE DAHURICAE RADIX, and naphthoquinone fraction in ARNEBIAE RADIX. In this way, our database is not only suitable to screen pure compounds but also helpful to identify bioactive fractions.

Ellman assay results showed that anthraquinones from RHEI RADIX ET RHIZOMA were the strongest AChEIs among these potential chemicals. In contrast, naphthoquinone from ARNEBIAE RADIX exhibited most potent attenuation activity against H_2O_2-induced apoptosis in both

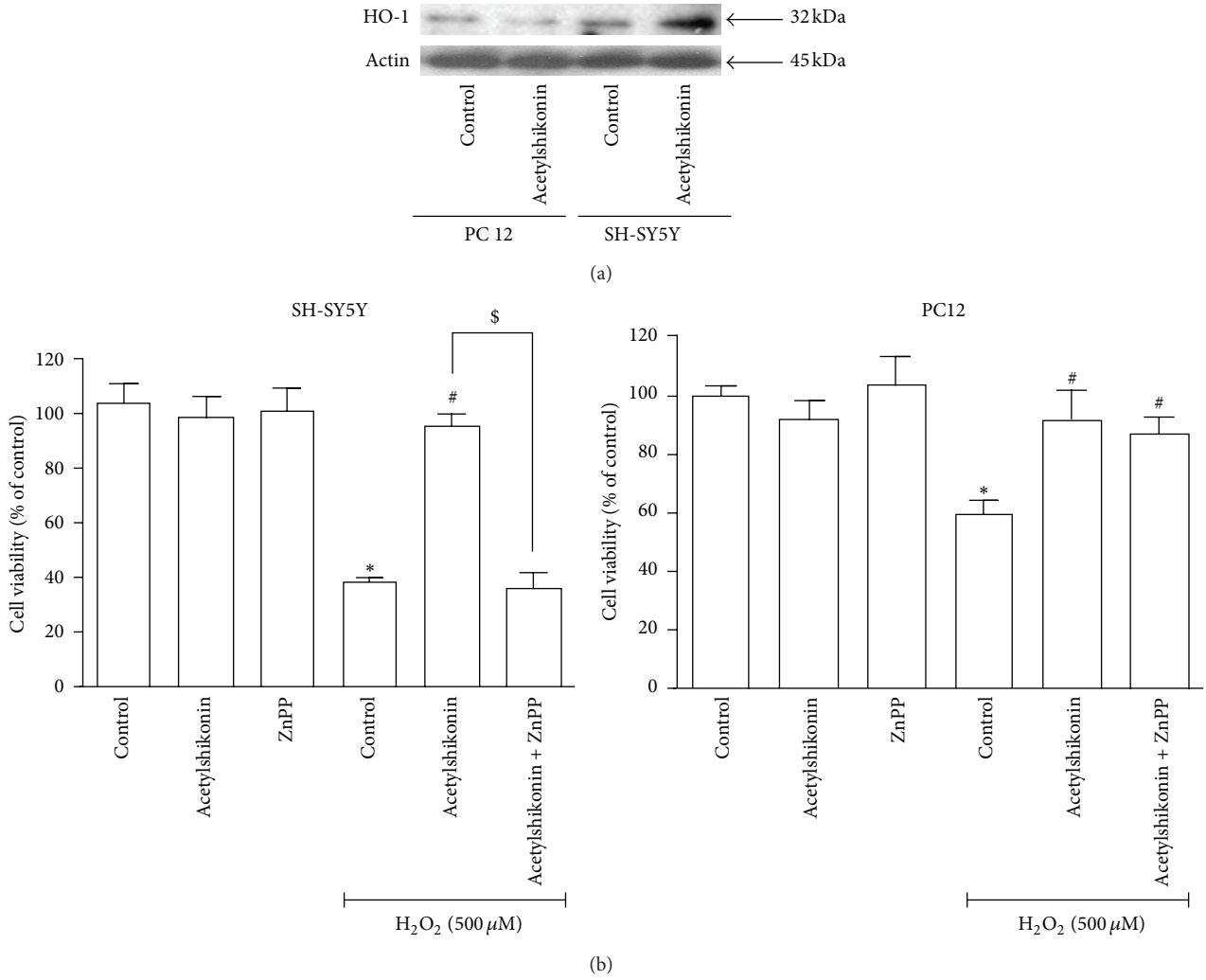

Figure 5: Antiapoptotic activity of acetylshikonin in H_2O_2 stimulation was related with induction of HO-1 expression in SH-SY5Y cells. (a) Both SH-SY5Y and PC12 cells were treated with desired concentration of acetylshikonin for 12 hours and then stimulated with H_2O_2 (500 μM) for 1 hours, and HO-1 protein expression was detected by western blot. (b) SH-SY5Y or PC12 cells were pretreated with HO-1 inhibitor (ZnPP, 10 μM) for 2 hours, then incubated with desired concentration of acetylshikonin for 12 hours, further stimulated with H_2O_2 (500 μM) for 4 hours, and the cell viability (right panel: SH-SY5Y; left panel: PC12) was measured by MTT. Data shown are means ± SEM of results from independent experiments in triplicate. $^{*}P < 0.05$ compared with control cells; $^{\#}P < 0.05$ compared with H_2O_2-stimulated cells; $^{\$}P < 0.05$ compared with acetylshikonin-treated cells.

SH-SY5Y and PC12 cells. Particularly, acetylshikonin, one naphthoquinone from ARNEBIAE RADIX, not only significantly inhibited AChE activity but also dramatically rescued oxidative stress-induced apoptosis in both SH-SY5Y and PC12 cells.

In addition to the role on the inhibition of Ach hydrolysis, there is evidence that all the FDA-approved AChEIs (tacrine, donepezil, rivastigmine, and galantamine) are neuroprotective agents. Three AChE inhibitors (tacrine, galanthamine, and donepezil) increased the activities of catalase (CAT) and glutathion peroxidase (GSH-Px) and protected PC12 cells from apoptosis generated by hydrogen peroxide. Donepezil also protected rat septal neurons from the toxicity induced by amyloid, while tacrine significantly attenuated hydrogen peroxide-induced injury and reversed hydrogen peroxide-induced overexpression of bax and p53 in PC12 cells [24–26].

Acetylshikonin, the major active components of ARNEBIAE RADIX, exhibit many biological effects including anticancer [27], antioxidant [28], and antiobesity [29]. Recent study also revealed that acetylshikonin might increase antioxidant enzyme activity and nitric oxide levels in ethanol-induced ulcer rat models [28]. Shikonin, the analogs of acetylshikonin, has been reported to protect PC12 against 6-hydroxydopamine-mediated neurotoxicity [30]. However, reports on the antioxidative stress effects of acetylshikonin on neuronal cells are limited.

Mitochondria have been identified as a key site of cell apoptosis and death. The dysfunction of mitochondria resulted in ROS generation as well as mitochondria membrane potential loss. The cleaved caspase-3 and PARP were upregulated by excessive ROS and mitochondria membrane potential loss, which subsequently triggered cell apoptosis

[31, 32]. Present study demonstrated that acetylshikonin rescued H_2O_2-mediated ROS production, $\Delta\Psi m$ loss, and upregulation of cleaved caspase-3. Furthermore, H_2O_2 stimulation resulted in upregulation of Bax expression and downregulation of Bcl-2 expression, therefore leading to the decline of Bcl-2/Bax ratio that served as another important indicator of mitochondrial dysfunction [33]. Western blot results confirmed that acetylshikonin increased the Bcl-2/Bax ratio by upregulation of Bcl-2 and downregulation of Bax, indicating that H_2O_2-induced mitochondrial dysfunction might be attenuated by acetylshikonin. In addition, p53, another proapoptotic factor [34], is essential for H_2O_2-induced apoptosis in glioma cells. A high level of p53 expression was observed in H_2O_2-induced apoptosis; however, this apoptosis was significantly reduced by antisense p53 oligonucleotide [35]. The increased p53 has been inhibited by acetylshikonin. Together, acetylshikonin has been reported to protect mitochondrial function from oxidative stress in both SH-SY5Y and PC12 cells.

Upregulation of HO-1 is the major approach to prevent H_2O_2-induced cells from apoptosis and cell death [36]. For further mechanistic exploration, the expression level of HO-1 was detected by western blot. Results showed the upregulation of HO-1 by acetylshikonin was observed in SH-SY5Y cells but not in PC12 cells. In cell proliferation assay, the specific antagonist of HO-1 ZnPP abolished the protective effects of acetylshikonin in SH-SY5Y cells. Consistent with western blot results, ZnPP cannot exert its effect on the neuroprotective activity of acetylshikonin in PC12 cells. Notably, shikonin, the analogs of acetylshikonin, has been reported to induce the Nrf2-ARE system that might upregulate the transcription of HO-1 genes [37]. Further systematic studies are needed to investigate whether upregulation of HO-1 effect by acetylshikonin is mediated by Nrf2-ARE pathway.

5. Conclusion

Together, we first reported that acetylshikonin, a novel AChEI, exhibited antiapoptotic activity through an HO-1 dependent mechanism in SH-SY5Y cells. Therefore, the findings suggested that acetylshikonin might provide potential benefits for Alzheimer's diseases treatment.

Acknowledgments

This work was partially supported by GRF (ref. no. 474808) and RFCID Grants (ref. no. 08070152) to David Chi-Cheong Wan.

References

[1] F. Mangialasche, A. Solomon, B. Winblad, P. Mecocci, and M. Kivipelto, "Alzheimer's disease: clinical trials and drug development," *The Lancet Neurology*, vol. 9, no. 7, pp. 702–716, 2010.

[2] L. M. Ittner and J. Götz, "Amyloid-β and tau—a toxic pas de deux in Alzheimer's disease," *Nature Reviews Neuroscience*, vol. 12, no. 2, pp. 67–72, 2011.

[3] H.C. Huang and Z.F. Jiang, "Accumulated amyloid-β peptide and hyperphosphorylated tau protein: relationship and links in Alzheimer's disease," *Journal of Alzheimer's Disease*, vol. 16, no. 1, pp. 15–27, 2009.

[4] E. Giacobini, "Invited review. Cholinesterase inhibitors for Alzheimer's disease therapy: from tacrine to future applications," *Neurochemistry International*, vol. 32, no. 5-6, pp. 413–419, 1998.

[5] N. Akula, L. Lecanu, J. Greeson, and V. Papadopoulos, "3D QSAR studies of AChE inhibitors based on molecular docking scores and CoMFA," *Bioorganic and Medicinal Chemistry Letters*, vol. 16, no. 24, pp. 6277–6280, 2006.

[6] M. Y. Mizutani and A. Itai, "Efficient method for high-throughput virtual screening based on flexible docking: discovery of novel acetylcholinesterase inhibitors," *Journal of Medicinal Chemistry*, vol. 47, no. 20, pp. 4818–4828, 2004.

[7] P. Kapková, N. Stiefl, U. Sürig, B. Engels, K. Baumann, and U. Holzgrabe, "Synthesis, biological activity, and docking studies of new acetylcholinesterase inhibitors of the bispyridinium type," *Archiv der Pharmazie*, vol. 336, no. 11, pp. 523–540, 2003.

[8] A. Klugman, "Antioxidant enzymatic activities in Alzheimer's disease: the relationship to acetylcholinesterase inhibitors," *Journal of Alzheimer's Disease*, vol. 30, pp. 467–474, 2012.

[9] R. Wang, J. Zhou, and X. C. Tang, "Tacrine attenuates hydrogen peroxide-induced apoptosis by regulating expression of apoptosis-related genes in rat PC12 cells," *Molecular Brain Research*, vol. 107, no. 1, pp. 1–8, 2002.

[10] R. Wang, Q. X. Xiao, and C. T. Xi, "Huperzine a attenuates hydrogen peroxide-induced apoptosis by regulating expression of apoptosis-related genes in rat PC 12 cells," *NeuroReport*, vol. 12, no. 12, pp. 2629–2634, 2001.

[11] C. McInnes, "Virtual screening strategies in drug discovery," *Current Opinion in Chemical Biology*, vol. 11, no. 5, pp. 494–502, 2007.

[12] J. Q. Araújo, J. A. Lima, A. D. C. Pinto, R. B. De Alencastro, and M. G. Albuquerque, "Docking of the alkaloid geissospermine into acetylcholinesterase: a natural scaffold targeting the treatment of Alzheimer's disease," *Journal of Molecular Modeling*, vol. 17, no. 6, pp. 1401–1412, 2011.

[13] T. Frembgen-Kesner and A. H. Elcock, "Computational sampling of a cryptic drug binding site in a protein receptor: explicit solvent molecular dynamics and inhibitor docking to p38 MAP Kinase," *Journal of Molecular Biology*, vol. 359, no. 1, pp. 202–214, 2006.

[14] P. Jia, R. Sheng, J. Zhang et al., "Design, synthesis and evaluation of galanthamine derivatives as acetylcholinesterase inhibitors," *European Journal of Medicinal Chemistry*, vol. 44, no. 2, pp. 772–784, 2009.

[15] D. H. Shi, W. Huang, C. Li, L. T. Wang, and S. F. Wang, "Synthesis, biological evaluation and molecular modeling of aloe-emodin derivatives as new acetylcholinesterase inhibitors," *Bioorganic & Medicinal Chemistry*, vol. 21, no. 5, pp. 1064–1073, 2013.

[16] S. A. Wildman, X. Zheng, D. Sept, J. T. Auletta, T. L. Rosenberry, and G. R. Marshall, "Drug-like leads for steric discrimination between substrate and inhibitors of human acetylcholinesterase," *Chemical Biology and Drug Design*, vol. 78, no. 4, pp. 495–504, 2011.

[17] K. K. Wong, J. C. K. Ngo, S. Liu et al., "Interaction study of two diterpenes, cryptotanshinone and dihydrotanshinone, to human acetylcholinesterase and butyrylcholinesterase by

molecular docking and kinetic analysis," *Chemico-Biological Interactions*, vol. 187, no. 1–3, pp. 335–339, 2010.

[18] Z.U. Zaheer-ul-Haq, S. A. Halim, R. Uddin, and J. D. Madura, "Benchmarking docking and scoring protocol for the identification of potential acetylcholinesterase inhibitors," *Journal of Molecular Graphics and Modelling*, vol. 28, no. 8, pp. 870–882, 2010.

[19] J. Egea, M. D. Martín-De-Saavedra, E. Parada et al., "Galantamine elicits neuroprotection by inhibiting iNOS, NADPH oxidase and ROS in hippocampal slices stressed with anoxia/reoxygenation," *Neuropharmacology*, vol. 62, no. 2, pp. 1082–1090, 2012.

[20] S. Li, D. T. M. Ip, H. Q. Lin et al., "High-level expression of functional recombinant human butyrylcholinesterase in silkworm larvae by Bac-to-Bac system," *Chemico-Biological Interactions*, vol. 187, no. 1–3, pp. 101–105, 2010.

[21] A. Ordentlich, D. Barak, C. Kronman et al., "Contribution of aromatic moieties of tyrosine 133 and of the anionic subsite tryptophan 86 to catalytic efficiency and allosteric modulation of acetylcholinesterase," *Journal of Biological Chemistry*, vol. 270, no. 5, pp. 2082–2091, 1995.

[22] K. Zhao, G. Luo, S. Giannelli, and H. H. Szeto, "Mitochondria-targeted peptide prevents mitochondrial depolarization and apoptosis induced by tert-butyl hydroperoxide in neuronal cell lines," *Biochemical Pharmacology*, vol. 70, no. 12, pp. 1796–1806, 2005.

[23] R. Motterlini, R. Foresti, R. Bassi, and C. J. Green, "Curcumin, an antioxidant and anti-inflammatory agent, induces heme oxygenase-1 and protects endothelial cells against oxidative stress," *Free Radical Biology and Medicine*, vol. 28, no. 8, pp. 1303–1312, 2000.

[24] M. Kimura, S. Akasofu, H. Ogura, and K. Sawada, "Protective effect of donepezil against Aβ(1-40) neurotoxicity in rat septal neurons," *Brain Research*, vol. 1047, no. 1, pp. 72–84, 2005.

[25] H. Y. Zhang and X. C. Tang, "Huperzine B, a novel acetylcholinesterase inhibitor, attenuates hydrogen peroxide induced injury in PC12 cells," *Neuroscience Letters*, vol. 292, no. 1, pp. 41–44, 2000.

[26] R. Wang, J. Zhou, and X. C. Tang, "Tacrine attenuates hydrogen peroxide-induced apoptosis by regulating expression of apoptosis-related genes in rat PC12 cells," *Molecular Brain Research*, vol. 107, no. 1, pp. 1–8, 2002.

[27] J. Liu, W. Zhou, S.-S. Li et al., "Modulation of orphan nuclear receptor Nur77-mediated apoptotic pathway by acetylshikonin and analogues," *Cancer Research*, vol. 68, no. 21, pp. 8871–8880, 2008.

[28] T. Aysun, A. Fatih, A. Hülya, S. Halis, Ö. Ufuk, and E. Havva, "The effects of acetyl shikonin isolated from onosma armeniacum on oxidative stress in ethanol-induced ulcer model of rats," *Turkish Journal of Medical Sciences*, vol. 43, pp. 315–320, 2013.

[29] S. Y. Gwon, J. Y. Ahn, C. H. Chung, B. Moon, and T. Y. Ha, "Lithospermum erythrorhizon suppresses high-fat diet-induced obesity, and acetylshikonin, a main compound of Lithospermum erythrorhizon, inhibits adipocyte differentiation," *Journal of Agricultural and Food Chemistry*, vol. 60, no. 36, pp. 9089–9096, 2012.

[30] E. Esmaeilzadeh, M. Gardaneh, E. Gharib, and F. Sabouni, "Shikonin protects dopaminergic cell line PC12 against 6-Hydroxydopamine-Mediated neurotoxicity Via both Glutathione-Dependent and independent pathways and by inhibiting apoptosis," *Neurochem Research*, vol. 38, no. 8, pp. 1590–1604, 2013.

[31] B. Liu, Z. Jian, Q. Li et al., "Baicalein protects human melanocytes from H_2O_2-induced apoptosis via inhibiting mitochondria-dependent caspase activation and the p38 MAPK pathway," *Free Radical Biology and Medicine*, vol. 53, no. 2, pp. 183–193, 2012.

[32] A. Das, N. L. Banik, and S. K. Ray, "Mechanism of apoptosis with the involvement of calpain and caspase cascades in human malignant neuroblastoma SH-SY5Y cells exposed to flavonoids," *International Journal of Cancer*, vol. 119, no. 11, pp. 2575–2585, 2006.

[33] L. L. Pan, X. H. Liu, Y. L. Jia et al., "A novel compound derived from danshensu inhibits apoptosis via upregulation of heme oxygenase-1 expression in SH-SY5Y cells," *Biochimica et Biophysica Acta*, vol. 1830, no. 4, pp. 2861–2871, 2013.

[34] Y. Kitamura, T. Ota, Y. Matsuoka et al., "Hydrogen peroxide-induced apoptosis mediated by p53 protein in glial cells," *Glia*, vol. 25, no. 2, pp. 154–164, 1999.

[35] K. Datta, P. Babbar, T. Srivastava, S. Sinha, and P. Chattopadhyay, "p53 dependent apoptosis in glioma cell lines in response to hydrogen peroxide induced oxidative stress," *International Journal of Biochemistry and Cell Biology*, vol. 34, no. 2, pp. 148–157, 2002.

[36] F. Zhang, S. Wang, M. Zhang et al., "Pharmacological induction of heme oxygenase-1 by a triterpenoid protects neurons against ischemic injury," *Stroke*, vol. 43, no. 5, pp. 1390–1397, 2012.

[37] K. N. Nam, M. S. Son, J. H. Park, and E. H. Lee, "Shikonins attenuate microglial inflammatory responses by inhibition of ERK, Akt, and NF-κB: neuroprotective implications," *Neuropharmacology*, vol. 55, no. 5, pp. 819–825, 2008.

Hindawi Publishing Corporation
Evidence-Based Complementary and Alternative Medicine
Volume 2013, Article ID 731385, 9 pages
http://dx.doi.org/10.1155/2013/731385

Research Article

Kai-Xin-San, a Chinese Herbal Decoction Containing Ginseng Radix et Rhizoma, Polygalae Radix, Acori Tatarinowii Rhizoma, and Poria, Stimulates the Expression and Secretion of Neurotrophic Factors in Cultured Astrocytes

Kevin Yue Zhu,[1,2] Sherry Li Xu,[1] Roy Chi-Yan Choi,[1] Artemis Lu Yan,[1] Tina Ting-Xia Dong,[1] and Karl Wah-Keung Tsim[1]

[1] *Division of Life Science, Center for Chinese Medicine and State Key Laboratory of Molecular Neuroscience, The Hong Kong University of Science and Technology, Clear Water Bay Road, Hong Kong*
[2] *Jiangsu Key Laboratory for High Technology Research of TCM Formulae and Jiangsu Collaborative Innovation Center of Chinese Medicinal Resources Industrialization, Nanjing University of Chinese Medicine, Nanjing, China*

Correspondence should be addressed to Karl Wah-Keung Tsim; botsim@ust.hk

Received 7 June 2013; Revised 16 August 2013; Accepted 21 August 2013

Academic Editor: Paul Siu-Po Ip

Kai-xin-san (KXS), a Chinese herbal decoction prescribed by Sun Simiao in *Beiji Qianjin Yaofang* about 1400 years ago, contains Ginseng Radix et Rhizoma, Polygalae Radix, Acori Tatarinowii Rhizoma, and Poria. In China, KXS has been used to treat stress-related psychiatric diseases with the symptoms of depression and forgetfulness. Although animal study has supported the antidepression function of KXS, the mechanism in cellular level is still unknown. Here, a chemically standardized water extract of KXS was applied onto cultured astrocytes in exploring the action mechanisms of KXS treatment, which significantly stimulated the expression and secretion of neurotrophic factors, including NGF, BDNF, and GDNF, in a dose-dependent manner: the stimulation was both in mRNA and protein levels. In addition, the water extracts of four individual herbs did not significantly stimulate the expression of neurotrophic factors, which could explain the optimized effect of KXS in a herbal decoction. The KXS-induced expression of neurotrophic factors did not depend on signaling mediated by estrogen receptor or protein kinase. The results suggested that the antidepressant-like action of KXS might be mediated by an increase of expression of neurotrophic factors in astrocytes, which fully supported the clinical usage of this decoction.

1. Introduction

Due to the fast speed of our daily life, more and more people are suffering from a depressive episode featured with these symptoms: (i) mood disturbance: anhedonia (loss of interest and pleasure), persistent depression, feeling helpless, or experiencing excessive guilt; (ii) cognitive disturbance: loss of memory and difficulty in concentrating; (iii) behavior disturbance: difficult in sleeping, loss of appetite or overeating, agitation, and suicidal tendency. If these symptoms occur together and last for more than two weeks without significant improvement, the result of major depression disorder (i.e., depression) will be diagnosed [1]. Now, depression has become one of the common psychiatric disorders, having the incidence of 15% of the total population and perhaps higher for women at 25% [2].

The deficiency of neurotransmitters, for example, norepinepherine, dopamine, and serotonin in brain, has long been regarded as the major cause of depression. Thus, all of the antidepression drugs available on the market are targeted on the restoration of decreased levels of neurotransmitters in synaptic cleft or in depressive brain by inhibiting the reuptake and degradation of neurotransmitters. However, 30%–40% of patients failed to respond to an initial 4–6-week treatment with an antidepression drug. Based on these phenomena, neurotrophic factor theory has been proposed [3]. Neurotrophic factors, including nerve growth factor (NGF), brain derived neurotrophic factor (BDNF),

glial derived neurotrophic factor (GDNF), neurotrophin 3 (NT3), neurotrophin 4/5 (NT4/5) secreted from astrocytes, or target tissues, play a major role in neuron survival, as well as the synapse formation [4, 5]. Low level of BDNF had been discovered clinically in hippocampus and prefrontal cortex of depressive patients [6, 7]. Postmortem analyses of brain tissues from depressive patients showed a reduction of BDNF in brain and serum [8, 9]. On the other hand, brain infusion of BDNF produced antidepressant-like action in animals [10], as well as for NGF [11]. Therefore, the newly developed antidepression drugs should be designed aiming at multitargets, instead of a single neurotransmitter target.

Traditional Chinese medicine (TCM) offers a possible therapy for the treatment of depression, and a herbal decoction named Kai-Xin-San (KXS) is the most popular one. The first description of KXS is recorded in *Beiji Qianjin Yaofang* (*Thousand Formulae for Emergency*) written by Sun Simiao in Tang Dynasty (i.e., 652 A.D.). This herbal formula composes of four herbs: Ginseng Radix et Rhizoma (root and rhizome of *Panax ginseng* C. A. Mey.), Polygalae Radix (root of *Polygala tenuifolia* Wild.), Acori Tatarinowii Rhizoma (rhizome of *Acorus tatarinowii* Schott), and Poria (sclerotium of *Poria cocos* (Schw.) Wolf).Interestingly, at least three KXS formulae having a variation of herb ratio were described in ancient books, and all of them are commonly used clinically. In our previous study, we have demonstrated that KXS relieved depression-like symptoms on a chronic mild stress (CMS) induced depressive rat model by increasing the amounts of neurotransmitters and neurotrophic factors in the brain [12]. Here, we aimed to explore the mechanism of KXS in regulating neurotrophic factors in cultured astrocytes. In addition, the roles of different formulations of KXS and individual herb in the expression of neurotrophic factors were elucidated.

2. Materials and Methods

2.1. Tissue Culture. Astrocytes from postnatal SD rat at day 1 were isolated and cultured. The cortex was dissected in Hank's Balanced Salt Solution without Ca^{2+} and Mg^{2+} (Sigma-Aldrich, St. Louis, MO). After being trypsinized for 15 min, the cortex was washed with culture medium and triturated several times. The culture medium was minimum essential medium (MEM) supplemented with 10% horse serum, 100 U/mL penicillin, and 100 μg/mL streptomycin. All culture reagents were purchased from Invitrogen Technologies (Carlsbad, CA). The cells were centrifuged at 250 ×g for 5 min. The cell pellet was suspended in the culture medium. The cells were seeded on plastic culture plates with the density of 2×10^4 cell/cm^2 and incubated at 37°C in 95% air, 5% CO_2. The culture medium was changed twice a week. Each time, the culture was pipetted up and down gently to remove loosely attached oligodendrocytes, microglia, and neurons.

2.2. Immunocytofluorescent Staining. Cultured astrocytes were grown on glass cover slip and fixed with 4% paraformaldehyde (PFA) in PBS for 15 min, followed by 50 mM ammonium chloride (NH_4Cl) treatment for 25 min. Cultures were permeablized by 0.1% Triton X-100 in PBS for 10 min and blocked by 5% BSA in PBS for 1 hour at room temperature. The primary antibodies were then applied onto the cells for 16 hours at 4°C, which were mouse antineurofilament 68 antibody (1 : 200, Sigma-Aldrich), mouse antiglial fibrillary acidic protein (GFAP)-Cy3 (1 : 500, Sigma-Aldrich), and anti-rabbit anti-oligo2 (1 : 200, Imgenex). Then, the culture was stained with Alexa Fluor@ 488 donkey anti-Mouse antibody (1 : 1000, Invitrogen) and DAPI (1 : 500, Sigma-Aldrich) for 1 hour at room temperature. After being washed with PBS for 4 × 15 min, the cells were dehydrated serially with ice-cold 50%, 75%, 95%, and 100% ethanol and mounted with fluorescence mounting medium. Samples were then examined by Zeiss confocal microscopy with Ex 488/Em 505–540 nm for green color, Ex 543/Em 560–615 nm for Cy3 red color.

2.3. KXS Decoction Preparation. KXS decoction was composed of the following dried raw materials: Ginseng Radix et Rhizome (root and rhizome of *P. ginseng*), Polygalae Radix (root of *P. tenuifolia*), Acori Tatarinowii Rhizoma (rhizome of *A. tatarinowii*), and Poria (sclerotium of *P. cocos*). The herbs were purchased from Qingping Market of Chinese herbs in Guangzhou China and were authenticated by one of the authors, Dr. Tina T. X. Dong, according to their morphological characteristics. The voucher specimens were deposited in Centre for Chinese Medicine at Hong Kong University of Science & Technology. According to different formulations of KXS including KXS-652, KXS-984, and DZW-652, the appropriate amounts of Ginseng Radix et Rhizome, Polygalae Radix, Acori Tatarinowii Rhizoma, and Poria were weighed separately to form a combined weight of 20 g. The herbal extraction was performed in 160 mL of boiling water for 2 hours, and the herbs were extracted twice. For the second extraction of KXS, the residue from the first extraction was filtered: the same extraction condition was applied on the filtered residue. Then, the extracts were combined, dried under vacuum, and stored at −80°C. This extraction condition was also applied to each individual herb as well as a combination of herbs under the same extraction method as described above. The herbal extract was chemically standardized as reported previously [13], and the representative fingerprinting chromatograms were developed.

2.4. Drug Treatment. During the treatment, cultured astrocytes were changed with medium for 3 hours in modified Eagle's medium supplemented with 0.5% horse serum, 100 U/mL penicillin, and 100 μg/mL streptomycin, and then the cultures were treated with KXS extracts and/or other reagents for 48 hours. In analyzing the signaling pathway, the cells were pretreated with the protein kinase A inhibitor H89 (2 μM) and the MEK1/2 inhibitor U0126 (20 μM) and ICI 182, 780 (1 μM) for 3 hours before the exposure to KXS extract, Bt_2-cAMP (1 mM), TPA (10 nM), and 17β-Estradiol (10 nM).

2.5. Total RNA Extraction. Total RNA from brain tissue was isolated with RNAzol reagent according to the manufacturer's protocol. The brain tissues were added with RNAzol reagent (1.5 mL/g) and homogenized. The homogenate was centrifuged at 16,100 ×g for 5 min at 4°C. The supernatants were removed, added with diethylpyrocarbonate (DEPC) treated water (prepared by autoclaving water with DEPC in a 1000 : 1 ratio) and vortex vigorously for 15 sec, followed by centrifugation at 16,100 ×g for 10 min at 4°C. The aqueous layer was collected and added with half volume of 70% ethanol in DEPC treated water for RNA precipitation. The RNA pallet was collected by centrifugation at 16,100 ×g for 10 min at 4°C and washed with 70% ethanol in DEPC-treated water twice. After air dry, the RNA was resuspended in 200 μL of DEPC treated water. The concentration of extracted RNA was calculated from UV absorbance at 260 nm. The quality of RNA was assessed by absorbance at 260 nm and 280 nm, with the ratio of 260/280 nm ranging from 1.90 to 2.10 being acceptable.

2.6. Real-Time Quantitative PCR. Isolated RNAs were reverse transcribed by Moloney Murine Leukemia Virus (MMLV) reverse transcriptase with oligo-d(T) primer in a 20 μL reaction by using High Capacity cDNA Reverse Transcription Kit of Invitrogen Technologies. In details, three μg of total RNA was mixed with 1 μL of 0.5 μg/mL oligo-d(T) primer, 1 μL of 10 mM dNTP mix, and RNAase/DNAase free water in a 12 μL reaction. The mixture was incubated in 65°C for 5 min. Two μL of 0.1 M dithiothreitol (DTT), 1 μL of 40 U/μL RNase out, and 4 μL of 5x first strand buffer (250 mM Tris-HCl, pH 8.3, 375 mM KCl, and 15 mM $MgCl_2$) were added into the reaction mix and incubated at 37°C for 5 min. One μL MMLV was added into the reaction and incubated at 37°C for 50 min. Then, the reaction was incubated at 70°C for 15 min. Quantification of the cDNA was determined by UV absorbance at 260 nm and 280 nm by NanoDrop.

Real-time quantitative PCR for the target genes was performed on equal amounts of cDNA by using Roche SYBR Green Master mix with Rox reference dye, according to the manufacturer's instructions. The SYBR green signal was detected by Applied Biosystems 7500 Fast Real-Time PCR System. Transcript levels were quantified by using the ΔΔCt value method. Calculation was done by using the Ct value of Glyceraldehyde 3-phosphate dehydrogenase (GAPDH) to normalize the Ct value of target gene in each sample to obtain the ΔCt value, which was then used to compare among different samples. Real-time PCR products were analyzed by gel electrophoresis on a 1.5% agarose gel, and the specificity of amplification was confirmed by the melting curves.

2.7. ELISA Analysis. The amounts of NGF, GDNF (both from Abfrontier, Seoul, Korea), and BDNF (Millipore, Billerica, MA) in astrocyte conditioned medium were measured using commercially available ELISA kits according to the manufacturer's instructions. Briefly, conditioned medium was applied onto a 96-well plate precoated with anti-neurotrophic factor antibodies and incubated on at 37°C for 90 min. After discarding plate content, the biotinylated anti-neurotrophic antibody was added and incubated at 37°C for 60 min. After washing four times, avidin-biotin-peroxidase, or streptavidin-peroxidase, complex solution was added and incubated at 37°C for 90 min. Tetramethylbenzidine solution was added and incubated at 37°C for 30 min. The reaction was stopped with 1 M sulfuric acid and absorbance recorded at 450 nm immediately. The values of standards and samples were corrected by subtracting the absorbance of nonspecific blinding. All samples were measured in duplicate in the same assay to minimize interassay variation.

Table 1: Historical record of different KXS formulae.

Notation[a]	Record	Ratio			
		GR	PR	ATR	PO
KXS-652	*Beiji Qianjin Yaofang*[b]	1	1	25	50
KXS-984	*Yixin Fang*[c]	1	1	1	2
DZW-652	*Beiji Qianjin Yaofang*[b]	3	2	2	3

[a]The notation of KXS was corresponding to the years of recording.
[b]*Beiji Qianjin Yaofang* was written by Sun Simiao in 652 A.D, which was re-edited in 1066 A.D.
[c]*Yixin Fang* was written by Nima Yasunori in 984 A.D.
Abbreviations: GR: Ginseng Radix et Rhizoma; PR: Polygalae Radix; ATR: Acori Tatarinowii Rhizoma; PO: Poria.

2.8. Protein and Statistical Analysis. The concentration of protein was determined following the instructions of Bradford's method with a kit from Bio-Rad Laboratories. Individual data was expressed as mean ± standard deviation (SD). Statistical tests were performed with t-test (version 13.0, SPSS). Statistically significant changes were classified as significant (*) where $P < 0.05$, more significant (**) where $P < 0.01$, and highly significant (***) where $P < 0.001$.

3. Results

3.1. KXS Stimulates the Expression of Neurotrophic Factors on Astrocytes. Cultured astrocytes reached confluence on the day in vitro (DIV) 12 having the mRNA level of glial fibrillary acidic protein (GFAP), a marker for astrocyte, reaching the peak on DIV 12 to 16 (Figure 1(a)). To test the culture purity, the astrocytes were seeded onto the glass cover slip. At DIV 12, the culture was fixed for immunofluorescent staining with GFAP and possible contamination of oligodendrocytes, which was viewed under the microscopy (Figure 1(b)). The result showed that the majority of cell population was astrocyte, and thus, this stage of astrocyte was used subsequently for all biochemical analyses.

Historically, three formulations of KXS have been described, denoted as KXS-652, KXS-984, and DZW-652 (Table 1), and all of them are commonly used today clinically. The notation was described according to the year of their publication. KXS-652 with a ratio of 1 : 1 : 25 : 50 of Ginseng Radix et Rhizoma : Polygalae Radix : Acori Tatarinowii Rhizoma : Poria. Meanwhile, a herbal formula named Ding-Zhi-Wan (DZW-652) was also described with the ratio of 3 : 2 : 2 : 3. In addition, KXS-984 was recorded in a herbal

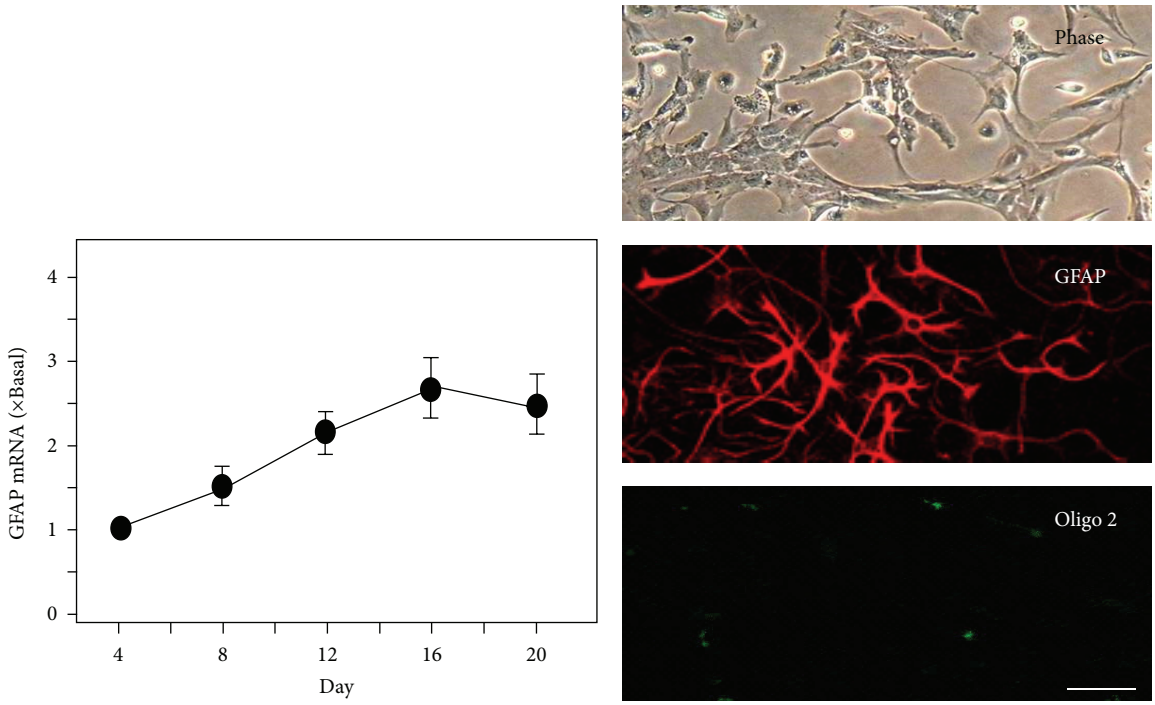

Figure 1: Cultures of rat astrocytes. (a) Cultured astrocytes were harvested on DIV4, 8, 12, 16, and 20, and the mRNA encoding GFAP was analyzed. Values are expressed as the percentage of increase to DIV 4 (set as 1) and in mean ± SEM, $n = 3$. (b) Cultured astrocytes were observed under the microscopy. Meanwhile, cultured astrocytes were stained by Cy3-anti-GFAP (shown in red) and anti-rabbit anti-oligo2 (shown in green) polyclonal antibodies observed under confocal microscopy in the presence of 0.1% Triton-X 100. Bar = 10 μm. Representative figures are showed here, $n = 3$.

ratio of 1 : 1 : 1 : 2. The chemical standardizations of these herbal decoctions were done by HPLC fingerprints and quantitation of chemical ingredients (Supplementary Figure 1), as described fully in Zhu et al. [13]. By determining the amounts of marker chemicals from the herbs, a standardized KXS extract was recommended in containing minimal amounts of ginsenoside Rb_1, ginsenoside Rd, ginsenoside Re, ginsenoside Rg_1, pachymic acid, 3, 6′-disinapoyl sucrose, α-asarone, and β-asarone (see Table 5 of [13] for detail). The chemical properties of these herbal extracts were prerequisite for all biochemical analyses.

The effect of the three formulations of KXS on the expression of neurotrophic factors was evaluated by quantitative PCR, which included NGF, BDNF, GDNF, NT3, NT4, and NT5. The specific primers of these neurotrophic factors were listed in Supplementary Table 1. Astrocytes cultured at DIV 12 were treated with KXS from 0.5–50 μg/mL for 24 hours, and then the amounts of mRNA were analyzed. The KXS treatment significantly increased the mRNA levels of NGF, BDNF, GDNF, and NT3 in dose-dependent manners (Figure 2). For NGF, the mRNA expression level showed over 2-fold enhancement under the treatment of KXS from 5 to 50 μg/mL, while the DZW-652 showed the best effect (~4-fold) at concentration of 15 μg/mL. For BDNF, DZW-652 increased the mRNA expression level over 2.5-fold. The best effect of DZW-652 could be also observed in GDNF induction. For NT3, K-984 showed better effect (~2-fold). For NT4 and NT5, there were slight changes observed after KXS treatment (Figure 2). Thus, KXS having a high ratio of Ginseng Radix et Rhizoma and Polygalae Radix could benefit the expression of neurotrophic factors, as this was in DZW-652 formulation.

The KXS-induced gene expression was robust for NGF, BDNF, and GDNF, and thus, the proteins of these factors in astrocytes' conditioned medium were further determined. Firstly, standard curves of three target proteins in ELISA assays were made by different concentrations of protein standards. NGF, BDND, and GDNF exerted good linearity in a range of 0~40 pg/mL (Figure 3(a)), and the square of linear correlation coefficient was all over 0.95. The recovery of spiked protein was greater than 90%. The coefficient of intra and interassay was over 0.90. In astrocytes treated with KXS extracts, the induction of NGF, GDNF, and BDNF was determined by ELISA. The amount of NGF of cultured astrocytes was 4.92 pg/mg proteins, while the value of BDNF and GDNF was 2.39 pg/mg protein and 21.6 pg/mg proteins, respectively. Under the treatment of KXS, the expressions of NGF, GDNF, and BDNF were increased in dose-dependent manners (Figure 3(b)). At 15 μg/mL of KXS in all cases, the inductions were significant higher than that of the control. The treatment of DZW-652 exerted the best stimulation in neurotrophic factor secretion: a maximal induction at 100% increase compared to control was revealed under

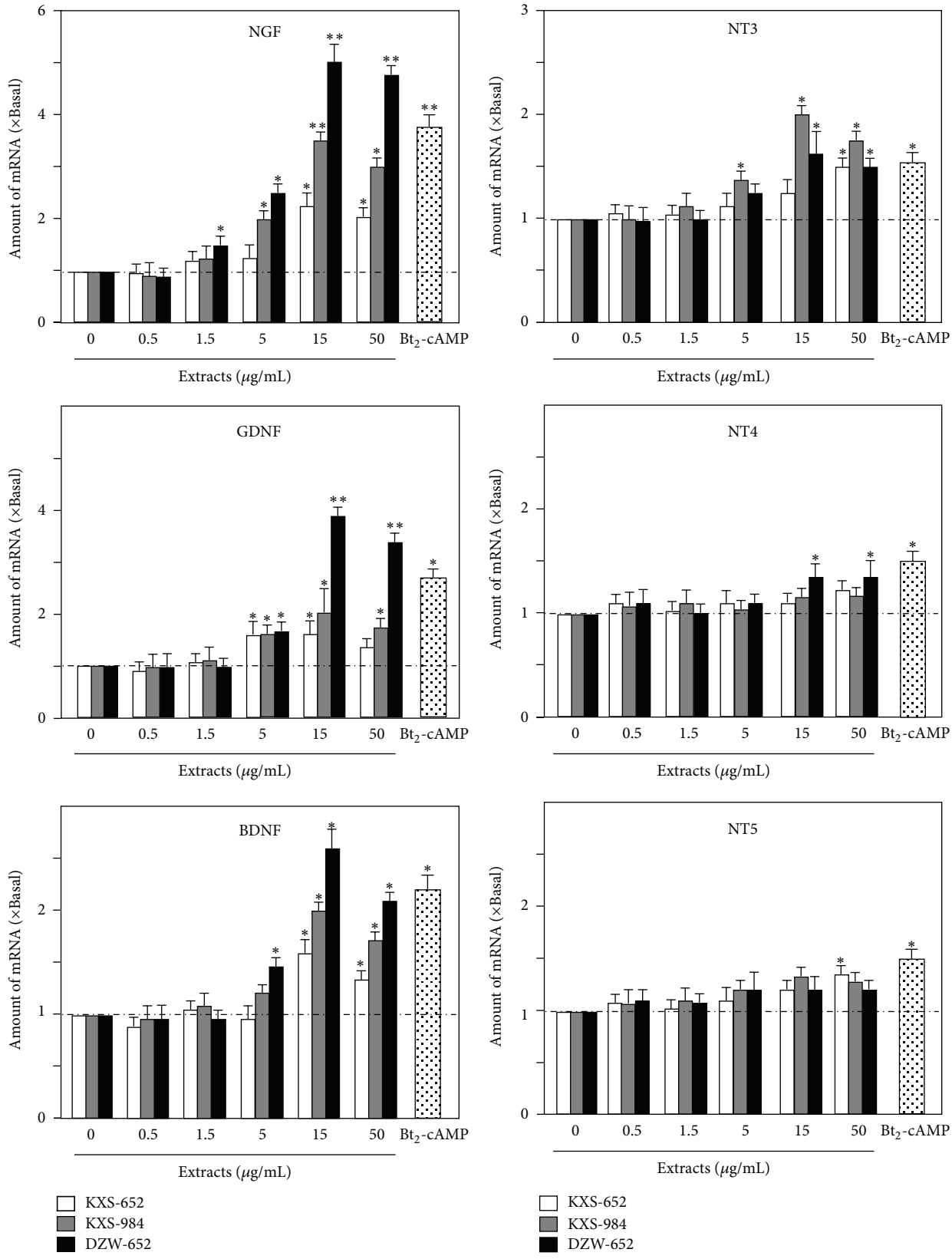

Figure 2: KXS stimulates the mRNA expression of neurotrophic factors in astrocytes. The mRNA expression levels of neurotrophic factors (NGF, GDNF, BDNF, NT3, NT4, and NT5) in astrocytes were analyzed. The astrocytes were treated with different formulations of KXS (0.5–50 μg/mL) for 24 hours. The mRNA was determined by quantitative PCR. Primers for neurotrophic factors were listed in Supplementary Table 1. Available online at http://dx.doi.org/10.1155/2013/731385 Bt_2-cAMP (1 mM) was used as a control. Data are expressed as x Basal where the value of control is set as 1 and in Mean ± SEM, $n = 4$.

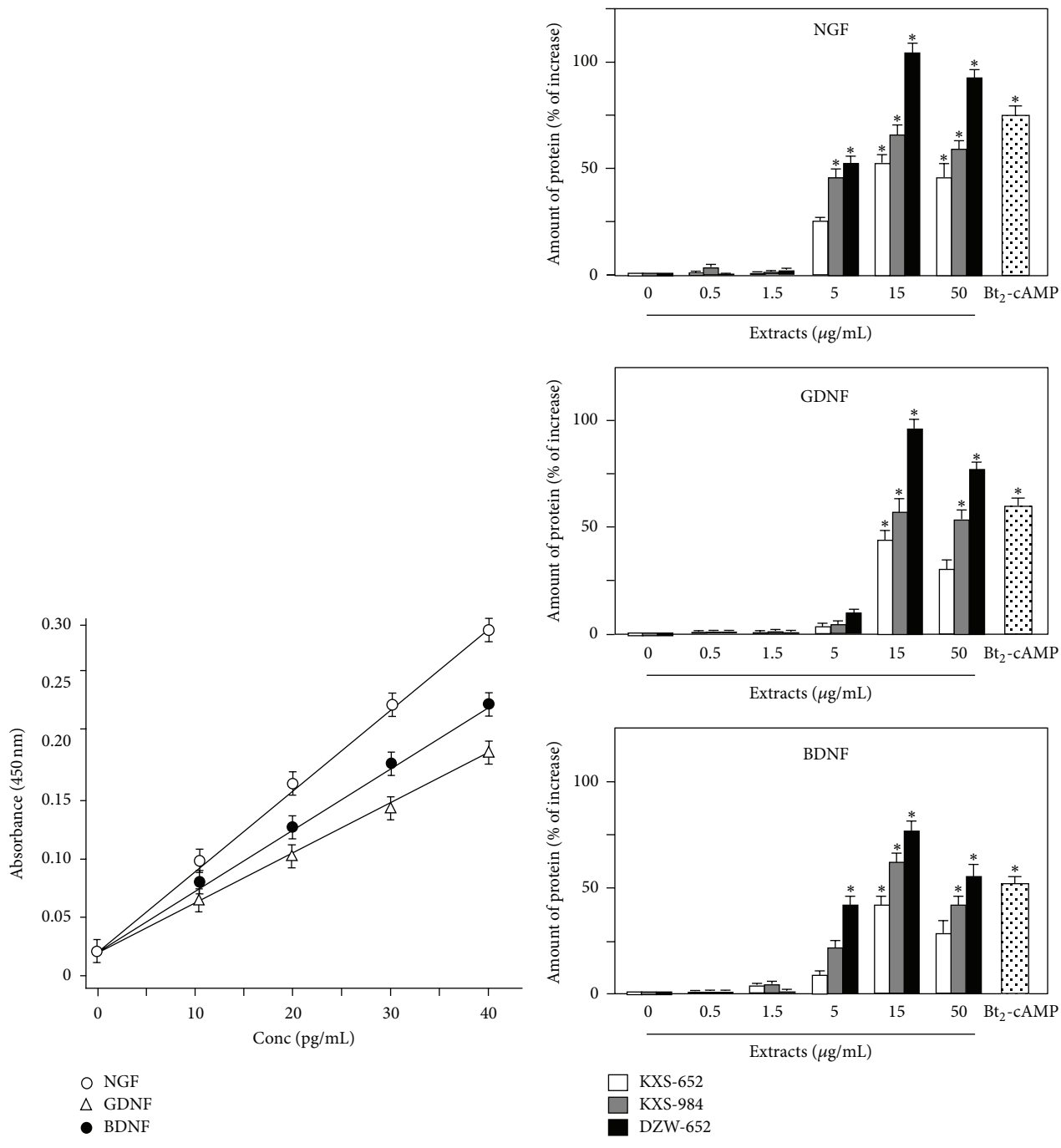

FIGURE 3: KXS stimulates the secretion of neurotrophic factor in astrocytes. (a) Different concentrations of neurotrophic factors (0–40 pg/mL) were applied onto ELISA kit, and the absorbance was detected at wavelength of 450 nm. The calibration curve of each target protein was constructed by plotting absorbance versus the concentration of each target protein. Each calibration curve was derived from 5 data points. (b) Astrocytes were treated with KXS (0.5–50 μg/mL) and Bt_2-cAMP (1 mM) for 48 hours. Then, the media were collected for analysis of NGF, BDNF, and GDNF with ELISA kit. Data are expressed as percentage of increase to control (no drug treatment, that is, 0 extract here). Values are showed as the Mean ± SEM, $n = 3$.

15 μg/mL of DZW-652 (Figure 3(b)). In addition, the inducing effect of KXS-984 was slightly better than that of KXS-652 (Figure 3(b)). Here, the application of Bt_2-cAMP was used as a control. In addition, the water extracts of four individual herbs were tested for their role in the induction of neurotrophic factors, and the effects were not significant. Here, the water extracts of Ginseng Radix et Rhizoma and Polygalae Radix could slightly stimulate the expression of

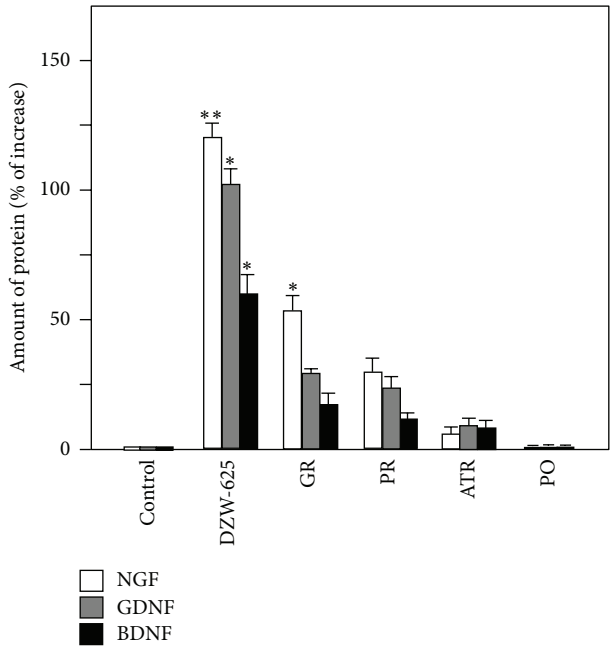

Figure 4: The comparison of KXS and single herb in stimulating the secretion of neurotrophic factors in astrocytes. Astrocytes were treated with DZW-652 (15 μg/mL), the extract of Ginseng Radix et Rhizoma (4.5 μg/mL), the extract of Polygalae Radix (3 μg/mL), the extract of Acori Tatarinowii Rhizoma (3 μg/mL), and the extract of Poria (4.5 μg/mL) for 48 hours, and then the media were collected to determine the amount of NGF, BDNF, and GDNF. Data are expressed as percentage of increase to control (no drug treatment, that is, 0 extract here). Values are showed as the Mean ± SEM, $n = 3$. Abbreviations: GR: Ginseng Radix et Rhizoma; PR: Polygalae Radix; ATR: Acori Tatarinowii Rhizoma; PO: Poria.

NGF and GDNF (Figure 4), while the other inductions were very small. In contrast, a combined herbal mixture (i.e., DZW-652) showed robust induction.

3.2. The Signaling of KXS-Induced Neurotrophic Factor Expression. To search for the possible mechanism of KXS-induced neurotrophic factor expression on astrocytes, the known signaling pathways, including cAMP-dependent, MAPK-dependent, and estrogen receptor-dependent [14–17], were probed here. The cultured astrocytes were treated with the corresponding agonists, for example, Bt_2-cAMP activating cAMP-dependent signal TPA activating MAPK-dependent signal, and 17-β-estradiol activating estrogen receptor-dependent signal. The application of these positive inducers activated robustly the mRNA expressions of NGF, GDNF, and BDNF (Figure 5) in cultured astrocytes. As expected, the application of H89, U0126, and ICI 182, 780 significantly reduced the inductions of Bt_2-cAMP, TPA, and 17-β-estradiol, respectively. However, the DZW-652-induced gene expressions were not affected by these signaling inhibitors (Figure 5). Thus, the role of KXS in inducing the expressions of neurotrophic factors was novel, at least not belonging to any known signaling pathways.

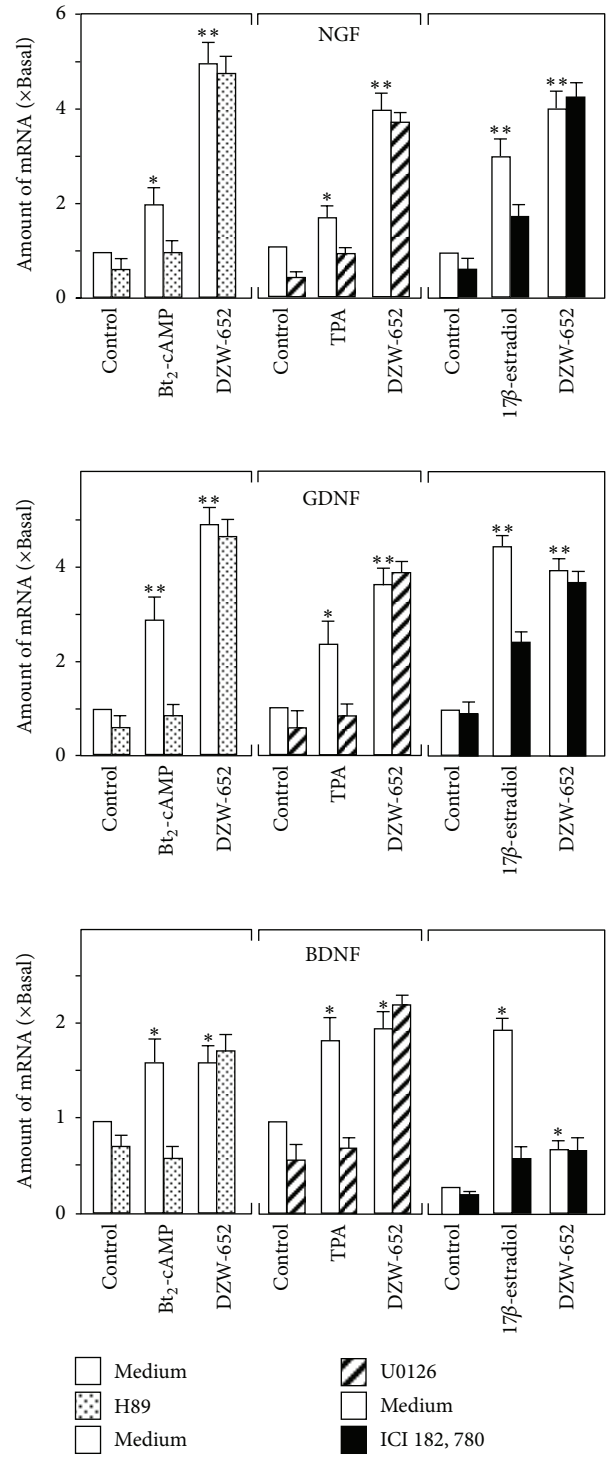

Figure 5: Effect of cAMP, MAPK, and estrogen signaling pathway on the expression of neurotrophic factors. Astrocytes were pretreated with H89 (2 μM; the PKA inhibitor), U0126 (10 μM; the MEK1/2 and PKC inhibitor), and ICI 182, 780 (1 μm; the estrogen receptor inhibitor) for 3 hours and then treated with Bt_2-cAMP (1 mM), TPA (100 nM), 17β-estradiol (10 nM), and DZW-652 (15 μg/mL) for 24 hours. The mRNA expression levels of neurotrophic factors in astrocytes were analyzed. Data are expressed as x Basal where the value of control is set as 1 and in mean ± SEM, where $n = 4$.

4. Discussions

Astrocyte is the prevailing glial cell in the central nervous system and constitutes the blood brain barrier, which is an essential component in protecting the inner environment of the brain. More importantly, there is an intensive bidirectional communication between neurons and glial cells at the synapses, which leads to a concept of "tripartite synapse," that is, a presynaptic neuron, a postsynaptic neuron and glial cells [18]. Astrocyte plays a role in the uptake of neurotransmitter from synaptic cleft, the synthesis of neurotransmitter precursors, and disposal of excess neurotransmitter [19]. On the other hand, astrocyte is an important regulator for the modulation of neurotrophic factors [20, 21].

Neurotrophic factors are a family of proteins responsible for the growth and survival of neurons during development and for maintenance of adult neurons, for example, NGF, BDNF, GDNF, NT3, and NT-4/5. The deficiency of neurotrophic factors in brain has been regarded as a biomarker for depression. The chronic stress in animals induced decreased synthesis of neurotrophic factors, which subsequently caused atrophy of neurons in hippocampus [22, 23]. In parallel, the stress was also reported to decrease the expression of BDNF in CA3 pyramidal and dentate gyrus of hippocampus in rat [24]. These observations led to the hypothesis that downregulation of BDNF contributed to an accelerated atrophy of CA3 neurons. Here, the treatment of KXS not only enhanced the expression of neurotrophic factors, for example, NGF, BDNF, GDNF, and NT3, but also stimulated the secretion of these neurotrophic factors in cultured astrocytes, which was in line to antidepression function of KXS in rats [12]. In depressive rats, total saponins of Ginseng Radix et Rhizoma reversed the stress-induced decreased BDNF level, and in parallel ginsenoside, Rg_1 upregulated the BDNF signaling pathway in hippocampus of mice [25, 26]. In addition, 3, 6′-disinapoyl sucrose derived from Polygalae Radix reversed the reduced BDNF levels in stress-induced depressive rats [27], while saponin from Polygalae Radix enhanced the production of NGF in rat astrocytes [28]. Eugenol derived from Acori Tatarinowii Rhizoma increased BDNF mRNA expression level in hippocampus of mice [29]. Among the tested three KXS formulations, the amount of Ginseng Radix et Rhizoma and Polygalae Radix was the highest in DZW-652, which therefore might explain the best effect of this ratio in enhancing neurotrophic factor expression.

There are several possibilities of having three formulations of KXS in history. Due to a lack of printing technologies in Tang Dynasty, the original edition of *Beiji Qianjin Yaofang* (652 A.D.) had never been seen. The earliest edition of *Beiji Qianjin Yaofang*, which could be found today, was edited by Lin Yi and Gao Bao-heng in Song Dynasty, who described one of the KXS formulae, KXS-652 with a ratio of 1 : 1 : 25 : 50 (Ginseng Radix et Rhizoma : Polygalae Radix : Acori Tatarinowii Rhizoma : Poria). Meanwhile, a herbal formula named Ding-Zhi-Wan (DZW-652) was also described having the herbal ratio of 3 : 2 : 2 : 3 in the same book. In addition, the composition of another herbal formula, named KXS-984, was recorded in *Yi Xin Fang* written by Nima Yasunori from Japan in 984 A.D. (Song Dynasty). The author recorded the herbal ratio of 1 : 1 : 1 : 2 for KXS-984 and cited *Beiji Qianjin Yaofang*. Despite the variations of herbal composition, all three KXS formulae have been used to treat the diseases with symptoms of depressed mood and morbid forgetfulness [30, 31]. The disappearance of the original manuscript of *Beiji Qianjin Yaofang* in Tang Dynasty might also be a reason for emerging different KXS formulae. More realistically, the original KXS formula might have been rearranged by other TCM practitioners according to syndrome differentiation.

The mechanism of KXS in stimulating mRNA expression levels of neurotrophic factors was unknown. It has been reported that cAMP-dependent pathway, MAPK-dependent pathways, and estrogen signaling pathway might be included in neurotrophic factor expression [14, 15]. Here, the effect of KXS in stimulating neurotrophic expression could not be inhibited by the corresponding inhibitors, that is, H89, U0126, or ICI 182, 780. KXS is a herbal extract having multichemicals, which therefore could have different roles in stimulating neurotrophic factor expression via multiple signal transduction pathways or unidentified kinase(s), that is, not only the reported cAMP-, MAPK- and estrogen-dependent pathway. Thus, we hypothesized that KXS might exert functions in stimulating neurotrophic factor expression through multitargets and multisignaling pathways. Some new pathways might be also involved instead of the single reported well-known pathways. Other method, such as phosphorylation proteomics, might be applied for further studies in the future.

5. Conclusions

The treatment of KXS in cultured astrocytes increased both the synthesis and the release of neurotrophic factors, including NGF, BDNF, and GDNF. Although the action mechanism was not fully revealed, this result was in parallel to our previous report that KXS was effective in treating antidepression. In line to the historical usage, this chemically standardized herbal extract could serve as alternative medicine or health food supplement for patients suffering from depression.

Acknowledgments

This research was supported by the Chinese National Nature Science Foundation for Young Scholars (81303190) to Kevin Y ZHU, Hong Kong Research Grants Council Theme-based Research Scheme (T13-607/12R) and GRF (661110, 662911, 663012), and Foundation of The Awareness of Nature (TAON12SC01) to KWKT.

References

[1] G. Parker, "Beyond major depression," *Psychological Medicine*, vol. 35, no. 4, pp. 467–474, 2005.

[2] M. D. Binder, N. Hirokawa, and U. Windhorst, *Encyclopedia of Neuroscience*, Springer, Berlin, Germany, 2009.

[3] R. S. Duman and L. M. Monteggia, "A neurotrophic model for stress-related mood disorders," *Biological Psychiatry*, vol. 59, no. 12, pp. 1116–1127, 2006.

[4] Y. Shirayama, A. C. Chen, S. Nakagawa, D. S. Russell, and R. S. Duman, "Brain-derived neurotrophic factor produces antidepressant effects in behavioral models of depression," *Journal of Neuroscience*, vol. 22, no. 8, pp. 3251–3261, 2002.

[5] A. Sahay and R. Hen, "Adult hippocampal neurogenesis in depression," *Nature Neuroscience*, vol. 10, no. 9, pp. 1110–1115, 2007.

[6] R. K. Schwarting and J. P. Huston, "Behavioral concomitants of regional changes in the brain's biogenic amines after apomorphine and amphetamine," *Pharmacology Biochemistry and Behavior*, vol. 41, no. 4, pp. 675–682, 1992.

[7] T. H. H. Pang, F. C. F. Ip, and N. Y. Ip, "Recent development in the search for effective antidepressants using traditional Chinese medicine," *Central Nervous System Agents in Medicinal Chemistry*, vol. 8, no. 1, pp. 64–71, 2008.

[8] E. Castrén, V. Võikar, and T. Rantamäki, "Role of neurotrophic factors in depression," *Current Opinion in Pharmacology*, vol. 7, no. 1, pp. 18–21, 2007.

[9] C. Aydemir, E. S. Yalcin, S. Aksaray et al., "Brain-derived neurotrophic factor (BDNF) changes in the serum of depressed women," *Progress in Neuro-Psychopharmacology and Biological Psychiatry*, vol. 30, no. 7, pp. 1256–1260, 2006.

[10] J. A. Siuciak, D. R. Lewis, S. J. Wiegand, and R. M. Lindsay, "Antidepressant-like effect of brain-derived neurotrophic factor (BDNF)," *Pharmacology Biochemistry and Behavior*, vol. 56, no. 1, pp. 131–137, 1997.

[11] D. H. Overstreet, K. Fredericks, D. Knapp, G. Breese, and J. McMichael, "Nerve growth factor (NGF) has novel antidepressant-like properties in rats," *Pharmacology Biochemistry and Behavior*, vol. 94, no. 4, pp. 553–560, 2010.

[12] K. Y. Zhu, Q. Q. Mao, S. P. Ip et al., "A standardized Chinese herbal decoction, Kai-Xin-San, restores decreased levels of neurotransmitters and neurotrophic factors in the brain of chronic stress-induced depressive rats," *Evidence-Based Complementary and Alternative Medicine*, vol. 2012, no. 149256, 2012.

[13] K. Y. Zhu, Q. Fu, H. Q. Xie et al., "Quality assessment of a formulated Chinese herbal decoction, Kaixinsan, by using rapid resolution liquid chromatography coupled with mass spectrometry: a chemical evaluation of different historical formulae," *Journal of Separation Science*, vol. 33, no. 23-24, pp. 3666–3674, 2010.

[14] S. R. D'mello and G. Heinrich, "Induction of nerve growth factor gene expression by 12-O-tetradecanoyl phorbol 13-acetate," *Journal of Neurochemistry*, vol. 55, no. 2, pp. 718–721, 1990.

[15] D. F. Condorelli, P. Dell'albani, G. Mudò, T. Timmusk, and N. Belluardo, "Expression of neurotrophins and their receptors in primary astroglial cultures: Induction by cyclic AMP-elevating agents," *Journal of Neurochemistry*, vol. 63, no. 2, pp. 509–516, 1994.

[16] T. Ivanova, M. Karolczak, and C. Beyer, "Estradiol stimulates GDNF expression in developing hypothalamic neurons," *Endocrinology*, vol. 143, no. 8, pp. 3175–3178, 2002.

[17] F. Sohrabji, R. C. G. Miranda, and C. D. Toran-Allerand, "Identification of a putative estrogen response element in the gene encoding brain-derived neurotrophic factor," *Proceedings of the National Academy of Sciences of the United States of America*, vol. 92, no. 24, pp. 11110–11114, 1995.

[18] G. Perea, M. Navarrete, and A. Araque, "Tripartite synapses: astrocytes process and control synaptic information," *Trends in Neurosciences*, vol. 32, no. 8, pp. 421–431, 2009.

[19] L. Hertz and H. R. Zielke, "Astrocytic control of glutamatergic activity: astrocytes as stars of the show," *Trends in Neurosciences*, vol. 27, no. 12, pp. 735–743, 2004.

[20] C. C. Wilson, K. M. Faber, and J. H. Haring, "Serotonin regulates synaptic connections in the dentate molecular layer of adult rats via 5-HT(1a) receptors: evidence for a glial mechanism," *Brain Research*, vol. 782, no. 1-2, pp. 235–239, 1998.

[21] M. Slezak and F. W. Pfrieger, "New roles for astrocytes: regulation of CNS synaptogenesis," *Trends in Neurosciences*, vol. 26, no. 10, pp. 531–535, 2003.

[22] R. M. Sapolsky, "Glucocorticoids, hippocampal damage and the glutamatergic synapse," *Progress in Brain Research*, vol. 86, pp. 13–23, 1990.

[23] A. M. Magariños, J. M. García Verdugo, and B. S. Mcewen, "Chronic stress alters synaptic terminal structure in hippocampus," *Proceedings of the National Academy of Sciences of the United States of America*, vol. 94, no. 25, pp. 14002–14008, 1997.

[24] M. A. Smith, S. Makino, R. Kvetnansky, and R. M. Post, "Effects of stress on neurotrophic factor expression in the rat brain," *Annals of the New York Academy of Sciences*, vol. 771, pp. 234–239, 1995.

[25] H. Dang, Y. Chen, X. Liu et al., "Antidepressant effects of ginseng total saponins in the forced swimming test and chronic mild stress models of depression," *Progress in Neuro-Psychopharmacology and Biological Psychiatry*, vol. 33, no. 8, pp. 1417–1424, 2009.

[26] B. Jiang, Z. Xiong, J. Yang et al., "Antidepressant-like effects of ginsenoside Rg1 produced by activation of BDNF signaling pathway and neurogenesis in the hippocampus," *British Journal of Pharmacology*, vol. 166, no. 6, pp. 1872–1887, 2012.

[27] Y. Hu, H. B. O. Liao, P. Liu, D. H. Guo, and K. Rahman, "A bioactive compound from Polygala tenuifolia regulates efficiency of chronic stress on hypothalamic-pituitary-adrenal axis," *Pharmazie*, vol. 64, no. 9, pp. 605–608, 2009.

[28] T. Yabe, S. Iizuka, Y. Komatsu, and H. Yamada, "Enhancements of choline acetyltransferase activity and nerve growth factor secretion by Polygalae radix-extract containing active ingredients in Kami-untan-to," *Phytomedicine*, vol. 4, no. 3, pp. 199–205, 1997.

[29] G. Tao, Y. Irie, D. J. Li, and M. K. Wing, "Eugenol and its structural analogs inhibit monoamine oxidase A and exhibit antidepressant-like activity," *Bioorganic and Medicinal Chemistry*, vol. 13, no. 15, pp. 4777–4788, 2005.

[30] Z. X. Bao, G. P. Zhao, W. Sun, and B. J. Chen, "Clinical curative effects of Kaixin powder on depression with mild or moderate degree," *Chinese Archives of Traditional Chinese Medicine*, vol. 28, no. 5, pp. 987–988, 2011.

[31] Z. X. Bao, Q. Tian, X. Y. Gao, B. J. Chen, Y. F. Zhong, and l. Li, "Analysis on medication rule for 235 formula e for depression," *Journal of Zhejiang University of Traditional Chinese Medicine*, vol. 34, no. 5, pp. 763–766, 2010.

Hindawi Publishing Corporation
Evidence-Based Complementary and Alternative Medicine
Volume 2013, Article ID 687958, 11 pages
http://dx.doi.org/10.1155/2013/687958

Research Article

Song Bu Li Decoction, a Traditional Uyghur Medicine, Protects Cell Death by Regulation of Oxidative Stress and Differentiation in Cultured PC12 Cells

Maitinuer Maiwulanjiang,[1] Kevin Y. Zhu,[1] Jianping Chen,[1] Abudureyimu Miernisha,[1] Sherry L. Xu,[1] Crystal Y. Q. Du,[1] Kitty K. M. Lau,[1] Roy C. Y. Choi,[1] Tina T. X. Dong,[1] Haji A. Aisa,[2] and Karl W. K. Tsim[1]

[1] *Division of Life Science and Centre for Chinese Medicine, The Hong Kong University of Science and Technology, Clear Water Bay Road, Hong Kong*
[2] *Xinjiang Key Laboratory of Plant Resources and Natural Products Chemistry, Xinjiang Technical Institute of Physics and Chemistry, Chinese Academy of Sciences, Urumqi 830011, China*

Correspondence should be addressed to Karl W. K. Tsim; botsim@ust.hk

Received 21 May 2013; Revised 2 August 2013; Accepted 26 August 2013

Academic Editor: Paul Siu-Po Ip

Song Bu Li decoction (SBL) is a traditional Uyghur medicinal herbal preparation, containing Nardostachyos Radix et Rhizoma. Recently, SBL is being used to treat neurological disorders (insomnia and neurasthenia) and heart disorders (arrhythmia and palpitation). Although this herbal extract has been used for many years, there is no scientific basis about its effectiveness. Here, we aimed to evaluate the protective and differentiating activities of SBL in cultured PC12 cells. The pretreatment of SBL protected the cell against tBHP-induced cell death in a dose-dependent manner. In parallel, SBL suppressed intracellular reactive oxygen species (ROS) formation. The transcriptional activity of antioxidant response element (ARE), as well as the key antioxidative stress proteins, was induced in dose-dependent manner by SBL in the cultures. In cultured PC12 cells, the expression of neurofilament, a protein marker for neuronal differentiation, was markedly induced by applied herbal extract. Moreover, the nerve growth factor- (NGF-) induced neurite outgrowth in cultured PC12 cells was significantly potentiated by the cotreatment of SBL. In accord, the expression of neurofilament was increased in the treatment of SBL. These results therefore suggested a possible role of SBL by its effect on neuron differentiation and protection against oxidative stress.

1. Introduction

Traditional Uyghur medicine (TUM), one of the main medicinal systems in central Asia, is based on four humors: fire, air, water, and earth, which generates four different body fluids: blood, phlegm, yellow bile, and black bile [1]. The main ingredients of TUM are flowers, seeds, fruits, minerals, and animal compartments. According to the TUM theory, diseases or impairments are resulted from imbalance between the four body fluids. TUM herbal formulation could regulate the balance of body fluids and cure diseases [2]. Song Bu Li decoction (SBL), a TUM formula described in Sherhi Alkanun by Emam Durdin during AD 840-1212, consists of only one herb named Nardostachyos Radix et Rhizoma (NRR, a root and rhizome of *Nardostachys jatamansi*). Recently, SBL has been used to treat neurological disorders (insomnia and neurasthenia) and heart disorders (palpitation and arrhythmia) in Xinjiang of China. According to ancient method of preparations of TUM [2], two methods of SBL preparation are commonly used in Xinjiang: (i) NRR is boiled with water, and the vapor generated is being collected as the volatile components of NRR. Condensed vapor and extracted water are mixed and (ii) NRR is boiled in water and filtered, and only the water extract is being used for treatment. Both preparation methods of SBL generate a problem of quality control and efficacy.

Neurasthenia is defined as a condition with symptoms of fatigue, forgetfulness, sleepless, anxiety, and depressed mood [3, 4], and the pathogenesis of neurasthenia still remains unknown [5]. During the brain development, neuronal stem cells undergo a stage called neurogenesis in which immature neurons grow, differentiate, and survive. However, for patients with neurasthenia and depression, the normal neurogenesis would be impaired, that is, the inability for neurons to differentiate normally. Amongst different causes of neuronal cell death, reactive oxygen species (ROS) mediated oxidative stress is one of the major origins of many neurological disorders [6–8]. The excess generation of ROS damages cells by peroxidizing lipids and disrupting structural proteins, enzymes, and nucleic acids [9, 10]. In defending the stress, antioxidant response element (ARE), located upstream of various genes, could regulate the expression of antioxidative stress proteins [11–13].

Neuronal differentiation of PC12 cells, mediated by nerve growth factor (NGF), shows the morphological change of cells possessing neurites. In addition, the neuronal differentiation could be determined biochemically by analyzing the expression of neurofilaments (NFs) that are the major structural components of differentiated neurons [14, 15]. Three mammalian neurofilament subunits, NF68, NF160, and NF200 are believed to form heterodimers in making the structural domain of neurites [16]. The differentiation status of neuron is also a critical parameter of neuron survival.

Having the questions of SBL efficacy under two distinct preparative methods, we aimed to establish quality control parameters of the herbal preparation and to reveal the role of SBL in preventing neuronal cell death. Chemical fingerprint and quantitation of ingredients, including ferulic acid, linarin, and volatile oil, were developed for quality control. In the bioassay, the role of SBL in preventing *tert*-Butyl hydroperoxide- (tBHP-) induced cell death as well as the gene activation of antioxidative stress proteins was determined. Lastly, the length of neurites and the expression of neurofilaments were determined in PC12 cells under the treatment of SBL.

2. Materials and Methods

2.1. Plant Materials and Preparation of SBL. NRR, the root and rhizome of *N. jatamansi*, was purchased from Hong Kong herbal market (Wong Chak Kee Co.). The authentication of plant material was performed by Dr. Tina T. X. Dong according to their morphological characteristics. The voucher specimens were deposited in the Centre for Chinese Medicine R&D at The Hong Kong University of Science and Technology. The herb NRR was minced and soaked in water in the proportion of 1 : 10 (w/v) overnight. The mixture was submitted to hydrodistillation in a Clevenger-type apparatus for 4 hours. Water extract and volatile oil of NRR were obtained at the same time. Volatile oil was dried over anhydrous sodium and stored at −20°C. The resulting water extract was filtered, vacuum-dried to powder, and kept at −20°C. This extract was considered as an NRR extract. The extraction efficiency reached over 95% within 4 hours. For SBL preparation, 1 g of dried NRR powder was dissolved in 20 mL DMSO and sonicated for 30 min. The extract was centrifuged at 13,200 rpm at 4°C for 5 min, and 170 μL of volatile oil was added onto the supernatant as the final SBL decoction.

2.2. Chemicals and Reagents. Ferulic acid (>98%), *tert*-Butyl hydroperoxide (tBHP) (>98%), *tert*-Butylhydroquinone (tBHQ) (>98%), 3-(4,5-dimethylthiazol-2-yl)-2,5-diphenyl tetrazolium bromide (MTT) (>98%) were purchased from Sigma Chemical Co. (St. Louis, MO, USA). Linarin (>98%) was kindly provided by Testing Laboratory for Chinese Medicine (Hong Kong, China). HPLC-grade acetonitrile and methanol were purchased from Merck (Darmstadt, Germany). Ultra-pure water was prepared from a Milli-Q purification system (Millipore, Molsheim, France).

2.3. GC-MS Analysis. Agilent 7000 GC-MS series system (Waldbronn, Germany) equipped with an Agilent 7890A gas chromatography and GC-QQQ Mass Hunter workstation software was adopted. The extract was separated in an Agilent HP-5MS capillary column (250 μm × 30 m × 0.25 μm) with controlled temperature at 100°C in the initial stage, and the temperature was adjusted to 280°C at the rate of 5°C/min. Pulsed splitless injection was conducted by injecting 1 μL of the sample extract. Helium was used as carrier gas at a flow rate of 2.25 mL/min; nitrogen was used as the collision gas at a flow rate of 1.5 mL/min. The spectrometer was operated in a full-scan electron-impact (EI) mode, and the ionization energy was 70 eV. The inlet and ionization source temperatures were 250°C and 230°C, respectively. The solvent delay time was 3.5 min. Retention indices of all compounds were determined according to the Kovats method using *n*-alkanes (Sigma) as standards. Identification of the volatile compounds was confirmed by comparing the mass spectra with the Kovats retention indices.

2.4. HPLC-DAD Analysis. HPLC-DAD analysis was conducted with an Agilent HPLC 1200 series system (Agilent Waldbronn, Germany), which was equipped with a degasser, a binary pump, an autosampler, a diode array detector (DAD), and thermo-stated column compartment. Chromatographic separation was carried out on an Intersil C18 column (particle size 5 μm, 4.6 × 250 mm) with water (as solvent A) and acetonitrile (as solvent B) as the mobile phase at flow rate of 1.0 mL/min at room temperature using the following gradient program: 0–20 min, isocratic gradient 19-19% (B); 20–25 min, linear gradient 19–25% (B); 25–45 min, linear gradient 25–35% (B); and 45–55 min, linear gradient 35–55% (B). A preequilibration period of 10 min was used between each run. The injection volume was 10 μL. The UV detector wavelength was set to 334 nm with full spectral scanning from 190 to 400 nm.

2.5. PC12 Cell Culture. Pheochromocytoma PC12 cells, a cell line derived from rat adrenal medulla, were obtained from American Type Culture Collection (ATCC, Manassas, VA) and maintained in Dulbecco's modified Eagle's medium

(DMEM) supplemented with 6% fetal bovine serum, 6% horse serum, 100 units/mL penicillin, and 100 μg/mL of streptomycin in a humidified CO_2 (7.5%) incubator at 37°C. Culture reagents were from Invitrogen (Carlsbad, CA). For the differentiation assay, cultured PC12 cells were serum starved for 4 hours in DMEM supplemented with 1% fetal bovine serum, 1% horse serum, and penicillin-streptomycin, and then they were treated with the SBL and/or other reagents for 72 hours.

2.6. MTT and ROS Formation Assay. PC12 cell viability was assayed by reduction of MTT [3-(4,5-dimethylthiazol-2-yl)-2,5-diphenyl tetrazolium bromide] reagent. Cells (2×10^4 cells/well) were plated in 96-well plate and pretreated with different concentrations of SBL and/or other reagents for 24 hours. Then, the cells were treated with 150 μM tBHP for 3 hours. The cultures were then treated with MTT solution for 1 hour, and the optical density was measured using spectrophotometer at 570 nm. The determination of ROS level in cell cultures was performed according to Zhu et al. [17]. In brief, cultured PC12 cells in a 96-well plate were pretreated with different concentrations of SBL and/or other reagents for 24 hours and labeled by 100 μM DCFH-DA (Sigma) in HBSS for 1 hour at room temperature. Cultures were then treated with 100 μM tBHP for 1 hour. The amount of intracellular tBHP-induced ROS formation was detected by fluorometric measurement with excitation at 485 nm and emission at 530 nm (Spectra max Gemini XS, Molecular Devices Crop., Sunnyvale, CA).

2.7. DNA Construction and Transfection. The pGL4.37[*luc2P*/ARE/Hygro] vector contains four copies of an antioxidant response element (ARE; 5′-TGACnnnGCA-3′) that drives transcription of the luciferase reporter gene *luc2P* (*Photinus pyralis*). *Luc2P* is a synthetically-derived luciferase sequence with humanized codon optimization that is designed for high expression and reduced anomalous transcription. The *luc2P* gene contains hPEST, a protein destabilization sequence, which allows *luc2P* protein levels to respond more quickly than those of *luc2* to induce transcription. Cultured PC12 cells were transfected with pARE-Luc (Promega, Fitchburg, WI) by Lipofectamine 2000 (Invitrogen) according to the manufacturer's instructions. The transfection efficiency was ~60%, as determined by another control plasmid having β-galactosidase, under a cytomegalovirus enhancer promoter.

2.8. Luciferase Activity. PC12 cells, cultured in 24-well plate (1×10^5 cells/well), were treated with SBL and/or other reagents for 24 hours. Afterward, the medium was aspirated, and cultures were washed by ice-cold PBS. The cells were lysed by a buffer containing 0.2% Triton X-100, 1 mM dithiothreitol, and 100 mM potassium phosphate buffer (pH 7.8) at 4°C. Followed by centrifugation at 13,200 rpm for 10 min at 4°C, the supernatant was collected and used to perform luciferase assay (Tropix Inc., Bedford, MA); the activity was normalized by amount of protein and the activity of β-galactosidase (a control plasmid).

2.9. Polymerase Chain Reaction (PCR) Analysis. PC12 cells were treated with SBL and/or other reagents for 24 hours. Total RNAs were isolated by TRIzol reagent (Invitrogen) and reverse-transcribed by Moloney Murine Leukemia Virus Reverse Transcriptase (Invitrogen) according to the manufacturer's instruction. Real-time PCR was performed by using SYBR green master mix and ROX reference dye according to the manufacturer's instruction (Applied Bioscience, Foster City, CA). The primers were as follows: 5′-GAC CTT GCT TTC CAT CAC CAC CGG-3′ and 5′-GTA GAG TGG TGA CTC CTC CCA GAC-3′ for NAD(P)H quinone oxidoreductase (NQO1; 241 bp); 5′-CCT GCT GTG TGA TGC CAC CAG ATT TT-3′ and 5′-TCT GCT TTT CAC GAT GAC CGA GTA CC-3′ for glutamate-cysteine ligase modulatory subunit (GCLM; 197 bp); 5′-CGT GGA CAC CCG ATG CAG TAT TCT G-3′ and 5′-GGG TCG CTT TTA CCT CCA CTG TAC T-3′ for glutamate-cysteine catalytic subunit (GCLC; 261 bp); 5′-CCT GGG CAT CTG AAA CCT TTT GAG AC-3′ and 5′-GCG AGC CAC ATA GGC AGA GAG C-3′ for glutathione *S*-transferase (GST; 180 bp). Glyceraldehyde 3-phosphate dehydrogenase (GAPDH) was used as an internal control in all cases, and its primer sequence was 5′-AAC GGA TTT GGC CGT ATT GG-3′ and 5′-CTT CCC GTT CAG CTC TGG G-3′ (657 bp). SYBR green signal was detected by Mx3000ptm multiplex quantitative PCR machine (Applied Bioscience, Foster City, CA). The transcript levels were quantified by using $\Delta\Delta C_t$ value method [18]. Calculations were done using the C_t value of GAPDH to normalize the C_t value of target genes in each sample to obtain the ΔC_t values which were used to compare among different samples. PCR products were analyzed by gel electrophoresis and melting curve analysis to confirm specific amplifications.

2.10. Neurite Outgrowth Assay. PC12 cells were treated with SBL or NGF for 72 hours. A light microscope (Diagnostic Instruments, Sterling Heights, MI) equipped with a phase-contrast condenser (Zeiss), 10X objective lens, and a digital camera (Diagnostic Instruments) was used to capture the image with manual setting. For analyzing the number and length of neurite, approximately 100 cells were counted from at least 10 randomly chosen visual fields for each culture. Using the Photoshop software, the number and length of neurite were analyzed. The cells were scored as differentiated if one or more neurites were longer than the diameter of the cell body, and they were also classified into different groups according to the lengths of neurites, which are <15 μm, 15–30 μm, and >30 μm.

2.11. Western Blot Analysis. After the indicated time of treatment, cultures were collected in the high salt lysis buffer (10 mM HEPES, pH 7.5, 1 M NaCl, 1 mM EDTA, 1 mM EGTA, 0.5% Triton X-100, 5 mM benzamidine HCl, 10 μM aprotinin, 10 μM leupeptin) and were analyzed immediately or stored frozen at −20°C. Proteins were separated on the 8% SDS-polyacrylamide gels and transferred to the nitrocellulose membrane. Successful transfer and equal loading of samples were confirmed by staining Ponceau-*S*. The nitrocellulose membrane was blocked with 5% fat-free milk in TBS-T

Table 1: Chemical composition of volatile oil from NRR.

Retention time (min)	Compound[a]	Molecular weight	RA (%)[b]
8.34	β-maaliene	204	7.9
8.62	9-aristolene	204	4.7
9.08	Calarene	204	37.9
9.29	α-maaliene	204	1.2
9.58	Guaia-6,9-diene	204	0.7
9.77	Valerena-4,1(11)-diene	204	6.6
10.79	α-humulene	204	1.6
12.49	Epi-α-selinene	204	1.5
14.64	β-lonone	192	2.1
15.08	4-epi-α-maaliol	222	1.9
19.24	Patchouli alcohol	222	5.5
19.68	Guaina-6,9-diene-4 β ol	220	3.7
22.44	Eudesma-3,11-dien-2-one	218	1.7
23.93	Aristolone	218	2.1

[a]The identified constituents are listed in their order of elution.
[b]RA indicates relative amount (peak area relative to the total peak area).
The extraction efficiency of NRR oil was over 95% within the 4 hours of distillation. In addition, the amount of extracted oil was $2.1 \pm 0.28\%$ ($n = 4$). The values are in mean of three individual experiments ($n = 3$). The SD values were less than 5% of the mean, not shown for clarity.

(20 mM Tris base, 137 mM NaCl, 0.1% Tween-20, pH 7.6) for 2 hours at room temperature, and then it was incubated in the primary antibody diluted in 2.5% fat-free milk in TBS-T for 16 hours at 4°C. The primary antibodies used were antiNF200 (Sigma), antiNF160 (Sigma), antiNF68 (Sigma), and antiGAPDH (Calbiochem, Germany). After that, the nitrocellulose was rinsed with TBS-T and incubated for 2 hours at the room temperature in horseradish peroxidase conjugated goat antimouse secondary antibody (Invitrogen) diluted in the 2.5% fat-free milk in TBS-T. After intensive washing with TBS-T, the immune complexes were visualized using the enhanced chemiluminescence (ECL) method (GE Healthcare, Piscataway, NJ). The intensities of the bands in the control and different samples were run on the same gel and under strictly standardized ECL conditions and compared on an image analyzer using a calibration plot constructed from a parallel gel with serial dilutions of one of the samples.

2.12. Other Assays. The protein concentrations were measured routinely by Bradford's method with kit from Bio-Rad Laboratories (Hercules, CA). Statistical tests were done by using one-way analysis by student's t-test on Prism 4.00. Differences from basal or control values (as shown in the plots) were classed as significant (*) where $P < 0.05$, (**) where $P < 0.01$.

3. Results

3.1. Chemical Analysis of SBL. According to the ancient method of preparation, two extracts were obtained from NRR extraction: (i) NRR extract without volatile oil, that is, NRR extract; and (ii) NRR plus volatile oil, that is, SBL. Both NRR and oil extracts were chemically standardized. The volatile oil from NRR was analyzed by GC-MS: 14 components were identified, which accounted for 79.1% of the total volatile oil. The amount of volatile oil within NRR was $2.1 \pm 0.28\%$ ($n = 4$), and the relative amounts of each chemical were given (Table 1). The major components of the oil were calarene (37.9%), β-maaliene (7.6%), and 9-aristolene (5.1%). Thus, a standardized NRR volatile oil should contain at least the chemicals as stated here. To standardize the water extract of NRR, HPLC fingerprint was generated. The amount of NRR extract from crude herb was $13.34 \pm 0.45\%$ ($n = 4$). The fingerprints of five different batches of NRR extract were compared, and this showed the consistence of the herbal extract (Figure 1). Ferulic acid and linarin were determined as chemical markers: these chemicals were reported to have known biological functions as described previously [19–21]. The quantification of chemical markers was carried out by measuring the peak area according to the regression equation (see Table 1 in Supplementary Material available online at http://dx.doi.org/10.1155/2013/687958). Using the established HPLC method, the calibration curves of ferulic acid and linarin exhibited good linearity within a specific range of concentration. The correlation coefficients (r^2) of those chemical markers were higher than 0.999. The limit of detection (LOD) and limit of quantification (LOQ) were determined at S/N of 3 and 10, respectively (Supplementary Table 1). The precision and repeatability of the chemical measurement were excellent, having a relative standard deviation (RSD) <5% (Supplementary Table 2). The recovery experiment was carried out to evaluate the method accuracy. The recoveries of ferulic acid and linarin were 99.31% and 100.12%, respectively. Thus, the employed HPLC method was validated by in performing the quantitative analysis. Here, we recommended that a standardized NRR extract should

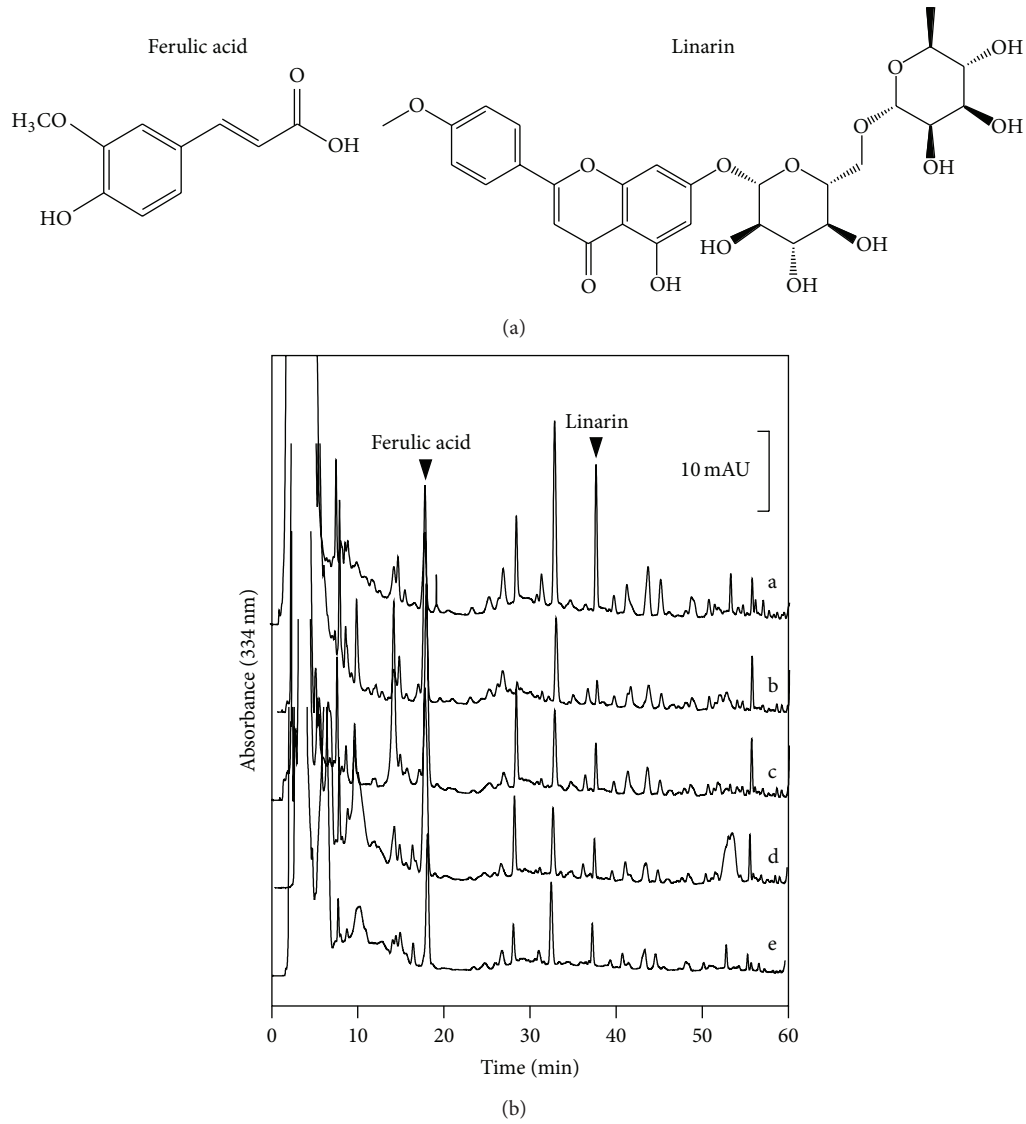

Figure 1: Chemical standardization of SBL by HPLC fingerprint analysis. Chemical structures of ferulic acid and linarin were shown (a). In the HPLC chromatogram at an absorbance of 334 nm (b), the peaks corresponding to ferulic acid and linarin in SBL are indicated by arrowheads. The fingerprints of different batches of NRR extracts (a–e) that were collected from (a) Songpan, (b) Abei, (c) Hongyuan, (d) Wing Lee Hong (HK), and (e) Wong Chak Kee (HK) of China are shown. The chromatographic method was described in Section 2. Representative chromatograms are shown, $n = 3$.

contain at least 24.8 μg ferulic acid and 114.9 μg linarin in 1 g of dried NRR extract. A well-standardized SBL was prepared with the mixture of NRR extract and volatile oil in a ratio of 6 (NRR water extract; w) : 1 (NRR volatile oil; v).

3.2. SBL on tBHP-Treated PC12 Cells. To elucidate the function of NRR extract and SBL, the herbal extract was applied onto cultured PC12 cells. Firstly, the concentrations (3–12 μg/mL) of applied SBL did not show cytotoxicity or proliferating effect on the cultures (Supplementary Figure 1). The cell viability, determined by MTT assay, was significantly decreased by tBHP in dose-dependent manner (Figure 2(a)). Cultured PC12 cells were pretreated with SBL (3–12 μg/mL) for 24 hours before the challenged tBHP. Higher concentrations (6 and 12 μg/mL) of SBL showed significant protection effect against the tBHP-induced cell death (Figure 2(b)). The applications of NRR extract (6 μg/mL) and volatile oil (2 μg/mL) in the cultures did not show any effect. Higher dose of NRR extract (12 μg/mL) showed the protection effect which, however, was lower than that of SBL (Figure 2(b)). Thus, the protection effect of SBL was better than that of NRR extract and volatile oil. The tBHP-induced cell mortality in PC12 cells was markedly reduced by the pretreatment of vitamin C, a positive control (Figure 2(b)).

The formation of ROS is one of the crucial causes in inducing neuronal cell death. By determining the formation of ROS in tBHP-treated PC12 cells, the role of SBL was

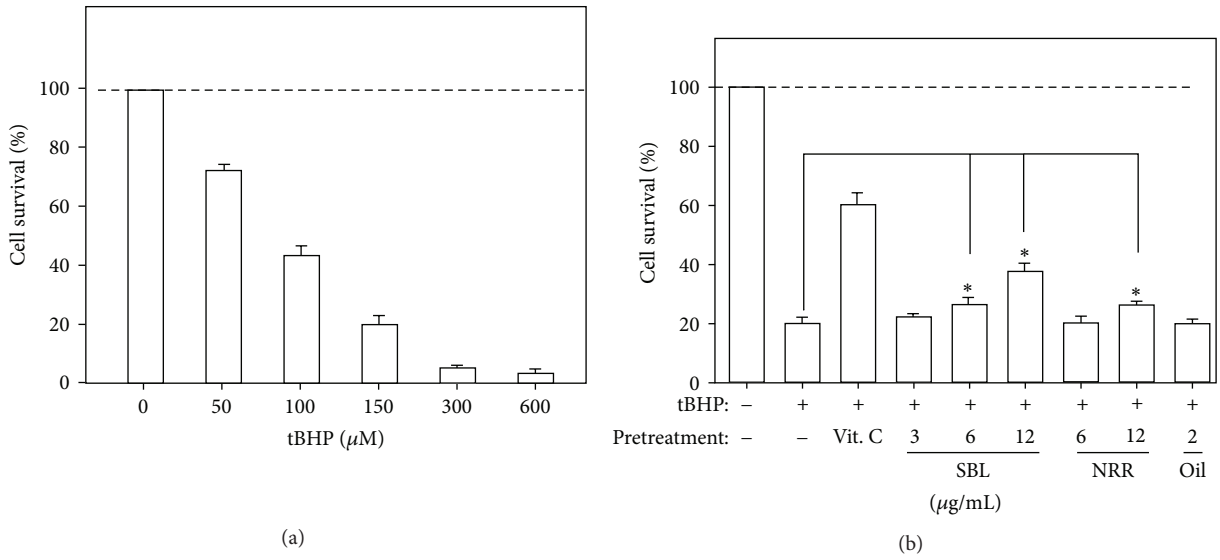

Figure 2: SBL prevents cell death in tBHP-treated PC12 cells. (a) Cultured PC12 cells were treated with tBHP (0–600 μM) for 3 hours to determine the cytotoxicity of tBHP by cell viability assay. (b) PC12 cells were pretreated with SBL (3–12 μg/mL), NRR (6 and 12 μg/mL) and volatile oil (2 μg/mL) for 24 hours before the addition of tBHP (150 μM) for 3 hours. The neuroprotective effect of SBL by cell viability assay was shown. Vitamin C (1 mM) served as a positive control. The viability of PC12 cells is shown in percentage of MTT value relative to normal control. Data are expressed as Mean ± SEM, where $n = 5$, each with triplicate samples. $^{*}P < 0.05$ and $^{**}P < 0.01$ as compared to the group (with tBHP alone).

analyzed. Application of tBHP in cultured PC12 cells induced the ROS formation in dose-dependent manner (Figure 3(a)). The tBHP-induced ROS formation was reduced by ~25% after the pretreatment of tBHQ, a known antioxidant. SBL, NRR extract and volatile oil were applied for 24 hours before the addition of tBHP (100 μM), and then the cultures were subjected to the determination of intracellular ROS formation. Pretreatment of SBL reduced tBHP-induced ROS formation in dose-dependent manner: the maximal reduction at ~40% was revealed after the treatment of 12 μg/mL SBL (Figure 3(b)). Although NRR extract (12 and 6 μg/mL) showed the reduction effect in ROS formation, compared with SBL, the reduction efficacy was not as good as SBL. Pretreatment of volatile oil (2 μg/mL) did not show any reduction effect.

ARE is a *cis*-acting regulatory element or enhancer sequence, which is found in promoter regions of genes encoding detoxifying enzymes and antioxidant proteins [12]. To study the signaling mechanism of SBL in neuroprotection, the transcriptional activity of ARE, triggered by SBL, was studied. PC12 cells were stably transfected with a promoter-reporter construct containing four repeats of ARE tagged with luciferace reporter gene (pARE-Luc) (Figure 4(a)). The pARE-Luc stably transfected PC12 cells were treated with SBL, NRR extract, and volatile oil for 24 hours, and then the cell lysates were collected to determine the luciferase activity. The application of SBL increased the transcriptional activity of pARE-Luc in dose-dependent manner, in which the maximal induction at ~5-fold was revealed at 12 μg/mL SBL (Figure 4(a)). NRR extract showed similar gene activation but at lower extend. NRR volatile oil could not increase the luciferase activity (Figure 4(a)). Based on the results of pARE-Luc activation, we investigated the role of SBL in the expression of detoxifying enzymes that were stimulated by the responsive element ARE. The ARE-derived genes, including GST, GCLC, GCLM, and NQO1, were investigated via real-time qPCR. Cultured PC12 cells were treated with SBL (12 μg/mL) for 24 hours. The levels of GST and GCLC mRNA were increased by ~3-fold with treatment of SBL. The expression level of GCLC was increased by ~2-fold. In the regulation of NQO1 expression, SBL showed a robust induction of NQO1 mRNA by over ~4-fold (Figure 4(b)). This gene induction was better than that of tBHQ (3 μM), a positive control.

3.3. SBL on the Differentiation of PC12 Cells. Neuronal differentiation effect of SBL on cultured PC12 cells was analyzed. After the treatment of NGF (50 ng/mL), the morphological change was observed. Longer neurites were protruded from the cell bodies (Figure 5(a)). This NGF treatment resulted in a 100% conversion of differentiated cells containing significant extension of neruites (Figure 5(b)). To evaluate the efficacies of SBL on PC12 differentiation, cells were treated with SBL (12 μg/mL) for 72 hours to induce a slight increase of neurite outgrowth with a conversion of differentiated cell by ~20% (Figures 5(a) and 5(b)). Here, we aimed to determine the treatment of SBL together with low dose of NGF. A low concentration of NGF at 0.5 ng/mL failed to induce the neurite extension (Figure 5(a)). However, the cotreatment of SBL with low dose of NGF significantly potentiated the number of differentiated cell (at ~60%) as well as the neurite outgrowth (Figure 5(b)).

The SBL-induced neurofilament expression was also determined. After the treatment of SBL for 72 hours, the cells

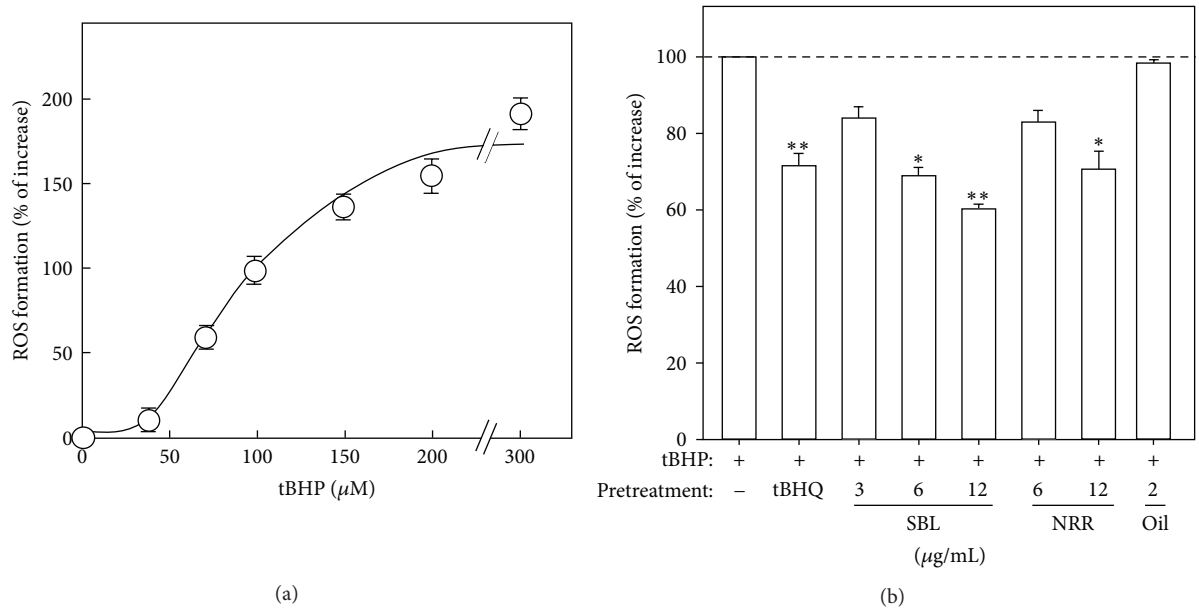

Figure 3: SBL suppresses the tBHP-induced ROS formation in PC12 cells. (a) Cultured PC12 cells were exposed to tBHP (0–300 μM) for 1 hour. The level of intracellular ROS formation was measured by fluorescence method. The results are shown in percentage of increase in ROS formation relative to the control (without tBHP). (b) Cultured PC12 cells were pretreated with SBL (3–12 μg/mL), NRR (6 and 12 μg/mL), and volatile oil (2 μg/mL) for 24 hours and then exposed to tBHP (100 μM) for 1 hour. The pretreatment of tBHQ (3 μM) was used for comparison. The results are shown in percentage of ROS formation relative to the control (with tBHP alone). Data are expressed as Mean ± SEM, where $n = 5$, each with triplicate samples. $^{*}P < 0.05$ and $^{**}P < 0.01$ as compared to the group (with tBHP alone).

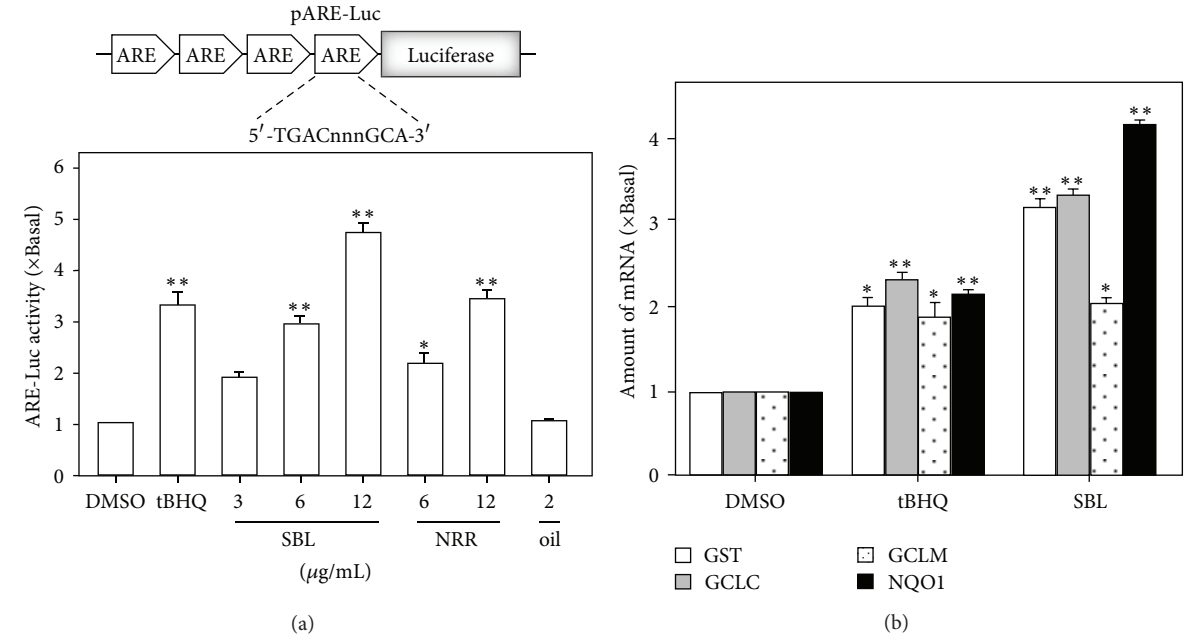

Figure 4: SBL induces ARE transcriptional activity and detoxifying enzymes in PC12 cells. (a) Four repeats of antioxidant responsive element (ARE: 5′-TGACnnnGCA-3′) tagged with luciferase-reporter vector called pARE-luc (upper panel). This reporter was stably transfected to PC12 cells, which were treated with SBL, NRR, and volatile oil for 24 hours (lower panel). tBHQ (3 μM) was used as a positive control. (b) Cultured PC12 cells treated with SBL (12 μg/mL) and tBHQ (3 μM) for 24 hours. Total RNAs were isolated from cultured PC12 cells and then reversed transcribed into cDNAs for the detection of mRNAs encoding for GST, GCLC, GCLM, and NQO1 by real-time PCR analysis. The GAPDH served as internal control. Values are expressed as the fold of increase to basal reading (untreated culture), and in Mean ± SEM, where $n = 4$, each with triplicate samples. $^{*}P < 0.05$ and $^{**}P < 0.01$.

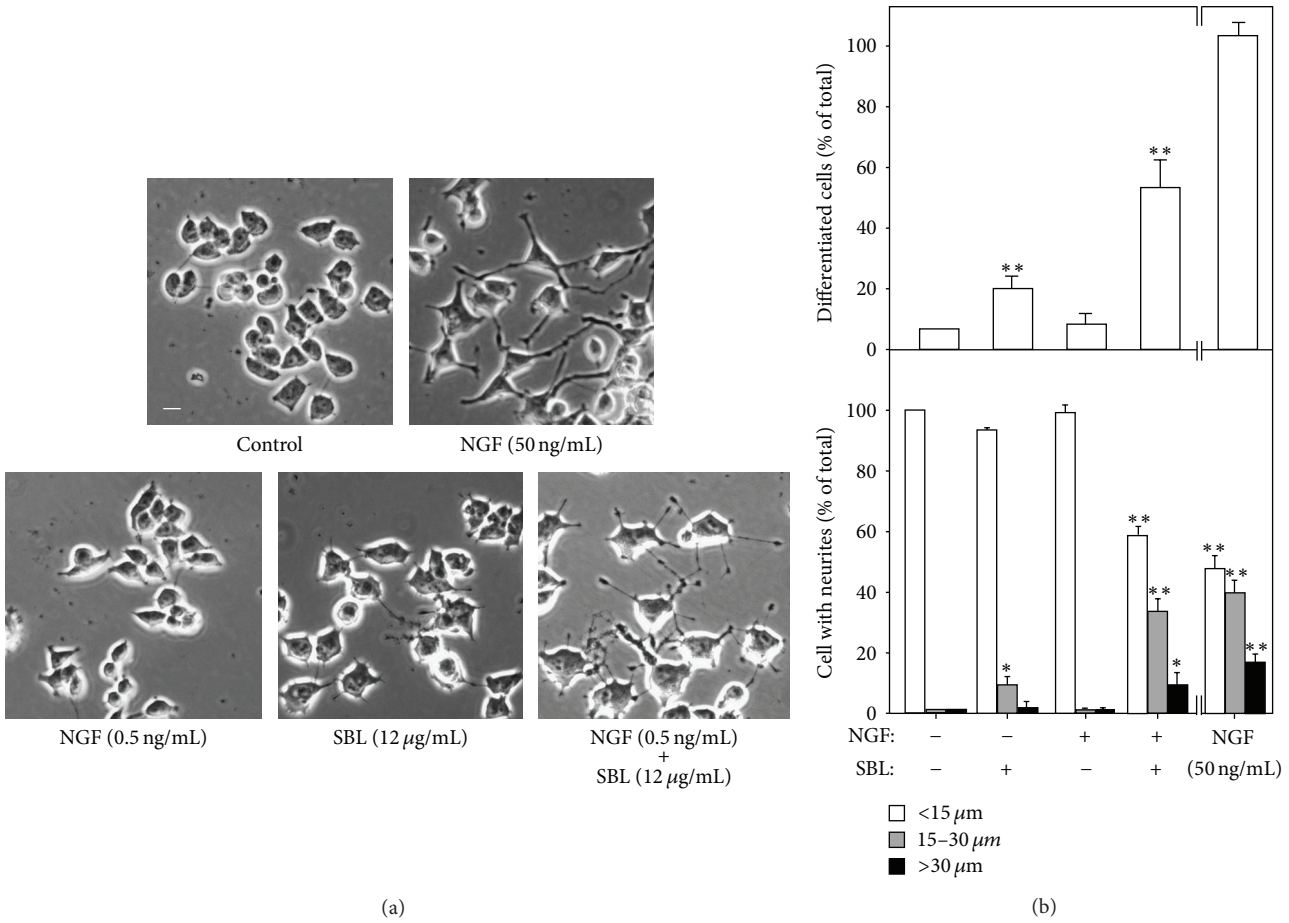

Figure 5: SBL potentiates the NGF-induced neurite outgrowth. (a) PC12 cells were treated with NGF (0.5 ng/mL and 50 ng/mL), SBL (12 μg/mL), and NGF (0.5 ng/mL) + SBL (12 μg/mL) for 72 hours. The cultures were fixed, and extension of neurite outgrowth was revealed. Bar = 10 μm. (b) The % of differentiated cell (upper panel) and length of neurite (lower panel) were counted as described in Section 2. Values are expressed as % of cells in 100 counted cells. Mean ± SEM, where $n = 4$. $^{*}P < 0.05$ and $^{**}P < 0.01$ compared with control.

were collected to perform western blot analysis to determine the expressions of NF68, NF160, and NF200. By treatment of 12 μg/mL SBL, the expression of NF68 was increased by ~5-fold, while NF160 and NF200 were altered by ~4-fold (Figure 6). The induction of neurofilament was also revealed in the cotreatment of SBL with low dose of NGF. High dose of NGF, a positive control, showed robust protein induction. The expression of control protein GAPDH remained unchanged (Figure 6).

4. Discussion

SBL decoction is one of the simplest herbal medicinal preparations of TUM containing only one herb NRR. Based on TUM theory, SBL can be used to treat functional reduction of brain and heart caused by wet-cold and phlegm [2, 22]. In line to ancient usage of SBL, here, we provided different lines of evidence to support the role of SBL in brain functions. First, SBL prevented the tBHP-induced cell death, which most likely was mediated by a reduction of ROS formation. Second, SBL induced the pARE-Luc activity as well as the gene activation of the key antioxidative stress proteins. Third, SBL induced differentiation of PC12 and the extension of neurites. More robustly, the cotreatment of SBL with NGF significantly induced the neuronal differentiation of PC12 cells. In parallel, the SBL-induced PC12 differentiation was shown to have a marked increase of neurofilament expression. These results strongly support the notion of SBL in treating neurasthenia clinically.

According to TUM practitioner's practice, two SBL preparation methods are performed in Xinjiang. The only difference between these two preparation methods is the collection of the vapor (i.e., volatile oil) during the boiling process. Indeed, NRR is well known to possess high amount of volatile oil [23]. To guarantee the consistency of SBL preparation chemically, we standardized both water extract and volatile oil of NRR. The amount of NRR extract and volatile oil within NRR by weight were 13.34% and 2.1%, respectively. According to this ratio, NRR water extract and volatile oil were mixed together in the ratio of 6 : 1 (w : v) to generate an authentic decoction of SBL. Here, we compared the biological

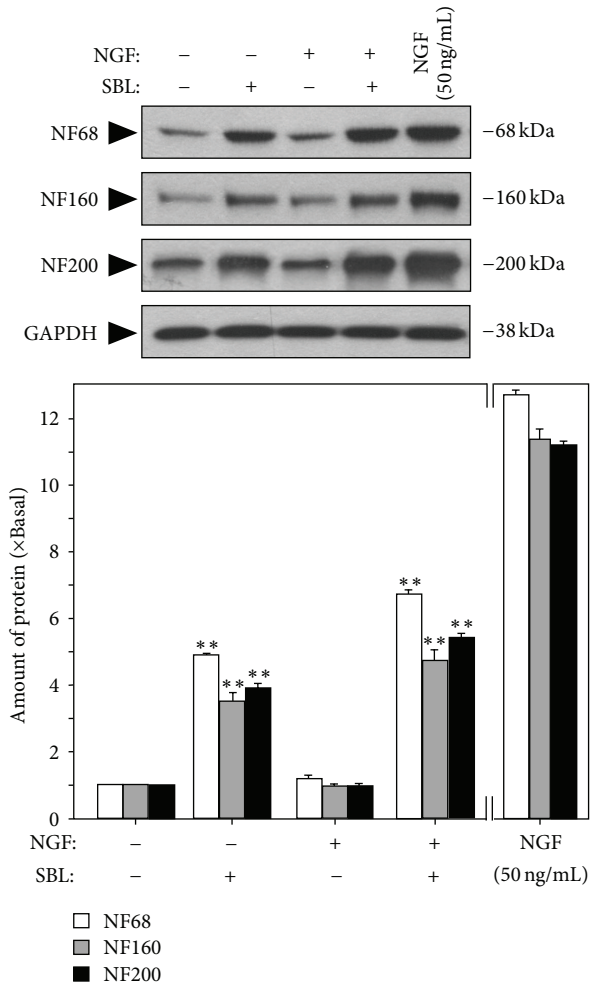

Figure 6: SBL potentiates the expression of neurofilaments. Cultured PC12 cells were treated with control, NGF (0.5 ng/mL or 50 ng/mL), SBL (12 μg/mL), and NGF (0.5 ng/mL) + SBL (12 μg/mL) for 72 hours. The cultures were collected to determine the change of neurofilaments expression (NF68, NF160, and NF200). NGF at 50 ng/mL was set as the positive control. GAPDH served as a loading control. Representative images are shown (upper panel). The lower panel shows the quantification from the blots by a densitometer. Values are expressed as the fold of change (x Basal) against the control (no treatment; set as 1), and in Mean ± SEM, where $n = 4$.

efficacy of NRR extract, volatile oil, and SBL. Our results suggested that SBL in general showed better effects than that of NRR extract. Interestingly, volatile oil alone had no biological effect. This synergetic effect of volatile oil and NRR water extract was fully revealed in the case of SBL. Thus, a completed preparation (i.e., NRR water extract + volatile oil) of SBL is recommended for decoction preparation.

The redox-sensitive transcription factor NF-E2-related factor-2 (Nrf2) has been demonstrated to be a critical transcription factor that binds to antioxidant response element (ARE) in the promoter region of genes that code for phase II detoxifying enzymes in several types of cells. Activation of phase II detoxifying enzymes, such as GST, GCLM, GCLC, and NQO1, by phytochemicals resulted in detoxifying ROS [24]. As demonstrated here, the antioxidative role of SBL could be in several aspects: (i) suppressing the formation of ROS, (ii) inducing the gene activation of pARE-Luc, and (iii) inducing antioxidative stress proteins. Amongst different antioxidative stress proteins, GST is involved in the detoxification of free radicals through catalyzing the conjugation of GSH: this is considered as one of the key enzymes associated with chemoprevention [11]. GSH is synthesized by the consecutive action of two enzymes, GCLC and GCLM [12]. Moreover, NQO1, a well-known Nrf2-ARE regulated enzyme, protects cells against deleterious reactive semiquinones by converting exogenous quinones into hydroquinones through two-electron reduction pathway [25]. Thus, the pretreatment of SBL protected the cells against oxidative-stress-induced cell death by scavenging ROS and activating the Nrf2-ARE self-defense mechanism.

Differentiation is a vital process for maturation of neuronal cells. When neurons differentiate, the neuron cell body (soma) would protrude long neurites in order to connect with other neurons to form synapses. Most of the neurological disorders are caused by the deficit of synaptic formation. During the neuronal differentiation, the expression level of neurofilaments and the neuronal cell specific cytoskeleton proteins, including 68, 160, 200 (kDa), were increased [14, 15]. In general, NF68 is expressed at the beginning of neurite outgrowth; then, NF160 is expressed shortly after with the emergence of neurite formation, and NF200 is expressed later when axonal radial growth is required for nervous system maturation. After the treatment of SBL, both neuron differentiation and expression of neurofilaments were promoted. More robustly, SBL showed a significant effect in potentiating the NGF-mediated neurite-inducing activity. A lot of neurological diseases are found to be associated with insufficiency of neurotropic factors, for example, depression [26] and Alzheimer's [27]. Neuronal cell death was found in depressed brain [28, 29]. Additionally, ROS also caused the hippocampal neurons loss [30]. In depressed brain, the secretion of neurotrophic factors could be reduced, and the neuron could not survive, grow, or differentiate normally [31]. For the property of potentiation effect on NGF-mediated neurite outgrowth, SBL would have the potential to be used to treat the differentiation obstruction caused by NGF deficiency. Besides, our preliminary results also suggested the induction of various trophic factors by SBL in cultured astrocytes (data not shown).

Reports of antioxidant and neuroprotective effect of NRR have been published [32, 33]. Lyle et al. [34] reported that NRR alleviated the symptoms of chronic fatigue syndrome (CFS) with the role of antioxidant properties of NRR. Here, our results supported the notion that functional roles of SBL might be derived from its antioxidant properties. Phenolic components have strong antioxidant role as a hydrogen ion donor, and our colorimetric study showed that SBL extract contains relatively high amount of phenolic compounds. In addition, ferulic acid and linarin were shown to have protective effect on neurons [19, 21]. In our study, ferulic acid and linarin showed promising effect in reducing the intracellular ROS formation (data not shown). On the other hand, the volatile oils of SBL are a mixture of lipids, terpenoids, ketones,

and phenols. β-Maaliene, aristolene, and calarene, isolated from NRR, were reported to have a strong sedative and sleep enhancing activity [35]: these chemicals account for 57.1% of total volatile oil of SBL. Moreover, a partially purified glycoside from NRR was able to induce the outgrowth of neurites and the expression of growth-associated protein 43 (GAP-43) [36]. Thus, the distinctive properties of SBL could depend on the synergistic effects of total phenols, terpenoids, and/or other chemical components in SBL.

5. Conclusion

In summary, our study focused on the neuro-beneficial role of SBL, a simple ancient TUM, in cultured PC 12 cells. We found that pretreatment of a chemically standardized SBL could protect the cells from oxidative stress, which could be mediated by scavenging of ROS formation and stimulating the Nrf2-ARE self-defense mechanism. In addition, SBL could increase the expression of neurofilaments in cultured PC 12 cells and potentiated the NGF-mediated neurite outgrowth. Lastly, we demonstrated that the inclusion of volatile oil is necessary for a complete function of SBL. Taken together, these results partially revealed the action mechanism of SBL by cell studies.

Acknowledgments

This research was supported by the Hong Kong Research Grants Council Theme-based Research Scheme (T13-607/12R) and GRF (661110, 662911, 663012), and the Foundation of The Awareness of Nature (TAON12SC01) to KWKT.

References

[1] A. Yusup, H. Upur, I. Baudrimont et al., "Inhibition of cell growth and cellular protein, DNA and RNA synthesis in human hepatoma (HepG2) cells by ethanol extract of abnormal Savda Munziq of traditional Uighur medicine," *Evidence-Based Complementary and Alternative Medicine*, vol. 2011, Article ID 251424, 9 pages, 2011.

[2] M. Yishakejiang, K. Abudureyimu, and R. Abulake, *China Medical Encyclopedia-Uyghur Medicine Volume*, Shanghai Science and Technology Press, Shanghai, China, 2005.

[3] D. Maquet, C. Demoulin, and J.-M. Crielaard, "Chronic fatigue syndrome: a systematic review," *Annales de Readaptation et de Medecine Physique*, vol. 49, no. 6, pp. 418–427, 2006.

[4] Y. Cao, Y. Zhang, D. F. Chang, G. Wang, and X. Zhang, "Psychosocial and immunological factors in neurasthenia," *Psychosomatics*, vol. 50, no. 1, pp. 24–29, 2009.

[5] S. B. Harvey, S. Wessely, D. Kuh, and M. Hotopf, "The relationship between fatigue and psychiatric disorders: evidence for the concept of neurasthenia," *Journal of Psychosomatic Research*, vol. 66, no. 5, pp. 445–454, 2009.

[6] M. F. Beal, "Oxidatively modified proteins in aging and disease," *Free Radical Biology and Medicine*, vol. 32, no. 9, pp. 797–803, 2002.

[7] J. T. T. Zhu, R. C. Y. Choi, J. Li et al., "Estrogenic and neuroprotective properties of scutellarin from erigeron breviscapus: a drug against postmenopausal symptoms and alzheimer's disease," *Planta Medica*, vol. 75, no. 14, pp. 1489–1493, 2009.

[8] J. T. T. Zhu, R. C. Y. Choi, H. Q. Xie et al., "Hibifolin, a flavonol glycoside, prevents β-amyloid-induced neurotoxicity in cultured cortical neurons," *Neuroscience Letters*, vol. 461, no. 2, pp. 172–176, 2009.

[9] J. T. Coyli and P. Puttfarcken, "Oxidative stress, glutamate, and neurodegenerative disorders," *Science*, vol. 262, no. 5134, pp. 689–695, 1993.

[10] M. Ebadi, S. K. Srinivasan, and M. D. Baxi, "Oxidative stress and antioxidant therapy in Parkinson's disease," *Progress in Neurobiology*, vol. 48, no. 1, pp. 1–19, 1996.

[11] A. Pompella, A. Visvikis, A. Paolicchi, V. De Tata, and A. F. Casini, "The changing faces of glutathione, a cellular protagonist," *Biochemical Pharmacology*, vol. 66, no. 8, pp. 1499–1503, 2003.

[12] J. M. Lee and J. A. Johnson, "An important role of Nrf2-ARE pathway in the cellular defense mechanism," *Journal of Biochemistry and Molecular Biology*, vol. 37, no. 2, pp. 139–143, 2004.

[13] S. Dhakshinamoorthy, A. K. Jain, D. A. Bloom, and A. K. Jaiswal, "Bach1 competes with Nrf2 leading to negative regulation of the antioxidant response element (ARE)-mediated NAD(P)H:quinone oxidoreductase 1 gene expression and induction in response to antioxidants," *Journal of Biological Chemistry*, vol. 280, no. 17, pp. 16891–16900, 2005.

[14] J. Schimmelpfeng, K.-F. Weibezahn, and H. Dertinger, "Quantification of NGF-dependent neuronal differentiation of PC-12 cells by means of neurofilament-L mRNA expression and neuronal outgrowth," *Journal of Neuroscience Methods*, vol. 139, no. 2, pp. 299–306, 2004.

[15] S. L. Xu, R. C. Y. Choi, K. Y. Zhu et al., "Isorhamnetin, a flavonoid aglycone from *Ginkgo biloba* L., induces neuronal differentiation of cultured PC12 cells: potentiating the effect of nerve growth factor," *Evidence-Based Complementary and Alternative Medicine*, vol. 2012, Article ID 278273, 11 pages, 2012.

[16] M. K. Lee and D. W. Cleveland, "Neuronal intermediate filaments," *Annual Review of Neuroscience*, vol. 19, pp. 187–217, 1996.

[17] J. T. T. Zhu, R. C. Y. Choi, G. K. Y. Chu et al., "Flavonoids possess neuroprotective effects on cultured pheochromocytoma PC12 cells: a comparison of different flavonoids in activating estrogenic effect and in preventing β-amyloid-induced cell death," *Journal of Agricultural and Food Chemistry*, vol. 55, no. 6, pp. 2438–2445, 2007.

[18] J. Winer, C. K. S. Jung, I. Shackel, and P. M. Williams, "Development and validation of real-time quantitative reverse transcriptase-polymerase chain reaction for monitoring gene expression in cardiac myocytes *in vitro*," *Analytical Biochemistry*, vol. 270, no. 1, pp. 41–49, 1999.

[19] J. Kanski, M. Aksenova, A. Stoyanova, and D. A. Butterfield, "Ferulic acid antioxidant protection against hydroxyl and peroxyl radical oxidation in synaptosomal and neuronal cell culture systems *in vitro* structure-activity studies," *Journal of Nutritional Biochemistry*, vol. 13, no. 5, pp. 273–281, 2002.

[20] S. Fernández, C. Wasowski, A. C. Paladini, and M. Marder, "Sedative and sleep-enhancing properties of linarin, a flavonoid-isolated from *Valeriana officinalis*," *Pharmacology Biochemistry and Behavior*, vol. 77, no. 2, pp. 399–404, 2004.

[21] H. Lou, P. Fan, R. G. Perez, and H. Lou, "Neuroprotective effects of linarin through activation of the PI3K/Akt pathway in amyloid-β-induced neuronal cell death," *Bioorganic and Medicinal Chemistry*, vol. 19, no. 13, pp. 4021–4027, 2011.

[22] J. N. Lu, "Study on the traditional Uyghur medicine Song Bu Li decoction," *Journal of Medicine & Pharmacy of Chinese Minorities*, vol. 9, pp. 13–14, 2003.

[23] J. H. Wang, J. Zhao, H. Liu et al., "Chemical analysis and biological activity of the essential oils of two valerianaceous species from China: *Nardostachys chinensis* and *Valeriana officinalis*," *Molecules*, vol. 15, no. 9, pp. 6411–6422, 2010.

[24] J. A. Johnson, D. A. Johnson, A. D. Kraft et al., "The Nrf2-ARE pathway: an indicator and modulator of oxidative stress in neurodegeneration," *Annals of the New York Academy of Sciences*, vol. 1147, pp. 61–69, 2008.

[25] D. Ross, J. K. Kepa, S. L. Winski, H. D. Beall, A. Anwar, and D. Siegel, "NAD(P)H:quinone oxidoreductase 1 (NQO1): chemoprotection, bioactivation, gene regulation and genetic polymorphisms," *Chemico-Biological Interactions*, vol. 129, no. 1-2, pp. 77–97, 2000.

[26] Y. Dwivedi, A. C. Mondal, H. S. Rizavi, and R. R. Conley, "Suicide brain is associated with decreased expression of neurotrophins," *Biological Psychiatry*, vol. 58, no. 4, pp. 315–324, 2005.

[27] S. Capsoni and A. Cattaneo, "On the molecular basis linking Nerve Growth Factor (NGF) to Alzheimer's disease," *Cellular and Molecular Neurobiology*, vol. 26, no. 4–6, pp. 619–633, 2006.

[28] H. K. Manji, W. C. Drevets, and D. S. Charney, "The cellular neurobiology of depression," *Nature Medicine*, vol. 7, no. 5, pp. 541–547, 2001.

[29] R. S. Duman, "Depression: a case of neuronal life and death?" *Biological Psychiatry*, vol. 56, no. 3, pp. 140–145, 2004.

[30] A. L. Lee, W. O. Ogle, and R. M. Sapolsky, "Stress and depression: possible links to neuron death in the hippocampus," *Bipolar Disorders*, vol. 4, no. 2, pp. 117–128, 2002.

[31] Y. Shirayama, A. C.-H. Chen, S. Nakagawa, D. S. Russell, and R. S. Duman, "Brain-derived neurotrophic factor produces antidepressant effects in behavioral models of depression," *Journal of Neuroscience*, vol. 22, no. 8, pp. 3251–3261, 2002.

[32] S. Salim, M. Ahmad, K. S. Zafar, A. S. Ahmad, and F. Islam, "Protective effect of *Nardostachys jatamansi* in rat cerebral ischemia," *Pharmacology Biochemistry and Behavior*, vol. 74, no. 2, pp. 481–486, 2003.

[33] M. B. Khan, M. N. Hoda, T. Ishrat et al., "Neuroprotective efficacy of *Nardostachys jatamansi* and crocetin in conjunction with selenium in cognitive impairment," *Neurological Sciences*, vol. 33, no. 5, pp. 1011–1020, 2012.

[34] N. Lyle, A. Gomes, T. Sur et al., "The role of antioxidant properties of *Nardostachys jatamansi* in alleviation of the symptoms of the chronic fatigue syndrome," *Behavioural Brain Research*, vol. 202, no. 2, pp. 285–290, 2009.

[35] H. Takemoto, T. Yagura, and M. Ito, "Evaluation of volatile components from spikenard: valerena-4,7(11)-diene is a highly active sedative compound," *Journal of Natural Medicines*, vol. 63, no. 4, pp. 380–385, 2009.

[36] J. H. Liu, F. Yin, and X. X. Zheng, "*Nardostachys chinensis* glycoside induces characteristics of neuronal differentiation in rat pheochromocytoma PC12 cells," *Biological and Pharmaceutical Bulletin*, vol. 28, no. 4, pp. 768–771, 2005.

Hindawi Publishing Corporation
Evidence-Based Complementary and Alternative Medicine
Volume 2013, Article ID 516741, 12 pages
http://dx.doi.org/10.1155/2013/516741

Research Article

The Aqueous Extract of Rhizome of *Gastrodia elata* Protected *Drosophila* and PC12 Cells against Beta-Amyloid-Induced Neurotoxicity

Chun-Fai Ng,[1,2] Chun-Hay Ko,[1,2] Chi-Man Koon,[1,2] Jia-Wen Xian,[3] Ping-Chung Leung,[1,2] Kwok-Pui Fung,[1,2,4] Ho Yin Edwin Chan,[5] and Clara Bik-San Lau[1,2]

[1] *Institute of Chinese Medicine, The Chinese University of Hong Kong, Shatin, New Territories, Hong Kong*
[2] *State Key Laboratory of Phytochemistry & Plant Resources in West China, The Chinese University of Hong Kong, Shatin, New Territories, Hong Kong*
[3] *School of Chinese Medicine, The Chinese University of Hong Kong, Shatin, New Territories, Hong Kong*
[4] *School of Biomedical Sciences, The Chinese University of Hong Kong, Shatin, New Territories, Hong Kong*
[5] *School of Life Sciences, The Chinese University of Hong Kong, Shatin, New Territories, Hong Kong*

Correspondence should be addressed to Clara Bik-San Lau; claralau@cuhk.edu.hk

Received 7 June 2013; Accepted 30 July 2013

Academic Editor: Paul Siu-Po Ip

This study aims to investigate the neuroprotective effect of the rhizome of *Gastrodia elata* (GE) aqueous extract on beta-amyloid(Aβ)-induced toxicity *in vivo* and *in vitro*. Transgenic *Drosophila* mutants with Aβ-induced neurodegeneration in pan-neuron and ommatidia were used to determine the efficacy of GE. The antiapoptotic and antioxidative mechanisms of GE were also studied in Aβ-treated pheochromocytoma (PC12) cells. *In vivo* studies demonstrated that GE (5 mg/g *Drosophila* media)-treated *Drosophila* possessed a longer lifespan, better locomotor function, and less-degenerated ommatidia when compared with the Aβ-expressing control (all $P < 0.05$). *In vitro* studies illustrated that GE increased the cell viability of Aβ-treated PC12 cells in dose-dependent manner, probably through attenuation of Aβ-induced oxidative and apoptotic stress. GE also significantly upregulated the enzymatic activities of catalase, superoxide dismutase, and glutathione peroxidase, leading to the decrease of reactive oxidation species production and apoptotic marker caspase-3 activity. In conclusion, our current data presented the first evidence that the aqueous extract of GE was capable of reducing the Aβ-induced neurodegeneration in *Drosophila*, possibly through inhibition of apoptosis and reduction of oxidative stress. GE aqueous extract could be developed as a promising herbal agent for neuroprotection and novel adjuvant therapies for Alzheimer's disease.

1. Introduction

Beta-amyloid (Aβ) protein plays a central role in Alzheimer's disease (AD). Although the exact mechanism of the disease is unknown, the devastating effect of beta-amyloid is quite clear. The protein would self-aggregate into a plaque [1], which lead to the generation of reactive oxygen species, disruption of membrane potential, and increased vulnerability to excitotoxicity, and eventually cause neuronal death [2] and related cognitive defects [3]. Recent report postulated an increasing prevalence of dementia all over the world, from 36 million in 2010 to 66 million by 2030, with majority of AD [4]. Nowadays, AD threatens our aging population with the possible loss of memory and cognitive functions and leads to increasingly heavy health care burden to our future economy. Despite advances in medical interventions, Alzheimer's disease is fatal, and presently, there is no cure. Due to the complexity of pathology, AD is not very responsive to current western medications [5, 6]. Increasing attentions have turned to the conventional medicinal herbs, which are multitargeting, to search for a novel way of AD treatment [7, 8].

Drosophila melanogaster was recently developed as a model organism for drug/herbal screening for neurodegenerative diseases. It provides several unique features such as highly stable and fully-known genetics, highly conserved disease pathways, high-throughput, and very low comparative costs [9]. Most of the genes implicated in human AD pathogenesis have *Drosophila* homologs, including amyloid precursor protein (APP), γ-secretase, and tau [10]. However, there are some dissimilarities, such as the absence of β-secretase, which cause a defect in endogenous production of Aβ42 [11]. In this study, the *Drosophila* models that overexpress human Aβ42 would be used. The neurodegeneration would result in reduced lifespan, reduced locomotor activity, histological change to the neuronal structure, and eye degeneration [10, 12]. These pathological phenotypes could be observed within a few weeks, much faster than the development of these phenotypes in transgenic mice [13]. Therefore, application of *Drosophila* as model of AD provides excellent tools for performing drug/herb screens to identify small molecules/herbal formula that can suppress the toxicity associated with Aβ accumulation.

There is a long history of the use of medicinal herbs in the treatment of neurological disorders, like convulsion, stroke, and epilepsy, that is, *Poria cocos*, *Polygala tenuifolia*, *Uncaria rhynchophylla*, *Ginkgo biloba*, and *Lycium barbarum* [8, 14]. Modern pharmacological studies revealed that *Ginkgo biloba* possessed neuroprotective effects towards D-galactose [15], beta-amyloid [16], and ischemia-induced neuronal death [17]. *Uncaria rhynchophylla* also prevented D-galactose [18], beta-amyloid [19], 6-hydroxydopamine [20], and kainic acid-induced neurotoxicity [21]. Similar neuroprotective effects were found in other commonly used herbs in China [22–25]. Rhizome of *Gastrodia elata* (Tianma, GE) is also one of the commonly used traditional Chinese medicines. Many studies have been performed to evaluate the neuroprotective effects of GE and its biologically active ingredients against different kinds of neuronal damages. The nonpolar extract of GE inhibited the 1-Methyl-4-phenylpyridinium and glutamate-induced apoptosis in neuronal cells [26, 27]. Additionally, the nonpolar extract of GE protected mice and rat against kainic acid [28] and aluminum chloride-induced neuronal damages [29]. Its active ingredient, gastrodin, has been shown to possess a protective effect against hypoxia injury on neurons [30]. Other active compounds, hydroxybenzyl alcohol and vanillin, could ameliorate ischemic cerebral injury in rats [31], and prevent ischemic death of hippocampal neuronal in gerbils [32], respectively. Recently, an *in vitro* study indicated that the aqueous extract of GE enhanced proteolytic processing of APP towards the noncytotoxic nonamyloidogenic pathway [33]. Previously, studies revealed that APP processing affected the production of Aβ, which strongly correlated to the neuronal degeneration in AD pathology [34]. Mishra et al. demonstrated that that GE was able to inhibit β-site APP-cleaving enzyme 1 activity and promote α-secretase activity [33]. The inhibition of β-site APP-cleaving enzyme 1 reduces the cleavage of APP into Aβ [35], and the activation of α-secretase increases the cleavage of APP into soluble-APP-α [36, 37].

Although the nonpolar extract of GE was found to have various neuroprotective effects, extraction of GE with water is the traditional way of preparing Chinese medicine for human consumption. The active ingredient content of aqueous extract and nonpolar extract is theoretically different, which aqueous extract should have a higher content of hydrophilic gastrodin and polysaccharides and a lower content of less hydrophilic ingredients, such as hydroxybenzaldehyde, hydroxybenzyl alcohol, vanillin, and vanillyl alcohol. According to the Chinese pharmacopeia 2010, aqueous extract of GE is a traditional Chinese medicine that is widely used for treatment of convulsive disorders, headache, dizziness, and vertigo [38]. However, there is a lack of scientific evidence to support these medical claims. Based on these previous studies and the traditional use of GE, we hypothesize that aqueous extract of GE may also be effective in protecting neurons against beta-amyloid-induced neuronal death. Moreover, there is a lack of information relating to the *in vivo* neuroprotective effects of GE aqueous extract. In hope of finding an extract which could modulate APP cleavage and reduce neurotoxic effect from beta-amyloid, in the present study, we aimed to investigate the neuroprotective effects of GE on beta-amyloid-induced neurodegeneration in *Drosophila* and its related mechanisms using pheochromocytoma (PC12) cells. The mechanism of the neuroprotective effects of GE on the downstream pathway after the cleavage of APP to Aβ were studied, including the reactive oxygen species production and the activity of the antioxidative enzyme. The apoptosis caused by Aβ was also determined by propidium iodide (PI)/Annexin V staining and confirmed by caspase-3 activity assay.

2. Materials and Methods

2.1. Materials. $A\beta_{25-35}$ peptide, 3-(4,5-dimethylthiazol-2-yl)-2,5-diphenyltetrazolium bromide (MTT), and caspase-3 assay kit were purchased from Sigma-Aldrich (St Louis, MO, USA). RPMI medium 1640, fetal bovine serum (FBS), horse serum (HS), and 2′,7′-dichlorodihydrofluorescein diacetate (H_2DCFDA) were obtained from Invitrogen (Carlsbad, CA, USA). Annexin V-FITC and propidium iodide (PI) were obtained from BD Biosciences (San Jose, CA, USA). Superoxide dismutase and glutathione peroxidase assay kits were from Cayman Chemical (Ann Arbor, MI, USA). Catalase fluorometric detection kit was obtained from Enzo Life Sciences (Farmingdale, NY, USA). Formula 4–24 instant *Drosophila* medium was obtained from Carolina Biological Supply Company (Burlington, NC, USA).

2.2. Herbal Materials and Extraction. The raw herbs of the rhizome of *Gastrodia elata* were purchased from Chinese herbal stores in the Guangdong province in Mainland China. It was chemically authenticated using thin layer chromatography in accordance to the Chinese Pharmacopoeia 2010 and deposited in the museum of the Institute of Chinese Medicine, the Chinese University of Hong Kong, with voucher specimen number of 2010-3294. For extraction, the raw herbs Tianma were firstly washed with tap water to remove any contaminants. They were then cut into small

pieces. The herbs were soaked with 10-fold of water (v/w) for 1 h, followed by extraction at 100°C for 1 h. Subsequent extractions were carried out with 10-fold of water (v/w) for another 1 h. The extracts were combined and concentrated under reduced pressure to give dry Tianma powdered extract. Ultimately, 48.90 g of the aqueous extract was obtained from 100.00 g of raw GE herb. The content of gastrodin was determined to be 2.2% w/w using high performance liquid chromatography, according to the method listed in the Chinese Pharmacopeia 2010 [38], which is higher than the requirement of 0.2% w/w.

2.3. Drosophila Strains. *Drosophila* strains used in this study were Oregon-R-C (OR) (#5), w^{1118} (#3605), and *elav-GAL4*^{C155} (#458) (Bloomington *Drosophila* Stock Center, Department of Biology, Indiana University, Bloomington, IN, USA). *UAS-Aβ42/CyO* and *GMR-Aβ42*^{K52}*; GMR-Aβ42*^{K53} heterozygous were gifts from Dr. M. Konsolaki (Rutgers University, USA). OR is a wild type *Drosophila*. w^{1118} is a white-eye mutant with a deletion in the sex-linked white gene. *Elav-GAL4*^{C155} is a mutant with an *embryonic lethal abnormal vision (elav)-GAL4* insert on the X chromosome. *UAS-Aβ42/CyO* is a mutant with an *UAS-Aβ42* insert and a *Curly of Oster (CyO)* balancer on the 2nd chromosome. *GMR-Aβ42*^{K52}; *GMR-Aβ42*^{K53} heterozygous is a mutant with 2 copies of *Glass Multiple Reporter (GMR)-Aβ42* inserts on the 3rd chromosome.

For longevity and climbing assay, genotypes of *Drosophila* used in this study were as follows: control: *elav-GAL4*^{c155}*/Y, Aβ42: elav-GAL4*^{c155}*/Y; UAS-Aβ42/+; +/+*. *Elav-GAL4*^{C155} line was crossed with w^{1118} line to produce control. *Elav-GAL4*^{C155} line was crossed with *UAS-Aβ42/CyO* to produce *elav-GAL4*^{c155}*/Y; UAS-Aβ42/+; +/+*. The genotypes of newly hatched *Drosophila* are different between male and female. The genotype of the male offspring is *elav-GAL4*^{c155}*/Y; UAS-Aβ42/+; +/+*, while that of female offspring is *elav-GAL4*^{c155}*/w; UAS-Aβ42/+; +/+*. The existence of the wild type gene in par with our *elav-GAL4*^{c155} promoter would half the overall expression of the transgene [39]. In order to minimize the error due to genetic difference, male was chosen in the present study. For the psuedopupil assay, *Drosophila* genotypes were as follows: Control: *OR*, Aβ42: *GMR- Aβ42*^{K52}*; GMR- Aβ42*^{K53} heterozygotes.

2.4. Effect of GE on Longevity of Aβ Expressing Drosophila. Genetic crosses were performed in the vials containing the diet with treatments. The normal control, which did not express Aβ, was maintained on the normal diet. The Aβ expressing control and the positive control were maintained on the normal diet and diet containing 10 mmol donepezil/g of *Drosophila* media, respectively, whereas the two GE groups were fed with diets containing 1 or 5 mg GE/g of *Drosophila* media, respectively. Newly hatched male *Drosophila* in each group was transferred to a new vial (30 *Drosophila* per vial), continued with their respective treatments, and incubated at 25°C. Dead *Drosophila* were counted on day 1 and 5 in a 7-day cycle, and the remaining live *Drosophila* were transferred to a new vial containing the same diet. The feeding lasted for 65 days. One hundred and fifty *Drosophila* were tested for each group.

2.5. Climbing Assay. Locomotor function of *Drosophila* was measured according to the climbing assay as previously reported by Lee et al. [40] with slight modifications. In brief, 30 male *Drosophila* were placed at the bottom of a 15 mL falcon tube and were given 10 s to climb up the tube. At the end of each trial, the number of *Drosophila* that climbed up to a vertical distance of 8 cm or above was recorded. *Drosophila* were tested on day 1 and 5 in a 7-day cycle. Each trial was performed three times. One hundred and fifty *Drosophila* were tested for each group.

2.6. Pseudopupil Assay. The control and Aβ42 *Drosophila* were treated with the same treatments as described above. *Drosophila* heads were examined under a light microscope (Olympus CX31; Olympus, Tokyo, Japan) as described previously [41]. Briefly, the compound eye of 5 days old *Drosophila* was viewed under microscope in a dark field. There were eight photoreceptors in each ommatidium, and seven of them were visible. Each photoreceptor projected a darkly staining rod, the rhabdomere, into the center of the ommatidium. Under the microscope, the rhabdomeres appeared as bright spots and rhabdomeres in each ommatidium were counted. In the control group, 7 rhabdomeres could be observed in each ommatidium. One hundred ommatidia were observed from 5 to 10 eyes, and the average rhabdomeres count per ommatidium was calculated. Three trials were conducted for each group.

2.7. Cell Culture and Drug Treatment. PC12 rat pheochromocytoma cells were obtained from American Type Culture Collection (Manassas, VA, USA) and maintained in RPMI medium 1640 supplemented with 10% (v/v) heat-inactivated HS and 5% (v/v) FBS at 37°C under 95% air/5% CO_2. Cells were utilized for experiments during exponential growth.

Aβ_{25-35} was dissolved in sterile distilled water at a concentration of 1.0 mM as a stock solution and preaggregated at 37°C for 7 days prior to use. Confluent cells were trypsinized, counted, and seeded on poly-L-lysine-coated 6-well culture plates at a density of 3×10^5 cells/well and incubated for 24 h. After that, cells were treated with various concentrations of GE and 20 μM of aggregated Aβ_{25-35} for 48 h.

2.8. Cell Viability Assay. Cell viability was determined using 3-(4,5-dimethylthiazol-2-yl)-2,5-diphenyltetrazolium (MTT) assay. Briefly, the cells were plated on poly-L-lysine-coated 96-well culture plates at the density of 1×10^4 cells/well and incubated for 24 h. After that, the medium was replaced with fresh medium, and the cells were incubated with Aβ_{25-35} (1 μM) in the presence or absence of aqueous extract of GE (250-1000 μg/mL) for 48 h. Thereafter, cells were incubated with 30 μL of MTT solution (final concentration, 1.5 mg/mL) for 4 h. The supernatant was then removed and 100 μL of dimethyl sulfoxide was added to dissolve the formazan crystal. Plates were shaken for 10 min and optical

density was determined with a microplate reader at 540 nm. The optical density of control cell was 100% viability.

2.9. Flow Cytometric Detection of Apoptosis. Apoptotic cells were quantified by Annexin V-FITC and PI staining by flow cytometry. Briefly, the treated cells were trypsinized and centrifuged at 450 ×g at 25°C for 5 min. The pellet was washed twice with ice cold PBS and resuspended with Annexin V binding buffer. Annexin V-FITC and PI were added according to manufacturer's instruction and incubated in dark at room temperature for 15 min. 300 μL of binding buffer was added to each sample. The stained cells were analyzed by fluorescence-activated cell sorter (FACS). Ten thousands events were analyzed per sample.

2.10. Measurement of Apoptosis. The treated cells were collected and washed twice with ice cold PBS. PC12 cells were lysed in cell lysis buffer (50 mM Tris-HCl pH 7.4, 2 mM $MgCl_2$, 0.1% Triton X-100) with 2 freeze/thaw cycles. The supernatant was collected after centrifugation at 15,000 ×g for 3 min; after that, the total protein concentration was determined by the bicinchoninic acid (BCA) assay, using bovine serum albumin (BSA) as a standard. The samples were then applied to caspase-3 activity assays, according to manufacturer's instructions. The activities were normalized using the total protein concentrations.

2.11. Measurement of Reactive Oxygen Species (ROS) Production. The 2,7-dichlorodihydrofluorescein diacetate (H_2DCF-DA) method was used to measure intracellular ROS production. H_2DCF-DA can pass through the cell membrane and oxidized by ROS to form the fluorochrome 2′,7′dichlorofluorescein (DCF). Therefore, H_2DCF-DA was widely used to reflect the intracellular ROS content [42–44]. The treated cells were collected, washed twice with ice cold PBS, and incubated with H_2DCF-DA (20 μM) in the dark at 37°C for 15 min. Then cells were washed once with PBS and harvested for fluorescence-activated cell sorter (FACS) analysis. Ten thousands events were analyzed per sample.

2.12. Measurement of the Antioxidative Enzyme Activities. The treated cells were collected and washed twice with ice cold PBS. The cells were lysed in cell lysis buffer (50 mM Tris-HCl pH 7.4, 2 mM $MgCl_2$, 0.1% Triton X-100) with 2 freeze/thaw cycles. The supernatant was collected after centrifugation at 14,000 ×g for 3 min, after that the total protein concentration was determined by the bicinchoninic acid (BCA) assay, using bovine serum albumin (BSA) as a standard. The samples were then applied to antioxidative enzyme activity assays, including glutathione peroxidase (GPx), superoxide dismutase (SOD), and catalase (CAT), according to manufacturer's instructions. The activities were normalized using the total protein concentrations.

2.13. Statistical Analysis. Multiple group comparisons were performed using one-way analysis of variance (ANOVA) followed by Dunnett's test to detect intergroup differences. Comparisons for survival assay were performed using Log-Rank analysis and chi-square comparison.

All statistical analyses were performed using GraphPad Prism version 5.0 for Windows (GraphPad Software Inc., California, USA). The data were expressed as mean ± standard deviation (SD). A value of $P < 0.05$ was considered statistically significant.

3. Results

3.1. Tianma Prolonged the Lifespan and Improved Locomotor Abilities of Aβ-Expressing Drosophila. In the present study, we evaluated the neuroprotective effect of aqueous extract of GE, using *Drosophila* AD model. Before performing the experiments, we evaluated the effect of 5 and 50 mg GE extract/g of *Drosophila* media on food intake of *Drosophila*. Both GE treatments did not affect the food intake of *Drosophila* (data not shown), which ensured no experimental differences were due to the alteration of feeding behavior. For lifespan experiment, Aβ42 *Drosophila* showed a reduction of median and maximum lifespan by 17 days and 32 days when compared with control, respectively. Both GE treatments significantly improved the survival of *Drosophila* (Figure 1(a)). At 1 mg GE extract/g of *Drosophila* media, median and maximum lifespan were increased by 4 days (12.0%) and 4 days, respectively ($P < 0.001$ for mean increases). At 5 mg GE extract/g of *Drosophila* media, median and maximum lifespan were increased by 7 days (26.9%) and 7 days, respectively ($P < 0.001$ for mean increases).

For locomotor abilities determination, Aβ42 *Drosophila* showed significant impaired locomotion from age of day 9 onwards (Figure 1(b-i)). GE-treated flies showed an improvement in locomotor activity from age of days 12 to 23. At day 12, 19, and 23, 5 mg GE extract/g of *Drosophila* media resulted in a 14.4%, 11.6%, and 9.74% improvement in locomotion, respectively ($P < 0.001$, $P < 0.01$, $P < 0.05$) (Figure 1(b-ii)) when compared with the Aβ42 *Drosophila* without GE treatment.

3.2. Tianma Rescued Neurodegeneration in Ommatidia of Aβ-Expressing Drosophila. We analyzed the effect of Aβ42 on degeneration of retinal tissue of *Drosophila*, which were mainly neurons. Aβ42 *Drosophila* contained significantly more degenerating rhabdomeres, compared with OregonR. The number of degenerated rhabdomeres was 3.82 ± 0.09. Aβ42 *Drosophila* treated with GE (1 and 5 mg/g of *Drosophila* media) had significantly rescued rhabdomere in each ommatidium, with an increase of 0.49 and 0.97 rhabdomere count per ommatidium, respectively (Figure 2), which reflected a preventive effect of GE on neurodegeneration. The preventive effect was comparable to donepezil medication (10 μmol/g of *Drosophila* media), in which there was an increase of 0.78 rhabdomere count per ommatidium than the Aβ42 *Drosophila*.

3.3. Tianma Reduced Aβ-Induced Cytotoxicity in PC12 Cells and Prevented Aβ-Induced Apoptosis. Exposure of PC12 cells to aggregated $A\beta_{25-35}$ (20 μM) for 48 h caused significant

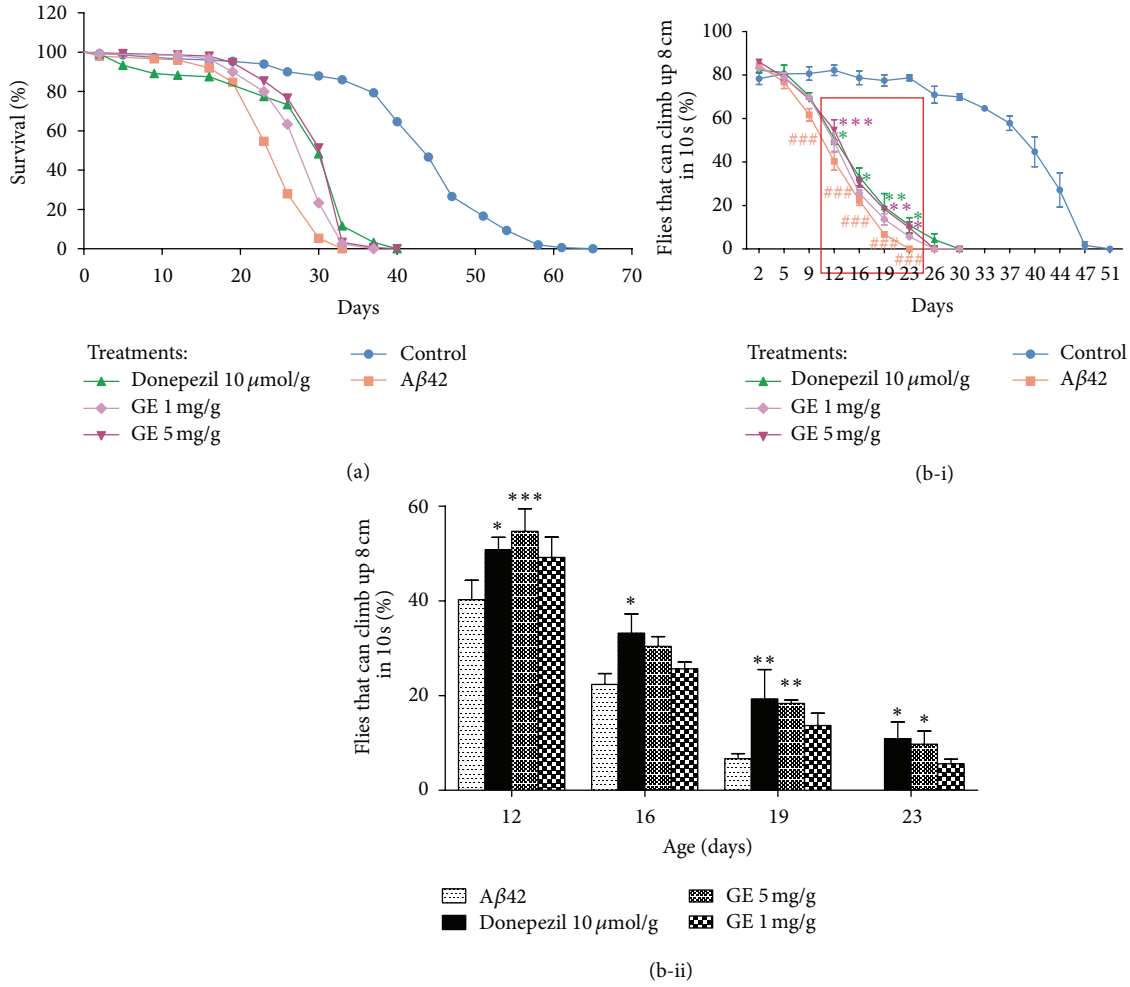

Figure 1: Intake of GE increases the (a) lifespan and (b-i) locomotor activity of Aβ-expressing *Drosophila*. The lifespan of Aβ42 group (squares in red) is shorter than the control group (circles in blue), while GE (asterisks and triangles in purple) or donepezil (triangles in green) treatments delay the mortality of the *Drosophila*. (b-ii) is an amplification of the region from days 12 to 23 showing the differences among the Aβ42 group and the treatment groups. The percentage of *Drosophila* climbing up 8 cm in 10 seconds was increased by GE or donepezil treatments when compared with Aβ42 group. Results are the means ± SEM from five independent crosses. $^{###}P < 0.001$ relative to control; $^{*}P < 0.05$, $^{**}P < 0.01$, $^{***}P < 0.001$ relative to Aβ42 *Drosophila* by one-way ANOVA for locomotor activity. Log-Rank analysis and chi-square comparison were applied to the survival data and $P < 0.001$ was obtained when comparing Aβ42 *Drosophila* and Donepezil 10 μmol/g or GE 1 mg/g or 5 mg/g treated ones ($n = 150$).

cytotoxicity. Concentration of GE in the range from 125 to 1000 μg/mL was identified to be non-toxic to PC12 cells by MTT assay (data not shown). The high concentration of GE used is also correlated to its high extraction yield in water (48.9%), compared with the yield of less than a few percent in extraction by nonpolar solvents. Our results demonstrated that GE imposed significant protective effect against Aβ_{25-35}-induced damage in a dose dependent manner, with the maximum effect observed at 1000 μg/mL (Figure 3). Therefore, concentration of GE in the range from 250 to 1000 μg/mL was selected for the further apoptosis study. In this regard, we investigated the effect of GE on Aβ_{25-35}-induced apoptosis using Annexin V-FITC and PI staining. Early apoptotic (PI: negative, Annexin V: positive) cells and late apoptotic (PI and Annexin V: positive) cells were quantified by flow cytometry. For the control group treated with Aβ_{25-35} only, the normalized percentages of early and late apoptosis induced by Aβ_{25-35} were 14.1 ± 3.5% and 2.6 ± 0.3%, respectively. For the treatment groups, the percentage of early and late apoptosis induced by Aβ_{25-35} with treatment of GE were 9.7 ± 2.4% and 0.9 ± 0.6% for 250 μg/mL, 8.2 ± 0.3% and 0.4 ± 0.7% for 500 μg/mL, and 3.1 ± 3.1% and 0.1 ± 0.1% for 1000 μg/mL (Figure 4(b)). The results suggested that GE can reduce Aβ_{25-35}-induced apoptosis dose dependently. To further confirm the antiapoptotic effects of GE against Aβ_{25-35}-induced toxicity, the activity of crucial mediator of apoptosis caspase-3 was assessed. Caspase-3 activity was increased by 31.8 ± 13.4% with Aβ_{25-35} treatment, and the increase in activity was attenuated dose dependently with treatment of GE (Figure 4(c)). At 1000 μg/mL of GE, the

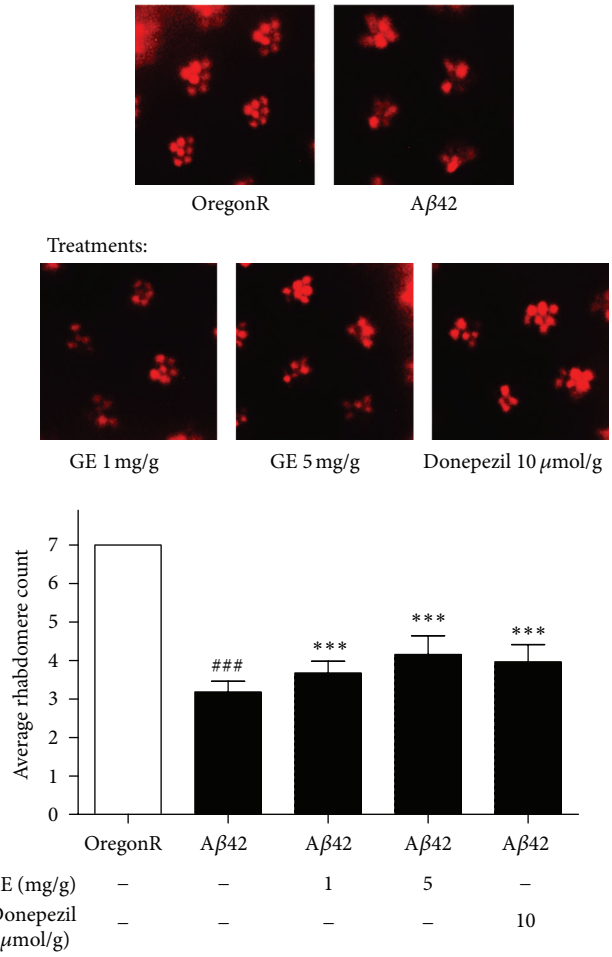

Figure 2: Rhabdomere count in the pseudopupil assay. Regular array of 7 ommatidia (bright red spots) was observed in OregonR eyes. Degeneration of ommatidia was observed in the Aβ42 group, while the degeneration is improved by GE or donepezil treatments. $^{###}P < 0.001$ relative to OregonR; $^{***}P < 0.001$ relative to Aβ42 *Drosophila* with no treatment by one-way ANOVA. Results are the means ± SEM from 3 independent crosses. One hundred ommatidia were observed from 10 eyes of 5 *Drosophila* from each group in each trial.

caspase-3 activation was totally abolished and reverted to the normal activity level of the PC12 cells without Aβ_{25-35} treatment.

3.4. Tianma Prevented Aβ-Induced Oxidative Stress. Figure 5(a) shows that 20 μM Aβ_{25-35} elevated the production of ROS from 100% to 145.2 ± 16.3%, whereas the fluorescence intensity in GE-treated groups decreased significantly (110.9 ± 7.5%, 103.7 ± 23.1%, and 99.0 ± 15.1%, resp.). The decrease of fluorescence by GE reflected the reduction of ROS content, which possibly caused by the activation of antioxidative enzymes.

The activities of antioxidative enzymes (SOD, CAT, and GPx) in untreated PC12 cells and in those treated with 20 μM Aβ_{25-35} alone or with GE together are presented in Figures 5(b)–5(d). Activity of SOD was decreased by 24.75 ± 9.07% in

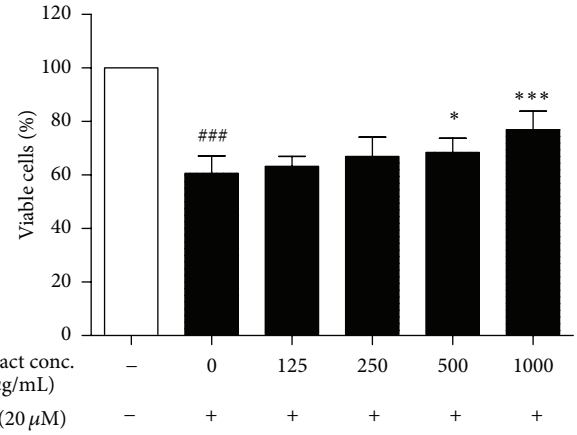

Figure 3: Protective effect of GE on Aβ-induced cytotoxicity in PC12 cells. Effect of 48 h treatment of GE extract on the viability of PC12 cells was determined by MTT assay. Results are the means ± SD from three separate experiments. $^{###}P < 0.001$ relative to control; $^{*}P < 0.05$, $^{***}P < 0.001$ relative to Aβ treatment only by one-way ANOVA.

the cells exposed to 20 μM Aβ_{25-35} (Figure 5(b)). Exposure to 20 μM Aβ_{25-35} did not significantly affect the activity of CAT (Figure 5(c)) and induced a 19.70 ± 4.87% increase in activity of GPx (Figure 5(d)). With 1000 μg/mL of GE treatment, the activity of SOD was reverted to the normal activity level of the PC12 cells without Aβ_{25-35} treatment, while the activity of CAT was enhanced by 63.30 ± 12.58% compared with the normal control. Moreover, 1000 μg/mL of GE further increase the activity of GPx to 45.00 ± 7.71% higher than the normal control. Overall, treatment with different doses of GE significantly and dose-dependently enhanced the activities of SOD, CAT, and GPx (Figures 5(b)–5(d)).

4. Discussion

In the present study, we have presented the first evidence that the aqueous extract of GE could significantly ameliorate the adverse morphological changes from Aβ protein in *Drosophila*, as indicated by improving locomotor abilities, prolonging the lifespan, and rescuing neurodegeneration in ommatidia in Aβ-expressing *Drosophila*. *In vitro* experiments showed that Aβ-treated cultures exhibited characteristic features of ROS production, apoptosis, and cell death in PC12 cells. GE aqueous extract attenuated Aβ-induced cytotoxicity effectively, probably through increasing the activities of antioxidative enzymes so as to reduce overall oxidative stress and subsequently inhibiting Aβ-induced apoptosis.

Two *Drosophila* lines were used to overexpress different levels of Aβ, one was using *GMR* promoter and one was using *GAL4-UAS* system. *GMR* promoter element directs the expression of the protein at the eye imaginal disc. The advantage of expressing only in the eye is that flies producing a highly toxic protein may still be viable. Rapid and severe degeneration of the ommatidia (eyes of *Drosophila*) was achieved due to the presence of two copies of gene encoding for Aβ in our *Drosophila* with *GMR* promoter [10]. For the

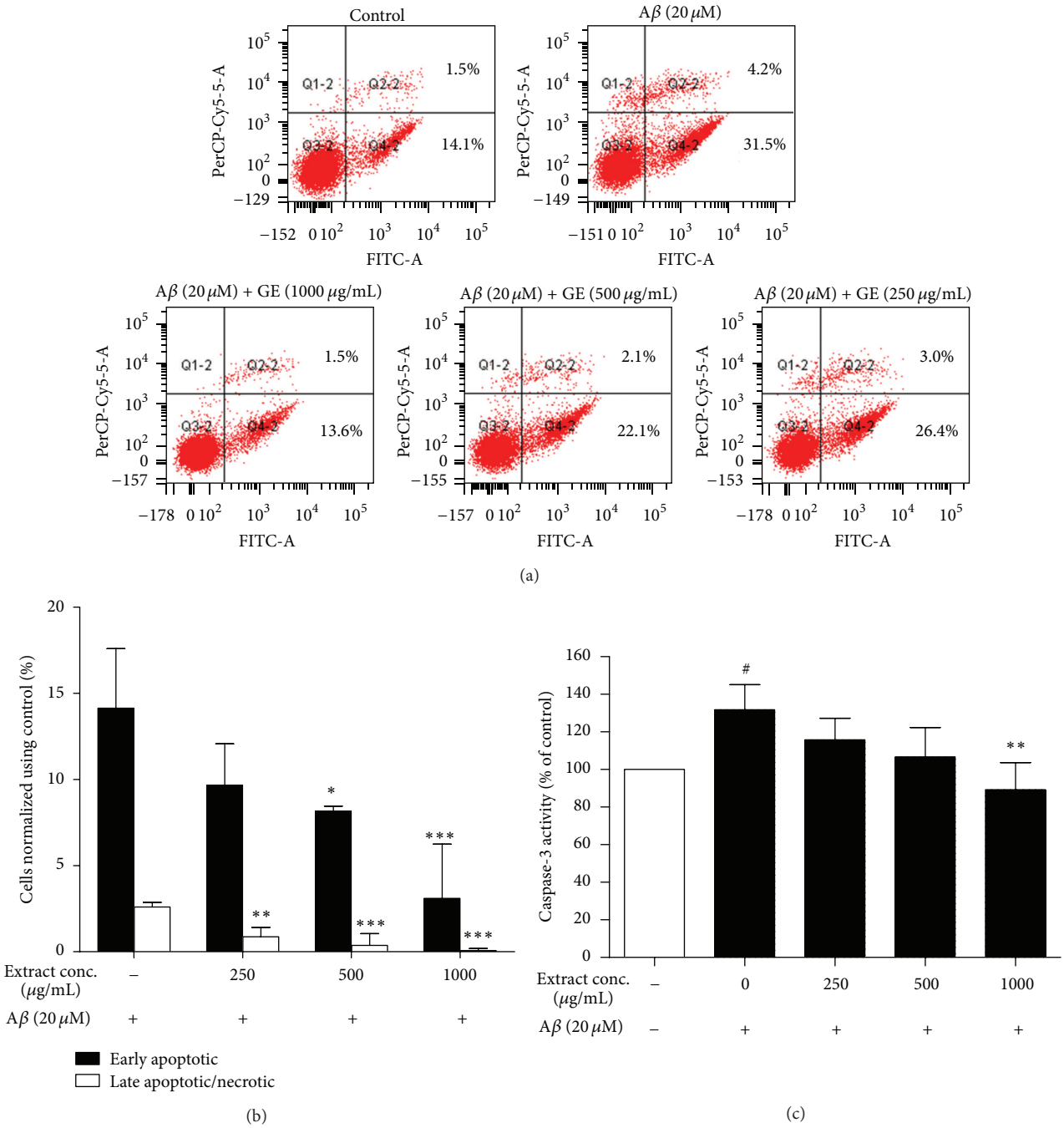

Figure 4: Antiapoptotic effect of GE on Aβ-induced cytotoxicity in PC12 cells. (a) Representative plots for the flow cytometric analysis. (b) GE extract reduced Aβ-induced apoptosis in flow cytometric analysis. The fluorescence intensity was measured after PC12 cells were exposed to 20 μM Aβ for 48 h, followed by incubation with Annexin V-FITC and PI for 15 min. (c) 48 h treatment of GE extract attenuated Aβ-induced activation of caspase-3. Results are the means ± SD from three separate experiments. $^{\#}P < 0.05$ relative to control; $^{*}P < 0.05$, $^{**}P < 0.01$, $^{***}P < 0.001$ relative to Aβ treatment only by one-way ANOVA.

latter one, the *GAL4-UAS* system is more complex. Tissue-specific expression of the *UAS-Aβ42* is achieved by crossing the transgenic *Drosophila* with driver lines that control tissue-specific expression *GAL4*, which would bind with *UAS* to activate gene transcription. *Elav-GAL4* is a commonly used pan-neuronal driver that directs the expression of transgene throughout the brain, neuronal system, and retina of the *Drosophila* [45]. The advantage of this model is that the lethal gene can be carried in the parents without affecting their viability and fecundity. In this study, *UAS-Aβ42* would be crossed with $elav^{C155}$*-GAL4* to express Aβ42 in the brain and the whole neuronal system and gradually accumulate to

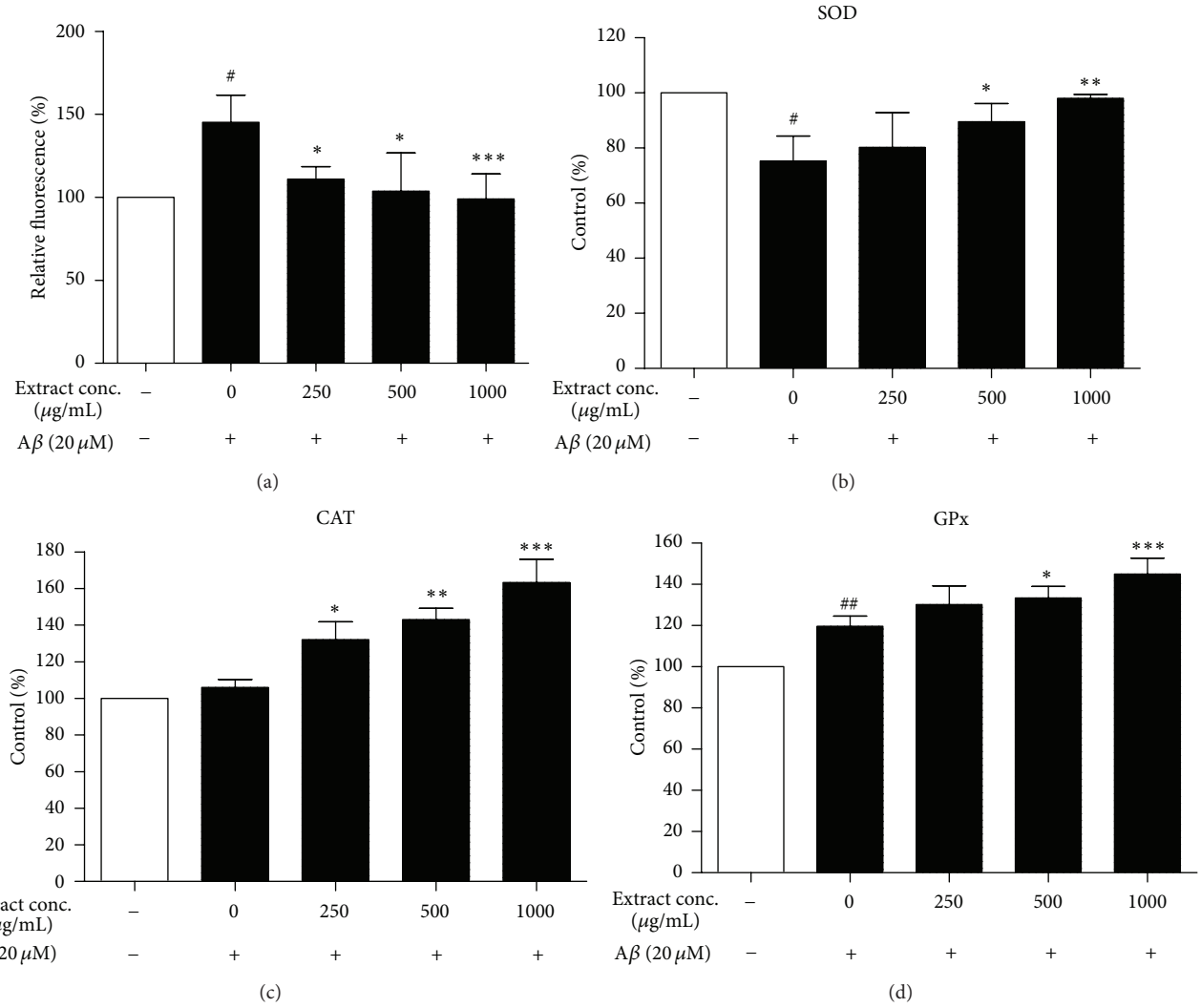

Figure 5: Antioxidative effect of GE on Aβ-induced cytotoxicity in PC12 cells. (a) GE extract reduced Aβ-induced oxidative stress in flow cytometric analysis of DCF positive cells. The fluorescence intensity of DCF was measured after PC12 cells were exposed to 20 μM Aβ for 48 h, followed by 20 μM H2DCF-DA for 15 min. 48 h treatment of GE extract increased the activities of antioxidative enzymes (b) superoxide dismutase (c) catalase and (d) glutathione peroxidase in 20 μM Aβ-treated cells. Results are the means ± SD from three separate experiments. $^{\#}P < 0.05$, $^{\#\#}P < 0.01$ relative to control; $^{*}P < 0.05$, $^{**}P < 0.01$, $^{***}P < 0.001$ relative to Aβ treatment only by one-way ANOVA.

induce the degenerative phenotypes, such as the pathological morphologies and behavioral changes, in weeks. Therefore, to identify the efficacy against Aβ toxicity, the rationale of the current assays aimed to see whether GE aqueous extract can rescue retinal degeneration, locomotion and climbing deficits, and increase the lifespan of the flies, restoration of normal activity.

Using these two *Drosophila* models, the *in vivo* effects of GE aqueous extract in Alzheimer's disease were studied. Firstly, we found that GE aqueous extract reduced the neurotoxic effect of Aβ to ommatidia. The degree of degeneration of ommatidia reflected the extent of neurodegeneration [46], based on the fact that photoreceptors were neurons in nature. Overexpression of Aβ causes plaque formation and neuronal degeneration, which was responsible for the eye morphological changes [10, 12]. The intake of GE extract reduced the adverse effect of Aβ-associated plaque formation and rescued the eye phenotype. Similar findings were observed in the other *Drosophila* model with systemic pan-neuronal Aβ42 expression. GE aqueous extract significantly prolonged the lifespan and improved locomotor dysfunction of the flies. We also found that the beneficial effects of GE were comparable with the medicine donepezil. Hong et al. recently reported that Chinese traditional medicinal prescription SuHeXiang Wan improved the longevity and locomotor ability using the same *Drosophila* model system [47]. The results of the current study suggested that GE aqueous extract confers a therapeutic potential to AD-like pathology of Aβ42 overexpressing in different *Drosophila* models. In our *Drosophila* model, the AD-like pathology was caused by the neurotoxic Aβ produced, secreted to and aggregated in the extracellular matrix [48], yet there was no previous report on the effect of Aβ on

apoptosis and oxidative stress on *Drosophila*. Previous reports revealed the direct proportional relationship between the manifestations of neuronal dysfunction in *Drosophila*, such as locomotor deficits and reduced lifespan, and aggregation rate of the Aβ, which provide evidence that the aggregated Aβ is the primary determinant of the pathological behavior in the *Drosophila* system [49]. To study pathogenic mechanisms, we have developed *in vitro* model that recapitulate many of the signature events in Aβ neurotoxicity including the accumulation extracellular aggregated Aβ, leading to apoptotic events and formation of reactive oxygen species. Basing on previous studies that were using PC12 cells as a platform to express and study the action mechanisms of *Drosophila* proteins [50], we postulate that the PC12 cells would be able to mimic the cellular environment of the *Drosophila*. Moreover, there was a well-established platform using PC12 cells and *Drosophila* toscreen and validate aggregation inhibitors of polyglutamine, which resulted in neurodegeneration [51, 52]. The platform suggested that PC12 cells and *Drosophila* would have correlation in neurodegeneration mechanisms. Therefore, PC12 cell line was used to explain the *in vivo* effects in the present study.

For the *in vitro* mechanistic studies, PC12 cell line, which is originated from transplantable rat adrenal pheochromocytoma, was used. Due to their similarity with sympathetic neurons and their reversible differentiation response to nerve growth factor [53], PC12 cells were widely used in the study of neuronal differentiation [54], neuronal function [55], and neurodegeneration [56, 57]. Aβ-induced cytotoxicity on PC12 cell line is widely used to study the AD-related neurodegeneration [58]. In the present study, we adopted this cell line and found that GE possessed protective effect against Aβ-induced cell death in MTT assay. Previously, Kim et al. had also demonstrated that the ethyl ether fraction of GE was able to protect Aβ-induced IMR-32 neuroblastoma cell death [59]. However, the content of active ingredients in the ethyl ether extract was expected to be different from the aqueous extract. Although the dose of extract used in the study was as low as 10 μg/mL, the extraction yield of the extract was only 1.12%. When comparing with the present study of extraction yield of 48.90%, the dose was equivalent to 420.61 μg/mL in the present study, which is similar to the present dose of 500 μg/mL. Moreover, the study only demonstrated the protective effect using MTT assay, but lacked further elucidation of any protective mechanisms. A complete picture from the *in vivo* effect to the downstream neuroprotective mechanisms was yet to be provided, and the present study was the novel one targeting this. Extensive evidence shows that neuron cell death in AD is mediated by apoptosis [60, 61]. For instance, postmortem analysis of AD brain shows that there is DNA fragmentation in neurons and glia of hippocampus and cortex as detected by TdT-mediated dUTP nick end labeling [62]. It was also found that the extracellular accumulation of Aβ, which triggers the intracellular formation of neurofibrillary tangles [63], leads to the loss of cholinergic neurons [64]. Hence, a common theory believed that the pathological neuronal loss in AD is through apoptosis, which may be caused by Aβ accumulation and cytotoxicity [2, 34]. In order to elucidate the possible mechanisms of the neuroprotective effect, the antiapoptotic effects of GE were determined by flow cytometry using PI/Annexin V staining method and caspase-3 activity assay. Our PI/Annexin V data demonstrated that GE could strongly attenuate not only the early stage but also the late stage of apoptosis/necrosis induced by Aβ. Besides, we also found that GE could suppress Aβ-induced caspase-3 activity, which provided further evidence in antiapoptosis.

Although the exact underlying mechanism leading to Aβ-induced apoptosis was not well understood, oxidative stress caused by the Aβ plaque was widely believed to seriously impair various cellular function and play an important role in apoptosis [65, 66]. Therefore, reducing reactive oxygen species (ROS) production was a promising approach to inhibit Aβ-induced apoptosis. It has been previously reported that the nonpolar fractions of GE and its active constituents could inhibit ROS generation [32, 67]. In this study, we found that the aqueous extract of GE also possessed strong antioxidative action, which decreased the H_2DCF-DA-labeled ROS accumulation in PC12 cells. Antioxidative action can be mediated by 2 mechanisms: activation of antioxidative enzymes and direct free radical scavenging [68]. Antioxidative enzymes, including superoxide dismutase and catalase, convert superoxides, a strong ROS, to hydrogen peroxide and then to water. Glutathione peroxidase catalyzes the reaction of glutathione and hydrogen peroxide, which is a crucial endogenous antioxidative mechanism, to water [69]. In the present study, although Aβ did not affect the activity of CAT, the impairment of the upstream SOD would cause the accumulation of superoxides. On the other hand, the upregulation of GPx by Aβ was possibly a response to the increased ROS and facilitated the action of glutathione. Due to the fact that CAT and GPx could not breakdown superoxides, the accumulation of superoxides may be the explanation for the observed oxidative stress after the Aβ treatment. Our results also demonstrated that GE up-regulated the activity of SOD, CAT, and GPx during Aβ-insult. The activity of SOD was retained, which resume the breakdown of superoxides to hydrogen peroxide. The up-regulation of CAT and GPx can promote the clearance of ROS, and that partially explained the antioxidative action for GE. Other studies also demonstrated that both nonpolar and polar fractions of GE have hydroxyl radical scavenging activity and reduce lipid peroxidation [67, 70, 71]. Its active constituents, including vanillyl alcohol, vanillin, hydroxybenzyl alcohol, and hydroxybenzaldehyde, were found to be potent antioxidants [32, 72]. These compounds can be found in aqueous extract of GE [73, 74].

As aqueous extract of GE was widely and traditionally used in Chinese medicine as a supplement in diet and an herbal medicine [75], and the further development of GE as novel non-toxic preventive/treatment interventions for life-threatening neurodegenerative diseases, such as AD, is possible. In order to confirm our current findings, further investigation of the neuroprotective effect of GE to mammalian AD model is necessary. Since the traditional way of consuming Chinese herbs is to be taken orally, the gastrointestinal metabolic ingredients of GE are the final effective elements. However, very limited information were

found regarding the pharmacokinetic data of GE aqueous extract, except that gastrodin was known to be metabolized to *p*-hydroxybenzyl alcohol [76], and both gastrodin and *p*-hydroxybenzyl alcohol possess significant free radical scavenging and memory consolidation effects [77, 78]. Hence, further pharmacokinetic studies are required to understand the post metabolism ingredients of GE. Besides, further investigation is needed to determine the clinical efficacy and safety of GE in human subjects because the presence of blood-brain barrier (BBB) may block those beneficial active ingredients from the brain. Although BBB exists in *Drosophila* and serves the function of blocking the passage of ions and small molecules [79, 80], the *Drosophila's* BBB is morphologically different from the mammalian one [81, 82]. Nevertheless, some previous studies demonstrated that intravenous administration of gastrodin and hydroxybenzyl alcohol were able to pass through BBB in rats [83, 84]. However, the pharmacokinetics of GE in the human brain is yet to be investigated.

5. Conclusions

In conclusion, the present study demonstrated the novel use of aqueous extract of GE against Aβ-induced neurodegeneration in *Drosophila*. Its effect is mediated through the increasing activity of antioxidative enzymes and reducing oxidative stress in cells, together with the inhibition of caspase-3, leading to the attenuation of apoptosis. Based on these findings, we suggest developing GE aqueous extract as a potential therapeutic intervention for neurodegenerative diseases, such as Alzheimer's disease.

Conflict of Interests

None of the authors has any conflict of interests regarding this study.

Acknowledgment

This project was supported by Ming Lai Foundation.

References

[1] J. Schnabel, "Amyloid: little proteins, big clues," *Nature*, vol. 475, no. 7355, pp. S12–S14, 2011.

[2] M. P. Mattson, "Pathways towards and away from Alzheimer's disease," *Nature*, vol. 430, no. 7000, pp. 631–639, 2004.

[3] J. Hardy and D. J. Selkoe, "The amyloid hypothesis of Alzheimer's disease: progress and problems on the road to therapeutics," *Science*, vol. 297, no. 5580, pp. 353–356, 2002.

[4] Alzheimer's Disease International, *World Alzheimer Report*, Alzheimer's Disease International, London, UK.

[5] L. Gravitz, "Drugs: a tangled web of targets," *Nature*, vol. 475, no. 7355, pp. S9–S11, 2011.

[6] P. T. Francis, A. M. Palmer, M. Snape, and G. K. Wilcock, "The cholinergic hypothesis of Alzheimer's disease: a review of progress," *Journal of Neurology Neurosurgery and Psychiatry*, vol. 66, no. 2, pp. 137–147, 1999.

[7] L. M. Fu and J. T. Li, "A systematic review of single chinese herbs for Alzheimer's disease treatment," *Evidence-Based Complementary and Alternative Medicine*, vol. 2011, Article ID 640284, 8 pages, 2011.

[8] M. J. R. Howes and P. J. Houghton, "Ethnobotanical treatment strategies against alzheimer's disease," *Current Alzheimer Research*, vol. 9, no. 1, pp. 67–85, 2012.

[9] R. J. Greenspan, *Fly Pushing: The Theory and Practice of Drosophila Genetics*, Cold Spring Harbor Laboratory Press, Cold Spring Harbor, NY, USA, 2nd edition, 2004.

[10] A. Finelli, A. Kelkar, H. J. Song, H. Yang, and M. Konsolaki, "A model for studying Alzheimer's Aβ42-induced toxicity in Drosophila melanogaster," *Molecular and Cellular Neuroscience*, vol. 26, no. 3, pp. 365–375, 2004.

[11] A. Moloney, D. B. Sattelle, D. A. Lomas, and D. C. Crowther, "Alzheimer's disease: insights from Drosophila melanogaster models," *Trends in Biochemical Sciences*, vol. 35, no. 4, pp. 228–235, 2010.

[12] K. Iijima, H. C. Chiang, S. A. Hearn et al., "Aβ42 mutants with different aggregation profiles induce distinct pathologies in Drosophila," *PLoS ONE*, vol. 3, no. 2, Article ID e1703, 2008.

[13] D. Paris, N. J. Ganey, V. Laporte et al., "Reduction of β-amyloid pathology by celastrol in a transgenic mouse model of Alzheimer's disease," *Journal of Neuroinflammation*, vol. 7, article 17, 2010.

[14] B. H. May, M. Lit, C. C. Xue et al., "Herbal medicine for dementia: a systematic review," *Phytotherapy Research*, vol. 23, no. 4, pp. 447–459, 2009.

[15] N. Wang, X. Chen, D. Geng, H. Huang, and H. Zhou, "Ginkgo biloba leaf extract improves the cognitive abilities of rats with D-galactose induced dementia," *Journal of Biomedical Research*, vol. 27, no. 1, pp. 29–36, 2013.

[16] C. Shi, L. Zhao, B. Zhu et al., "Protective effects of Ginkgo biloba extract (EGb761) and its constituents quercetin and ginkgolide B against β-amyloid peptide-induced toxicity in SH-SY5Y cells," *Chemico-Biological Interactions*, vol. 181, no. 1, pp. 115–123, 2009.

[17] B. Spinnewyn, N. Blavet, and F. Clostre, "Effects of Ginkgo biloba extract on a cerebral ischaemia model in gerbils," *Presse Medicale*, vol. 15, no. 31, pp. 1511–1515, 1986.

[18] Y. F. Xian, Z. X. Lin, M. Zhao, Q. Q. Mao, S. P. Ip, and C. T. Che, "Uncaria rhynchophylla ameliorates cognitive deficits induced by D-galactose in mice," *Planta Medica*, vol. 77, no. 18, pp. 1977–1983, 2011.

[19] Y. F. Xian, Z. X. Lin, Q. Q. Mao et al., "Bioassay-guided isolation of neuroprotective compounds from Uncaria rhynchophylla against beta-amyloid-induced neurotoxicity," *Evidence-Based Complementary and Alternative Medicine*, vol. 2012, Article ID 802625, 8 pages, 2012.

[20] J. S. Shim, H. G. Kim, M. S. Ju, J. G. Choi, S. Y. Jeong, and M. S. Oh, "Effects of the hook of Uncaria rhynchophylla on neurotoxicity in the 6-hydroxydopamine model of Parkinson's disease," *Journal of Ethnopharmacology*, vol. 126, no. 2, pp. 361–365, 2009.

[21] C. L. Hsieh, C. H. Liu, Y. W. Lin, N. Y. Tang, and H. J. Liu, "Neuroprotective effect of Uncaria rhynchophylla in Kainic acid-induced epileptic seizures by modulating hippocampal mossy fiber sprouting, neuron survival, astrocyte proliferation, and S100b expression," *Evidence-based Complementary and Alternative Medicine*, vol. 2012, Article ID 194790, 2012.

[22] Z. Lin, J. Gu, J. Xiu, T. Mi, J. Dong, and J. K. Tiwari, "Traditional chinese medicine for senile dementia," *Evidence-Based Complementary and Alternative Medicine*, vol. 2012, Article ID 692621, 13 pages, 2012.

[23] K. Y. Zhu, Q. Q. Mao, S. P. Ip et al., "A standardized chinese herbal decoction, kai-xin-san, restores decreased levels of neurotransmitters and neurotrophic factors in the brain of chronic stress-induced depressive rats," *Evidence-Based Complementary and Alternative Medicine*, vol. 2012, Article ID 149256, 13 pages, 2012.

[24] R. Naito and C. Tohda, "Characterization of anti-neurodegenerative effects of Polygala tenuifolia in Aβ(25-35)-treated cortical neurons," *Biological and Pharmaceutical Bulletin*, vol. 29, no. 9, pp. 1892–1896, 2006.

[25] C. Rui, L. Yuxiang, H. Yinju et al., "Protective effects of Lycium barbarum polysaccharide on neonatal rat primary cultured hippocampal neurons injured by oxygen-glucose deprivation and reperfusion," *Journal of Molecular Histology*, vol. 43, no. 5, pp. 535–542, 2012.

[26] H. An, I. S. Kim, S. Koppula et al., "Protective effects of Gastrodia elata Blume on MPP+-induced cytotoxicity in human dopaminergic SH-SY5Y cells," *Journal of Ethnopharmacology*, vol. 130, no. 2, pp. 290–298, 2010.

[27] Z. B. Huang, Z. Wu, F. K. Chen, and L. B. Zou, "The protective effects of phenolic constituents from Gastrodia elata on the cytotoxicity induced by KCl and glutamate," *Archives of Pharmacal Research*, vol. 29, no. 11, pp. 963–968, 2006.

[28] H. J. Kim, K. D. Moon, S. Y. Oh, S. P. Kim, and S. R. Lee, "Ether fraction of methanol extracts of Gastrodia elata, a traditional medicinal herb, protects against kainic acid-induced neuronal damage in the mouse hippocampus," *Neuroscience Letters*, vol. 314, no. 1-2, pp. 65–68, 2001.

[29] H. Shuchang, N. Qiao, N. Piye et al., "Protective effects of gastrodia elata on aluminium-chloride-induced learning impairments and alterations of amino acid neurotransmitter release in adult rats," *Restorative Neurology and Neuroscience*, vol. 26, no. 6, pp. 467–473, 2008.

[30] X. Xu, Y. Lu, and X. Bie, "Protective effects of gastrodin on hypoxia-induced toxicity in primary cultures of rat cortical neurons," *Planta Medica*, vol. 73, no. 7, pp. 650–654, 2007.

[31] S. S. Yu, J. Zhao, S. P. Lei, X. M. Lin, L. L. Wang, and Y. Zhao, "4-hydroxybenzyl alcohol ameliorates cerebral injury in rats by antioxidant action," *Neurochemical Research*, vol. 36, no. 2, pp. 339–346, 2011.

[32] H. J. Kim, I. K. Hwang, and M. H. Won, "Vanillin, 4-hydroxybenzyl aldehyde and 4-hydroxybenzyl alcohol prevent hippocampal CA1 cell death following global ischemia," *Brain Research*, vol. 1181, no. 1, pp. 130–141, 2007.

[33] M. Mishra, J. Huang, Y. Y. Lee et al., "Gastrodia elata modulates amyloid precursor protein cleavage and cognitive functions in mice," *BioScience Trends*, vol. 5, no. 3, pp. 129–138, 2011.

[34] M. P. Mattson, "Cellular actions of β-amyloid precursor protein and its soluble and fibrillogenic derivatives," *Physiological Reviews*, vol. 77, no. 4, pp. 1081–1132, 1997.

[35] R. Vassar, B. D. Bennett, S. Babu-Khan et al., "β-Secretase cleavage of Alzheimer's amyloid precursor protein by the transmembrane aspartic protease BACE," *Science*, vol. 286, no. 5440, pp. 735–741, 1999.

[36] F. Colciaghi, B. Borroni, M. Zimmermann et al., "Amyloid precursor protein metabolism is regulated toward alpha-secretase pathway by Ginkgo biloba extracts," *Neurobiology of Disease*, vol. 16, no. 2, pp. 454–460, 2004.

[37] M. Nistor, M. Don, M. Parekh et al., "Alpha- and beta-secretase activity as a function of age and beta-amyloid in Down syndrome and normal brain," *Neurobiology of Aging*, vol. 28, no. 10, pp. 1493–1506, 2007.

[38] Chinese Pharmacopoeia Commission, *Pharmacopoeia of the People's Republic of China*, Chemical Industry Press, 2010.

[39] J. M. Warrick, H. Y. E. Chan, G. L. Gray-Board, Y. Chai, H. L. Paulson, and N. M. Bonini, "Suppression of polyglutamine-mediated neurodegeneration in Drosophila by the molecular chaperone HSP70," *Nature Genetics*, vol. 23, no. 4, pp. 425–428, 1999.

[40] F. K. M. Lee, A. K. Y. Wong, Y. W. Lee, O. W. Wan, H. Y. Edwin Chan, and K. K. K. Chung, "The role of ubiquitin linkages on α-synuclein induced-toxicity in a Drosophila model of Parkinson's disease," *Journal of Neurochemistry*, vol. 110, no. 1, pp. 208–219, 2009.

[41] S. L. A. Wong, M. C. Wing, and H. Y. E. Chan, "Sodium dodecyl sulfate-insoluble oligomers are involved in polyglutamine degeneration," *FASEB Journal*, vol. 22, no. 9, pp. 3348–3357, 2008.

[42] C. Xiao, J. Li, X. Dong et al., "Anti-oxidative and TNF-α suppressive activities of puerarin derivative (4AC) in RAW264.7 cells and collagen-induced arthritic rats," *European Journal of Pharmacology*, vol. 666, no. 1–3, pp. 242–250, 2011.

[43] R. C. Choi, Z. Jiang, H. Q. Xie et al., "Anti-oxidative effects of the biennial flower of Panax notoginseng against H2O2-induced cytotoxicity in cultured PC12 cells," *Chinese Medicine*, vol. 5, article 38, 2010.

[44] A. Boldyrev, E. Bulygina, T. Leinsoo, I. Petrushanko, S. Tsubone, and H. Abe, "Protection of neuronal cells against reactive oxygen species by carnosine and related compounds," *Comparative Biochemistry and Physiology B*, vol. 137, no. 1, pp. 81–88, 2004.

[45] J. B. Duffy, "GAL4 system in Drosophila: a fly geneticist's Swiss army knife," *Genesis*, vol. 34, no. 1-2, pp. 1–15, 2002.

[46] G. R. Jackson, I. Salecker, X. Dong et al., "Polyglutamine-expanded human huntingtin transgenes induce degeneration of Drosophila photoreceptor neurons," *Neuron*, vol. 21, no. 3, pp. 633–642, 1998.

[47] Y. K. Hong, S. H. Park, S. Lee et al., "Neuroprotective effect of SuHeXiang Wan in Drosophila models of Alzheimer's disease," *Journal of Ethnopharmacology*, vol. 134, no. 3, pp. 1028–1032, 2011.

[48] D. Ling, H. J. Song, D. Garza, T. P. Neufeld, and P. M. Salvaterra, "Abeta42-induced neurodegeneration via an age-dependent autophagic-lysosomal injury in Drosophila," *PLoS ONE*, vol. 4, no. 1, Article ID e4201, 2009.

[49] L. M. Luheshi, G. G. Tartaglia, A. C. Brorsson et al., "Systematic in vivo analysis of the intrinsic determinants of amyloid beta pathogenicity," *PLoS Biology*, vol. 5, no. 11, p. e290, 2007.

[50] J. Van De Goor and R. B. Kelly, "Association of Drosophila cysteine string proteins with membranes," *FEBS Letters*, vol. 380, no. 3, pp. 251–256, 1996.

[51] B. L. Apostol, A. Kazantsev, S. Raffioni et al., "A cell-based assay for aggregation inhibitors as therapeutics of polyglutamine-repeat disease and validation in Drosophila," *Proceedings of the National Academy of Sciences of the United States of America*, vol. 100, no. 10, pp. 5950–5955, 2003.

[52] J. Wang, C. M. Pfleger, L. Friedman et al., "Potential application of grape derived polyphenols in huntington's disease," *Translational Neuroscience*, vol. 1, no. 2, pp. 95–100, 2010.

[53] L. A. Greene and A. S. Tischler, "Establishment of a noradrenergic clonal line of rat adrenal pheochromocytoma cells which respond to nerve growth factor," *Proceedings of the National Academy of Sciences of the United States of America*, vol. 73, no. 7, pp. 2424–2428, 1976.

[54] S. L. Xu, R. C. Choi, K. Y. Zhu et al., "Isorhamnetin, a flavonol aglycone from Ginkgo biloba L., induces neuronal differentiation of cultured PC12 cells: potentiating the effect of nerve growth factor," *Evidence-Based Complementary and Alternative Medicine*, vol. 2012, Article ID 278273, 11 pages, 2012.

[55] M. C. Chuang, H. Y. Lai, J. A. Annie Ho, and Y. Y. Chen, "Multifunctional microelectrode array (mMEA) chip for neural-electrical and neural-chemical interfaces: characterization of comb interdigitated electrode towards dopamine detection," *Biosensors and Bioelectronics*, vol. 41, pp. 602–607, 2013.

[56] A. M. Wang, Y. Miyata, S. Klinedinst et al., "Activation of Hsp70 reduces neurotoxicity by promoting polyglutamine protein degradation," *Nature Chemical Biology*, vol. 9, no. 2, pp. 112–118, 2013.

[57] S. B. Lee, C. K. Kim, K. H. Lee, and J. Y. Ahn, "S-nitrosylation of B23/nucleophosmin by GAPDH protects cells from the SIAH1-GAPDH death cascade," *Journal of Cell Biology*, vol. 199, no. 1, pp. 65–76, 2012.

[58] B. Jayaprakasam, K. Padmanabhan, and M. G. Nair, "Withanamides in Withania somnifera fruit protect PC-12 cells from β-amyloid responsible for Alzheimer's disease," *Phytotherapy Research*, vol. 24, no. 6, pp. 859–863, 2010.

[59] H. J. Kim, K. D. Moon, D. S. Lee, and S. H. Lee, "Ethyl ether fraction of Gastrodia elata Blume protects amyloid β peptide-induced cell death," *Journal of Ethnopharmacology*, vol. 84, no. 1, pp. 95–98, 2003.

[60] S. Shimohama, "Apoptosis in Alzheimer's disease: an update," *Apoptosis*, vol. 5, no. 1, pp. 9–16, 2000.

[61] J. Yuan and B. A. Yankner, "Apoptosis in the nervous system," *Nature*, vol. 407, no. 6805, pp. 802–809, 2000.

[62] M. Ankarcrona and B. Winblad, "Biomarkers for apoptosis in Alzheimer's disease," *International Journal of Geriatric Psychiatry*, vol. 20, no. 2, pp. 101–105, 2005.

[63] F. M. LaFerla, K. N. Green, and S. Oddo, "Intracellular amyloid-β in Alzheimer's disease," *Nature Reviews Neuroscience*, vol. 8, no. 7, pp. 499–509, 2007.

[64] J. T. Coyle, D. L. Price, and M. R. DeLong, "Alzheimer's disease: a disorder of cortical cholinergic innervation," *Science*, vol. 219, no. 4589, pp. 1184–1190, 1983.

[65] M. P. Mattson, W. A. Pedersen, W. Duan, C. Culmsee, and S. Camandola, "Cellular and molecular mechanisms underlying perturbed energy metabolism and neuronal degeneration in Alzheimer's and Parkinson's diseases," *Annals of the New York Academy of Sciences*, vol. 893, pp. 154–175, 1999.

[66] L. Annunziato, S. Amoroso, A. Pannaccione et al., "Apoptosis induced in neuronal cells by oxidative stress: role played by caspases and intracellular calcium ions," *Toxicology Letters*, vol. 139, no. 2-3, pp. 125–133, 2003.

[67] T. Y. Jung, S. I. Suh, H. Lee et al., "Protective effects of several components of Gastrodia elata on lipid peroxidation in gerbil brain homogenates," *Phytotherapy Research*, vol. 21, no. 10, pp. 960–964, 2007.

[68] D. A. Butterfield and C. M. Lauderback, "Lipid peroxidation and protein oxidation in Alzheimer's disease brain: potential causes and consequences involving amyloid β-peptide-associated free radical oxidative stress," *Free Radical Biology and Medicine*, vol. 32, no. 11, pp. 1050–1060, 2002.

[69] T. Finkel and N. J. Holbrook, "Oxidants, oxidative stress and the biology of ageing," *Nature*, vol. 408, no. 6809, pp. 239–247, 2000.

[70] E. J. Shin, J. H. Bach, T. T. L. Nguyen et al., "Gastrodia elata Bl attenuates methamphetamine-induced Dopaminergic toxicity via inhibiting oxidative burdens," *Current Neuropharmacology*, vol. 9, no. 1, pp. 118–121, 2011.

[71] Y. L. Ji, W. J. Young, S. K. Hyo, H. Moon, S. S. Sang, and J. K. Chang, "Anti-inflammatory action of phenolic compounds from Gastrodia elata root," *Archives of Pharmacal Research*, vol. 29, no. 10, pp. 849–858, 2006.

[72] I. S. Kim, D. K. Choi, and H. J. Jung, "Neuroprotective effects of vanillyl alcohol in gastrodia elata blume through suppression of oxidative stress and anti-apoptotic activity in toxin-induced dopaminergic MN9D cells," *Molecules*, vol. 16, no. 7, pp. 5349–5361, 2011.

[73] C. C. Teo, S. N. Tan, J. W. H. Yong, C. S. Hew, and E. S. Ong, "Evaluation of the extraction efficiency of thermally labile bioactive compounds in Gastrodia elata Blume by pressurized hot water extraction and microwave-assisted extraction," *Journal of Chromatography A*, vol. 1182, no. 1, pp. 34–40, 2008.

[74] Y. Wang, S. Lin, M. Chen et al., "Chemical constituents from aqueous extract of Gastrodia elata," *China Journal of Chinese Materia Medica*, vol. 37, no. 12, pp. 1775–1781, 2012.

[75] C. J. Bulpitt, Y. Li, P. F. Bulpitt, and J. Wang, "The use of orchids in Chinese medicine," *Journal of the Royal Society of Medicine*, vol. 100, no. 12, pp. 558–563, 2007.

[76] C. R. Wu, M. T. Hsieh, S. C. Huang, W. H. Peng, Y. S. Chang, and C. F. Chen, "Effects of Gastrodia elata and its active constituents on scopolamine-induced amnesia in rats," *Planta Medica*, vol. 62, no. 4, pp. 317–321, 1996.

[77] M. T. Hsieh, C. R. Wu, and C. F. Chen, "Gastrodin and p-hydroxybenzyl alcohol facilitate memory consolidation and retrieval, but not acquisition, on the passive avoidance task in rats," *Journal of Ethnopharmacology*, vol. 56, no. 1, pp. 45–54, 1997.

[78] C. R. Wu, M. T. Hsieh, and J. Liao, "p-Hydroxybenzyl alcohol attenuates learning deficits in the inhibitory avoidance task: involvement of serotonergic and dopaminergic systems," *Chinese Journal of Physiology*, vol. 39, no. 4, pp. 265–273, 1996.

[79] J. L. Juang and S. D. Carlson, "Analog of vertebrate anionic sites in blood-brain interface of larval Drosophila," *Cell and Tissue Research*, vol. 277, no. 1, pp. 87–95, 1994.

[80] T. Stork, D. Engelen, A. Krudewig, M. Silies, R. J. Bainton, and C. Klämbt, "Organization and function of the blood-brain barrier in Drosophila," *Journal of Neuroscience*, vol. 28, no. 3, pp. 587–597, 2008.

[81] M. R. Freeman and J. Doherty, "Glial cell biology in Drosophila and vertebrates," *Trends in Neurosciences*, vol. 29, no. 2, pp. 82–90, 2006.

[82] R. Daneman and B. A. Barres, "The blood-brain barrier—lessons from moody flies," *Cell*, vol. 123, no. 1, pp. 9–12, 2005.

[83] Q. Wang, G. Chen, and S. Zeng, "Distribution and metabolism of gastrodin in rat brain," *Journal of Pharmaceutical and Biomedical Analysis*, vol. 46, no. 2, pp. 399–404, 2008.

[84] Q. Wang, G. Chen, and S. Zeng, "Pharmacokinetics of Gastrodin in rat plasma and CSF after i.n. and i.v," *International Journal of Pharmaceutics*, vol. 341, no. 1-2, pp. 20–25, 2007.

Hindawi Publishing Corporation
Evidence-Based Complementary and Alternative Medicine
Volume 2013, Article ID 971712, 15 pages
http://dx.doi.org/10.1155/2013/971712

Research Article

P90RSK and Nrf2 Activation via MEK1/2-ERK1/2 Pathways Mediated by Notoginsenoside R2 to Prevent 6-Hydroxydopamine-Induced Apoptotic Death in SH-SY5Y Cells

Xiang-Bao Meng, Gui-Bo Sun, Min Wang, Jing Sun, Meng Qin, and Xiao-Bo Sun

Key Laboratory of Bioactive Substances and Resources Utilization of Chinese Herbal Medicine, Ministry of Education, Institute of Medicinal Plant Development, Chinese Academy of Medical Sciences and Peking Union Medical College, No. 151, Malianwa North Road, Haidian District, Beijing 100193, China

Correspondence should be addressed to Gui-Bo Sun; sunguibo@126.com and Xiao-Bo Sun; sun_xiaobo163@163.com

Received 17 June 2013; Revised 27 July 2013; Accepted 12 August 2013

Academic Editor: Paul Siu-Po Ip

6-Hydroxydopamine (6-OHDA) is known to contribute to neuronal death in Parkinson's disease. In this study, we found that the preincubation of SH-SY5Y cells for 24 h with 20 μM notoginsenoside R2 (NGR2), which is a newly isolated notoginsenoside from *Panax notoginseng*, showed neuroprotective effects against 6-OHDA-induced oxidative stress and apoptosis. NGR2 incubation successively resulted in the activation of P90RSK, inactivation of BAD, and inhibition of 6-OHDA-induced mitochondrial membrane depolarization, thus preventing the mitochondrial apoptosis pathway. NGR2 incubation also led to the activation of Nrf2 and subsequent activity enhancement of phase II detoxifying enzymes, thus suppressing 6-OHDA-induced oxidative stress, and these effects could be removed by Nrf2 siRNA. We also found that the upstream activators of P90RSK and Nrf2 were the MEK1/2–ERK1/2 pathways but not the JNK, P38, or PI3K/Akt pathways. Interestingly, NGR2 incubation could also activate MEK1/2 and ERK1/2. Most importantly, NGR2-mediated P90RSK and Nrf2 activation, respective downstream target activation, and neuroprotection were reversed by the genetic silencing of MEK1/2 and ERK1/2 by using siRNA and PD98059 application. These results suggested that the neuroprotection elicited by NGR2 against 6-OHDA-induced neurotoxicity was associated with NGR2-mediated P90RSK and Nrf2 activation through MEK1/2-ERK1/2 pathways.

1. Introduction

Parkinson's disease (PD) is a neurodegenerative disorder characterized by severe motor deficits including resting tremor, rigidity, bradykinesia, and postural instability. The pathophysiological changes responsible for these motor deficits are known to be associated with the selective loss of dopaminergic neurons in the substantia nigra pars compacta and subsequent depletion of striatal dopamine content.

To date, although L-dopa or MAO-B inhibitors such as rasagiline show symptomatic relief, no available therapy can delay or halt the neurodegenerative process of PD [1]. Therefore, an urgent clinical need exists for effective PD drugs and therapies. A promising effective therapy for PD may be achieved by target- and mechanism-based drug development [2]. Previous studies consistently implicated that oxidative stress and mitochondrial dysfunction are common mechanisms that lead to the demise of dopaminergic neurons in both familial and sporadic PD [3, 4]. Neuroprotective therapies are presumed approaches to suppress oxidative stress and reverse mitochondrial dysfunction in PD.

We mimicked the pathogenesis of PD by using an *in vitro* PD model of 6-OHDA-induced cell death in SH-SY5Y cells [5]. SH-SY5Y cells are widely used for studies of neuronal survival, apoptosis, and their underlying mechanisms [6], and 6-OHDA can lead to oxidative stress, mitochondrial dysfunction, and apoptosis in SH-SY5Y cells [7]. This model can be used to determine the possible neuroprotective compounds and investigate the underlying mechanism.

P. notoginseng saponins, the main active ingredients of *P. notoginseng* (Burk.) F. H. Chen, have neuroprotective properties against PD *in vivo* [8]. Furthermore, ginsenosides Rg1 [9]

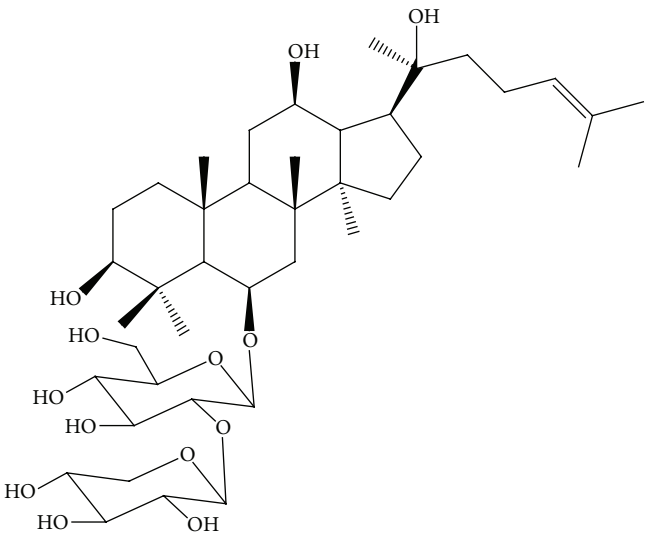

Figure 1: Chemical structure of NGR2.

and Re [10], which are the main saponins in *P. notoginseng* saponins, protect dopaminergic neurons *in vivo*. Notoginsenoside R2 (NGR2), whose chemical structure is shown in Figure 1, is a new notoginsenoside isolated from *P. notoginseng*. We hypothesized that NGR2 might be neuroprotective because NGR2 has a similar chemical structure to ginsenosides Rg1 and Re. However, the neuroprotective properties of NGR2 are largely unknown. Since our preliminary experiments found that NGR2 has an ability to protect neurons against various toxic stimuli, in the present study, multiple approaches were conducted to explore the neuroprotective effects of NGR2 and underlying mechanisms.

Phase II detoxifying enzymes including heme oxygenase-1 (HO-1), glutathione peroxidase (GSH-PX), and glutathione peroxidase (GR) are believed to play a central role in neuronal defense [11]. They can reportedly be upregulated in neurons via the activation of nuclear factor-erythroid 2-related factor 2 (Nrf2) by pharmacological inducers such as ginsenoside Rg1 [12]. Moreover, activated P90RSK can phosphorylate and inactivate a proapoptotic protein BAD [13] and subsequently inhibit the apoptotic pathways, which emphasizes the importance of P90RSK. Targeting the P90RSK and Nrf2 signaling pathways may provide neuroprotection advantages. Furthermore, P90RSK and Nrf2 activation is regulated by multiple signaling pathways such as ERK1/2, JNK, p38, and PI3K/Akt [14–20]. Whether these mechanisms are responsible for NGR2-mediated neuroprotection remains to be seen.

In this study, we demonstrated that NGR2 possessed neuroprotective effects against 6-OHDA-induced apoptotic death in SH-SY5Y cells by the activation of P90RSK and Nrf2 via MEK1/2-ERK1/2 signaling pathways.

2. Materials and Methods

2.1. Materials. NGR2 (molecular weight = 871.01; purity > 98%) was purchased from Shanghai Winherb Medical S&T Development (China). Human SH-SY5Y neuroblastoma cell line was obtained from the Cell Resource Center of the Institute of Basic Medical Sciences, Peking Union Medical College/Chinese Academy of Medical Sciences (China). Dulbecco's modified Eagle's medium (DMEM) and fetal bovine serum (FBS) were purchased from Gibco Life Technologies (USA). Primary and secondary antibodies were all purchased from Santa Cruz Biotechnology (USA). All other chemicals used were obtained from Sigma (USA).

2.2. Cell Culture. SH-SY5Y cells were maintained in a 1 : 1 mixture of F12 nutrient and DMEM supplemented with 10% (v/v) heat-inactivated FBS, 2 mM L-glutamine, 50 U/mL penicillin, and 50 μg/mL streptomycin. Rat pheochromocytoma PC12 cells were grown in DMEM that contains 10% heat-inactivated horse serum, 5% heat-inactivated FBS, 50 U/mL penicillin, and 50 μg/mL streptomycin. SH-SY5Y and PC12 cells were maintained at 37°C in a humidified atmosphere of 95% air and 5% CO_2. Cells at a passage below 10 and in the exponential growth phase were used in all experiments. Primary cortical neurons were prepared from embryonic day 18 Sprague-Dawley rat fetuses according to a previously described method with a slight modification [21]. The protocol was performed according to the Guide for the Care and Use of Laboratory Animals of the National Institute of Health and approved by the Animal Ethics Committee of Peking Union Medical College. All efforts were made to minimize the number of animals used and reduce their suffering. The cerebral cortex was collected, mechanically fragmented, and incubated at 37°C for 10 min with 0.125% trypsin. The cortical neurons were incubated in DMEM/F12 supplemented with 20% heat-inactivated FBS for 4 h in a humidified atmosphere of 95% air and 5% CO_2 at 37°C. After the cells attached to the substrate, the culture medium was replaced with a serum-free neurobasal medium supplemented with 2% B27 (Gibco, USA) and changed twice a week. The experiments were performed on day seven of the cell culture.

2.3. Drug Preparation. NGR2 was stored at 4°C as a stock solution (100 mM) in dimethyl sulfoxide (DMSO). 6-OHDA was dissolved in sterile distilled water containing 0.1% ascorbic acid as a stock solution (1 M). NGR2 and 6-OHDA stock solutions were diluted in DMEM/F-12 immediately before use.

2.4. Analysis of Cell Viability and Morphological Changes. Cell viability was determined by cell counting kit-8 (Dojindo Laboratories, Japan). SH-SY5Y cells were cultured in 96-well plates at a density of 1×10^4 cells/well and grown for 24 h. The cells were treated with 6-OHDA or preincubated with NGR2 followed by treatment with 6-OHDA or coincubation with NGR2 and 6-OHDA. Cells incubated in DMEM/F12 that contain an equivalent concentration of DMSO (the highest concentration less than 0.1%) were used as the control. Thereafter, a 10 μL cell counting kit-8 solution was added to each well. The absorbance was detected at 450 nm on a microplate reader after 1 h (Spectra Fluor, Tecan, Sunrise, Austria). Cell viability was expressed as a percentage of the control. The morphological changes in the SH-SY5Y cells were visualized by an inverted microscope connected to a digital camera (Canon, Japan).

2.5. Quantization of Cell Apoptosis Rate. Cell apoptosis was determined by flow cytometry by using Annexin V-propidium iodide (PI) double staining kits (Invitrogen, USA). SH-SY5Y cells (5×10^4 cells/well) were cultured in 24-well plates. The cells were preincubated with 20 μM NGR2 for 24 h followed by treatment with 50 μM 6-OHDA for 24 h. Then, the cells were washed twice with ice-cold PBS and collected by trypsinization and centrifugation. The cells were incubated in the dark in 100 μL of 1× binding buffer with 5 μL Annexin V and 1 μL PI for 15 min. After 400 μL of 1× binding buffer was added, the cells were subjected to FACSCalibur analysis (BD Biosciences, USA).

2.6. Detection of Cell DNA Fragmentation. The DNA fragmentation in the apoptotic SH-SY5Y cells was detected by TUNEL assay by using ApopTag Fluoresce *in situ* Apoptosis Detection Kits (Millipore, MA, USA). SH-SY5Y cells were cultured on cover slips. The cells were preincubated with 20 μM NGR2 for 24 h followed by treatment with 50 μM 6-OHDA for 24 h. The cells were washed twice with PBS and fixed in 4% neutral-buffered formalin solution for 30 min. The cells were rinsed with PBS and incubated with a methanol solution containing 0.3% H_2O_2 for 30 min. Thereafter, the cells were incubated by a permeabilizing solution (0.1% sodium citrate and 0.1% Triton X-50) for 10 min. After rinsing in the equilibration buffer, the cells were incubated with a working-strength TdT enzyme in a humidified chamber at 37°C for 1 h. The cells were then rinsed in the stop/wash buffer and incubated with the working-strength antidigoxigenin conjugate at room temperature for 30 min. After washing in PBS, the cells were counterstained by diamidino-2-phenylindole (DAPI) and viewed under a fluorescence microscope (Leica, Germany).

2.7. Detection of Intracellular ROS. To detect intracellular reactive oxygen species (ROS), the molecular probe 5-(and -6)-carboxy-2′,7′-dichlorodihydrofluorescein diacetate (carboxy-H2DCFDA) was used. SH-SY5Y cells (1×10^4 cells/well) were cultured in 96-well plates. The cells were preincubated with 20 μM NGR2 for 24 h followed by treatment with 50 μM 6-OHDA for 24 h. The cells were harvested and washed with 1× washing buffer and incubated with carboxy-H2DCFDA (final concentration of 25 μM) in the dark at 37°C for 30 min. The fluorescence was immediately detected on a microplate reader. Excitation and emission wavelengths were 495 and 529 nm, respectively. The level of cellular ROS was expressed as a percent of the control.

2.8. Determination of LDH and MDA Levels and HO-1, GSH-PX, and GR Activities. Lactate dehydrogenase (LDH) and malondialdehyde (MDA) levels, as well as GSH-PX and GR activities, were measured by using the respective assay kits according to the manufacturer's protocol (Nanjing Jiancheng Bioengineering Institute, China). HO-1 activities were determined by using HO-1 ELISA kits (RapidBio Lab, USA). SH-SY5Y cells (1×10^5 cells/well) were cultured in 6-well plates. The cells were preincubated with 20 μM NGR2 for 24 h followed by treatment with 50 μM 6-OHDA for 24 h. The cell culture media were collected to measure the level of extracellular LDH. The cells were harvested to measure the level of intracellular LDH and MDA and detect HO-1, GSH-PX, and GR activities. LDH release was expressed as the rate of extracellular LDH to total LDH (intracellular plus extracellular). HO-1 activity was expressed as the fold change of the control.

2.9. Measurement of Mitochondrial Membrane Potential. JC-1 (5′,6,6′-tetrachloro-1,1′,3,3′-tetraethylbenzimidazolylcarbocyanine iodide, Enzo Life Sciences International, USA) was used to measure the changes in mitochondrial membrane potential. SH-SY5Y cells (1×10^5 cells/well) were cultured in 6-well plates. The cells were preincubated with 20 μM NGR2 for 24 h followed by treatment with 50 μM 6-OHDA for 24 h. The cells were washed with PBS and incubated in the dark at 37°C with JC-1 (final concentration of 2 μM) for 30 min. After washing twice with PBS, the cells labeled with JC-1 were analyzed by a high content screening system (Molecular devices, USA).

2.10. siRNA Transfection. MEK1/2 siRNA, ERK1/2 siRNA, Nrf2 siRNA, and control siRNA were purchased from Santa Cruz Biotechnology (USA). SH-SY5Y cells were cultured in 6-well plates. When 50% confluence was achieved, SH-SY5Y cells were transfected with MEK1/2 siRNA (100 nM), ERK1/2 siRNA (100 nM), Nrf2 siRNA (50 nM), or equivalent concentrations of control siRNA by using a Lipofectamine 2000 reagent (Invitrogen, USA). The cells were transfected for 48 h in Opi-MEM medium without serum and antibiotics and incubated with 20 μM NGR2 for 24 h.

2.11. Preparation of Cytosolic and Nuclear Proteins. Reagents and kits used were all purchased from Santa Cruz Biotechnology (USA). Cytosolic and nuclear proteins were prepared by using cell nuclear protein extraction kits. SH-SY5Y cells were briefly washed with cold PBS, scraped in cold buffer A supplemented with protease inhibitor cocktail, and incubated on ice for 15 min. The supernatant that contains cytosolic proteins was collected by centrifugation at 12,000 rpm for 10 min at 4°C. A pellet-containing nuclear fraction was re-suspended in buffer *C* supplemented with a protease inhibitor cocktail and incubated on ice for 30 min. Thereafter, the supernatant that contains nuclear proteins was collected by centrifugation at 12,000 rpm for 10 min at 4°C. The total protein concentration was determined by bicinchoninic acid assay kits and boiled with a sodium dodecyl sulfate-polyacrylamide gel electrophoresis loading buffer for 5 min. The cytosolic and nuclear proteins were stored at −80°C until use.

2.12. Western Blot Analysis. Protein expression was determined by western blot analysis. Briefly, equal amounts of protein were separated by electrophoresis on 10% SDS polyacrylamide gels and transferred onto nitrocellulose membranes. The membranes were incubated with 5% (w/v) nonfat milk powder in tris-buffered saline containing 0.1% (v/v) Tween 20 for 2 h to block nonspecific binding sites. Thereafter, the membranes were incubated overnight at 4°C with the respective primary antibodies. The primary antibodies used were as follows: rabbit polyclonal anti-p-MEK-1/2 (Ser218/Ser222);

rabbit polyclonal anti-MEK-1/2 (12-B); rabbit polyclonal anti-p-ERK1/2 (Thr177/Thr160)-R; mouse monoclonal anti-ERK 1/2 (MK1); rabbit polyclonal anti-p-Rsk-1 (Ser363); mouse monoclonal anti-Rsk (B-4); rabbit polyclonal anti-Nrf2 (C-20); Lamin A (H-102): sc-20680; goat polyclonal anti-p-BAD (Ser112); rabbit polyclonal anti-BAD (C-20); mouse monoclonal anti-Bcl-XL (H-5); rabbit polyclonal anti-BAX (N-20); mouse monoclonal anticytochrome C (6H2); goat polyclonal anticleaved caspase-9 p10 (h331); goat polyclonal anticleaved caspase-3 p11 (h176); mouse monoclonal anti-β-actin (C4). After washing with tris-buffered saline and Tween 20 (TBST), the membranes were incubated for 1 h at room temperature with the respective peroxidase-conjugated secondary antibodies. The membranes were rewashed with TBST, and the bands were developed by using an enhanced chemiluminescence reagent. The protein levels were quantified by densitometry by using Image J software.

2.13. Statistical Analysis. The data were expressed as the mean ± standard deviation (SD) of three independent experiments. ANOVA followed by the Newman-Keuls post hoc test or Student's t-test were used for multiple group comparison and two-group comparison, respectively. $P < 0.05$ was considered statistically significant.

3. Results

3.1. NGR2 Inhibited 6-OHDA-Induced Cell Death in SH-SY5Y Cells. The potential protective effects of NGR2 were investigated in SH-SY5Y cells exposed to 6-OHDA.

First, we investigated the effect of 6-OHDA on SH-SY5Y cells. The SH-SY5Y cell treatment at different concentrations (25, 50, 100, and 200 μM) of 6-OHDA for various periods (4, 8, 16, 24, and 32 h) decreased cell viability in concentration- and time-dependent manners (Figure 2(a)). Cell viability was reduced approximately to 50% of the control when SH-SY5Y cells were exposed to 50 μM of 6-OHDA for 24 h. Thus, the concentration (50 μM) and period (24 h) were used for further investigations.

Second, we investigated the effect of NGR2 on SH-SY5Y cells. The results indicated that no significant difference in cell viability was found when SH-SY5Y cells were incubated for 32 h at different concentrations (10, 20, and 40 μM) of NGR2 compared with the control. This finding suggested that NGR2 had no toxic effect on SH-SY5Y cells (Figure 2(b)).

Third, we explored the potential protective effect of NGR2 on 6-OHDA-induced cell death in SH-SY5Y cells. The pre-incubation of SH-SY5Y cells with increasing concentrations (10, 20, and 40 μM) of NGR2 for different time periods (4, 8, 16, and 24 h) reversed the decreased cell viability induced by 6-OHDA (Figure 2(c)). In this study, rasagiline was used as a positive control drug for it is a specific monoamine oxidase B inhibitor and used as a monotherapy in early Parkinson's disease or as an adjunct therapy in more advanced cases. As shown in Figure 2(c), the pre-incubation of SH-SY5Y cells with 10 μM of rasagiline for different time periods (4, 8, 16, and 24 h) markedly inhibited the reduction of cell viability induced by 6-OHDA. However, NGR2 pre-incubation of SH-SY5Y cells with 40 μM NGR2 for 32 h had almost no incremental protective action compared with that of 20 μM NGR2 for 24 h, and the cell viability resumed to 80% of control. This result suggested that the maximum protective effect was achieved with 20 μM NGR2 for 24 h. Nevertheless, the maximum protective effect of NGR2 is lower than rasagiline. Therefore, the concentration (20 μM) and time period (24 h) were selected for further investigations.

We confirmed the protective effect of NGR2 by using LDH release assay. SH-SY5Y cell pre-incubation with 20 μM of NGR2 or 10 μM of rasagiline for 24 h decreased LDH release in cells treated with 6-OHDA (Figure 2(d)). In contrast, NGR2 treatment alone had no effect on LDH release.

Both the cell counting kit-8 test (Figure 2(e)) and LDH assay (Figure 2(f)) demonstrated that almost no protection was obtained when NGR2 (10, 20, and 40 μM) was co-incubated with 6-OHDA for 24 h. This finding suggested that the protective effect of NGR2 was exerted only by pretreatment and not by co-treatment with 6-OHDA.

Finally, we assessed whether the observed neuroprotective action of NGR2 was cell type specific by using pheochromocytoma PC12 cells and rat primary cortical neurons. The neuroprotection of NGR2 against 6-OHDA toxic effects was confirmed in these two types of cells by both cell counting kit-8 test (Figure 2(g)) and LDH release assay (Figure 2(h)). This result suggested that the neuroprotective effect of NGR2 was independent of cell type.

3.2. NGR2 Ameliorated 6-OHDA-Induced Morphological Changes in SH-SY5Y Cells. The control SH-SY5Y cells had normal shapes with a smooth cellular profile and extensive neurite processes, whereas cells treated with 6-OHDA lost their neurite processes and became round (Figure 3(a)). An obvious amelioration of the morphological changes induced by 6-OHDA was observed in cells preincubated with NGR2. However, NGR2 treatment alone did not alter the morphology of the SH-SY5Y cells.

3.3. NGR2 Inhibited 6-OHDA-Induced Apoptosis in SH-SY5Y Cells. DNA fragmentation is a typical marker of apoptosis. Therefore, the nuclear fragmentation in apoptotic cells was detected to investigate the possible effects of NGR2 on 6-OHDA-induced apoptosis. The DNA fragmentation and TUNEL-positive cell rate were dramatically augmented in SH-SY5Y cells exposed to 6-OHDA compared with the control (Figures 3(b) and 3(d)). In contrast, pretreatment with NGR2 effectively reversed these changes induced by 6-OHDA, but NGR2 treatment alone had no effect on DNA fragmentation. We then corroborated the protective effect of NGR2 in SH-SY5Y cells by Annexin V-PI double staining by using flow cytometry. An early indicator of apoptosis is the translocation of the membrane phospholipid phosphatidylserine from the cytoplasmic interface to the extracellular surface. The phospholipid phosphatidylserine that accumulates on the extracellular surface can be detected by Annexin V. PI is a fluorescent dye that binds to the nuclei of dead cells. Annexin−/PI−, Annexin+/PI−, and Annexin+/PI+ represented the viable cells, early apoptotic cells, and late apoptotic cells, respectively. Figures 3(c) and

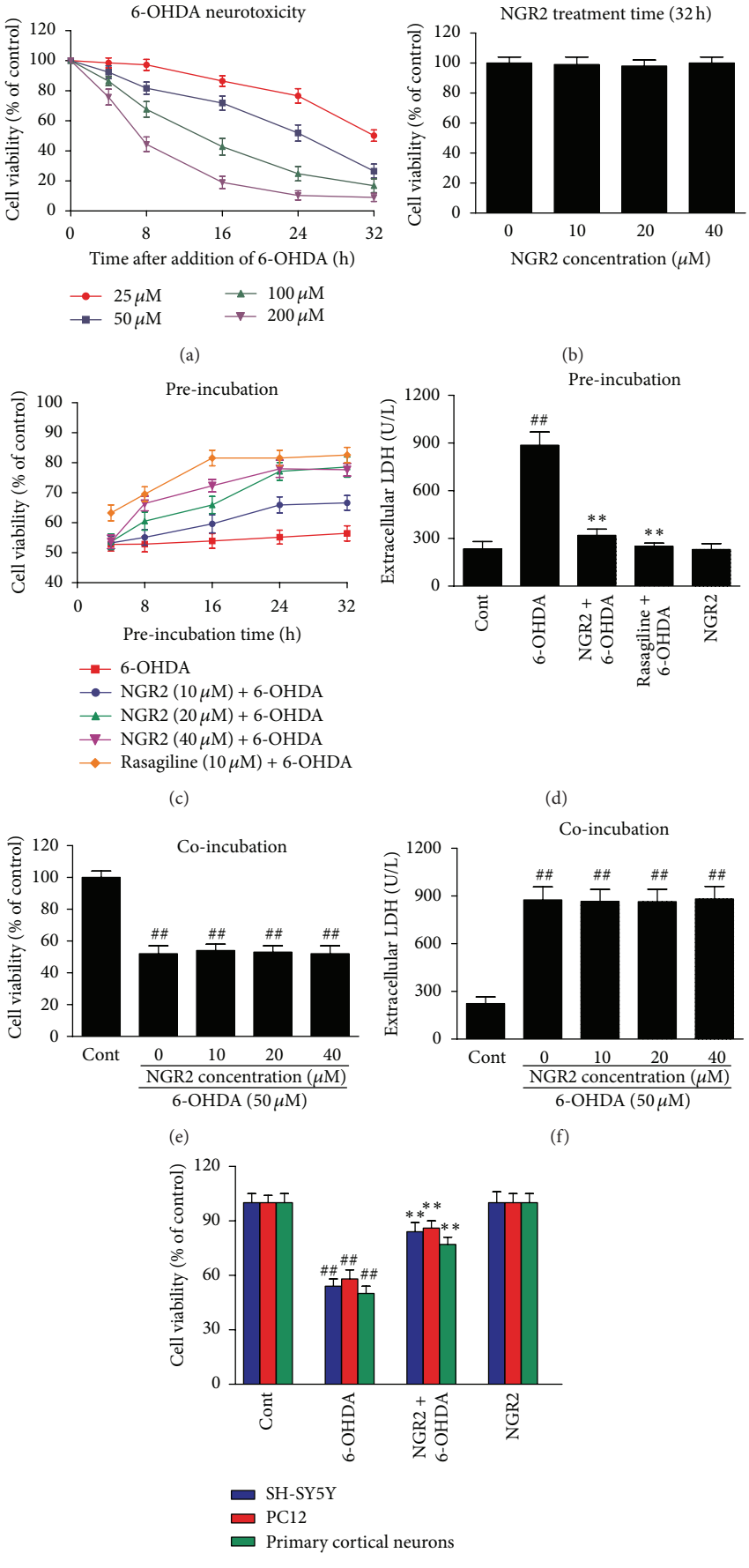

Figure 2: Continued.

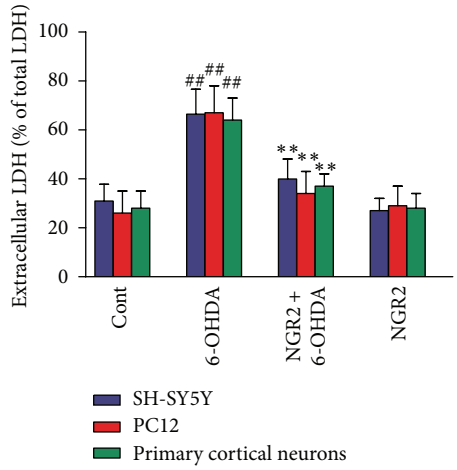

(h)

Figure 2: Protective effects of NGR2 on 6-OHDA-induced cell death in SH-SY5Y cells. Cell viability was measured by cell counting kit-8 test or LDH assay. (a) 6-OHDA could induce cell death in SH-SY5Y cells in concentration- and time-dependent manners. (b) NGR2 had no toxic effect on cell viability. Preincubation with different concentrations of NGR2 for different periods of time had protective effect on 6-OHDA-induced cell death (c) and LDH release (d) in SH-SY5Y cells. Coincubation with NGR2 had almost no protective effect on 6-OHDA-induced cell death (e) and LDH release (f) in SH-SY5Y cells. Both the cell counting kit-8 test (g) and LDH assay (h) showed that the neuroprotective effects of NGR2 was independent of cell type. The results were expressed as the mean ± SD of three independent experiments. ## indicates a significant difference from the control ($P < 0.01$). ** indicates a significant difference from the 6-OHDA treatment alone ($P < 0.01$).

3(e) show that Annexin+/PI− and Annexin+/PI+ substantially increased in the 6-OHDA-treated cells. This result suggested that the apoptosis rate was significantly increased when SH-SY5Y cells were challenged by 6-OHDA. However, these changes were markedly reversed by NGR2 pre-incubation. NGR2 treatment alone had no effect on the apoptosis rate. These results suggested that NGR2 was capable of rescuing SH-SY5Y cells from 6-OHDA-induced apoptotic death.

3.4. NGR2 Activated P90RSK and Nrf2 Pathways in SH-SY5Y Cells. Given that P90RSK and Nrf2 activation has beneficial effects on cell survival, we examined the effect of NGR2 on P90RSK and Nrf2 activation in SH-SY5Y cells. The time-dependent stimulation of SH-SY5Y cells with NGR2 increased the phosphorylation of P90RSK and the subsequent phosphorylation of BAD, which is a downstream target of activated P90RSK. SH-SY5Y cells receiving NGR2 similarly exhibited enhanced levels of nuclear Nrf2 accumulation (Figure 4(a)) and subsequent increase in phase II detoxifying enzyme activities such as HO-1, GSH-PX, and GR in a time-dependent manner (Figure 4(b)).

3.5. NGR2 Inhibited 6-OHDA-Induced Oxidative Stress in SH-SY5Y Cells. 6-OHDA kills dopaminergic neurons by inducing oxidative stress through the increase of ROS production and the decrease of antioxidative enzyme activities in cells. We investigated the effect of NGR2 on 6-OHDA-induced oxidative stress in SH-SY5Y cells. The exposure of SH-SY5Y cells to 6-OHDA increased H2DCFDA fluorescence and MDA production compared with the control cells. This finding indicated that 6-OHDA elevated ROS production and lipid peroxidation in SH-SY5Y cells. 6-OHDA treatment also decreased levels of nuclear Nrf2 accumulation and the activities of HO-1, GSH-PX, and GR in SH-SY5Y cells. However, these effects were significantly suppressed by NGR2 pre-incubation (Figure 5(a)). These results suggested that the enhanced cellular levels of phase II detoxifying enzymes by NGR2 provided neuroprotection against 6-OHDA-induced oxidative stress.

3.6. NGR2 Reversed 6-OHDA-Induced Depolarization of Mitochondrial Membrane in SH-SY5Y Cells. Mitochondrial membrane depolarization is the hallmark of apoptosis. Thus, we used JC-1 to detect the mitochondrial membrane potential. In nonapoptotic cells, JC-1 emits green fluorescence as the monomeric form in cytosol and red fluorescence as aggregates in the mitochondria. In apoptotic cells, JC-1 emits only green fluorescence in cytosol. Therefore, mitochondrial membrane depolarization can be detected as a reduction in the ratio of the red-to-green fluorescence intensity. In this study, the treatment of SH-SY5Y cells with 6-OHDA resulted in a significant decrease in the ratio of red-to-green fluorescence intensity. This decrease suggested that 6-OHDA could depolarize the mitochondrial membrane of SH-SY5Y cells. However, NGR2 pre-incubation prevented this 6-OHDA effect. NGR2 treatment alone did not change the red-to-green fluorescence intensity ratio (Figures 5(b) and 5(c)). These results demonstrated that NGR2 could reverse the 6-OHDA-induced depolarization of the mitochondrial membrane in SH-SY5Y cells.

3.7. NGR2 Inhibited 6-OHDA-Induced Deregulation of Apoptosis-Related Proteins in SH-SY5Y Cells. We examined

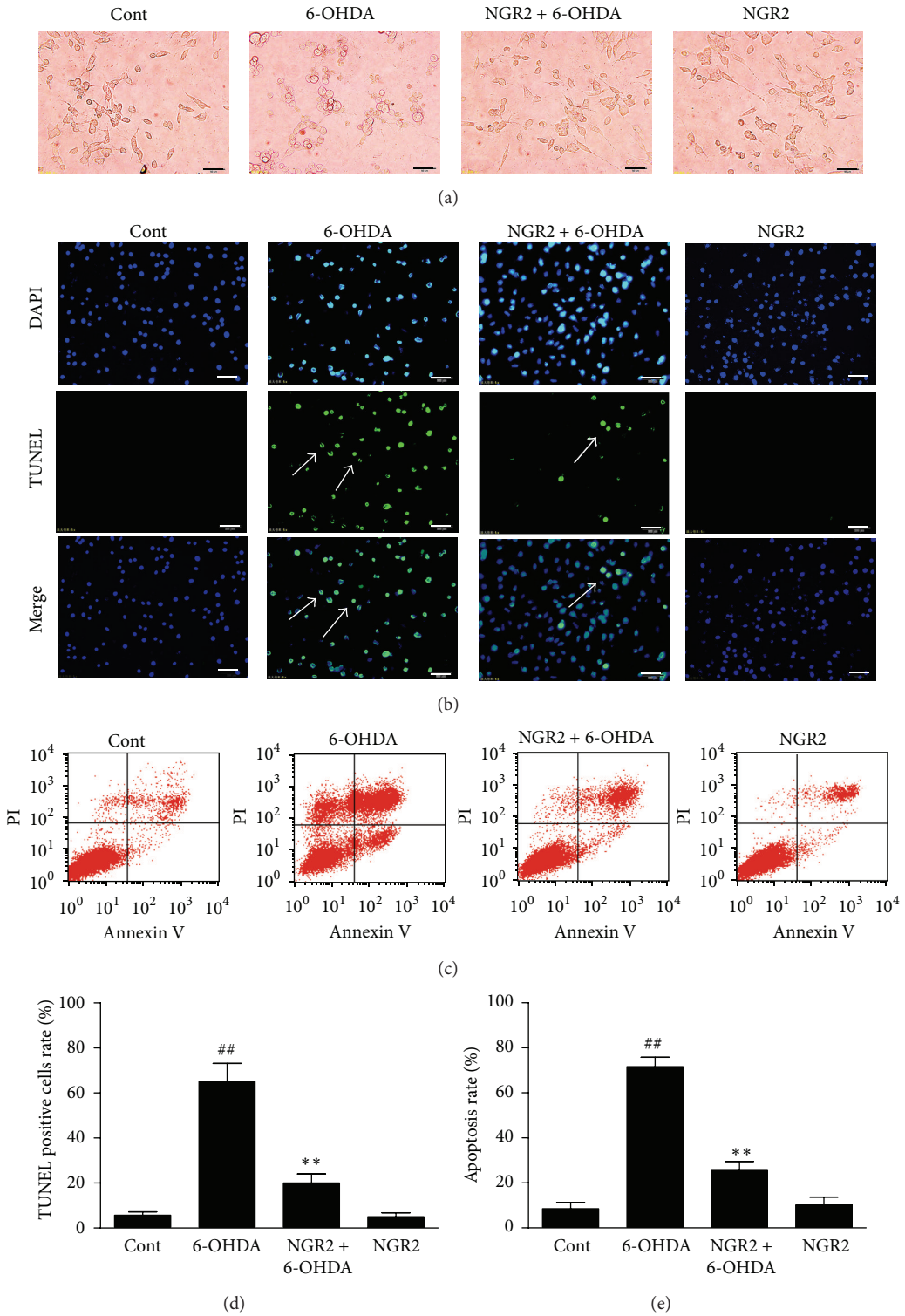

Figure 3: Protective effect of NGR2 on 6-OHDA-induced apoptosis in SH-SY5Y cells. The SH-SY5Y cells were preincubated with 20 μM NGR2 for 24 h followed by treatment with 50 μM 6-OHDA for 24 h. (a) Photographs of morphological changes in SH-SY5Y cells were visualized by an inverted microscope connected to a digital camera, bar = 50 μm. (b) Photographs of DNA fragmentation were detected by TUNEL assay in the apoptotic SH-SY5Y cells, bar = 50 μm. Arrows represent TUNEL-positive cells. (c) Cell apoptosis was determined by Annexin V-PI double staining kits by using flow cytometry. (d) Quantification of the TUNEL-positive cell rate. (e) Quantification of the apoptosis rate. The results were expressed as the mean ± SD of three independent experiments. ## indicates a significant difference from the control ($P < 0.01$). ** indicates a significant difference from the 6-OHDA treatment alone ($P < 0.01$).

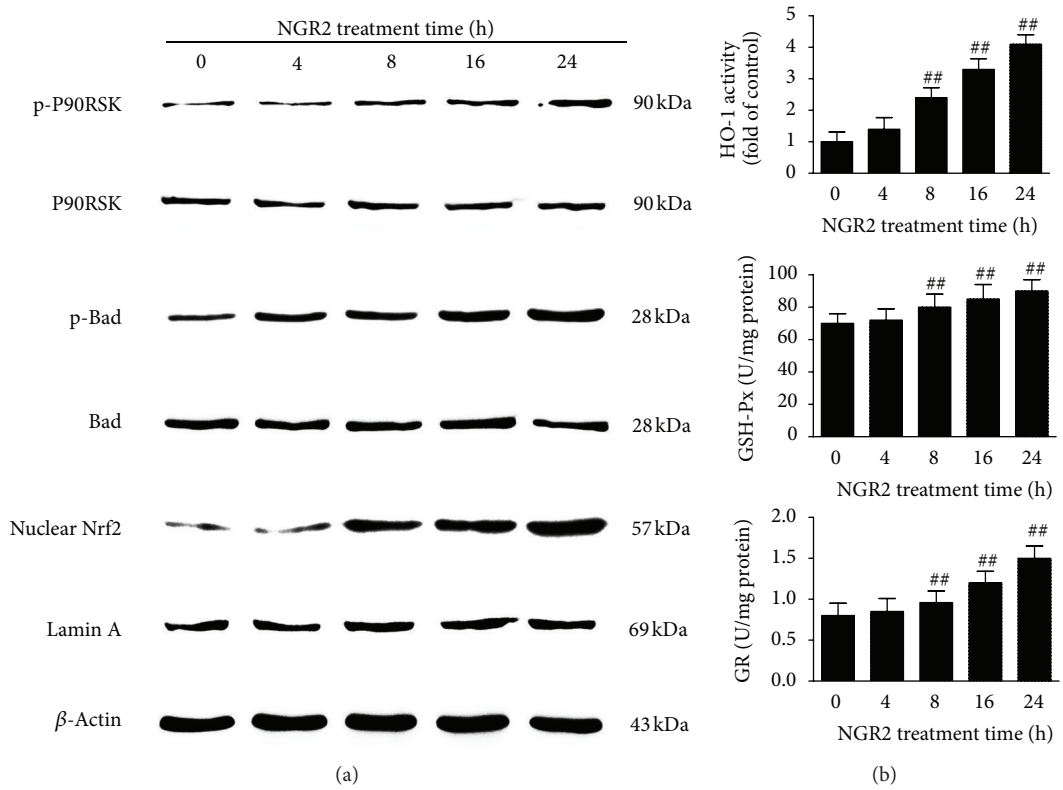

Figure 4: NGR2 could activate P90RSK and Nrf2 pathways in SH-SY5Y cells. The expression of proteins was determined by western blot analysis. HO-1 activities were measured by HO-1 ELISA kits. GSH-PX and GR activities were measured by GSH-PX and GR assay kits, respectively. The SH-SY5Y cells were treated with 20 μM NGR2 for different periods of time (4, 8, 16, and 24 h). (a) NGR2 time dependently increased p-P90RSK and p-BAD expression and nuclear Nrf2 accumulation. (b) NGR2 increased the activities of HO-1, GSH-PX, and GR in a time-dependent manner. The results are expressed as the mean ± SD of three independent experiments. ## indicates a significant difference from the control ($P < 0.01$).

the markers of the apoptotic pathway to delineate the mechanism for NGR2-mediated neuroprotection. Figure 5(d) shows that 6-OHDA treatment significantly increased the release of cytochrome c and the expression of cleaved caspase-9 and cleaved caspase-3. The expression of p-BAD in SH-SY5Y cells decreased compared with that of the control cells. However, NGR2 pre-incubation markedly blocked these effects. This finding suggested that NGR2-mediated neuroprotection was associated with the inhibition of 6-OHDA-induced altered expression of apoptosis-related proteins.

3.8. Dependence and Independence of NGR2-Mediated P90RSK and Nrf2 Activation on MEK1/2-ERK1/2 Pathways and JNK, P38, or PI3K/Akt Pathways. To delineate the pathway involved in NGR2-mediated activation of P90RSK and Nrf2, we pretreated the SH-SY5Y cells with various inhibitors for 2 h, followed by incubation of NGR2 for 24 h. The MEK1/2 inhibitor PD98059 (20 μM) effectively prevented the phosphorylation of P90RSK and nuclear Nrf2 accumulation mediated by NGR2 (Figure 6(a)). However, the JNK inhibitor SP600125 (20 μM), p38 inhibitor SB203580 (20 μM), and PI3K/Akt inhibitor LY294002 (10 μM) all failed to affect the NGR2-mediated phosphorylation of P90RSK and nuclear Nrf2 accumulation. We then investigated the time course of MEK1/2 and ERK1/2 phosphorylation after NGR2 incubation. The results depicted in Figure 6(b) show that the treatment of SH-SY5Y cells with 20 μM NGR2 for 24 h resulted in the phosphorylation of MEK1/2 and ERK1/2. MEK1/2 phosphorylation reached a peak point at 16 h. This finding was similar to ERK1/2 phosphorylation, which reached maximal elevation at 20 h. The aforementioned results indicated the involvement of MEK1/2-ERK1/2 but not of JNK, p38, or PI3K/Akt in NGR2-mediated P90RSK and Nrf2 activation.

3.9. NGR2-Mediated Neuroprotective Effects by P90RSK and Nrf2 Activation via MEK1/2-ERK1/2 Pathways. MEK1/2 siRNA and ERK1/2 siRNA were used to determine whether P90RSK and Nrf2 activation occurs downstream of the MEK1/2-ERK1/2 pathway. When SH-SY5Y cells were transfected with MEK1/2 siRNA, MEK1/2 expression in SH-SY5Y cells was successfully blocked (Figure 7(a)). Moreover, NGR2-mediated ERK1/2 phosphorylation, P90RSK phosphorylation, and BAD phosphorylation, as well as Nrf2 activation and the activity enhancement of phase II detoxifying enzymes (i.e., HO-1, GSH-PX, and GR), were all simultaneously inhibited (Figures 7(a) and 7(c)). Similarly, increased ERK1/2, p-P90RSK, and p-BAD expressions, as well as

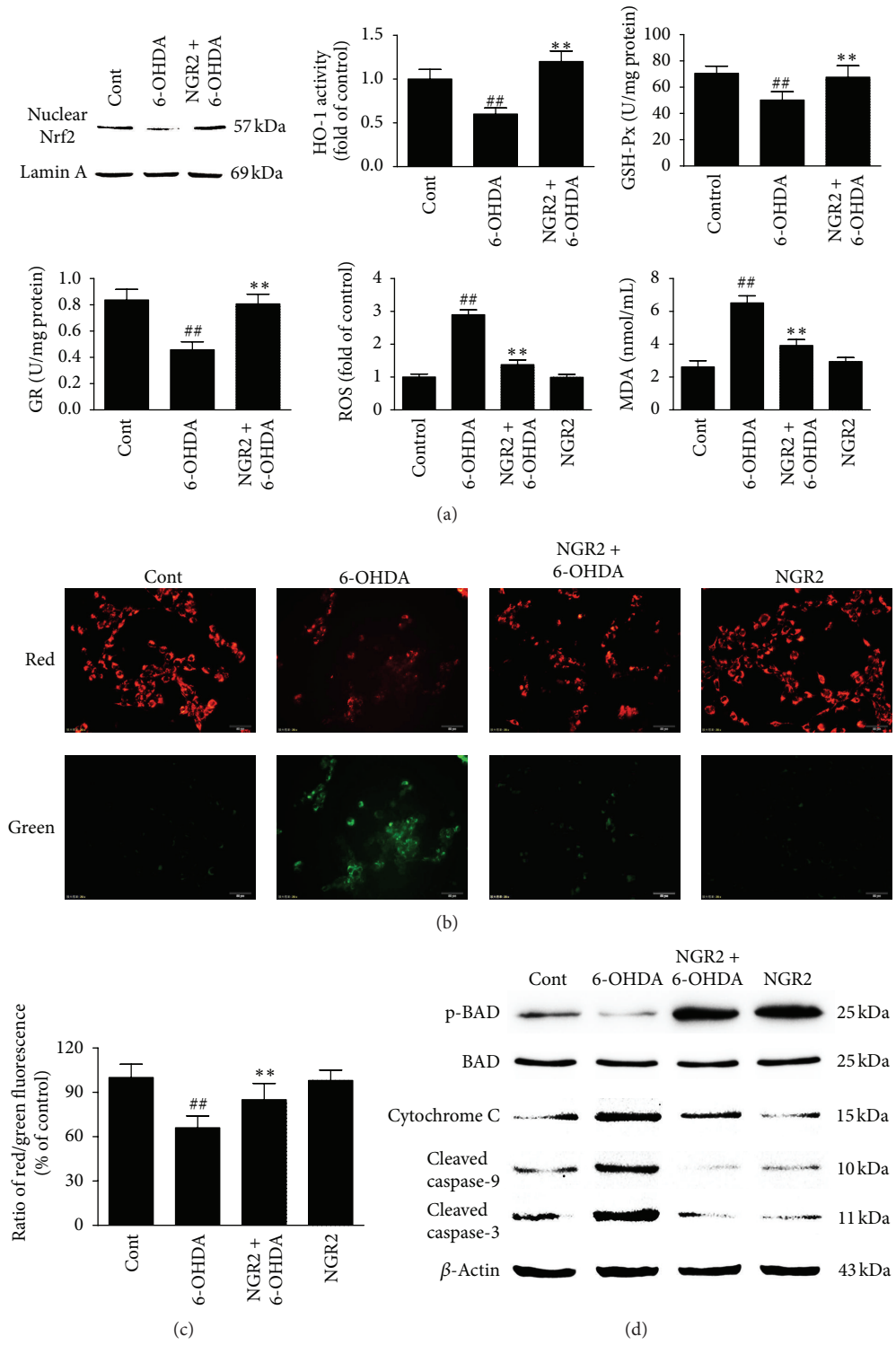

Figure 5: NGR2 reversal of 6-OHDA-induced oxidative stress, mitochondrial membrane depolarization, and apoptosis-related protein deregulation in SH-SY5Y cells. The SH-SY5Y cells were preincubated with 20 μM NGR2 for 24 h followed by treatment with 50 μM 6-OHDA for 24 h. (a) NGR2 reversal of 6-OHDA induced the increase in MDA production and ROS generation, as well as the decrease of nuclear Nrf2, HO-1, GSH-PX, and GR activities in SH-SY5Y cells. (b) NGR2 reversal of mitochondrial membrane depolarization. (c) The cells labeled by JC-1 were analyzed by a high content screening system. (d) NGR2 suppression of 6-OHDA induced increase in cytochrome c release, upregulation of cleaved caspase-9 and cleaved caspase-3, and downregulation of p-BAD. The results are expressed as the mean ± SD of three independent experiments. ## indicates a significant difference from the control ($P < 0.01$). ∗∗ indicates a significant difference from the 6-OHDA treatment alone ($P < 0.01$).

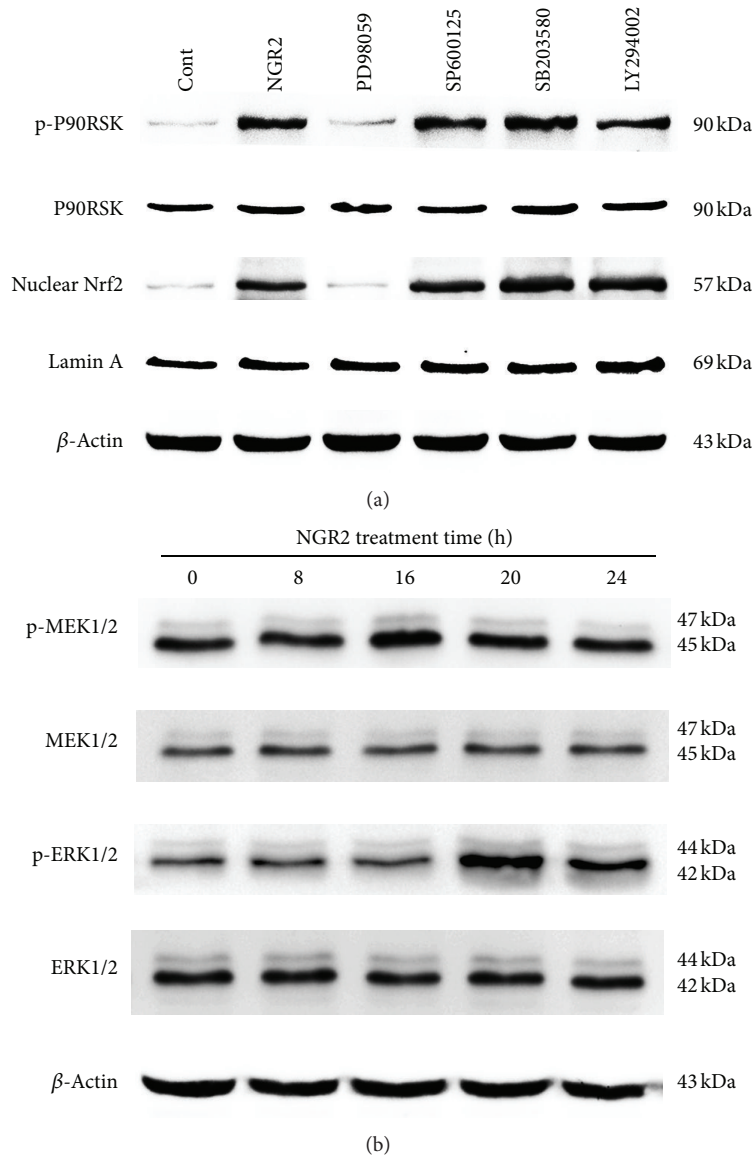

Figure 6: NGR2-mediated activation of P90RSK and Nrf2 was dependent of MEK1/2-ERK1/2 pathways but independent on JNK, P38, or PI3K/Akt pathways. The expression of proteins was determined by western blot analysis. The SH-SY5Y cells were preincubated with different inhibitors for 1 h followed by treatment with 20 μM NGR2 for 24 h. (a) NGR2-mediated the phosphorylation of P90RSK and the nuclear Nrf2 accumulation were effectively prevented by MEK inhibitor PD98059 but not by JNK inhibitor SP600125, p38 inhibitor SB203580, or PI3K/Akt inhibitor LY294002. (b) Treatment of SH-SY5Y cells with 20 μM NGR2 for different periods of time (4, 8, 16, 24 h) resulted in the activation of MEK1/2-ERK1/2 pathways.

nuclear Nrf2 accumulation and the NGR2-mediated activity enhancement of HO-1, GSH-PX, and GR, were all effectively diminished by the suppression of ERK1/2 expression with siRNA (Figures 7(b) and 7(c)). The NGR2-mediated activity enhancement of HO-1, GSH-PX, and GR was also abolished by the transfection of SH-SY5Y cells with Nrf2 siRNA (Figure 7(c)). These results were corroborated by cell counting kit-8 test, where the protective effect of NGR2 against 6-OHDA was completely abolished by the genetic silencing of MEK1/2 and ERK1/2 and the pharmacologic blockade of MEK1/2 by using PD98059. However, the protective effect of NGR2 was partly inhibited by Nrf2 siRNA (Figure 7(d)).

4. Discussion

PD is a neurodegenerative disease that causes the selective loss of dopaminergic neurons in the substantia nigra. Although the etiology and pathogenesis of PD are not completely elucidated, accumulating evidence indicates that 6-OHDA, a hydroxylated dopamine metabolite, contributes to neuronal cell death in PD [22, 23].

6-OHDA can selectively kill dopaminergic neurons because of its high affinity to the dopamine transporter [24]. Once inside the neuron, 6-OHDA undergoes auto-oxidation or metabolic degradation and produces hydrogen peroxide, superoxide, and hydroxyl radicals. This process causes lipid

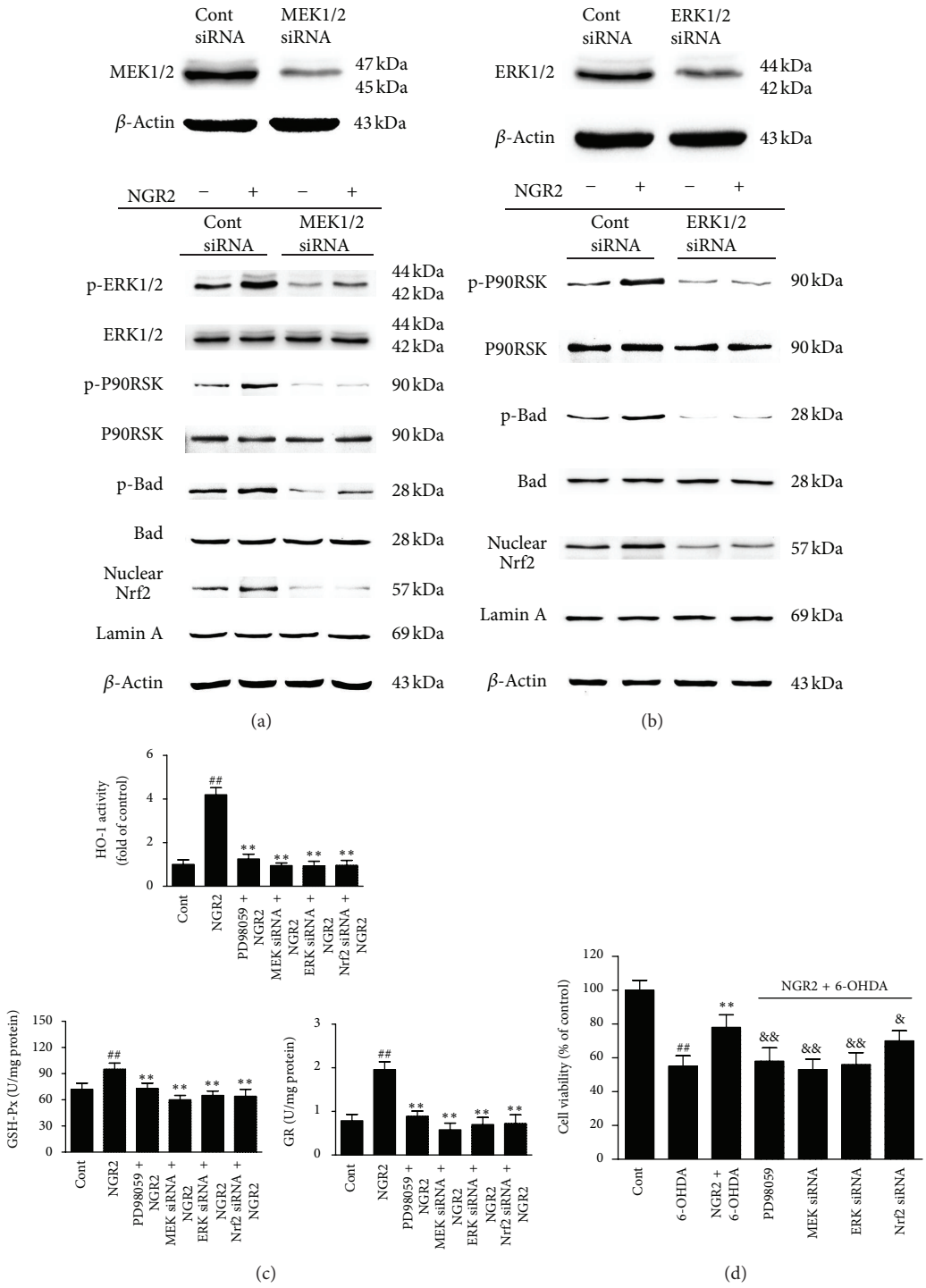

Figure 7: Neuroprotection of NGR2 involved the activation of P90RSK and Nrf2 through MEK1/2-ERK1/2 pathway. Protein expression was determined by western blot analysis. Both MEK1/2 siRNA (a) and ERK1/2 siRNA (b) suppressed NGR2-mediated activation of P90RSK and Nrf2. (c) NGR2-mediated activity enhancement of HO-1, GSH-PX, and GR was abolished by transfection of SH-SY5Y cells with MEK1/2 siRNA, ERK1/2 siRNA, and Nrf2 siRNA and by MEK inhibitor PD98059. The results are expressed as the mean ± SD of three independent experiments. ## indicates a significant difference from the control ($P < 0.01$). ∗∗ indicates a significant difference from the NGR2 treatment alone ($P < 0.01$). (d) The protective effect of NGR2 against 6-OHDA was partly abolished by Nrf2 siRNA and completely abolished by MEK1/2 siRNA, ERK1/2 siRNA, and PD98059. The results are expressed as the mean ± SD of three independent experiments. ## indicates a significant difference from the control ($P < 0.01$). ∗∗ indicates a significant difference from the 6-OHDA treatment alone ($P < 0.01$). & indicates a significant difference from NGR2+6-OHDA group ($P < 0.05$). && indicates a significant difference from NGR2+6-OHDA group ($P < 0.01$).

peroxidation, protein oxidation, and DNA oxidation and finally results in oxidative stress, mitochondrial dysfunction, and apoptosis [3, 25]. 6-OHDA is widely accepted as a toxin for induction of the PD model *in vivo* and *in vitro* [23, 26, 27]. We investigated the neuroprotective effect of NGR2 and underlying mechanisms by using an *in vitro* model of 6-OHDA-induced cell death in SH-SY5Y cells.

6-OHDA caused oxidative stress in SH-SY5Y cells, which is consistent with the results of a previous study [28]. Oxidative stress occurs when ROS production overwhelms the antioxidative ability in cells. In this study, a significant increase in ROS production and MDA levels and a striking decrease in the activities of phase II detoxifying enzymes (HO-1, GSH-PX, and GR) were observed in 6-OHDA-treated cells. However, these 6-OHDA effects were suppressed by NGR2 preincubation.

Phase II detoxifying enzymes have a central function in neuronal defense against oxidative stress. The induction of phase II detoxifying enzymes also contributes to neuroprotection. HO-1 is a rate-limiting enzyme that catalyzes the oxidative catabolism of heme and produces biliverdin, carbon monoxide, and ferrous iron. GSH-PX can catalyze the reaction between reduced glutathione and hydrogen peroxide and convert reduced glutathione to oxidized glutathione. GR can convert oxidized glutathione to reduced glutathione. A cycle exists between reduced glutathione and oxidized glutathione by GSH-PX and GR. These phase II detoxifying enzymes generate potent antioxidative abilities. The expression of HO-1, GSH-PX, and GR is regulated by the activation of an important transcription factor Nrf2. In normal status, Nrf2 is sequestrated in the cytoplasm with Keap1 (Nrf2-Kelch-like ECH-associated protein 1). When activated, Nrf2 detaches itself from the Nrf2-Keap1 complex and translocates to the nucleus. Then, Nrf2 binds to the antioxidant responsive element and initiates the expression of phase II detoxifying enzymes [29]. We found that the nuclear translocation of Nrf2 in SH-SY5Y cells time dependently increased in response to NGR2 stimulation. The abilities of HO-1, GSH-PX, and GR all increased in a time-dependent manner by NGR2 incubation. To determine whether the elevation of HO-1, GSH-PX, and GR activities is dependent on Nrf2 activation, we transfected SH-SY5Y cells with Nrf2 siRNA. The NGR2-mediated upregulation of HO-1, GSH-PX, and GR activities was effectively inhibited by Nrf2 siRNA. The neuroprotective effect of NGR2 was also partly suppressed by Nrf2 siRNA. Moreover, nuclear Nrf2 accumulation and the activities of HO-1, GSH-PX, and GR were all decreased by 6-OHDA. However, NGR2 preincubation effectively inhibits the effects of 6-OHDA. These results suggested that the neuroprotective effect of NGR2 pre-incubation may be partly caused by Nrf2-dependent activity enhancement of HO-1, GSH-PX, and GR.

The results agreed well with a previous study in which 6-OHDA resulted in mitochondrial dysfunction and apoptosis in SH-SY5Y cells [25]. This phenomenon was manifested by mitochondrial membrane depolarization, cytochrome c release, caspase-9 and caspase-3 activation, DNA fragmentation, and increased apoptosis rate. However, NGR2 preincubation was effective in protecting SH-SY5Y cells against 6-OHDA-induced apoptosis. This is the first study to report the neuroprotective effect of NGR2 against 6-OHDA-induced apoptosis. The deregulation of Bcl-2 family protein is responsible for mitochondrial dysfunction induced by 6-OHDA. In the presence of apoptotic factors, the proapoptotic protein BAD interacts with the antiapoptotic protein Bcl-xl, thereby releasing the proapoptotic protein BAX from the Bcl-xl-BAX complex. BAX can disrupt the mitochondrial membrane, thus leading to the release of cytochrome c from the mitochondria. Consequently, caspase-9 and caspase-3 are subsequently activated, and apoptosis is initiated [30]. However, BAD can be inhibited when it is phosphorylated at serine 112. Therefore, promoting the phosphorylation of BAD at serine 112 contributed to apoptosis inhibition. A previous study showed that P90RSK could phosphorylate and inhibit BAD [31]. Therefore, the effect of NGR2 on P90RSK and BAD was investigated. NGR2 time dependently activated P90RSK and increased BAD phosphorylation, thereby preventing 6-OHDA-induced apoptotic cell death. To our knowledge, this is the first study that involves P90RSK in the neuroprotection against 6-OHDA-induced apoptosis.

Given that NGR2 activated Nrf2 and P90RSK in a time-dependent manner, the fact that NGR2-mediated protection was achieved by pre-incubation only rather than cotreatment with 6-OHDA was not surprising. This result may be attributed to the requirement of sufficient time for transcriptional and translational alterations to activate Nrf2 and P90RSK.

However, the mechanism of the activation of Nrf2 and P90RSK is still unclear. Previous reports showed that ERK1/2, JNK, P38, and PI3K/Akt pathways might be involved in P90RSK or Nrf2 activation in various cell types [14–20]. To ascertain which pathway participated in the activation of P90RSK and Nrf2, different inhibitors including MEK1/2 inhibitor PD98059, JNK inhibitor SP600125, p38 inhibitor SB203580, and PI3K/Akt inhibitor LY294002 were used in the present study. We found that the MEK1/2 inhibitor PD98059, rather than inhibitors against JNK, p38, or PI3 K/Akt, achieved a nearly complete inhibition of P90RSK and Nrf2 activation. This finding suggested that MEK1/2 was involved in NGR2-mediated P90RSK and Nrf2 activation.

MEK1/2, which is located upstream of ERK1/2, plays an important role in a variety of biological responses such as cell differentiation, proliferation, survival, and apoptosis [32]. Once activated, ERK1/2 leads to P90RSK phosphorylation and Nrf2 activation. We then explored the duration of MEK1/2 and ERK1/2 phosphorylations after NGR2 incubation. The treatment of SH-SY5Y cells with NGR2 led to MEK1/2 and ERK1/2 activation. The phosphorylation of MEK1/2 and ERK1/2 reached their respective peak points chronologically at 16 and 20 h. The question remains on whether ERK1/2 was activated by MEK1/2 and whether P90RSK and Nrf2 activation occurs downstream of the ERK1/2 pathway. To clarify this issue, SH-SY5Y cells were transfected with MEK1/2 siRNA or ERK1/2 siRNA. MEK1/2 siRNA simultaneously blocked NGR2-mediated the activation of ERK1/2, P90RSK, and Nrf2 as well as the subsequent activation of their respective downstream targets. NGR2-mediated activation of P90RSK and Nrf2, and the subsequent activation of their respective downstream targets were also simultaneously

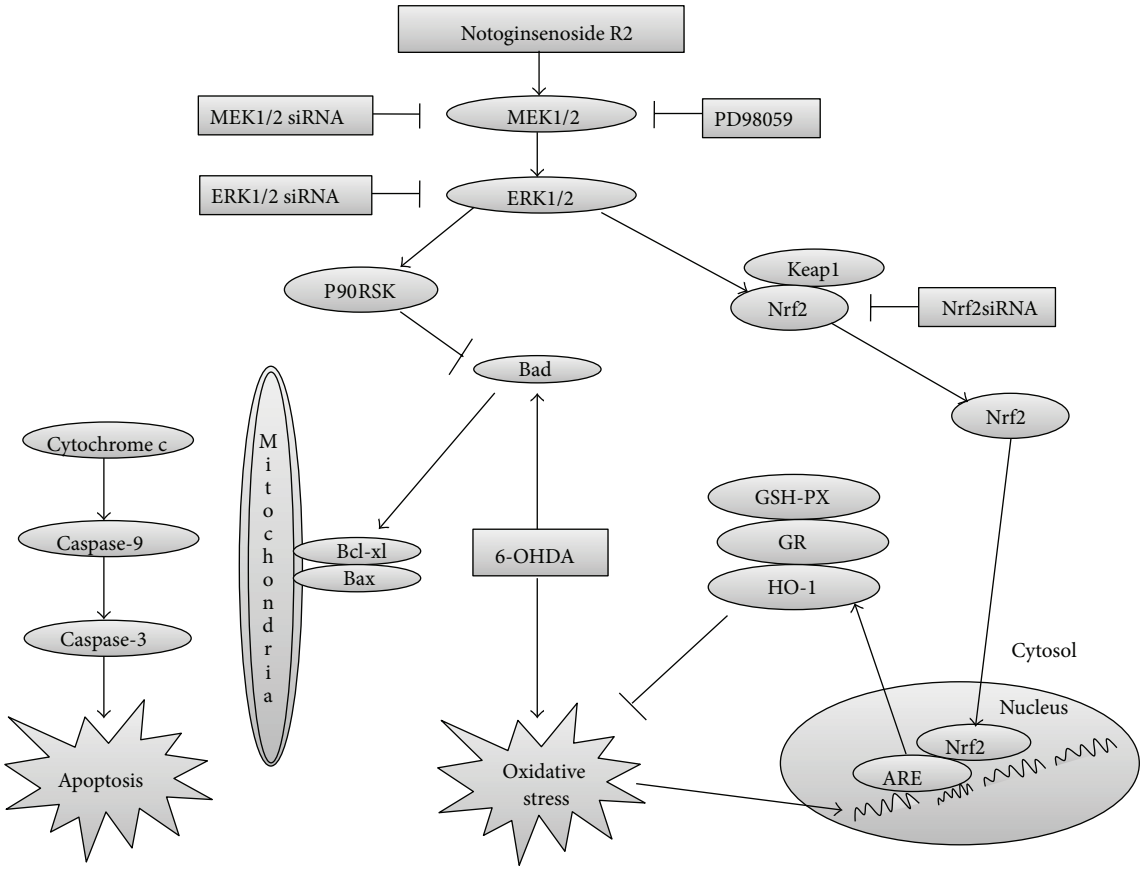

Figure 8: Schematic of the neuroprotective effects of NGR2 against 6-OHDA-induced neurotoxicity. NGR2 activates P90RSK and Nrf2 via MEK1/2-ERK1/2 pathways. P90RSK activation could inhibit BAD, thereby inhibiting 6-OHDA-induced mitochondrial membrane depolarization, cytochrome c release, caspase-9 and caspase-3 activation, and apoptosis. Nrf2 activation could enhance the activities of phase II detoxifying enzymes such as HO-1, GSH-PX, and GR. This phenomenon suppressed 6-OHDA-induced oxidative stress and DNA fragmentation.

reversed by ERK1/2 siRNA. Moreover, NGR2-mediated neuroprotection was partly inhibited by Nrf2 siRNA and completely abolished by the genetic silencing of MEK1/2 and ERK1/2 or the application of a pharmacological inhibitor against MEK1/2. These results suggested that the immediate upstream activator of P90RSK and Nrf2 was ERK1/2, and the immediate upstream activator of ERK1/2 was MEK1/2, and these factors were all involved in NGR2-mediated neuroprotection either directly or indirectly.

Although P90RSK and Nrf2 activation was clearly activated by MEK1/2-ERK1/2 signaling pathways, the occurrence of a cross-talk between P90RSK and Nrf2 was not clearly elucidated. Detailed experiments are needed to investigate the exact underlying mechanism.

However, the successful application of the protective effect of NGR2 on different neuronal cell types remains to be determined. In this study, the neuroprotective effects of NGR2 against 6-OHDA toxic effects were confirmed in PC12 cells and rat primary cortical neurons. These results suggested that the neuroprotection of NGR2 was independent of cell type.

5. Conclusion

NGR2 exhibited neuroprotective effects against 6-OHDA-induced apoptosis in SH-SY5Y cells. The mechanism of this neuroprotection was associated with NGR2-mediated P90RSK and Nrf2 activation via MEK1/2-ERK1/2 pathways (Figure 8). NGR2 provides a potential promising alternative option as adjunctive medication for the treatment of PD in clinic.

Acknowledgments

This work was supported by the Key Projects of the National Science and Technology Pillar Program (Grant no. 2008BAI51B02), the Major Scientific and Technological Special Project for "Significant New Drugs Formulation" (Grants no. 2012ZX09501001004 and no. 2012ZX09301002-001), and the Graduate Innovation Foundation of Peking Union Medical College (Grant no. 2011-1007-002).

References

[1] K. L. Lim and C. W. Zhang, "Molecular events underlying Parkinson's disease: an interwoven tapestry," *Frontiers in Neurology*, vol. 4, article 33, 2013.

[2] P. C. Trippier, K. Jansen Labby, D. D. Hawker, J. J. Mataka, and R. B. Silverman, "Target- and mechanism-based therapeutics for neurodegenerative diseases: strength in numbers," *Journal of Medicinal Chemistry*, vol. 56, no. 8, pp. 3121–3147, 2013.

[3] O. Hwang, "Role of oxidative stress in Parkinson's disease," *Experimental Neurobiology*, vol. 22, no. 1, pp. 11–17, 2013.

[4] M. H. Yan, X. Wang, and X. Zhu, "Mitochondrial defects and oxidative stress in Alzheimer disease and Parkinson disease," *Free Radical Biology and Medicine*, vol. 62, pp. 90–101, 2013.

[5] Y.-C. Lo, Y.-T. Shih, I.-J. Chen, and Y.-C. Wu, "San-Huang-Xie-Xin-Tang protects against activated microglia- and 6-OHDA-induced toxicity in neuronal SH-SY5Y cells," *Evidence-Based Complementary and Alternative Medicine*, vol. 2011, Article ID 429384, 11 pages, 2011.

[6] H. Kumar, I. S. Kim, S. V. More et al., "Gastrodin protects apoptotic dopaminergic neurons in a toxin-induced Parkinson's disease model," *Evidence-Based Complementary and Alternative Medicine*, vol. 2013, Article ID 514095, 13 pages, 2013.

[7] S.-H. Kwon, S.-I. Hong, Y.-H. Jung et al., "Lonicera japonica THUNB. protects 6-hydroxydopamine-induced neurotoxicity by inhibiting activation of MAPKs, PI3K/Akt, and NF-κB in SH-SY5Y cells," *Food and Chemical Toxicology*, vol. 50, no. 3-4, pp. 797–807, 2012.

[8] F.-C. Luo, S.-D. Wang, L. Qi, J.-Y. Song, T. Lv, and J. Bai, "Protective effect of panaxatriol saponins extracted from Panax notoginseng against MPTP-induced neurotoxicity in vivo," *Journal of Ethnopharmacology*, vol. 133, no. 2, pp. 448–453, 2011.

[9] L. Xu, W.-F. Chen, and M.-S. Wong, "Ginsenoside Rg1 protects dopaminergic neurons in a rat model of Parkinson's disease through the IGF-I receptor signalling pathway," *British Journal of Pharmacology*, vol. 158, no. 3, pp. 738–748, 2009.

[10] K. H. Kim, K. Song, S. H. Yoon et al., "Rescue of PINK1 protein null-specific mitochondrial complex IV deficits by ginsenoside Re activation of nitric oxide signaling," *Journal of Biological Chemistry*, vol. 287, no. 53, pp. 44109–44120, 2012.

[11] B. K. Barlow, D. W. Lee, D. A. Cory-Slechta, and L. A. Opanashuk, "Modulation of antioxidant defense systems by the environmental pesticide maneb in dopaminergic cells," *NeuroToxicology*, vol. 26, no. 1, pp. 63–75, 2005.

[12] X. Du, H. Xu, H. Jiang, and J. Xie, "Akt/Nrf2 activated upregulation of heme oxygenase-1 involves in the role of Rg1 against ferrous iron-induced neurotoxicity in SK-N-SH cells," *Neurotoxicity Research*, vol. 24, no. 1, pp. 71–79, 2013.

[13] S. R. Boston, R. Deshmukh, S. Strome, U. D. Priyakumar, A. D. MacKerell Jr., and P. Shapiro, "Characterization of ERK Docking domain inhibitors that induce apoptosis by targeting Rsk-1 and caspase-9," *BMC Cancer*, vol. 11, article 7, 2011.

[14] B. S. Bowser, S. Alam, and C. Meyers, "Treatment of a human papillomavirus type 31b-positive cell line with benzo[a]pyrene increases viral titer through activation of the Erk1/2 signaling pathway," *Journal of Virology*, vol. 85, no. 10, pp. 4982–4992, 2011.

[15] L. Li, J. K. Du, L. Y. Zou et al., "Decursin isolated from *Angelica gigas* Nakai rescues PC12 cells from amyloid beta-protein-induced neurotoxicity through Nrf2-mediated upregulation of Heme oxygenase-1: potential roles of MAPK," *Evidence-Based Complementary and Alternative Medicine*, vol. 2013, Article ID 467245, 14 pages, 2013.

[16] G. B. Sun, X. Sun, M. Wang et al., "Oxidative stress suppression by luteolin-induced heme oxygenase-1 expression," *Toxicology and Applied Pharmacology*, vol. 265, no. 2, pp. 229–240, 2012.

[17] E. J. Park, Y. M. Kim, S. W. Park et al., "Induction of HO-1 through p38 MAPK/Nrf2 signaling pathway by ethanol extract of *Inula helenium* L. reduces inflammation in LPS-activated RAW 264. 7 cells and CLP-induced septic mice," *Food and Chemical Toxicology*, vol. 55, pp. 386–395, 2013.

[18] J. Xu, M. Xilouri, J. Bruban et al., "Extracellular progranulin protects cortical neurons from toxic insults by activating survival signaling," *Neurobiology of Aging*, vol. 32, no. 12, pp. 2326.e5–2326.e16, 2011.

[19] A. Zoubeidi, A. Zardan, R. M. Wiedmann et al., "Hsp27 promotes insulin-like growth factor-I survival signaling in prostate cancer via p90Rsk-dependent phosphorylation and inactivation of BAD," *Cancer Research*, vol. 70, no. 6, pp. 2307–2317, 2010.

[20] X. Wang, J. Z. Liu, J. X. Hu et al., "ROS-activated p38 MAPK/ERK-Akt cascade plays a central role in palmitic acid-stimulated hepatocyte proliferation," *Free Radical Biology and Medicine*, vol. 51, no. 2, pp. 539–551, 2011.

[21] Y. Yuan, C. Y. Jiang, H. Xu et al., "Cadmium-induced apoptosis in primary rat cerebral cortical neurons culture is mediated by a calcium signaling pathway," *PLoS ONE*, vol. 8, no. 5, Article ID e64330, 2013.

[22] R. Andrew, D. G. Watson, S. A. Best, J. M. Midgley, H. Wenlong, and R. K. H. Petty, "The determination of hydroxydopamines and other trace amines in the urine of parkinsonian patients and normal controls," *Neurochemical Research*, vol. 18, no. 11, pp. 1175–1177, 1993.

[23] J. W. Chambers, S. Howard, and P. V. LoGrasso, "Blocking c-Jun N-terminal kinase (JNK) translocation to the mitochondria prevents 6-hydroxydopamine-induced toxicity in vitro and in vivo," *Journal of Biological Chemistry*, vol. 288, no. 2, pp. 1079–1087, 2013.

[24] V. Lehmensiek, E.-M. Tan, S. Liebau et al., "Dopamine transporter-mediated cytotoxicity of 6-hydroxydopamine in vitro depends on expression of mutant α-synucleins related to Parkinson's disease," *Neurochemistry International*, vol. 48, no. 5, pp. 329–340, 2006.

[25] J. C. Tobon-Velasco, J. H. Limon-Pacheco, M. Orozco-Ibarra et al., "6-OHDA-induced apoptosis and mitochondrial dysfunction are mediated by early modulation of intracellular signals and interaction of Nrf2 and NF-kappaB factors," *Toxicology*, vol. 304, pp. 109–119, 2013.

[26] G. Tovilovic, N. Zogovic, V. Soskic et al., "Arylpiperazine-mediated activation of Akt protects SH-SY5Y neuroblastoma cells from 6-hydroxydopamine-induced apoptotic and autophagic death," *Neuropharmacology*, vol. 72, pp. 224–235, 2013.

[27] N. Sriraksa, J. Wattanathorn, S. Muchimapura, S. Tiamkao, K. Brown, and K. Chaisiwamongkol, "Cognitive-enhancing effect of quercetin in a rat model of Parkinson's disease induced by 6-hydroxydopamine," *Evidence-Based Complementary and Alternative Medicine*, vol. 2012, Article ID 823206, 9 pages, 2012.

[28] M. P. Cunha, M. D. Martin-de-Saavedra, A. Romero et al., "Protective effect of creatine against 6-hydroxydopamine-induced cell death in human neuroblastoma SH-SY5Y cells: involvement of intracellular signaling pathways," *Neuroscience*, vol. 238, pp. 185–194, 2013.

[29] J.-W. Kim, M.-H. Li, J.-H. Jang et al., "15-Deoxy-Δ12,14-prostaglandin J2 rescues PC12 cells from H2O2-induced apoptosis through Nrf2-mediated upregulation of heme oxygenase-1: potential roles of Akt and ERK1/2," *Biochemical Pharmacology*, vol. 76, no. 11, pp. 1577–1589, 2008.

[30] E. Yang, J. Zha, J. Jockel, L. H. Boise, C. B. Thompson, and S. J. Korsmeyer, "Bad, a heterodimeric partner for Bcl-x(L), and Bcl-2, displaces Bax and promotes cell death," *Cell*, vol. 80, no. 2, pp. 285–291, 1995.

[31] A. Bonni, A. Brunet, A. E. West, S. R. Datta, M. A. Takasu, and M. E. Greenberg, "Cell survival promoted by the Ras-MAPK signaling pathway by transcription-dependent and -independent mechanisms," *Science*, vol. 286, no. 5443, pp. 1358–1362, 1999.

[32] M. C. Lawrence, A. Jivan, C. Shao et al., "The roles of MAPKs in disease," *Cell Research*, vol. 18, no. 4, pp. 436–442, 2008.

Hindawi Publishing Corporation
Evidence-Based Complementary and Alternative Medicine
Volume 2013, Article ID 347525, 5 pages
http://dx.doi.org/10.1155/2013/347525

Research Article

Open Randomized Clinical Trial on JWSJZ Decoction for the Treatment of ALS Patients

Weidong Pan,[1] Xiaojing Su,[2] Jie Bao,[1] Jun Wang,[1] Jin Zhu,[1] Dingfang Cai,[1,3] Li Yu,[1] and Hua Zhou[4]

[1] *Department of Neurology, Shuguang Hospital Affiliated to Shanghai University of TCM, 528 Zhangheng Road, Pudong New Area, Shanghai 201203, China*
[2] *Department of Rehabilitation, First Hospital of Yinchuan, 40 Liqun East Road, Xing Qing Area, Yinchuan 750001, China*
[3] *Laboratory of Neurology, Institute of Integrative Medicine, Zhongshan Hospital, Fudan University, 180 Fenglin Road, Shanghai 200032, China*
[4] *Department of Cardiology, Shuguang Hospital Affiliated to Shanghai University of TCM, 528 Zhangheng Road, Pudong New Area, Shanghai 201203, China*

Correspondence should be addressed to Hua Zhou; huazhoum@gmail.com

Received 27 April 2013; Revised 21 July 2013; Accepted 23 July 2013

Academic Editor: Paul Siu-Po Ip

Objective. To investigate the efficacy and safety of the traditional Chinese medicine Jiawei Sijunzi (JWSJZ) decoction for the treatment of patients with amyotrophic lateral sclerosis (ALS). *Methods*. Forty-eight patients with ALS were divided into a JWSJZ group ($n = 24$) and a control group ($n = 24$) using a randomized number method. Together with the basic treatment for ALS, JWSJZ decoction was added to the treatment regimen of patients in the JWSJZ group or Riluzole was administered to the control group for 6 months. Neurologists evaluated the treated and control patients using the ALS functional rating scale (ALSFRS) before, 3 and 6 months after starting the additional treatments. *Results*. The ALSFRS scores in both groups were lower 3 and 6 months after treatment than before. There was a significant difference at 6 months after treatment between the subgroups of patients with ALS whose limbs were the initial site of attack. No serious adverse effects were observed in the JWSJZ group. *Conclusion*. JWSJZ decoction may be a safe treatment for ALS, and may have delayed the development of ALS, especially in the subgroup of patients in whom the limbs were attacked first when compared with Riluzole treatment.

1. Introduction

Amyotrophic lateral sclerosis (ALS), also known as Lou Gehrig's disease, is a relatively rare, adult-onset, rapidly progressive, and fatal disease that involves degeneration of spinal cord motor neurons [1]. This disorder causes muscle weakness and atrophy throughout the body, and patients with ALS ultimately lose all voluntary movement. Regardless of the region of onset, however, muscle weakness and atrophy invariably spread to other parts of the body as the disease progresses. Although disease progression varies between individuals, toward the end stages of disease, most patients require ventilator support. Individuals with ALS most commonly die of respiratory failure or pneumonia within 2–5 years of diagnosis. There are no current treatments for ALS. ALS is diagnosed as "flaccidity syndrome" by traditional Chinese theory based on the weakness and atrophy of limbs and body and the fact that most patients are eventually unable to stand or walk, get in or out of bed on their own, use their hands and arms, and have difficulty with chewing, swallowing, and breathing, which ultimately lead to progressive weight loss and increased risk of choking and aspiration pneumonia. Most traditional Chinese doctors believe that the pathogenesis of motor neuron degeneration in ALS has its origin in a deficiency in the spleen, which is the organ that controls the creation of muscle, or deficiency of spleen accompanied by excess expending [2]. "Deal with Yangming meridian alone when treating flaccidity syndrome" is described in the ancient Chinese medicine book Huangdi Neijing [3]. The Yangming meridian means the functions of

the spleen. It could be thought that dealing with the spleen alone might improve the flaccidity syndrome. In previous studies, Sijunzi decoction appeared to positively improve and optimize cellular immune function and nutritional status in postsurgical gastric cancer patients [4], as well as improving neuroendocrine regulation in rats with "spleen-deficiency and spleen dysfunction" [5]. Jiawei Sijunzi decoction (JWSJZ) is made from Sijunzi decoction which can nourish the spleen and enrich the vitality of the body, plus the 2 herbs *Radix astragali* and *Desertliving cistanche*. Here we investigated the effects of JWSZJ decoction in the treatment of patients with ALS at 6 months and compared them with those of Riluzole, the only possibly effective "orphan drug" for treating ALS, in an attempt to demonstrate an evidence-based quantitative study of the effects of JWSJZ decoction.

2. Subjects and Methods

2.1. Subjects. An open randomized study design was used. Forty-eight patients with probable or definite ALS as defined by the El Escorial criteria [6] diagnosed at the Department of Neurology of Shuguang Hospital Affiliated to Shanghai University of TCM were invited to participate in the study. The age of the patients ranged from 20 to 80 years old ($\overline{x} \pm s$, 50.4±6.7 years), and signed informed consent was obtained before participation. The baseline clinical characteristics of the two ALS groups, including age, gender, mean symptom duration at baseline, in months, mean time from diagnosis to baseline in months, and mean ALSFRS scores at baseline are presented in Table 1. The study was approved by The Ethics Committee of Shuguang Hospital Affiliated to Shanghai University of TCM and was performed in accordance with the principles outlined in the Declaration of Helsinki.

2.2. Randomization, Masking, and Drug Administration. An unblinded pharmacist generated randomization codes using an Excel (Microsoft Office) random number generator (Microsoft, USA) in blocks of two and four participants. Kits were given sequential numbers that corresponded to the randomization key and were maintained in a secure location. When randomized, each successive participant was assigned by an electronic clinical trial management system to the next numbered kit in sequence at each site. The ALS patients were randomized into either the JWSJZ group ($n = 24$) or the control group ($n = 24$). There was no stratification of patients according to the onset region, age, or respiratory function since all the patients enrolled were supposed to receive both treatments.

Patients who had a forced vital capacity of less than 30%, those with signs of a major psychiatric disorder and/or dementia, acute cholecystitis, or bile duct occlusion, or patients who had another concomitant condition thought to be likely to interfere with drug compliance and outcome assessment were excluded. Additional exclusion criteria were pregnancy and participation in other clinical trials. The patients in the JWSJZ group took the JWSJZ decoction (*Panax Jinseng 9* g, *Radix Astragali 30* g, *Desert Cistanche 12* g, *Rhizoma Atractylodis Macrocephalae 9* g, *Poria Cocos 9* g, *Glycyrrhiza 9* g; Place all of the herbs into 400 mL of cold water, soak for 30 min, and boil for 30 min using a small flame to obtain about 100 mL of decoction. The decoctions were prepared by the manufacturing laboratory of Shuguang Hospital) (50 mL) twice per day while the other patients were treated with Riluzole tablets (Sanofi-Aventis Co., Ltd., France; 50 mg) twice per day for 6 consecutive months. They were not treated by any other complementary and/or alternative treatments such as other traditional Chinese medicine, Tai Chi exercise, or acupuncture.

2.3. Clinical Efficacy and Safety Evaluation. A detailed history and neurological examination were performed 3 times by a neurologist in all subjects at baseline (before treatment), 3 months, and 6 months throughout the 6-month study period. Disease severity was graded using the revised ALS functional rating scale (ALSFRS) [7]. We used the improvement rate of ALSFRS as the primary result to evaluate the efficacy of the additional treatment. The improvement rates were calculated using the formula (1). Treatment compliance was checked monthly by a pharmacist, and noncompliant patients who took less than 80% of the study medications were considered to have violated the treatment protocol. Changes in the SF-36 physical functioning (PF) subscale [8] and the mean distal limb muscle strength scale were used as secondary results. Standard laboratory tests including red blood cell count, chemistry, renal and liver function, and electrocardiograms were performed at baseline and at the posttreatment discontinuation visit. Safety was evaluated as the incidence and severity of adverse events, and their relationships to treatment were determined based on the results of laboratory tests, patient reports, and the judgment of the investigator.

Consider the following:

$$\text{improvement rate} = \left|\frac{\text{after} - \text{before}}{\text{before}}\right| \times 100\%. \quad (1)$$

2.4. Statistical Analysis. Repeated-measure ANOVA was conducted to test the differences among changes in outcomes at baseline, at 3 months, and 6 months later for both groups. Differences at baseline between the JWSJZ group and control group were analyzed using the t-test. A significant difference was defined as $P < 0.05$. SPSS (Windows version 17.0) software was used for statistical analyses. All data are expressed as the mean ± standard deviation.

3. Results

There were no differences in gender, age, and ALSFRS scores before the additional treatments were started between the two groups (Table 1). In the JWSJZ group, 18 patients first developed ALS in the limbs (defined as subgroup), 3 via bulbar paralysis, and 3 from both syndromes. In the control group, 19 patients first developed ALS in the limbs, 2 via bulbar paralysis, and 3 were attacked by both. Except for the patient who died from development of the disease at the end of the trial, all patients completed the investigation with less side effects (treatment related gastrointestinal side effects: 2 with nausea and 2 with constipation) in the JWSJZ group.

Table 1: Baseline clinical characteristics of the two ALS groups.

Subjects	JWSJZ group ($n = 23$)	Control group ($n = 19$)	P value
Age (years)	51.6 ± 7.2	50.1 ± 4.2	0.89
Men/Women	14/9	11/8	—
Disease duration (months)	25.9 ± 24.7	26.1 ± 24.9	0.37
Mean time from diagnosis (months)	18.35 ± 16.78	17.59 ± 13.51	0.29
Area where ALS first developed—limbs/bulbar/both	18/3/3	19/2/3	—
ALSFRS	37.1 ± 7.6	37.4 ± 9.2	0.65

No liver/kidney damage was observed in the JWSZJ group. Two patients died from development of the disease, including one limb first attack patient, and 12 patients had drug related gastrointestinal side effects in the control group (including 9 cases with nausea, 6 with dizziness, 7 with anorexia, 3 with constipation, and 3 with diarrhea). Three cases withdrew from the study due to side effects or economic reasons or both in the control group (Figure 1). Four patients had drug related liver/kidney damage.

The changes in ALSFRS score were as follows: the scores of both groups had decreased significantly after 6 months of treatment compared with those before treatment; however, the slope of the decrease in the JWSJZ group was less than that in the control group. No significant differences were found between the endpoint of the two groups (Table 2). The limbs first attack patients (subgroup) in the JWSJZ group had a significantly smaller rate of change (%) of ALSFRS scores after 6 months of treatment compared with the subgroup in the control group (Table 3). The changes in SF-36 physical functioning (PF) sub-scale and muscle strength were as follows: both groups had significant decreases in the PF sub-scale, but there were no significant changes in muscle strength (Table 4) compared with baseline after 6 months of treatment. The PF sub-scale was slightly higher in the JWSJZ group than in the control group at the endpoint, but the difference was not significant.

4. Discussion

Amyotrophic lateral sclerosis (ALS) is a fatal neurodegenerative disorder characterized by progressive degeneration of motor neurons in the motor cortex, brain stem, and spinal cord, leading to paralysis and death, typically within 3–5 years from symptom onset. Riluzole is the only FDA-approved "orphan drug" for ALS and prolongs median survival by only 2-3 months in patients treated for at least 18 months. Importantly, the greatest benefit of Riluzole is observed when treatment is initiated early in the course of the disease, highlighting the importance of early intervention in ALS [9]. Identifying effective treatments for ALS is the most important task for neurologists. Traditional Chinese medicine is one treatment choice for ALS due to its benefits that have been reported in clinical studies [10, 11]. The progressive weakness, muscle atrophy, dysphagia, weight loss, and even respiratory paralysis associated with ALS belong to "flaccidity syndrome or Wei Zheng" in Chinese traditional medicine theory. "Deal with Yangming meridian alone when treating flaccidity syndrome" is one proven theory currently in use for flaccidity treatment. According to traditional Chinese medicine, the functions of the stomach and spleen belong to the Yang Ming meridian. The "Stomach is the reservoir of food and drink" and "the sources of Qi (vitality) and blood manufacture" according to Huangdi Neijing [3], which demonstrates that "Yang Ming is the sea of the viscera internal organs of the body, it can embellish muscle tendons, and the muscle tendons can modify the movement of the joints." The Yang Ming meridian can manufacture all muscles of the organs and limbs and control their activities. If the Yang Ming is deteriorating, the muscles will atrophy and flaccidity will develop. We based JWSJZ on the famous traditional nourishing spleen and enriching vitality formula, Sijunzu decoction (*Panax ginseng* (Ren Shen), *Rhizoma Atractylodis Macrocephalae* (Bai Zhu), *Poria cocos* (Fu Ling), and *honey-fried licorice root* (Zhi Gan Cao)) [2], plus more potent nourishing spleen and enriching vitality herbs, *Astragalus mongholicus* (Huang Qi) and *Herba cistanche* (Cong Rong), to increase the nourishing functions of the decoction. Previous studies have demonstrated that *Panax ginseng* can improve the immunity of the body [12] and that *Rhizoma Atractylodis Macrocephalae* has neuroprotective effects and can protect against excitotoxicity-induced apoptosis in cultured cerebral cortical neurons [13]. *Poria cocos* and *honey-fried licorice root* have been found to inhibit the development of senile dementia and improve the degeneration of neurons [14]. *Astragalus mongholicus* inhibited high mobility group protein 1-(HMGB1-) induced endothelial cell permeability in endothelial cells and modulates some endothelial functions of the body [15]. The JWSJZ decoction might improve the activity and condition of the muscles, and this may agree with the treatment policy of "Deal with Yangming meridian alone in treating for flaccidity syndrome" when treating ALS. After 6 months of treatment, the severity of the ALS worsened in both groups and the symptoms of the ALS patients were not improved by the JWSJZ decoction, but compared with the Riluzole group, the JWSJZ decoction seemed to be slightly superior at slowing down the speed of development of ALS (Table 1). JWSJZ showed significant effects in the limbs first attacked subgroup patients on reducing development of the disease compared with Riluzole (Table 2). Limbs first attacked patients with limb atrophy and flaccidity syndrome belong to the "flaccidity syndrome or Wei Zheng" and conform more to traditional Chinese medicine theory, while bulbar paralysis first attack patients just suffer a deficiency of vital energy. It is

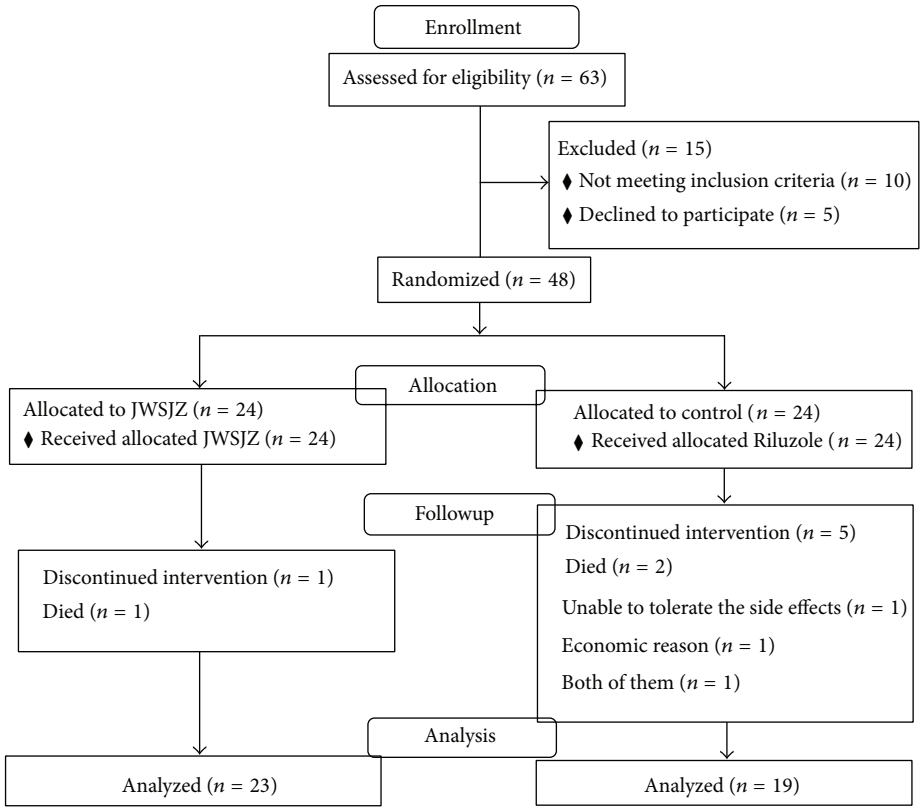

Figure 1: CONSORT flow diagram of JWSJZ decoction for the treatment of patients with ALS.

Table 2: Comparison of ALSFRS before and after treatment for JWSJZ group and control group ($\chi \pm S$).

Variable	n		ALSFRS			Rate of change (%)
	Before	After	Before	3 m	6 m	
JWSJZ	24	23	38.2 ± 6.3	36.1 ± 8.7	34.4 ± 7.9*	13.57
Control	24	19	37.9 ± 7.7	34.3 ± 6.8	30.6 ± 9.1*	19.26

JWSJZ: Jiawei Sijunzi decoction; ALSFRS: amyotrophic lateral sclerosis functional rating scale; *$P < 0.05$ compared with before treatment for the same group; rate of change: counted between before treatment and 6 months for the same group.

Table 3: Comparison of ALSFRS before and after treatment for limbs first attacked subgroups of JWSJZ group and control group ($\chi \pm S$).

Variable	n of limbs first attacked		ALSFRS			Rate of change (%)
	Before	After	Before	3 m	6 m	
JWSZJ	18	18	37.1 ± 7.6	35.2 ± 7.4	33.9 ± 6.2*	10.68#
Control	19	18	37.4 ± 9.2	34.5 ± 4.5	31.6 ± 8.9*	19.03

JWSJZ: Jiawei Sijunzi decoction; ALSFRS: amyotrophic lateral sclerosis functional rating scale; *$P < 0.05$ compared with before treatment for the same group; #$P < 0.01$, compared with JWSJZ group; rate of change; counted between before treatment and 6 months for the same group.

Table 4: Comparison of SF-36 physical function (PF) sub-scale and mean distal limb muscle strength between JWSJZ group and control group before and after treatment ($\chi \pm S$).

Variable	n		PF sub-scale			Distal limb muscle strength		
	Before	After	Before	3 m	6 m	Before	3 m	6 m
JWSJZ	24	23	43.1 ± 5.2	42.4 ± 7.3	38.9 ± 4.9*	3.7 ± 0.5	3.7 ± 0.3	3.5 ± 0.7
Control	24	19	42.9 ± 4.9	42.3 ± 6.8	37.6 ± 7.7*	3.7 ± 0.7	3.6 ± 0.6	3.5 ± 0.4

JWSJZ: Jiawei Sijunzi decoction; PF sub-scale: physical function sub-scale; *$P < 0.05$ compared with before treatment for the same group.

easy to understand why patients whose limbs were attacked first responded more sensitively to treatment with the JWSJZ decoction. No significant differences were observed between the subgroups in the Riluzole group. Furthermore, compared with the Riluzole group, the JWSJZ group demonstrated better dependency, less side effects, and a cheaper price. From 2008 to 2012 in China, the mean price of JWSJZ decoction was about 22.8 yuan/per day, while Riluzole cost was 160 yuan/per day (exchange rate; approximately 6 yuan/US dollar); therefore, the JWSJZ decoction is superior to Riluzole from a price perspective.

Inefficient GluR2 Q/R site editing is a disease-specific molecular dysfunction found in the motor neurons of sporadic ALS patients [16]. Genetically modified mice (designated as AR2) showed a decline in motor function commensurate with the slow death of ADAR2-deficient motor neurons in the spinal cord and cranial motor nerve nuclei [17]. The efficacy of JWSJZ decoction for treating ALS was also observed in vivo using this AR2 mouse model [18]; however, the molecular mechanism is not yet clear and further studies are needed. We have reported the clinical effects of the nourishing spleen and enriching vitality method, JWSJZ decoction, for treating ALS, especially in patients whose limbs were the first point of attack of the disease, compared with the ALS "orphan drug" Riluzole. The traditional Chinese decoction may be one adjuvant treatment for ALS; however, studies with larger sample sizes and/or different dosages will be needed to confirm the efficacy.

Acknowledgments

This study was sponsored by the National High Technology Research and Development Programme of China (863 Programme: Hua Zhou, 2010AA0221396001), the Special Fund of National Traditional Chinese Medicine (The promotion of base for standard research of traditional Chinese medicine: Hua Zhou, ZYYS-2010), the Three-Year Developmental Plan Project for Traditional Chinese Medicine (major research) of the Shanghai Municipal Health Bureau (ZYSNXD-CC-ZDYJ028), and the Shanghai Pujiang Programme of the Science and Technology Commission of Shanghai Municipality (Weidong Pan, 09PJ1409300).

References

[1] R. Tandan and W. G. Bradley, "Amyotrophic lateral sclerosis: part I. Clinical features, pathology, and ethical issues in management," *Annals of Neurology*, vol. 18, no. 3, pp. 271–280, 1985.

[2] B. Peng and J. Xie, *Traditional Chinese Internal Medicine*, People's Medical Publishing House, Beijing, China, 2nd edition, 2007.

[3] B. Wang, *The Yellow Emperor's Classic of Internal Medicine—Simple Questions*, People's Health Publishing House, Beijing, China, 1979.

[4] J. Cai, H. Wang, S. Zhou, B. Wu, H.-R. Song, and Z.-R. Xuan, "Effect of Sijunzi decoction and enteral nutrition on T-cell subsets and nutritional status in patients with gastric cancer after operation: a randomized controlled trial," *Journal of Chinese Integrative Medicine*, vol. 6, no. 1, pp. 37–40, 2008.

[5] Q. Liu and G. Cai, "Content of somatostatin and cholecystokinin-8 in hypothalamus and colons in a rat model of spleen-deficiency syndrome," *Journal of Chinese Integrative Medicine*, vol. 5, no. 5, pp. 555–558, 2007.

[6] B. R. Brooks, R. G. Miller, M. Swash, and T. L. Munsat, "El Escorial revisited: revised criteria for the diagnosis of amyotrophic lateral sclerosis," *Amyotrophic Lateral Sclerosis*, vol. 1, no. 5, pp. 293–299, 2000.

[7] J. M. Cedarbaum, N. Stambler, E. Malta et al., "The ALSFRS-R: a revised ALS functional rating scale that incorporates assessments of respiratory function," *Journal of the Neurological Sciences*, vol. 169, no. 1-2, pp. 13–21, 1999.

[8] J. E. Ware Jr. and C. D. Sherbourne, "The MOS 36-item short-form health survey (SF-36). I. Conceptual framework and item selection," *Medical Care*, vol. 30, no. 6, pp. 473–483, 1992.

[9] M. C. Zoing, D. Burke, R. Pamphlett, and M. C. Kiernan, "Riluzole therapy for motor neurone disease: an early Australian experience (1996–2002)," *Journal of Clinical Neuroscience*, vol. 13, no. 1, pp. 78–83, 2006.

[10] X. Wenjie, R. Hongli, and Z. Huiping, "Effects of Kidney-tonifying, Spleen-strengthening and Liver-soothing Method on Amyotrophic Lateral Sclerosis," *Shang Hai Zhong Yi Yao Da Xue Xue Bao*, vol. 25, no. 5, pp. 46–49, 2011.

[11] W. Jun, G. Junpeng, G. Yongmei et al., "Clinical study of the effect of Fuyuan shengji granule on symptoms of the patients with Amyotrophic Lateral Sclerosis," *Journal of Neurology and Neurorehabilitation*, vol. 6, no. 3, pp. 173–175, 2009.

[12] L. Zhai, Y. Li, W. Wang, Y. Wang, and S. Hu, "Effect of oral administration of ginseng stem-and-leaf saponins (GSLS) on the immune responses to Newcastle disease vaccine in chickens," *Vaccine*, vol. 29, no. 31, pp. 5007–5014, 2011.

[13] Q. Gao, Z. H. Ji, Y. Yang, R. Cheng, and X. Y. Yu, "Neuroprotective effect of Rhizoma Atractylodis macrocephalae against excitotoxicity-induced apoptosis in cultured cerebral cortical neurons," *Phytotherapy Research*, vol. 27, no. 6, p. 948, 2013.

[14] Z. Lin, J. Gu, J. Xiu, T. Mi, J. Dong, and J. K. Tiwari, "Traditional Chinese medicine for senile dementia," *Evidence-Based Complementary and Alternative Medicine*, vol. 2012, Article ID 692621, 13 pages, 2012.

[15] Y. J. Zheng, B. Zhou, Z. F. Song et al., "Study of Astragalus mongholicus Polysaccharides on endothelial cells permeability induced by HMGB1," *Carbohydrate Polymers*, vol. 92, no. 1, pp. 934–941, 2013.

[16] Y. Kawahara, K. Ito, H. Sun, H. Aizawa, I. Kanazawa, and S. Kwak, "Glutamate receptors: RNA editing and death of motor neurons," *Nature*, vol. 427, no. 6977, p. 801, 2004.

[17] T. Hideyama, T. Yamashita, T. Suzuki et al., "Induced loss of ADAR2 engenders slow death of motor neurons from Q/R site-unedited GluR2," *Journal of Neuroscience*, vol. 30, no. 36, pp. 11917–11925, 2010.

[18] P. Weidong, S. Xiaojing, W. Jun et al., "The study for the effects of "Jiawei Sijunzi Decoction" in treating for movement dysfunction of amyotrophic lateral sclerosis AR2 mice," *Shang Hai Zhong Yi Yao Da Xue Xue Bao*, vol. 27, no. 1, pp. 60–63, 2013.

Hindawi Publishing Corporation
Evidence-Based Complementary and Alternative Medicine
Volume 2013, Article ID 957875, 15 pages
http://dx.doi.org/10.1155/2013/957875

Review Article

Advances in Neuroprotective Ingredients of Medicinal Herbs by Using Cellular and Animal Models of Parkinson's Disease

Sandeep Vasant More, Hemant Kumar, Seong Mook Kang, Soo-Yeol Song, Kippeum Lee, and Dong-Kug Choi

Department of Biotechnology, College of Biomedical and Health Science, Konkuk University, Chungju 380-701, Republic of Korea

Correspondence should be addressed to Dong-Kug Choi; choidk@kku.ac.kr

Received 6 June 2013; Revised 25 July 2013; Accepted 26 July 2013

Academic Editor: Paul Siu-Po Ip

Parkinson's disease (PD) is a multifactorial disorder, which is neuropathologically identified by age-dependent neurodegeneration of dopaminergic neurons in the substantia nigra. Development of symptomatic treatments has been partly successful for PD research, but there remain a number of inadequacies in therapeutic strategies for the disease. The pathogenesis of PD remains intricate, and the present anti-PD treatments appears to be clinically insufficient. Comprehensive research on discovery of novel drug candidates has demonstrated that natural products, such as medicinal herbs, plant extracts, and their secondary metabolites, have great potential as therapeutics with neuroprotective activity in PD. Recent preclinical studies suggest that a number of herbal medicines and their bioactive ingredients can be developed into optimum pharmaceuticals for treating PD. In many countries, traditional herbal medicines are used to prevent or treat neurodegenerative disorders, and some have been developed as nutraceuticals or functional foods. Here we focus on recent advances of the evidence-linked neuroprotective activity of bioactive ingredients of herbal origin in cellular and animal models of PD research.

1. Introduction

Parkinson's disease (PD) is a chronic neurological disorder, characterized by a selective loss of dopaminergic neurons in the substantia nigra (SN) of ventral midbrain area, causing a subsequent reduction of dopamine (DA) levels in the striatum. Loss of dopaminergic supply to striatum causes imbalance with neurotransmitters like acetylcholine and DA, resulting in PD symptoms. Some typical characteristic symptoms observed in PD patients are tremor, myotonia, and dyskinesia [1]. The three main strategic developments in drug discovery that have advanced the progress in therapeutic management of PD patients have focused on the alleviation of motor symptoms by the use of dopaminergic mimetics, the development of novel nondopaminergic drugs for symptomatic improvement, and lastly, the discovery of neuroprotective compounds that have disease modifying effects in PD [2]. The pathogenesis and etiology of PD are not completely understood. Extensive study of various models mimicking key features of PD has outlined important cellular factors of dopaminergic cell death, including neuroinflammation, oxidative stress, mitochondrial dysfunction, and excitotoxicity [3, 4]. Although no model has thus far been able to reiterate all the pathological features of PD [5], the neurotoxic models have proved themselves to be a worthy tool for developing novel therapeutic strategies and assessing the efficacy and adverse effects of symptomatic treatments of PD [6].

Since ancient times, PD has been documented in various parts of the world. Based on their experience-based theories as well as practices from elsewhere, Asian countries, such as India, China, Japan, and Korea, have been using different combinations of herbal materials to treat PD within the context of ancient herbal medical systems [7]. Ayurveda, an ancient form of alternative traditional medicine followed in the Indian subcontinent describes PD as "Kampavata" [8] wherein seed preparations of mucuna are used as contemporary medicine for the treatment of PD [7]. Upon scientific investigations, it was found that *Mucuna pruriens* contains levodopa, which provides long-term amelioration of Parkinsonism [9, 10]. Formulation of powdered seed of

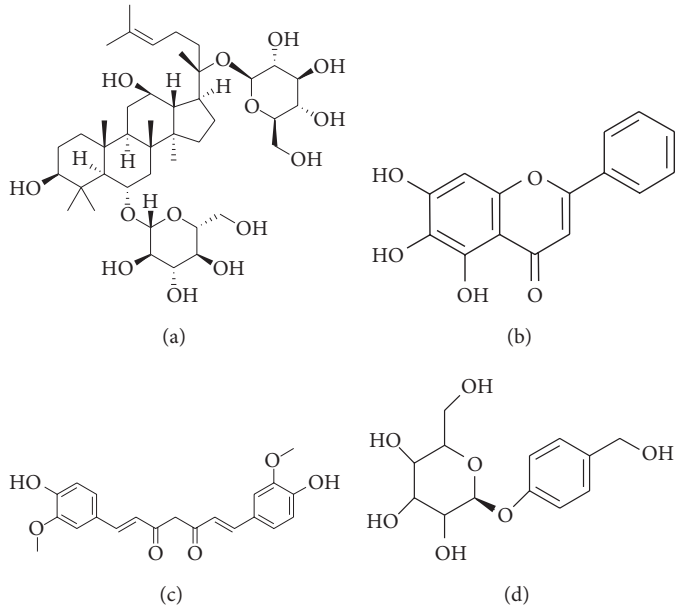

Figure 1: Chemical structure of ginsenoside Rg1 (a), baicalein (b), curcumin (c), and gastrodin (d).

Mucuna pruriens also showed positive effects on PD patients in clinical trials, with quick onset of action and without concomitant increase in dyskinesia [11]. Zandopa (HP-200), a commercial preparation of *Mucuna pruriens*, is also available for the treatment of PD [12]. In Chinese traditional medicine, 22,500 medicinal herbs are in use throughout China, of which only a few have been successfully investigated in animal experiments or clinical trials for potential development into herbal formulations for treating PD [13].

The past decade has substantiated considerable interest in phytochemical bioactive constituents from herbal medicines, which can have long-term medicinal or health-promoting qualities in PD [14]. In comparison, many medicinal plants exhibit specific medicinal actions without serving a nutritional role in the human diet and may be used in response to specific health problems over short- or long-term intervals [15, 16]. Therefore, a scientific re-examination of these therapies in preclinical models is valuable for the development of novel neuroprotective drugs for PD [17]. According to estimates from the World Health Organization, by 2040, neurodegenerative diseases will exceed cancer as the principal cause of death in industrialized countries. Irrespective of our advances in understanding the pathogenesis of PD, pharmacological treatments by conventional medicine have not transpired into satisfactory results. Therefore, it is plausible that the use of bioactive compounds from natural sources may yield more appropriate potential candidates for the preventive treatment of PD [18].

Comprehensive research on the discovery of novel neuroprotective drug candidates has proven that natural products, such as plant extracts and their bioactive compounds, can have tremendous potential as lead neuroprotective candidates in PD treatment. To list a few compounds from herbal origin, apomorphine, rivastigmine, and PYM-50028 are under clinical investigation to be used as potential neuroprotective agents in PD [19]. Here, we have focused on recent advances in the research of herbal medicines and their bioactive ingredients used in animal and cellular neurotoxic models of PD, so as to facilitate future basic and clinical investigations.

2. Neuroprotective Activity of Bioactive Compounds from Herbal Medicines

2.1. Ginsenoside Rg1. Ginseng is the dried root and rhizome of *Panax ginseng* and *Panax notoginseng* (Araliaceae) [13]. Ginseng is a valuable herb in traditional medicine, which has been utilized for over many centuries, based on the theory that it is a general tonic for the promotion of vitality, health, and longevity. The aqueous extract of ginseng has been used to treat many kinds of disease including ischemia, anemia, diabetes mellitus, gastritis, and insomnia [20]. There are over 30 ginsenosides among which the main active ingredients responsible for its vivid pharmaceutical actions are ginsenoside Rb1, Rd, Re, and Rg1 [21].

Recently, the aqueous extract of *Panax ginseng* was investigated for its protective effects against cellular model of parkinsonism like 1-methyl-4-phenylpyridine (MPP^+)-induced cytotoxicity in SH-SY5Y human neuroblastoma cells. In this study, the aqueous extract of *Panax ginseng* decreased the overproduction of reactive oxygen species (ROS), release of cytochrome c and activation of caspase-3, elevated Bax/Bcl-2 ratio, and thus, increased cell survival in MPP^+-treated SH-SY5Y cells [20]. Apart from *Panax ginseng*, saponins, obtained from *Panax notoginseng* by the induction of thioredoxin-1, elicit a very potent neuroprotective effect on MPP^+ induced toxicity to PC12 cells and Kunming mice [22, 23]. In a very recent report, ginsenoside Rg1 (Figure 1(a)) was studied for the mechanistic activity behind its antioxidant

effect on hydrogen peroxide (H_2O_2)-induced oxidative stress to PC12 cells. Pretreatment with Rg1 at concentrations of 0.1–10 μM significantly decreases the cytotoxicity induced by 400 μM of H_2O_2 in PC12 cells. Ginsenoside Rg1 abates the phosphorylation and nuclear translocation of nuclear factor-kappa B (NF-κB)/p65, phosphorylation, and degradation of inhibitor protein of κB (IκB), as well as the phosphorylation of IκB-kinase complex (IKK). Furthermore, Rg1 also inhibited the activation of Akt and the extracellular signal-regulated kinase 1/2 (ERK1/2). These results indicate that ginsenoside Rg1 protects the cell injury induced by H_2O_2 via downregulating ERK1/2 and by decreasing the activation of the NF-κB signaling pathway [24].

In a report by Xu et al., it was observed that pretreatment with ginsenoside Rg1 to MES23.5 cells renews an iron-induced reduction in mitochondrial transmembrane potential. Pretreatment with ginsenoside Rg1 also decreases the increase of iron influx by inhibiting 6-hydroxydopamine (6-OHDA)-induced upregulation of an iron importer protein divalent metal transporter 1 with iron responsive element (DMT1-IRE). Further findings demonstrated that, due to the antioxidant effect of ginsenoside Rg1, it inhibits iron regulatory proteins, and thereby downregulating DMT1 and IRE expression [25]. In a parallel study, pretreatment with ginsenoside Rg1 was seen to inhibit the MPP^+-induced upregulation of DMT1-IRE, which was associated with the production of ROS and translocation of NF-κB to nuclei in MES23.5 cells [26]. Similar results were reported in a 1-methyl-4-phenyl-1,2,3,6-tetrahydropyridine (MPTP) model of PD in C57BL/6 mice, wherein pretreatment with ginsenoside Rg1 significantly attenuated MPTP-induced elevated iron levels decreased the expression of DMT1 and increased ferroportin-1 expression in the SN [27]. Antiinflammatory effects of ginsenoside Rg1 were also evident in lipopolysaccharide (LPS)-induced microglial activation in male C57BL/6 mice. In this study, ginsenoside Rg1 is found to inhibit proinflammatory markers, including inducible nitric oxide synthase (iNOS), nitric oxide (NO), tumor necrosis factor alpha (TNF-α), and expression of ionized calcium binding adaptor molecule 1 (Iba-1) in both the cerebral cortex and hippocampus of C57BL/6 mice. Treatment with ginsenoside Rg1 suppresses downstream inflammatory markers by inhibiting the phosphorylation levels of IκB, nuclear translocation of p65 subunit of NF-κB, and phosphorylation level of ERK1/2 kinase induced by LPS [28]. Ginsenoside Rg1 is also reported to have protective effects on dopaminergic neurons in ovariectomized female SD rat injected intracerebroventricularly with 6-OHDA [29]. In a similar 6-OHDA-induced nigrostriatal injury model of PD, ginsenoside Rg1 was observed to have a neuroprotective effects on dopaminergic neurons through the insulin-like growth factor-I receptor signaling pathway [30].

2.2. Baicalein. Baicalein (Figure 1(b)) is a flavonoid and one of the active constituents obtained from a dried root of *Scutellaria baicalensis* (Labiatae). Recently, ethanolic extract of *Scutellaria baicalensis* was demonstrated to decrease LPS-induced expression of iNOS, NO, cyclooxygenase-2 (COX-2), and prostaglandin E_2 levels in BV-2 and RAW 264.7 cells [31]. In a latest study by Li et al., they investigated the effects of baicalein on rotenone-induced neurotoxicity in PC12 cells. The results demonstrated that baicalein, in a concentration-dependent manner, inhibits the accumulation of ROS, deficiency of ATP, dissipation of mitochondrial membrane potential, and activation of caspase-3/7. Baicalein suppresses rotenone-induced apoptosis, indicating that baicalein likely improves mitochondrial function. Moreover, isolated rat brain mitochondria were used by the author to evaluate the effect of baicalein. It was found that treatment with baicalein promotes mitochondrial active respiration and prevents the rotenone-induced production of ROS, deficiency of ATP, and swelling of isolated brain mitochondria [32]. In addition to the rotenone model, baicalein was also explored for its neuroprotective effect in 6-OHDA-induced cellular and animal models of experimental parkinsonism. Baicalein at 0.5 and 5 μg/mL promotes neurite outgrowth in PC12 cells and significantly attenuates the 6-OHDA-induced cell apoptosis in SH-SY5Y cells. In animal experiments, treatment with baicalein significantly attenuates muscle tremor in 6-OHDA-lesioned rats but does not have any effect on apomorphine induced rotations. Furthermore, baicalein treatment mitigates astroglial response and increases tyrosine-hydroxylase-(TH-) positive neurons in SN [33].

Analogous to this study, treatment with baicalein at 100, 200, and 400 mg/kg significantly attenuates muscle tremor in 6-OHDA-lesioned rats. Baicalein was demonstrated to modulate the balance between glutamate and gamma amino butyric acid. Baicalein was also demonstrated to inhibit cytochrome oxidase subunit I (CO-I) mRNA expression in the subthalamic nucleus [34]. In a similar study, baicalein was seen to improve impaired spontaneous motor activity and rotarod performance induced by MPTP in C57BL/6 mice. Besides, baicalein at 280 and 560 mg/kg displays a protective effect against the MPTP-induced fall of TH-positive neurons in the SN. Treatment with baicalein also abates an MPTP-induced decrease in DA levels in the striatum by changing dopamine catabolism and inhibiting dopamine turnover [35]. In a similar model of MPTP-induced loss of dopaminergic fibers in mice, pretreatment with baicalein was found to increase the levels of DA and 5-hydroxytryptamine in the striatum, increase the counts of dopaminergic neurons, and inhibit both the oxidative stress and the astroglial response [36].

Baicalein is also reported to decrease fibrillization of E46K and E46K α-synuclein-(α-syn-) induced aggregation and toxicity in N2A cells. It was also demonstrated that baicalein significantly attenuates both E46K-induced mitochondrial depolarization, significantly attenuates the inhibition of proteasome, and protects N2A cells against E46K-induced toxicity [37]. In a related study, baicalein was found to inhibit the oligomerisation of α-syn in cell-free and cellular systems, as well to act as an efficient inhibitor of α-syn fibrillation in cell-free systems. Furthermore, baicalein was demonstrated to inhibit the formation of α-syn oligomers in Hela and SH-SY5Y cells and protect SH-SY5Y cells from α-syn oligomer-induced toxicity [38].

2.3. Curcumin. Rhizomes of *Curcuma longa* (Zingiberaceae) with the common name of turmeric along with its active components have been comprehensively used in the Indian subcontinent as food additives and cosmetics, exhibiting several medicinal properties [39]. The multiple pharmacological activities of *Curcuma longa* are mainly attributed to its polyphenolic fraction, curcuminoids, comprised of curcumin (Figure 1(c)), demethoxy curcumin (DMC), and bisdemethoxy curcumin (BDMC). Following extensive research on curcumin, the major active component of curcuminoids has revealed its bioactivities, including antiinflammatory, antioxidant, proapoptotic, chemopreventive, chemotherapeutic, antiproliferative, wound healing, antinociceptive, antiparasitic, and antimalarial properties [40]. In a latest study by Jiang and coworkers, curcumin was found to ameliorate A53T α-syn-induced SH-SY5Y cell death by downregulating rapamycin/p70 ribosomal protein S6 kinase signaling [41]. In a similar study by Wang et al., curcumin was observed to decrease α-syn-induced intracellular ROS generation and inhibit caspase-3 activation in SH-SY5Y cells [42]. In a recent experiment by Ojha et al., they investigated curcuminoids for their neuroprotective effects on inflammation-mediated neurodegeneration of dopaminergic neurons of C57BL/6 mice in the acute MPTP-model. Authors found that oral pretreatment with curcuminoids (150 mg/kg/day) significantly prevents MPTP mediated loss of TH-positive neurons and depletion of DA. Furthermore, pretreatment with curcuminoids mitigates cytokines, generation of total nitrite, and the expression of protein inflammatory markers, such as glial fibrillary acidic protein (GFAP) and iNOS, in the striatum of MPTP-intoxicated mice. Moreover, curcuminoids also improved motor deficits produced by MPTP, as evidenced by rotarod and open field tests [43].

In a comparable study carried out by Pan et al., curcumin was observed to protect dopaminergic neurons from apoptosis in an MPTP mouse model of PD. Curcumin markedly ameliorated the loss of dopaminergic axons in the striatum as well as the demise of dopaminergic neurons, in an MPTP mouse model. Further mechanistic studies demonstrated that curcumin inhibits MPTP-induced hyperphosphorylation of c-Jun N-terminal kinase (JNK). Phosphorylation of JNKs is known to cause translocation of Bax to mitochondria as well as the release of cytochrome c, which ultimately results in mitochondria-mediated apoptosis. Authors have established that curcumin prevents the degeneration of nigrostriatal neurons by inhibiting the dysfunction of mitochondria through abolishing the hyperphosphorylation of JNKs induced by MPTP [44]. Apart from MPTP model, curcumin is also reported to be neuroprotective in a 6-OHDA-induced hemiparkinsonian mice model. Posttreatment with curcumin following a unilateral intrastriatal 6-OHDA injection to mice was found to decrease the 6-OHDA-induced loss of striatal TH fibers and nigral TH-immunoreactive neurons. The neuroprotection was accompanied with a significant weakening of astroglial and microglial reaction in the striatum and the substantia nigra pars compacta (SNpc). These results indicate that the neuroprotective effects of curcumin in 6-OHDA-lesioned mice may be mediated via its antiinflammatory properties, or direct protection on nigral DA neurons [45].

2.4. Gastrodin. *Gastrodia elata* (GE), belonging to the family of Orchidaceae, has been traditionally used as a folk medicine in Oriental countries for many centuries due to its vivid exhibition of therapeutic benefits [46]. The major compounds in GE are gastrodin, vanillyl alcohol, 4-hydroxybenzaldehyde, and vanillin (Figure 1(d)). These compounds are known to cross the blood brain barrier and also to display various biological activities, such as antioxidant, antiasthmatic, antimicrobial, and antimutagenic activities [47]. In a study by An et al., pretreatment with GE extract (10, 100, 200 μg/mL) for 4 h prior to the addition of MPP^+ significantly rescued the MPP^+-induced decrease in viability of SH-SY5Y cells. Pretreatment with GE at 10, 100, and 200 μg/mL for 4 h prior to the addition of 0.5 mM MPP^+ significantly improves cell viability in Neuro-2a cells [46]. Pretreatment with GE (10, 100, and 200 μg/mL) reduces the proportion of apoptotic cells, ROS, and Bax/Bcl-2 ratio in a concentration-dependent manner in MPP^+-induced toxicity to SH-SY5Y cells [46]. These findings suggest that treatment with GE shifts the balance between pro- and antiapoptotic members towards cell survival.

Application of vanillyl alcohol to MPP^+ intoxicated MN9D dopaminergic cells effectively improves cell viability and inhibits cytotoxicity. The underlying mechanisms of vanillyl alcohol were found to be attenuation of the elevated ROS levels, as well as initiating a decrease in the Bax/Bcl-2 ratio and poly (ADP-ribose) polymerase (PARP) proteolysis. These results demonstrate that vanillyl alcohol protects dopaminergic MN9D cells against MPP^+-induced apoptosis by relieving oxidative stress and modulating the apoptotic process [47]. In a recent study, treatment with gastrodin significantly and dose dependently protected dopaminergic neurons against neurotoxicity, through regulating free radicals, Bax/Bcl-2 mRNA, and caspase-3 and cleaved PARP in SH-SY5Y cells stressed with MPP^+ [48]. Gastrodin also shows neuroprotective effects in the subchronic MPTP mouse PD model by ameliorating bradykinesia and motor impairment in the pole and rotarod tests, respectively [48]. Consistent with this finding, gastrodin prevents DA depletion and reduces reactive astrogliosis caused by MPTP in SN and striatum of C57BL/6 mice. Moreover, gastrodin is also effective in preventing neuronal apoptosis by attenuating oxidative stress and apoptosis in SN and striatum of C57BL/6 mice. Gastrodin is also reported to significantly inhibit levels of neurotoxic proinflammatory mediators and cytokines including iNOS, COX-2, TNF-α, and IL-1β by inhibiting the NF-κB signaling pathway and phosphorylation of MAPKs in LPS-stimulated microglial cells [49]. These results indicate that gastrodin has protective effects in experimental PD models and might be suitable for development as a clinical candidate to ameliorate PD symptoms [48].

2.5. Resveratrol. Resveratrol (Figure 2(a)) is a naturally occurring polyphenolic phytoalexin which occurs in plants such as grapes, peanuts, berries, and pines [50]. Resveratrol is reported to have several pharmacological properties, such as cardioprotection, scavenging of free radicals, and inhibition of COX and hydroperoxidase [50, 51]. In a recent study by Chang et al., resveratrol was found to markedly reduce

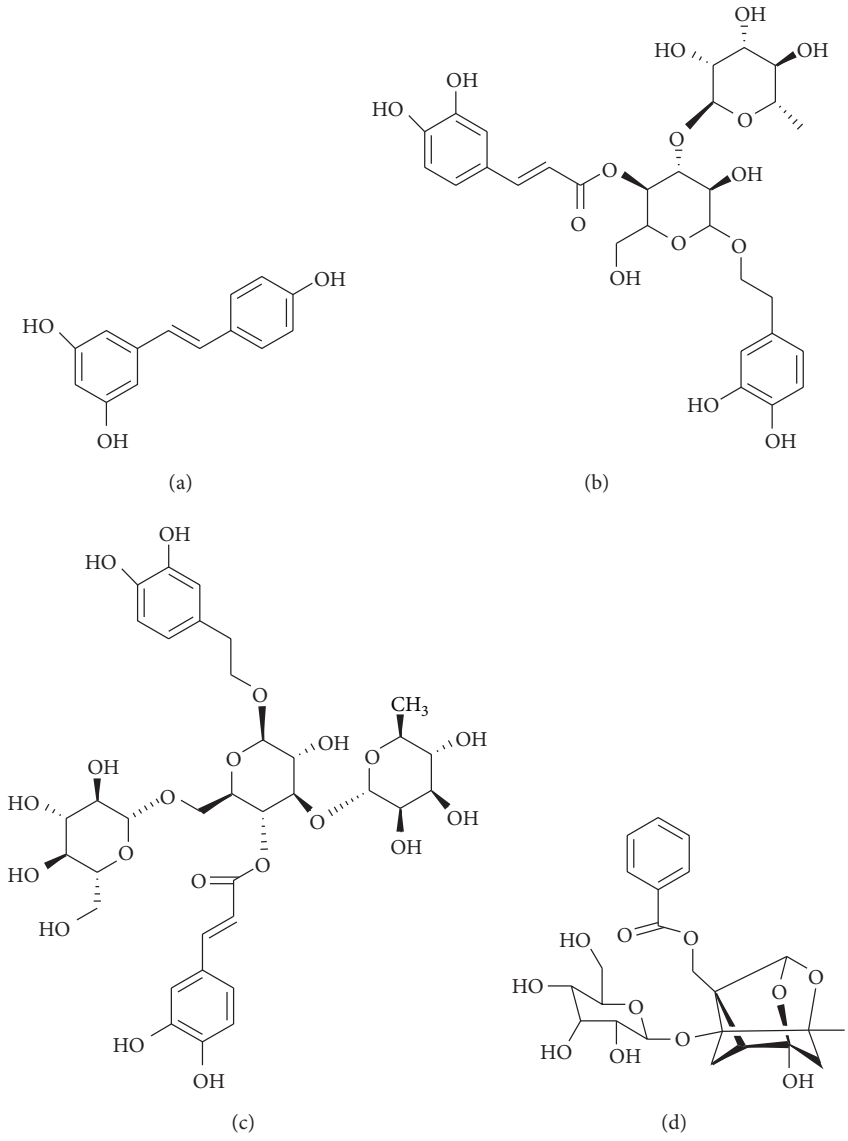

Figure 2: Chemical structure of resveratrol (a), acteoside (b), echinacoside (c), and paeoniflorin (d).

levels of myeloperoxidase (MPO) in microglia and astrocytes, without increasing the levels of NO. Resveratrol-induced downregulation of MPO significantly attenuates rotenone-triggered inflammatory responses, including the production of ROS and phagocytic activity in primary microglia and astrocytes [52]. In addition, pretreatment with resveratrol also alleviates impaired responses to rotenone from primary mixed glia in MPO deficient mice. The authors further demonstrated that resveratrol attenuates rotenone-induced dopaminergic cell death in neuron-glia cocultures, as compared to *perse* neuronal culture. Similar effects were also shown by resveratrol in modulating MPO levels in microglia treated with MPP^+, which supports its antiinflammatory profile in PD [52]. In an adjacent study by Wu et al., resveratrol was observed to protect SH-SY5Y cells against rotenone-induced apoptosis, and to enhance the degradation of α-syn in α-syn-expressing PC12 cell line via the induction of autophagy. After observing that suppression of silent information regulator 2 (SIRT1) and metabolic energy sensor AMP-activated protein kinase (AMPK) causes a decrease in protein levels of LC3-phosphatidylethanolamine conjugate (LC3-II), the authors concluded that AMPK and/or SIRT1 are required for the resveratrol-mediated induction of autophagy [53]. A similar study of the PC12 cell line demonstrated that pretreatment with resveratrol for 3 h before MPP^+ significantly reduced apoptosis-mediated neuronal cell death [54]. The authors also established that resveratrol tunes mRNA levels and protein expression of Bax and Bcl-2. Further investigation revealed that resveratrol reduces apoptotic neuronal cell death by decreasing cytochrome c and nuclear translocation of the apoptosis-inducing factor (AIF) [54]. As compared to earlier neuroprotective mechanism reported for resveratrol, it was found that antiapoptotic effects elicited against MPP^+ in rat cerebellar granule neurons by resveratrol

are independent of the stimulation of mammalian SIRT-2, but dependent on its antioxidant properties [55].

In a chronic MPTP model in Balb/c mice, resveratrol was observed to show significant neuroprotection by alleviating MPTP-induced impairments in motor coordination, oxidative stress, and loss of TH neurons [56]. Furthermore, resveratrol at (10 mg/kg, daily) significantly attenuated toxicity induced by paraquat and maneb, by increasing the levels of cytochrome P450 2D6 gene, as well as the expressions of vesicular monoamine transporter type 2 (VMAT-2). Resveratrol also relieves the increased accumulation of paraquat in nigrostriatal tissues, as well as relieving oxidative stress, microglial activation, neuroinflammation, and increasing the number of TH-positive cells and DA content [57]. Daily oral doses of resveratrol (10, 20 and 40 mg/kg) to rats with 6-OHDA-induced degeneration of the nigrostriatal network revealed that resveratrol alleviates 6-OHDA-induced swelling of mitochondria, condensation of chromatin, and vacuolization of dopaminergic neurons in rat SN. Moreover, resveratrol treatment significantly decreases the m-RNA levels of COX-2 and TNF-α in the SN [58]. Other reports also support the neuroprotective effects of resveratrol on nigral cells, wherein it mitigated oxidative damage and depletion of DA in 6-OHDA-induced dopaminergic cell death in a rat model [59–61]. These findings support the role of these natural polyphenols in preventive and/or complementary therapies for several human neurodegenerative diseases caused by oxidative stress and apoptosis.

2.6. Acteoside and Echinacoside. Cistanches Herba is the dried juicy stem of *Cistanche deserticola* or *Cistanche tubulosa* (Orobanchaceae) [62]. Total glycosides obtained from Cistanches Herba have been demonstrated to have neuroprotective effects on dopaminergic neurons of SN in a chronically intoxicated MPTP mice model of PD [62]. Treatment with 400 mg/kg of total glycosides significantly improves the altered neurobehavioral pattern of MPTP-intoxicated mice and inhibits the reduction of nigral dopaminergic neurons and the expression of TH in the striatum [62]. Acteoside (Figure 2(b)) extracted from Cistanches Herba has neuroprotective effects against rotenone-induced damage to SH-SY5Y cells. Pretreatment of SH-SY5Y cells with acteoside (10, 20, or 40 mg/L) for 6 h significantly reduces the release of lactate dehydrogenase induced by rotenone (0.5 μM/L). Pretreatment of SH-SY5Y cells with acteoside at the same dose ranges for 6 h, dose dependently decreases the cleavage of parkin induced by 0.5 μM/L of rotenone, decreases α-syn-positive SH-SY5Y cells, and stops the dimerization of α-syn. These findings indicate that the neuroprotective effects elicited by pretreatment of acteoside are due to its ability to reduce the cleavage of parkin and inhibit the expression of α-syn induced by rotenone in SH-SY5Y cells [63]. It is also found that pretreatment with acteoside significantly attenuates LPS-induced release of NO in RAW 264.7 cells via inhibition of NF-κB and activator protein-1 (AP-1) [64]. Acteoside has also been studied for its neuroprotective effects in MPTP models of PD. Pretreatment with acteoside at 10 and 30 mg/kg significantly improved MPTP-induced behavioral deficits in C57BL/6 mice. Acteoside also increases the dopaminergic neurons and content of DA [65]. Echinacoside (Figure 2(c)) is an important bioactive compound obtained and purified from the stems of *Cistanche tubulosa*, a Chinese herbal medicine [66]. Simultaneous treatment with 3.5 and 7.0 mg/kg of echinacoside is observed to prevent the 6-OHDA-induced extracellular loss of monoamine neurotransmitters, including DA, 3,4-dihydroxyphenylacetic acid (DOPAC), and homovanillic acid (HVA), in rat striatum [67]. Further authors suggested that alleviation of MPTP-induced behavioral deficits in C57BL/6 mice by pretreatment of echinacoside might result from a decrease in the biliverdin reductase B level [68]. In this study, acteoside selectively suppressed AP-1 activation, which may be essential for iNOS induction in the LPS-treated macrophages. In another study, prior treatment with echinacoside to MPTP-intoxicated mice was found to increase levels of striatal DA and its metabolite, reduce behavioral deficits, cell death, and lead to a significant rise in TH expression as compared to mice treated with MPTP alone. In addition, pretreatment with echinacoside markedly reduces MPP^+-induced activations of caspase-3 and caspase-8 in cerebellar granule neurons. These findings indicate that echinacoside uplifts neurochemical and behavioral outcomes in MPTP mice models of PD and inhibits caspase-3 and caspase-8 activation in cerebellar granule neurons [69]. In a comparable study, oral administration of echinacoside (30 mg/kg/day for 14 days) to MPTP-induced sub-acute mice model of PD significantly overcomes the reduction of striatal fibers, nigral dopaminergic neurons, dopamine transporter, and dopamine in MPTP-lesioned animals. As compared to vehicle-treated mice, echinacoside treatment increases mRNA and protein expression of glial cell-derived neurotrophic factor (GDNF) and brain-derived neurotrophic factor in MPTP-lesioned mice. In addition, echinacoside treatment decreases the increased apoptotic cells and mRNA/protein ratio of Bax/Bcl-2 in MPTP-lesioned mice. Echinacoside treatment was also found to improve motor deficits produced by MPTP. These findings demonstrate that echinacoside is an orally active inhibitor of apoptosis, as well as an inducer of neurotrophic factors, and thus providing preclinical support for its therapeutic potential in the treatment of PD [70].

2.7. Paeoniflorin. *Paeoniae alba* Radix is the red root of *Paeonia lactiflora* or *Paeonia veitchii*, used extensively as a component of traditional Chinese prescriptions to treat amenorrhea, traumatic injuries, epistaxis, inflammation, boils, and sores and to relieve pain in the chest and costal regions [71]. Paeoniflorin (PF) (Figure 2(d)) is a main principal bioactive component of *P. alba Radix* [72]. PF has been cited to exhibit many pharmacological effects, such as antiinflammatory and antiallergic effects, anti-hyperglycemic effects, analgesic effects, neuromuscular blocking effect, cognition-enhancing effects, and inhibitory effects on steroid protein binding [71]. Pretreatment of PF (2.5 and 5 mg/kg) for 11 days has been shown to protect striatal nerve fibers and TH-positive neurons in SN mitigate bradykinesia observed in an acute MPTP model of PD [71]. Posttreatment with PF for 60 min (2.5 and 5 mg/kg) once a day for the subsequent 3 days after MPTP administration significantly ameliorated the dopaminergic

neurodegeneration in a dose-dependent manner [71]. MPTP-induced activation of microglia and astrocytes, accompanied with the upregulation of proinflammatory genes, is also significantly attenuated by posttreatment with PF. Further mechanistic studies revealed that the neuroprotective and antineuroinflammatory effects of PF are associated with the activation of adenosine A_1 receptor [71]. The effect of PF was also studied in neurological impairments following 6-OHDA-induced unilateral striatal lesion in Sprague-Dawley (SD) rat. Subchronic treatment with PF (2.5, 5 and 10 mg/kg, subcutaneously, twice daily for 11 days dose dependently reduces apomorphine-induced rotation, indicating that PF has an alleviative effect on the 6-OHDA-induced neurological impairments). Since PF had no direct action on dopamine D_1 receptor or dopamine D_2 receptor, these results suggest that PF might provide an opportunity to develop a nondopaminergic management of PD [73].

In a recent report, PF was observed to protect PC12 cells from MPP^+ and acid-induced damage via an autophagic pathway. Treatment with 50 μM of PF protects PC12 cells against both MPP^+ and acid-induced injury, as determined by MTT assay, and decreases the release of lactate dehydrogenase and apoptotic rate. PF also reduces the influx of Ca^{2+} and reduces its cytosolic content. Further mechanistic study found that the neuroprotective effects of PF were closely associated with the upregulation of LC3-II protein, which is specifically associated with autophagic vacuole membranes. In addition to this, PF also inhibits the MPP^+-induced overexpression of LAMP2a, which is directly correlated with the activity of the chaperone-mediated autophagy pathway [74]. In a similar study by Sun et al., PF was observed to increase the autophagic degradation of α-syn by regulating the expression and activity of acid-sensing ion channels and thus eliciting protective effects against its cytotoxicity in PC12 cells [75].

2.8. Tenuigenin. Polygalae radix (PRE) is the dried root of *Polygala tenuifolia* (polygalaceae). PRE is composed of various xanthones, saponins, and oligosaccharide esters [76–78]. PRE is one of the most frequently prescribed herbal remedies in traditional Korean medicine and is used for the treatment of various cognitive symptoms associated with aging, senile dementia, and PD [79, 80]. In a recent finding, PRE (0.05–1 μg/mL) was demonstrated to significantly inhibit 6-OHDA induced damage to PC12 cells, with a maximal effect observed at a dose of 0.1 μg/mL. PRE at 0.1 μg/mL ameliorates the production of ROS, NO, and activity of caspase-3. At the same dose, PRE prevents the abnormal shrinking of dendrites and promotes the survival of mesencephalic dopaminergic neurons from MPP^+-induced toxicity. In an acute MPTP model of PD, pretreatment with PRE (100 mg/kg/day, 3 days) guards dopaminergic neurons and fibers from MPTP-induced toxicity in striatum and SNpc in C57BL/6 mice [81]. Tenuigenin (Figure 3(a)) is a bioactive principle found in *Polygala tenuifolia* root extracts [82]. In one study by Liang et al., tenuigenin was evaluated for its neuroprotective activity in 6-OHDA-induced cytotoxicity in SH-SY5Y cells. This study found that a 10 μM dose of tenuigenin significantly increased cell viability and reduced cell death [82].

Tenuigenin also protects against 6-OHDA induced damage of the mitochondrial membrane and markedly increases glutathione and superoxide dismutase (SOD) expression. Tenuigenin is observed to downregulate caspase-3 activity at the translational level and also to upregulate the expression of TH in 6-OHDA, damaged SH-SY5Y cells. These results establish that tenuigenin has neuroprotective effects on dopaminergic neurons via its antioxidant and antiapoptotic profile [82]. In a very recent report, tenuigenin was discovered to show the neuroprotective effect on neuroinflammation produced by a single unilateral intranigral dose of LPS (10 μg) in adult male SD rat. The authors observed that treatment with 300 mg/kg/day tenuigenin over 14 weeks improved the survival rate of TH-immunoreactive neurons in the SNpc, as compared to a contralateral side. A single dose (200 or 300 mg/kg/day) of tenuigenin significantly improved levels of DA in the striatum. Furthermore, LPS-induced upregulation of cytokines, such as TNF-α and IL-1β, was also nullified by tenuigenin administration [83].

2.9. Peurarin. Puerarin (Figure 3(b)), also known as daidzein-8-C-glucoside, is a major isoflavonoid derived from the Chinese medical herb *Pueraria lobata* belonging to the family of Leguminosae. In China, this herb has been used as a traditional medicine for treating various diseases including cardiovascular disorders, gynecological disease, osteoporosis, and cognitive dysfunction [84, 85]. In a recent report by Zhu et al., puerarin was observed to upregulate the phosphorylation of Akt in MPP^+-induced cytotoxicity in SH-SY5Y cells. This effect was further confirmed when puerarin-induced activation of Akt phosphorylation was completely blocked by phosphoinositide 3-kinase (PI3K) inhibitor (LY294002). Treatment with LY294002 also blocked the protective effect elicited by puerarin in MPP^+-induced toxicity to SH-SY5Y cells. Further mechanistic investigation demonstrated that puerarin inhibits the MPP^+-induced nuclear translocation of p53, Puma (p53-upregulated mediator of apoptosis), expression of Bax, and caspase-3-dependent programmed cell death. This protection was also abolished by treatment with PI3K/Akt inhibitor [86]. In addition to the involvement of the PI3K/Akt pathway in puerarin mediated neuroprotection to SH-SY5Y cells, puerarin is also reported to prevent the dysfunction of the proteasomal system and thereby avoid the accumulation of ubiquitin-conjugated proteins. Meanwhile, pretreatment of SH-SY5Y cells with puerarin significantly reduces the ratio of bcl-2/bax and caspase-3 activity [87]. In a latest study by Li et al., treatment with puerarin to 6-OHDA-lesioned rats was observed to significantly increase the protein expression of DJ-1 and superoxide dismutase-2 in the SN [88]. In recent report by Zheng et al., puerarin was found to suppress LPS-induced release of iNOS and phosphorylation of MAPKs in N9 cells [89]. Similar *in vitro* effects of puerarin are also evident in 6-OHDA-induced neurotoxicity to PC12 cells, wherein puerarin inhibits the MPP^+-induced phosphorylation of JNK [90]. These antiapoptotic mechanisms of puerarin were also reflected in 6-OHDA-mediated nigrostriatal damage in rats. Intraperitoneal administration of puerarin 0.12 mg/kg/day for 10 days inhibits the 6-OHDA mediated

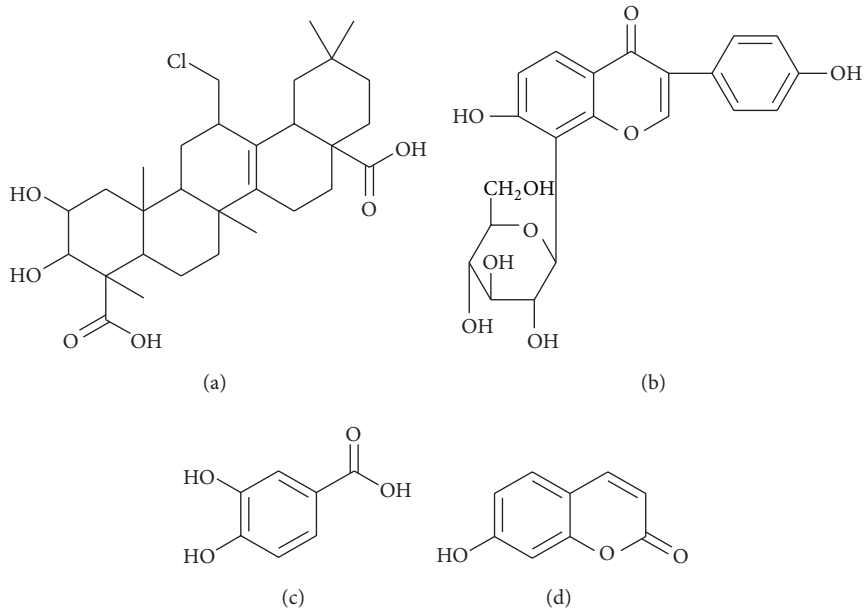

Figure 3: Chemical structure of tenuigenin (a), puerarin (b), protocatechuic acid (c), and umbelliferone (d).

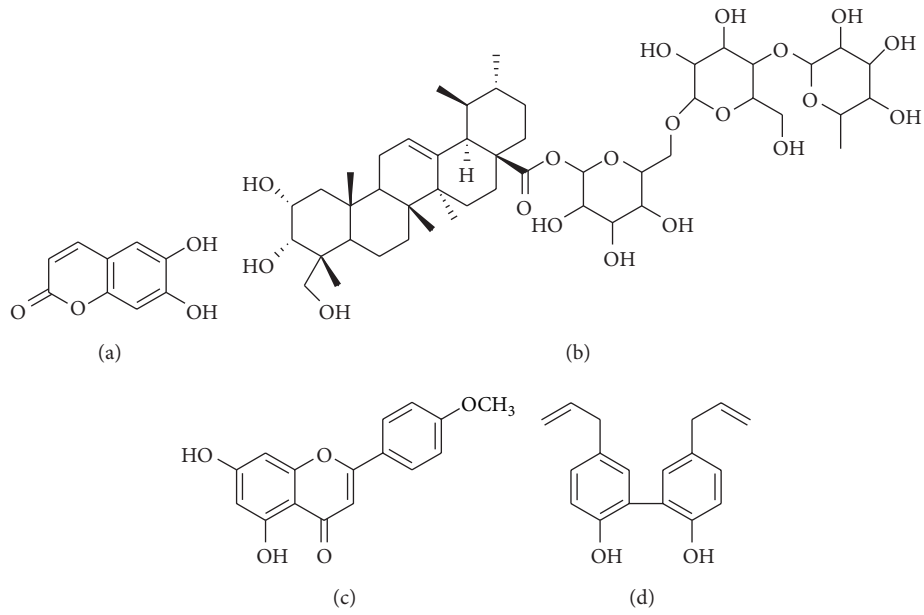

Figure 4: Chemical structure of esculetin (a), asiaticoside (b), acacetin (c), and magnolol (d).

damage to TH-positive neurons and restores the contents of DA and its metabolites. Furthermore, puerarin also increases the expression level of GDNF in the striatum in rats intoxicated with 6-OHDA [91].

2.10. Protocatechuic Acid. Alpiniae Oxyphyllae Fructus (AOE) is the dried and ripe seed of *Alpinia oxyphylla* (Zingiberaceae). Ethanolic extract of AOE prevented and renewed 6-OHDA-induced degeneration of dopaminergic neuron and also attenuated deficits in locomotor activity in a zebrafish model of PD. AOE, by attenuating cellular apoptosis, also increased the viability of 6-OHDA-toxined PC12 cells in a dose-dependent manner. A mechanistic study revealed that AOE protected the dopaminergic neuron from 6-OHDA-induced injury by its antioxidant effect, by inhibition of NO production and iNOS expression in PC12 cells, and by its antiinflammatory action, by downregulation of gene expression of IL-1β and TNF-α. In addition to this, the PI3K-Akt pathway might also be a part of the neuroprotective mechanism of AOE. Protocatechuic acid (PCA) (Figure 3(c)) is one of the active ingredients obtained from AOE [92]. PCA is found to inhibit the decreased expression of TH, apoptotic

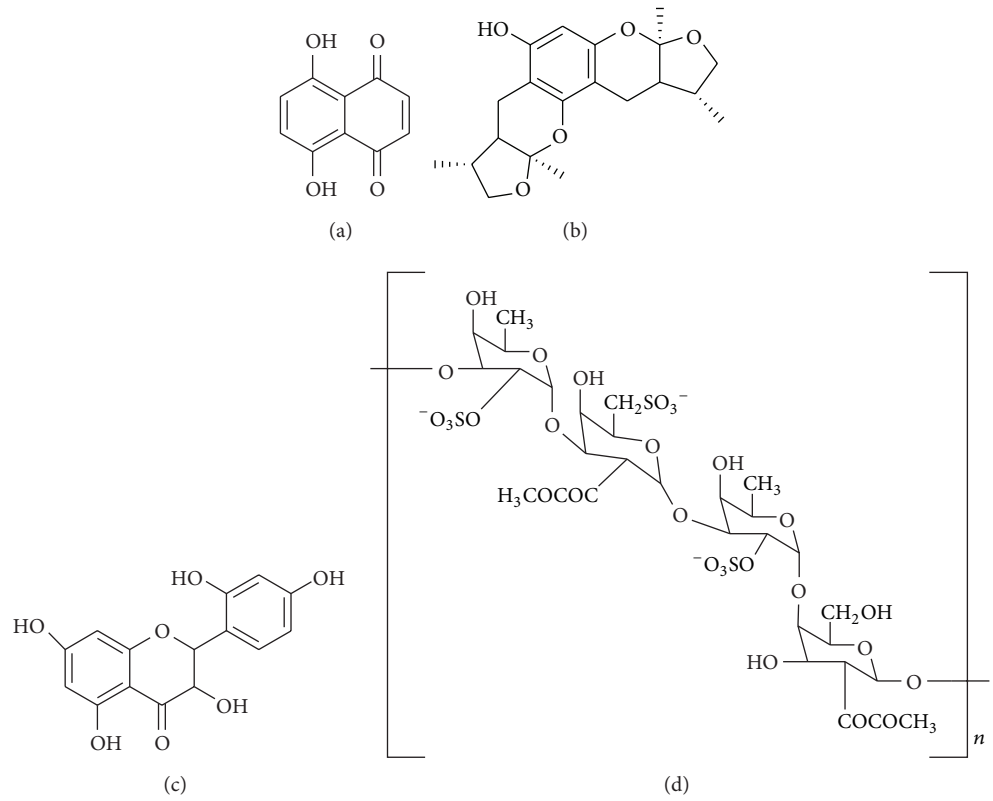

Figure 5: Chemical structure of naphthazarin (a), xyloketal B (b), morin (c), and fucoidan (d).

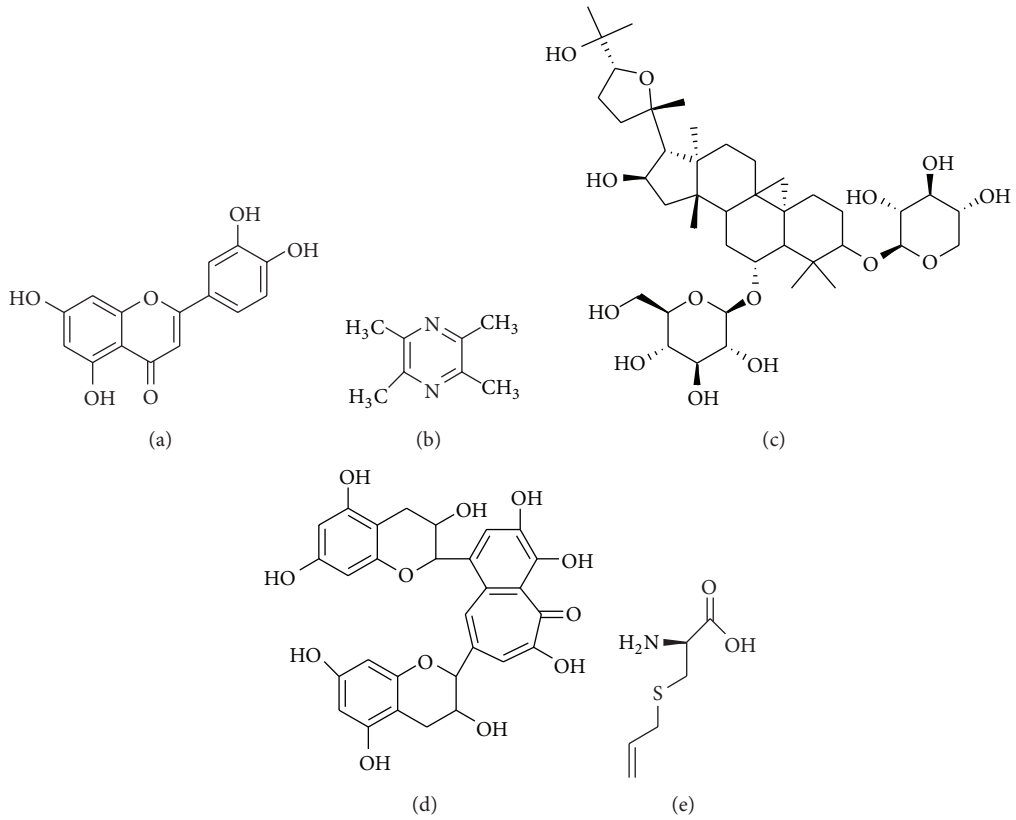

Figure 6: Chemical structure of luteolin (a), tetramethylpyrazine (b), astragaloside IV (c), theaflavin (d), and S-allylcysteine (e).

Table 1

Bioactive compound	Biological source	Model	Biological effect	References
Umbelliferone (Figure 3(d)) and esculetin (Figure 4(a))	Various plant species	Subacute MPTP model of PD in mice	Decrease in nitrosative stress, protection of tyrosine-hydroxylase-(TH-) positive neurons- and attenuation of caspase-3 activity	[96]
Asiaticoside (Figure 4(b))	*Centella Asiatica*	MPTP-induced parkinsonism in rats	Protection of dopaminergic neuron, alleviation of oxidative stress and motor dysfunction	[97]
Acacetin (Figure 4(c))	Chrysanthemum, safflower, *Calamintha* and *Linaria* species	MPP^+-induced toxicity in primary mesencephalic culture	Protection of dopaminergic neuron and inhibition of production of inflammatory factors	[98, 99]
		Subacute MPTP model of PD in mice	Protection of dopaminergic neuron, avoidance of dopamine (DA) depletion, and alleviation of behavioral deficits	
		Lipopolysaccharide stimulated BV-2 microglial cells	Significant inhibition of NO, prostaglandin E2, iNOS, COX-2, TNF-α, and IL-1β in LPS stimulated BV-2 cells	
Magnolol (Figure 4(d))	*Magnolia obovata*	MPP^+-induced toxicity in SH-SY5Y cells	Protection of MPTP-induced cytotoxicity and mitigation of oxidative stress	[100–102]
		Acute MPTP model of PD in mice	Attenuation of MPTP-induced decrease in DAT and TH protein levels and lipid peroxidation in striatum	
		6-OHDA model of PD in mice	Amelioration of apomorphine-induced contralateral rotation and increase of TH protein expression in striatum	
		Lipopolysaccharide + Interferon-γ-(IFN-γ) stimulated BV-2 and HAPI cells	Inhibition of LPS + IFN-γ-induced NO, cytokine, and ROS expression in BV-2 and HAPI cells	
Naphthazarin (Figure 5(a))	*Lomatia obliqua*	Acute MPTP model of PD in mice	Protection of dopaminergic neuron and suppression of astroglial response	[103]
Xyloketal B (Figure 5(b))	Xylaria species	MPP^+-induced neurotoxicity in Caenorhabditis elegans (C. elegans) and PC12 cells	Increases cell viability in C. elegans and PC12 cells, attenuation of intracellular ROS accumulation, and restoration of GSH level in PC12 cells	[104]
Morin (Figure 5(c))	Onion, red wine and Osage orange	MPP^+-induced toxicity in PC12 cells	Attenuation of cell viability, reactive oxygen species (ROS), and apoptosis in PC12 cells	[105]
		Subacute MPTP model of PD in mice	Attenuation of behavioral deficits, dopaminergic neuronal death, and striatal dopamine depletion	
Fucoidan (Figure 5(d))	*Laminaria japonica*	MPP^+-induced toxicity in MN9D cells	Protection of MN9D cells	[106, 107]
		Acute MPTP model of PD in mice	Reduced behavioral deficits, oxidative stress and cell death, increase in striatal dopamine and TH expression	
		LPS-induced damage to rat neurons and primary microglia	Downregulation of intracellular ROS and cytokines release in LPS-activated microglia	
Luteolin (Figure 6(a))	Celery, perilla leaf and chamomile tea.	LPS-induced cell toxicity in primary mesencephalic neuron-glia cultures	Inhibition of LPS-induced activation of microglia and excessive production of TNF-α, NO, and superoxide	[108]

Table 1: Continued.

Bioactive compound	Biological source	Model	Biological effect	References
Tetramethylpyrazine (Figure 6(b))	*Ligusticum chuanxiong*	MPP^+-induced toxicity to rat mesencephalic neurons	Increase of dopaminergic neurons and its neurite length	[109, 110]
		Subacute MPTP model of PD in mice	Increase in density of dopaminergic neurons	
		LPS-stimulated N9 microglial cells	Inhibition of NO and iNOS through blocking MAPK and PI3K/Akt activation and reducing ROS production	
Astragaloside IV (Figure 6(c))	*Astragalus membranaceus*	MPP^+-induced toxicity in SH-SY5Y cells	Reduction in cell loss, activity of caspase-3, ROS, and increase in Bax/Bcl-2 ratio	[111, 112]
		6-OHDA-induced toxicity in primary nigral culture	Promotion of neurite outgrowth and increase in TH-positive neurons	
Theaflavin (Figure 6(d))	*Camellia sinensis*	Subacute MPTP model of PD in mice	Reduction in oxidative stress, motor deficits, and increase in the expression of dopamine transporter (DAT) and VMAT2 in striatum and SN	[113, 114]
		Chronic MPTP/probenecid model of PD in mice	Attenuation of caspase-3, 8, 9 expression, increase in nigral TH and DAT	
S-Allylcysteine (Figure 6(e))	*Allium sativum*	Subacute MPTP model of PD in mice	Reduction in TNF-α, inducible iNOS, and glial fibrillary acidic protein (GFAP) expression	[115, 116]
		MPP^+-induced striatal damage in mice	Attenuation of MPP^+-induced loss of striatal DA level, oxidative stress, and behavioral deficits	

morphology, cytotoxicity, mitochondrial dysfunction [93], and abnormal tangling of α-syn in PC12 cells treated with MPP^+ [94]. Neuroprotective activity of PCA is also reported in MPTP-induced neurotoxicity C57BL/6 mice. PCA improved the motor deficits in rotarod test, contents of DA in striatum, and expression of TH in SN of C57BL/6 mice intoxicated by MPTP [95].

3. Evidence-Linked Bioactive Components Exhibiting Neuroprotective Activity in *In Vivo* and *In Vitro* Models of PD

See Table 1 and Figures 4, 5, and 6.

4. Conclusion

PD as a disease has multifactorial pathological mechanisms, and till now currently available conventional treatments are not been able to elicit disease modifying effects by targeting each of these pathomechanisms. Herbal medicines have been known to possess a combination of bioactive components which might target different pathomechanisms in neurodegenerative diseases. Recently, the identification and characterization of medicinal plants to cure PD by conventional medicine is one of the major increasing scientific interest. Although there are more than 120 traditional medicines being used for therapy of central nervous system (CNS) disorders in Asian countries, lack of their quality control data and safety in consumption across the population limits their use in modern world of medicines. A significant amount of people in the developing countries now consume CAM as they are viewed as being innately safer than synthetic chemical compounds. From the ethnobotanical and ethnopharmaceutical resources, many of the bioactive compounds from natural sources have recently been reported to exert neuroprotective effects in various experimental models of PD. Although demand for bioactive compounds from natural sources is increasing, a large-scale, double-blind, and placebo-controlled trials and there pharmacokinetic data to optimize the dosage form are still required to establish the clinical effect of CAM on PD. In addition to this, a very important property of a neuroprotective agent depends on its ability to cross the blood-brain barrier (BBB), in order to reach the target sites of the CNS. Whereas there have been a limited number of animal and cell a based studies focusing on penetration of BBB. Here, we have searched the literature for the most recent available data about bioactive constituents from natural sources that possess neuroprotective activity in various experimental models of PD. Bioactive constituents listed in this current write-up belong to different chemical classes like including, Terpenes (ginsenoside Rg1, tenuigenin, astragaloside IV), flavones (puerarin, luteolin and baicalein, morin), stilbenoids (resveratrol), phenylpropanoid (echinacoside), phenylethyl glycoside (acteoside), coumarin (umbelliferone and esculetin), and catechol (curcumin and protocatechuic acid). The bioactive ingredients discussed have traditionally been used in many countries for different ailments, and thus providing a basis for their validation in

comparison with modern day supplements. Even though the range of these studies reported are not vast, all the mentioned bioactive compounds have demonstrated a significant neuroprotective effect in PD models. Hence, bioactive compounds from natural sources can be used as alternative and valuable sources for anti-Parkinsonian drugs.

Acknowledgment

This research was supported by the High Value Added Food Technology Development Program and by the Ministry for Food, Agriculture, Forestry, and Fisheries, of Korea.

References

[1] S.-M. Liu, X.-Z. Li, Y. Huo, and F. Lu, "Protective effect of extract of Acanthopanax senticosus harms on dopaminergic neurons in Parkinson's disease mice," *Phytomedicine*, vol. 19, pp. 631–638, 2012.

[2] A. H. V. Schapira, E. Bezard, J. Brotchie et al., "Novel pharmacological targets for the treatment of Parkinson's disease," *Nature Reviews Drug Discovery*, vol. 5, no. 10, pp. 845–854, 2006.

[3] S. Singh and M. Dikshit, "Apoptotic neuronal death in Parkinson's disease: involvement of nitric oxide," *Brain Research Reviews*, vol. 54, no. 2, pp. 233–250, 2007.

[4] S. V. More, H. Kumar, I. S. Kim, S. Koppulla, B. W. Kim, and D. K. Choi, "Strategic selection of neuroinflammatory models in Parkinson's disease: evidence from experimental studies," *CNS & Neurological Disorders Drug Targets*, vol. 12, no. 5, pp. 680–697, 2013.

[5] J. R. Cannon and J. T. Greenamyre, "Neurotoxic in vivo models of Parkinson's disease. Recent advances," *Progress in Brain Research*, vol. 184, pp. 17–33, 2010.

[6] S. H. Fox and J. M. Brotchie, "The MPTP-lesioned non-human primate models of Parkinson's disease. Past, present, and future," *Progress in Brain Research*, vol. 184, pp. 133–157, 2010.

[7] B. V. Manyam and J. R. Sánchez-Ramos, "Traditional and complementary therapies in Parkinson's disease," *Advances in Neurology*, vol. 80, pp. 565–574, 1999.

[8] B. V. Manyam, "Paralysis agitans and levodopa in 'Ayurveda': ancient Indian medical treatise," *Movement Disorders*, vol. 5, no. 1, pp. 47–48, 1990.

[9] C. A. Lieu, A. R. Kunselman, B. V. Manyam, K. Venkiteswaran, and T. Subramanian, "A water extract of *Mucuna pruriens* provides long-term amelioration of parkinsonism with reduced risk for dyskinesias," *Parkinsonism and Related Disorders*, vol. 16, no. 7, pp. 458–465, 2010.

[10] B. V. Manyam, M. Dhanasekaran, and T. A. Hare, "Neuroprotective effects of the antiparkinson drug *Mucuna pruriens*," *Phytotherapy Research*, vol. 18, no. 9, pp. 706–712, 2004.

[11] R. Katzenshlager, A. Evans, A. Manson et al., "*Mucuna pruriens* in Parkinson's disease: a double blind clinical and pharmacological study," *Journal of Neurology, Neurosurgery and Psychiatry*, vol. 75, no. 12, pp. 1672–1677, 2004.

[12] J.-X. Song, S. C.-W. Sze, T.-B. Ng et al., "Anti-Parkinsonian drug discovery from herbal medicines: what have we got from neurotoxic models?" *Journal of Ethnopharmacology*, vol. 139, no. 3, pp. 698–711, 2012.

[13] X. Z. Li, S. N. Zhang, S. M. Liu, and F. Lu, "Recent advances in herbal medicines treating Parkinson's disease," *Fitoterapia*, vol. 84, pp. 273–285, 2013.

[14] V. Chung, L. Liu, Z. Bian et al., "Efficacy and safety of herbal medicines for idiopathic Parkinson's disease: a systematic review," *Movement Disorders*, vol. 21, no. 10, pp. 1709–1715, 2006.

[15] G. P. Kumar and F. Khanum, "Neuroprotective potential of phytochemicals," *Pharmacognosy Reviews*, vol. 6, pp. 81–90, 2012.

[16] V. Lobo, A. Patil, A. Phatak, and N. Chandra, "Free radicals, antioxidants and functional foods: impact on human health," *Pharmacognosy Reviews*, vol. 4, no. 8, pp. 118–126, 2010.

[17] Q. Li, D. Zhao, and E. Bezard, "Traditional Chinese medicine for Parkinson's disease: a review of Chinese literature," *Behavioural Pharmacology*, vol. 17, no. 5-6, pp. 403–410, 2006.

[18] P. S. Ip, K. W. Tsim, K. Chan, and R. Bauer, "Application of complementary and alternative medicine on neurodegenerative disorders: current status and future prospects," *Evidence-Based Complementary and Alternative Medicine*, vol. 2012, Article ID 930908, 2 pages, 2012.

[19] A. Saklani and S. K. Kutty, "Plant-derived compounds in clinical trials," *Drug Discovery Today*, vol. 13, no. 3-4, pp. 161–171, 2008.

[20] S. Hu, R. Han, S. Mak, and Y. Han, "Protection against 1-methyl-4-phenylpyridinium ion (MPP^+)-induced apoptosis by water extract of ginseng (Panax ginseng C.A. Meyer) in SH-SY5Y cells," *Journal of Ethnopharmacology*, vol. 135, no. 1, pp. 34–42, 2011.

[21] K. Radad, G. Gille, R. Moldzio, H. Saito, and W.-D. Rausch, "Ginsenosides Rb1 and Rg1 effects on mesencephalic dopaminergic cells stressed with glutamate," *Brain Research*, vol. 1021, no. 1, pp. 41–53, 2004.

[22] F.-C. Luo, S.-D. Wang, K. Li, H. Nakamura, J. Yodoi, and J. Bai, "Panaxatriol saponins extracted from Panax notoginseng induces thioredoxin-1 and prevents 1-methyl-4-phenylpyridinium ion-induced neurotoxicity," *Journal of Ethnopharmacology*, vol. 127, no. 2, pp. 419–423, 2010.

[23] F.-C. Luo, S.-D. Wang, L. Qi, J.-Y. Song, T. Lv, and J. Bai, "Protective effect of panaxatriol saponins extracted from Panax notoginseng against MPTP-induced neurotoxicity in vivo," *Journal of Ethnopharmacology*, vol. 133, no. 2, pp. 448–453, 2011.

[24] Q. Liu, J.-P. Kou, and B.-Y. Yu, "Ginsenoside Rg1 protects against hydrogen peroxide-induced cell death in PC12 cells via inhibiting NF-κB activation," *Neurochemistry International*, vol. 58, no. 1, pp. 119–125, 2011.

[25] H. Xu, H. Jiang, J. Wang, and J. Xie, "Rg1 protects iron-induced neurotoxicity through antioxidant and iron regulatory proteins in 6-OHDA-treated MES23.5 cells," *Journal of Cellular Biochemistry*, vol. 111, no. 6, pp. 1537–1545, 2010.

[26] H. Xu, H. Jiang, J. Wang, and J. Xie, "Rg1 protects the MPP^+-treated MES23.5 cells via attenuating DMT1 up-regulation and cellular iron uptake," *Neuropharmacology*, vol. 58, no. 2, pp. 488–494, 2010.

[27] J. Wang, H.-M. Xu, H.-D. Yang, X.-X. Du, H. Jiang, and J.-X. Xie, "Rg1 reduces nigral iron levels of MPTP-treated C57BL6 mice by regulating certain iron transport proteins," *Neurochemistry International*, vol. 54, no. 1, pp. 43–48, 2009.

[28] J.-F. Hu, X.-Y. Song, S.-F. Chu et al., "Inhibitory effect of ginsenoside Rg1 on lipopolysaccharide-induced microglial activation in mice," *Brain Research*, vol. 1374, pp. 8–14, 2011.

[29] L. Xu, L. X. Liu, W. F. Chen, J. X. Xie, and W. X. Huang, "The protective effect of ginsenoside Rg1 on dopaminergic neurons of substantia in the ovariectomized rat model of Parkinson's disease," *Zhongguo Ying Yong Sheng Li Xue Za Zhi*, vol. 24, pp. 1–5, 2008.

[30] L. Xu, W.-F. Chen, and M.-S. Wong, "Ginsenoside Rg1 protects dopaminergic neurons in a rat model of Parkinson's disease through the IGF-I receptor signalling pathway," *British Journal of Pharmacology*, vol. 158, no. 3, pp. 738–748, 2009.

[31] K. Jeong, Y.-C. Shin, S. Park et al., "Ethanol extract of Scutellaria baicalensis Georgi prevents oxidative damage and neuroinflammation and memorial impairments in artificial senescense mice," *Journal of Biomedical Science*, vol. 18, no. 1, article 14, 2011.

[32] X.-X. Li, G.-R. He, X. Mu et al., "Protective effects of baicalein against rotenone-induced neurotoxicity in PC12 cells and isolated rat brain mitochondria," *European Journal of Pharmacology*, vol. 674, no. 2-3, pp. 227–233, 2012.

[33] X. Mu, G. He, Y. Cheng, X. Li, B. Xu, and G. Du, "Baicalein exerts neuroprotective effects in 6-hydroxydopamine-induced experimental parkinsonism in vivo and in vitro," *Pharmacology Biochemistry and Behavior*, vol. 92, no. 4, pp. 642–648, 2009.

[34] X. Yu, G. R. He, L. Sun et al., "Assessment of the treatment effect of baicalein on a model of Parkinsonian tremor and elucidation of the mechanism," *Life Sciences*, vol. 91, pp. 5–13, 2012.

[35] X. Mu, G.-R. He, X. Yuan, X.-X. Li, and G.-H. Du, "Baicalein protects the brain against neuron impairments induced by MPTP in C57BL/6 mice," *Pharmacology Biochemistry and Behavior*, vol. 98, no. 2, pp. 286–291, 2011.

[36] Y. Cheng, G. He, X. Mu et al., "Neuroprotective effect of baicalein against MPTP neurotoxicity: behavioral, biochemical and immunohistochemical profile," *Neuroscience Letters*, vol. 441, no. 1, pp. 16–20, 2008.

[37] M. Jiang, Y. Porat-Shliom, Z. Pei et al., "Baicalein reduces E46K α-synuclein aggregation in vitro and protects cells against E46K α-synuclein toxicity in cell models of familiar Parkinsonism," *Journal of Neurochemistry*, vol. 114, no. 2, pp. 419–429, 2010.

[38] J.-H. Lu, M. T. Ardah, S. S. K. Durairajan et al., "Baicalein inhibits formation of alpha-synuclein oligomers within living cells and prevents Abeta peptide fibrillation and oligomerisation," *ChemBioChem*, vol. 12, no. 4, pp. 615–624, 2011.

[39] A. Marchiani, C. Rozzo, A. Fadda, G. Delogu, and P. Ruzza, "Curcumin and curcumin-like molecules: from spice to drugs," *Current Medicinal Chemistry*. In press.

[40] S. C. Gupta, S. Patchva, W. Koh, and B. B. Aggarwal, "Discovery of curcumin, a component of golden spice, and its miraculous biological activities," *Clinical and Experimental Pharmacology and Physiology*, vol. 39, no. 3, pp. 283–299, 2012.

[41] T. F. Jiang, Y. J. Zhang, H. Y. Zhou et al., "Curcumin ameliorates the neurodegenerative pathology in A53T alpha-synuclein cell model of Parkinson's disease through the downregulation of mTOR/p70S6K signaling and the recovery of macroautophagy," *Journal of NeuroImmune Pharmacology*, vol. 8, pp. 356–369, 2013.

[42] M. S. Wang, S. Boddapati, S. Emadi, and M. R. Sierks, "Curcumin reduces α-synuclein induced cytotoxicity in Parkinson's disease cell model," *BMC Neuroscience*, vol. 11, article 57, 2010.

[43] R. P. Ojha, M. Rastogi, B. P. Devi, A. Agrawal, and G. P. Dubey, "Neuroprotective effect of curcuminoids against inflammation-mediated dopaminergic neurodegeneration in the MPTP model of Parkinson's disease," *Journal of Neuroimmune Pharmacology*, vol. 7, pp. 609–618, 2012.

[44] J. Pan, H. Li, J. F. Ma et al., "Curcumin inhibition of JNKs prevents dopaminergic neuronal loss in a mouse model of Parkinson's disease through suppressing mitochondria dysfunction," *Translational Neurodegeneration*, vol. 1, no. 1, p. 16, 2012.

[45] W. Tripanichkul and E.-O. Jaroensuppaperch, "Curcumin protects nigrostriatal dopaminergic neurons and reduces glial activation in 6-hydroxydopamine hemiparkinsonian mice model," *International Journal of Neuroscience*, vol. 122, no. 5, pp. 263–270, 2012.

[46] H. An, I. S. Kim, S. Koppula et al., "Protective effects of Gastrodia elata Blume on MPP^+-induced cytotoxicity in human dopaminergic SH-SY5Y cells," *Journal of Ethnopharmacology*, vol. 130, no. 2, pp. 290–298, 2010.

[47] I. S. Kim, D.-K. Choi, and H. J. Jung, "Neuroprotective effects of vanillyl alcohol in gastrodia elata blume through suppression of oxidative stress and anti-apoptotic activity in toxin-induced dopaminergic MN9D cells," *Molecules*, vol. 16, no. 7, pp. 5349–5361, 2011.

[48] H. Kumar, I. S. Kim, S. V. More, B. W. Kim, Y. Y. Bahk, and D. K. Choi, "Gastrodin protects apoptotic dopaminergic neurons in a toxin-induced Parkinson's disease model," *Evidence-Based Complementary and Alternative Medicine*, vol. 2013, Article ID 514095, 13 pages, 2013.

[49] J.-N. Dai, Y. Zong, L.-M. Zhong et al., "Gastrodin inhibits expression of inducible no synthase, cyclooxygenase-2 and proinflammatory cytokines in cultured LPS-Stimulated microglia via MAPK pathways," *PLoS ONE*, vol. 6, no. 7, Article ID e21891, 2011.

[50] L. Frémont, "Biological effects of resveratrol," *Life Sciences*, vol. 66, no. 8, pp. 663–673, 2000.

[51] K. P. L. Bhat, J. W. Kosmeder II, and J. M. Pezzuto, "Biological effects of resveratrol," *Antioxidants and Redox Signaling*, vol. 3, no. 6, pp. 1041–1064, 2001.

[52] C. Y. Chang, D. K. Choi, D. K. Lee, Y. J. Hong, and E. J. Park, "Resveratrol confers protection against rotenone-induced neurotoxicity by modulating myeloperoxidase levels in glial cells," *PLoS ONE*, vol. 8, Article ID e60654, 2013.

[53] Y. Wu, X. Li, J. X. Zhu et al., "Resveratrol-activated AMPK/SIRT1/autophagy in cellular models of Parkinson's disease," *NeuroSignals*, vol. 19, no. 3, pp. 163–174, 2011.

[54] J. Bournival, P. Quessy, and M.-G. Martinoli, "Protective effects of resveratrol and quercetin against MPP^+-induced oxidative stress act by modulating markers of apoptotic death in dopaminergic neurons," *Cellular and Molecular Neurobiology*, vol. 29, no. 8, pp. 1169–1180, 2009.

[55] D. Alvira, M. Yeste-Velasco, J. Folch et al., "Comparative analysis of the effects of resveratrol in two apoptotic models: inhibition of complex I and potassium deprivation in cerebellar neurons," *Neuroscience*, vol. 147, no. 3, pp. 746–756, 2007.

[56] K.-T. Lu, M.-C. Ko, B.-Y. Chen et al., "Neuroprotective effects of resveratrol on MPTP-induced neuron loss mediated by free radical scavenging," *Journal of Agricultural and Food Chemistry*, vol. 56, no. 16, pp. 6910–6913, 2008.

[57] G. Srivastava, A. Dixit, S. Yadav, D. K. Patel, O. Prakash, and M. P. Singh, "Resveratrol potentiates cytochrome P450 2 d22-mediated neuroprotection in maneb- and paraquat-induced parkinsonism in the mouse," *Free Radical Biology and Medicine*, vol. 52, no. 8, pp. 1294–1306, 2012.

[58] F. Jin, Q. Wu, Y.-F. Lu, Q.-H. Gong, and J.-S. Shi, "Neuroprotective effect of resveratrol on 6-OHDA-induced Parkinson's disease in rats," *European Journal of Pharmacology*, vol. 600, no. 1–3, pp. 78–82, 2008.

[59] M. M. Khan, A. Ahmad, T. Ishrat et al., "Resveratrol attenuates 6-hydroxydopamine-induced oxidative damage and dopamine depletion in rat model of Parkinson's disease," *Brain Research*, vol. 1328, pp. 139–151, 2010.

[60] Y. Wang, H. Xu, Q. Fu, R. Ma, and J. Xiang, "Protective effect of resveratrol derived from Polygonum cuspidatum and its liposomal form on nigral cells in Parkinsonian rats," *Journal of the Neurological Sciences*, vol. 304, no. 1-2, pp. 29–34, 2011.

[61] J. Chao, H. Li, K.-W. Cheng, M.-S. Yu, R. C.-C. Chang, and M. Wang, "Protective effects of pinostilbene, a resveratrol methylated derivative, against 6-hydroxydopamine-induced neurotoxicity in SH-SY5Y cells," *Journal of Nutritional Biochemistry*, vol. 21, no. 6, pp. 482–489, 2010.

[62] W.-W. Li, R. Yang, and D.-F. Cai, "Protective effects of Cistanche total glycosides on dopaminergic neuron in substantia nigra of model mice of Parkinson's disease," *Chinese Journal of Integrated Traditional and Western Medicine*, vol. 28, no. 3, pp. 248–251, 2008.

[63] Y. Gao and X.-P. Pu, "Neuroprotective effect of acteoside against rotenone-induced damage of SH-SY5Y cells and its possible mechanism," *Chinese Pharmacological Bulletin*, vol. 23, no. 2, pp. 161–165, 2007.

[64] J. Y. Lee, E.-R. Woo, and K. W. Kang, "Inhibition of lipopolysaccharide-inducible nitric oxide synthase expression by acteoside through blocking of AP-1 activation," *Journal of Ethnopharmacology*, vol. 97, no. 3, pp. 561–566, 2005.

[65] L. Zhao and X.-P. Pu, "Neuroprotective effect of acteoside against MPTP-induced mouse model of Parkinsons disease," *Chinese Pharmacological Bulletin*, vol. 23, no. 1, pp. 42–46, 2007.

[66] J. Xie, J. Deng, F. Tan, and J. Su, "Separation and purification of echinacoside from *Penstemon barbatus* (Can.) Roth by recycling high-speed counter-current chromatography," *Journal of Chromatography B*, vol. 878, no. 28, pp. 2665–2668, 2010.

[67] H. Chen, F. C. Jing, C. L. Li, P. F. Tu, Q. S. Zheng, and Z. H. Wang, "Echinacoside prevents the striatal extracellular levels of monoamine neurotransmitters from diminution in 6-hydroxydopamine lesion rats," *Journal of Ethnopharmacology*, vol. 114, no. 3, pp. 285–289, 2007.

[68] X. Zhao, X.-P. Pu, and X.-C. Geng, "Effects of echinacoside on protein expression from substantia nigra and striatal tissue in mouse MPTP model of Parkinsons disease by using 2-dimensional electrophoresis analysis," *Chinese Pharmacological Bulletin*, vol. 24, no. 1, pp. 28–32, 2008.

[69] X. Geng, X. Tian, P. Tu, and X. Pu, "Neuroprotective effects of echinacoside in the mouse MPTP model of Parkinson's disease," *European Journal of Pharmacology*, vol. 564, no. 1–3, pp. 66–74, 2007.

[70] Q. Zhao, J. Gao, W. Li, and D. Cai, "Neurotrophic and neurorescue effects of Echinacoside in the subacute MPTP mouse model of Parkinson's disease," *Brain Research*, vol. 1346, pp. 224–236, 2010.

[71] H.-Q. Liu, W.-Y. Zhang, X.-T. Luo, Y. Ye, and X.-Z. Zhu, "Paeoniflorin attenuates neuroinflammation and dopaminergic neurodegeneration in the MPTP model of Parkinson's disease by activation of adenosine A1 receptor," *British Journal of Pharmacology*, vol. 148, no. 3, pp. 314–325, 2006.

[72] D.-Z. Liu, K.-Q. Xie, X.-Q. Ji, Y. Ye, C.-L. Jiang, and X.-Z. Zhu, "Neuroprotective effect of paeoniflorin on cerebral ischemic rat by activating adenosine A1 receptor in a manner different from its classical agonists," *British Journal of Pharmacology*, vol. 146, no. 4, pp. 604–611, 2005.

[73] D.-Z. Liu, J. Zhu, D.-Z. Jin et al., "Behavioral recovery following sub-chronic paeoniflorin administration in the striatal 6-OHDA lesion rodent model of Parkinson's disease," *Journal of Ethnopharmacology*, vol. 112, no. 2, pp. 327–332, 2007.

[74] B.-Y. Cao, Y.-P. Yang, W.-F. Luo et al., "Paeoniflorin, a potent natural compound, protects PC12 cells from MPP^+ and acidic damage via autophagic pathway," *Journal of Ethnopharmacology*, vol. 131, no. 1, pp. 122–129, 2010.

[75] X. Sun, Y.-B. Cao, L.-F. Hu et al., "ASICs mediate the modulatory effect by paeoniflorin on alpha-synuclein autophagic degradation," *Brain Research*, vol. 1396, pp. 77–87, 2011.

[76] Y. Jiang and P.-F. Tu, "Xanthone O-glycosides from *Polygala tenuifolia*," *Phytochemistry*, vol. 60, no. 8, pp. 813–816, 2002.

[77] Y. Jiang and P. Tu, "Four new phenones from the cortexes of *Polygala tenuifolia*," *Chemical and Pharmaceutical Bulletin*, vol. 53, no. 9, pp. 1164–1166, 2005.

[78] Y. Jiang, W. Zhang, P. Tu, and X. Xu, "Xanthone glycosides from *Polygala tenuifolia* and their conformational analyses," *Journal of Natural Products*, vol. 68, no. 6, pp. 875–879, 2005.

[79] M. Yan, "Studies on antiaging action of *Polygala tenuifolia* Wild," *Journal of Clinical Pharmacy and Therapeutics*, vol. 6, 2006.

[80] H. Zhang, T. Han, L. Zhang et al., "Effects of tenuifolin extracted from radix polygalae on learning and memory: a behavioral and biochemical study on aged and amnesic mice," *Phytomedicine*, vol. 15, no. 8, pp. 587–594, 2008.

[81] J. G. Choi, H. G. Kim, M. C. Kim et al., "Polygalae radix inhibits toxin-induced neuronal death in the Parkinson's disease models," *Journal of Ethnopharmacology*, vol. 134, no. 2, pp. 414–421, 2011.

[82] Z. Liang, F. Shi, Y. Wang et al., "Neuroprotective effects of tenuigenin in a SH-SY5Y cell model with 6-OHDA-induced injury," *Neuroscience Letters*, vol. 497, no. 2, pp. 104–109, 2011.

[83] H. L. Yuan, B. Li, J. Xu et al., "Tenuigenin protects dopaminergic neurons from inflammation-mediated damage induced by the lipopolysaccharide," *CNS Neuroscience & Therapeutics*, vol. 18, pp. 584–590, 2012.

[84] Y. Chang, C.-Y. Hsieh, Z.-A. Peng et al., "Neuroprotective mechanisms of puerarin in middle cerebral artery occlusion-induced brain infarction in rats," *Journal of Biomedical Science*, vol. 16, no. 1, article 9, 2009.

[85] R.-M. Han, Y.-X. Tian, E. M. Becker, M. L. Andersen, J.-P. Zhang, and L. H. Skibsted, "Puerarin and conjugate bases as radical scavengers and antioxidants: molecular mechanism and synergism with β-carotene," *Journal of Agricultural and Food Chemistry*, vol. 55, no. 6, pp. 2384–2391, 2007.

[86] G. Zhu, X. Wang, S. Wu, and Q. Li, "Involvement of activation of PI3K/Akt pathway in the protective effects of puerarin against MPP^+-induced human neuroblastoma SH-SY5Y cell death," *Neurochemistry International*, vol. 60, no. 4, pp. 400–408, 2012.

[87] Y.-F. Cheng, G.-Q. Zhu, M. Wang et al., "Involvement of ubiquitin proteasome system in protective mechanisms of Puerarin to MPP^+-elicited apoptosis," *Neuroscience Research*, vol. 63, no. 1, pp. 52–58, 2009.

[88] R. Li, N. Zheng, T. Liang, Q. He, and L. Xu, "Puerarin attenuates neuronal degeneration and blocks oxidative stress to elicit a neuroprotective effect on substantia nigra injury in 6-OHDA-lesioned rats," *Brain Research*, vol. 1517, pp. 28–35, 2013.

[89] G.-M. Zheng, C. Yu, and Z. Yang, "Puerarin suppresses production of nitric oxide and inducible nitric oxide synthase in lipopolysaccharide-induced N9 microglial cells through regulating MAPK phosphorylation, O-GlcNAcylation and NF-κB translocation," *International Journal of Oncology*, vol. 40, no. 5, pp. 1610–1618, 2012.

[90] G. Wang, L. Zhou, Y. Zhang et al., "Implication of the c-Jun-NH2-terminal kinase pathway in the neuroprotective effect

of puerarin against 1-methyl-4-phenylpyridinium (MPP^+)-induced apoptosis in PC-12 cells," *Neuroscience Letters*, vol. 487, no. 1, pp. 88–93, 2011.

[91] G. Zhu, X. Wang, Y. Chen et al., "Puerarin protects dopaminergic neurons against 6-hydroxydopamine neurotoxicity via inhibiting apoptosis and upregulating glial cell line-derived neurotrophic factor in a rat model of Parkinson's disease," *Planta Medica*, vol. 76, no. 16, pp. 1820–1826, 2010.

[92] Z.-J. Zhang, L. C. V. Cheang, M.-W. Wang et al., "Ethanolic extract of fructus alpinia oxyphylla protects against 6-hydroxydopamine-induced damage of PC12 cells in vitro and dopaminergic neurons in zebrafish," *Cellular and Molecular Neurobiology*, vol. 32, no. 1, pp. 27–40, 2012.

[93] S. Guan, B. Jiang, Y. M. Bao, and L. J. An, "Protocatechuic acid suppresses MPP^+-induced mitochondrial dysfunction and apoptotic cell death in PC12 cells," *Food and Chemical Toxicology*, vol. 44, no. 10, pp. 1659–1666, 2006.

[94] H.-N. Zhang, C.-N. An, M. Xu, D.-A. Guo, M. Li, and X.-P. Pu, "Protocatechuic acid inhibits rat pheochromocytoma cell damage induced by a dopaminergic neurotoxin," *Biological and Pharmaceutical Bulletin*, vol. 32, no. 11, pp. 1866–1869, 2009.

[95] H.-N. Zhang, C.-N. An, H.-N. Zhang, and X.-P. Pu, "Protocatechuic acid inhibits neurotoxicity induced by MPTP in vivo," *Neuroscience Letters*, vol. 474, no. 2, pp. 99–103, 2010.

[96] S. R. Subramaniam and E. M. Ellis, "Neuroprotective effects of umbelliferone and esculetin in a mouse model of Parkinson's disease," *Journal of Neuroscience Research*, vol. 91, pp. 453–461, 2013.

[97] C.-L. Xu, Q.-Z. Wang, L.-M. Sun et al., "Asiaticoside: attenuation of neurotoxicity induced by MPTP in a rat model of Parkinsonism via maintaining redox balance and up-regulating the ratio of Bcl-2/Bax," *Pharmacology Biochemistry and Behavior*, vol. 100, no. 3, pp. 413–418, 2012.

[98] H. G. Kim, M. S. Ju, S. K. Ha, H. Lee, S. Y. Kim, and M. S. Oh, "Acacetin protects dopaminergic cells against 1-methyl-4-phenyl-1, 2, 3, 6-tetrahydropyridine-induced neuroinflammation in vitro and in vivo," *Biological & Pharmaceutical Bulletin*, vol. 35, pp. 1287–1294, 2012.

[99] S. K. Ha, E. Moon, P. Lee, J. H. Ryu, M. S. Oh, and S. Y. Kim, "Acacetin attenuates neuroinflammation via regulation the response to LPS stimuli in vitro and in vivo," *Neurochemical Research*, vol. 37, pp. 1560–1567, 2012.

[100] A. Muroyama, A. Fujita, C. Lv, S. Kobayashi, Y. Fukuyama, and Y. Mitsumoto, "Magnolol protects against MPTP/MPP^+-Induced toxicity via Inhibition of oxidative stress in In vivo and In vitro models of parkinson's disease," *Parkinson's Disease*, vol. 2012, Article ID 985157, 9 pages, 2012.

[101] H.-H. Chen, S.-C. Lin, and M.-H. Chan, "Protective and restorative effects of magnolol on neurotoxicity in mice with 6-hydroxydopamine-induced hemiparkinsonism," *Neurodegenerative Diseases*, vol. 8, no. 5, pp. 364–374, 2011.

[102] D. Y. Chuang, M. H. Chan, Y. Zong et al., "Magnolia polyphenols attenuate oxidative and inflammatory responses in neurons and microglial cells," *Journal of Neuroinflammation*, vol. 10, p. 15, 2013.

[103] S. Y. Choi, T. G. Son, H. R. Park et al., "Naphthazarin has a protective effect on the 1-methyl-4-phenyl-1,2,3,4-tetrahydropyridine-induced Parkinson's disease model," *Journal of Neuroscience Research*, vol. 90, pp. 1842–1849, 2012.

[104] X.-L. Lu, X.-L. Yao, Z. Liu et al., "Protective effects of xyloketal B against MPP^+-induced neurotoxicity in Caenorhabditis elegans and PC12 cells," *Brain Research*, vol. 1332, pp. 110–119, 2010.

[105] Z.-T. Zhang, X.-B. Cao, N. Xiong et al., "Morin exerts neuroprotective actions in Parkinson disease models in vitro and in vivo," *Acta Pharmacologica Sinica*, vol. 31, no. 8, pp. 900–906, 2010.

[106] D. Luo, Q. Zhang, H. Wang et al., "Fucoidan protects against dopaminergic neuron death in vivo and in vitro," *European Journal of Pharmacology*, vol. 617, no. 1–3, pp. 33–40, 2009.

[107] Y. Q. Cui, Y. J. Jia, T. Zhang, Q. B. Zhang, and X. M. Wang, "Fucoidan protects against lipopolysaccharide-induced rat neuronal damage and inhibits the production of proinflammatory mediators in primary microglia," *CNS Neuroscience & Therapeutics*, vol. 18, pp. 827–833, 2012.

[108] H.-Q. Chen, Z.-Y. Jin, X.-J. Wang, X.-M. Xu, L. Deng, and J.-W. Zhao, "Luteolin protects dopaminergic neurons from inflammation-induced injury through inhibition of microglial activation," *Neuroscience Letters*, vol. 448, no. 2, pp. 175–179, 2008.

[109] J. Du, L. C. Shan, G. X. Zhang, and Y. Q. Wang, "Effect of TMP on dopaminergic neuron injury induced by MPTP in vivo and vitro," *Lishizhen Medicine and Materia Medica Research*, vol. 22, pp. 1564–1565, 2011.

[110] H.-T. Liu, Y.-G. Du, J.-L. He et al., "Tetramethylpyrazine inhibits production of nitric oxide and inducible nitric oxide synthase in lipopolysaccharide-induced N9 microglial cells through blockade of MAPK and PI3K/Akt signaling pathways, and suppression of intracellular reactive oxygen species," *Journal of Ethnopharmacology*, vol. 129, no. 3, pp. 335–343, 2010.

[111] Z.-G. Zhang, L. Wu, J.-L. Wang et al., "Astragaloside IV prevents MPP^+-induced SH-SY5Y cell death via the inhibition of Bax-mediated pathways and ROS production," *Molecular and Cellular Biochemistry*, vol. 364, pp. 209–216, 2012.

[112] W.-S. Chan, S. S. K. Durairajan, J.-H. Lu et al., "Neuroprotective effects of Astragaloside IV in 6-hydroxydopamine-treated primary nigral cell culture," *Neurochemistry International*, vol. 55, no. 6, pp. 414–422, 2009.

[113] A. Anandhan, U. Janakiraman, and T. Manivasagam, "Theaflavin ameliorates behavioral deficits, biochemical indices and monoamine transporters expression against subacute 1-methyl-4-phenyl-1, 2, 3, 6-tetrahydropyridine (MPTP)-induced mouse model of Parkinson's disease," *Neuroscience*, vol. 218, pp. 257–267, 2012.

[114] A. Anandhan, K. Tamilselvam, T. Radhiga, S. Rao, M. M. Essa, and T. Manivasagam, "Theaflavin, a black tea polyphenol, protects nigral dopaminergic neurons against chronic MPTP/probenecid induced Parkinson's disease," *Brain Research*, vol. 1433, pp. 104–113, 2012.

[115] E. García, J. Villeda-Hernández, J. Pedraza-Chaverrí, P. D. Maldonado, and A. Santamaría, "S-allylcysteine reduces the MPTP-induced striatal cell damage via inhibition of pro-inflammatory cytokine tumor necrosis factor-α and inducible nitric oxide synthase expressions in mice," *Phytomedicine*, vol. 18, no. 1, pp. 65–73, 2010.

[116] P. Rojas, N. Serrano-García, O. N. Medina-Campos, J. Pedraza-Chaverri, P. D. Maldonado, and E. Ruiz-Sánchez, "S-Allylcysteine, a garlic compound, protects against oxidative stress in 1-methyl-4-phenylpyridinium-induced parkinsonism in mice," *Journal of Nutritional Biochemistry*, vol. 22, no. 10, pp. 937–944, 2011.

Hindawi Publishing Corporation
Evidence-Based Complementary and Alternative Medicine
Volume 2013, Article ID 127075, 10 pages
http://dx.doi.org/10.1155/2013/127075

Research Article

Flavonoids Induce the Synthesis and Secretion of Neurotrophic Factors in Cultured Rat Astrocytes: A Signaling Response Mediated by Estrogen Receptor

Sherry L. Xu, Cathy W. C. Bi, Roy C. Y. Choi, Kevin Y. Zhu, Abudureyimu Miernisha, Tina T. X. Dong, and Karl W. K. Tsim

Division of Life Science and Center for Chinese Medicine, The Hong Kong University of Science and Technology, Clear Water Bay, Kowloon, Hong Kong

Correspondence should be addressed to Karl W. K. Tsim; botsim@ust.hk

Received 23 April 2013; Revised 30 May 2013; Accepted 10 June 2013

Academic Editor: Paul Siu-Po Ip

Neurotrophic factors are playing vital roles in survival, growth, and function of neurons. Regulation of neurotrophic factors in the brain has been considered as one of the targets in developing drug or therapy against neuronal disorders. Flavonoids, a family of multifunctional natural compounds, are well known for their neuronal beneficial effects. Here, the effects of flavonoids on regulating neurotrophic factors were analyzed in cultured rat astrocytes. Astrocyte is a major secreting source of neurotrophic factors in the brain. Thirty-three flavonoids were screened in the cultures, and calycosin, isorhamnetin, luteolin, and genistein were identified to be highly active in inducing the synthesis and secretion of neurotrophic factors, including nerve growth factor (NGF), glial-derived neurotrophic factor (GDNF), and brain-derived neurotrophic factor (BDNF). The inductions were in time- and dose-dependent manners. In cultured astrocytes, the phosphorylation of estrogen receptor was triggered by application of flavonoids. The phosphorylation was blocked by an inhibitor of estrogen receptor, which in parallel reduced the flavonoid-induced expression of neurotrophic factors. The results proposed the role of flavonoids in protecting brain diseases, and therefore these flavonoids could be developed for health food supplement for patients suffering from neurodegenerative diseases.

1. Introduction

Astrocytes are the most abundant type of glial cell in nervous system, and various brain functions have been attributed to astrocytes. During the last decade, it is recognized that the functions of astrocyte are not limited in supporting neurons, but they have a number of essential activities in the brain, including the development of central nervous system (CNS), ion homeostasis, uptake of neurotransmitters, maintenance of the blood-brain barrier (BBB), and modulation of CNS immune system, as well as the synthesis of neurotrophic factors [1]. Neurotrophic factors are a group of proteins mainly synthesized and secreted by neurons and astrocytes [2, 3]: these factors are playing vital roles in maintaining the survival, growth, differentiation, and normal functions of neurons [4, 5]. Nerve growth factor (NGF) is one of the key neurotrophic factors of neurite outgrowth during development. Many diseases of nervous system are associated with NGF insufficiency, especially neurodegenerative diseases [6], for example, depression [7] and Alzheimer's disease [8]. The expressions of glial cell-derived neurotrophic factor (GDNF) and brain-derived neurotrophic factor (BDNF) are also regulated by stress-related mood disorder and depression. The amount and effectiveness of the neurotrophic factors in the brain were found to be decreased during the process of aging, and the decrease was robust in the pathological condition of Parkinson's and Alzheimer's diseases [9, 10]. Much attention has been attracted to the correlation between neurotrophic factors and neurodegenerative diseases and depression. The upregulation of NGF, BDNF, GDNF, and other neurotrophic factors is considered for treatment of depression and neurodegenerative diseases [11]. In animal model of Parkinson's disease, the delivery of GDNF gene to damaged nigrostriatal system could alleviate the symptoms in rats, which therefore implied a potential clinical use of GDNF for human [12]. The expression of BDNF is closely related

to estrogen: the activation of estrogen receptor (ER) could potentially lead to production of BDNF [13]. Flavonoids, also known as phytoestrogen, have been reported to have neuronal beneficial effects including neuroprotection against neurotoxin stress, promotion of memory, learning and cognitive functions [14, 15]. Previously, it has been stated that flavonoids could protect the neurons against cell toxicity induced by oxidative stress [16] and by aggregated β-amyloid [17]: these stress inducers are considered as the causes of Alzheimer's disease. In addition, flavonoids were also shown to significantly potentiate NGF-induced neurite outgrowth [18], as demonstrated in cultured PC12 cells. Having a close resemblance to estrogen, the roles of various flavonoids in inducing the expression of neurotrophic factors could be an interesting question. Here, we are testing the hypothesis that the regulation of NGF, BDNF, and GDNF in cultured astrocytes could be triggered by flavonoids, and this effect could be mediated by a signaling of ER.

2. Materials and Methods

2.1. Materials. Calycosin and other flavonoids were purchased from the National Institute for the Control of Pharmaceutical Biology Products (NICPBP; Beijing, China), Sigma (St. Louis, MO) Wakojunyaku (Osaka, Japan), or Kunming Institute of Botany, Chinese Academy of Science (Kunming, China). All of them were at over 98% purity. The flavonoids were solubilized in dimethylsulfoxide (DMSO) to give stock solution at a series of concentration from 25 to 100 mM, stored at −20°C.

2.2. Cell Culture and Flavonoid Treatment. Primary cultured rat astrocyte was isolated from 1-day-old neonatal rat as described previously [19] with little modification. Cells were maintained in Minimum Essential Medium (MEM) supplemented with 10% horse serum, 100 U/mL penicillin, and 100 μg/mL streptomycin in a humidified CO_2 (5%) incubator at 37°C. Fresh medium was supplied every three days. All culture reagents were purchased from Invitrogen Technologies (Carlsbad, CA). During the treatment with flavonoids, cultured astrocyte cells were serum starved for 3 days in MEM supplemented with 0.5% fetal horse serum and penicillin-streptomycin, which were then treated with the flavonoids and/or other reagents for 48 hours.

2.3. Real-Time Quantitative PCR. Total RNA was isolated from cell cultures by RNAzol RT reagent according to the manufacture's instruction (Molecular Research Center, Cincinnati, OH). The purities of the RNAs were detected by UV absorbance at 260 nm. Total RNA was used to do the reverse transcription with Moloney murine leukemia virus (MMLV) reverse transcriptase according to the protocol provided by manufacturer. Real-time PCR was performed by using Roche SYBR FAST qPCR Master Mix and Rox reference dye, according to manufacturer's instruction (Roche Woburn, MA). The SYBR green signal was detected by Mx3000P multiplex quantitative PCR machine. The primers used for PCR were 5′-CAC TCT GAG GTG CAT AGC GTA ATG TC-3′ and 5′-CTG TGA GTC CTG TTG AAG GAG ATT GTA C-3′ for NGF (XP_001067130.2, 374 bp); 5′-GAG CTG AGC GTG TGT GAC AGT ATT AG-3′ and 5′-ATT GGG TAGT TCG GCA TTG CGA GTT C-3′ for BDNF (BC087634, 229 bp); 5′-GCG CTG ACC AGT GAC TCC AAT ATG-3′ and 5′-CGC TTC ACA GGA ACC GCT ACA ATAT C-3′ for GDNF (AF497634, 318 bp); 5′-AAC GGA TTT GGC CGT ATT GG-3′ and 5′-CTT CCC GTT CAG CTC TGG G-3′ for GAPDH ([20], 516 bp).

2.4. Measurement of Secretion of NGF, BDNF, and GDNF. To measure the protein level of secreted neurotrophic factors in primary cultured rat astrocyte, the method of enzyme-linked immunosorbent assay (ELISA) was employed. Rat astrocytes were plated in a 12-well plate in MEM supplemented with 10% horse serum, 100 U/mL penicillin, and 100 μg/mL. When the confluence of cells was higher than 80%, the medium was changed into MEM with 0.5% horse serum, 100 U/mL penicillin, and 100 μg/mL streptomycin for other weeks and was changed again to get equal volume 3 hours before the drug treatment. Flavonoids and other drugs were applied to cell culture and lasted for 48 hours. Then the medium and cell culture were collected and stored in −80°C. The protein amount of neurotrophic factors in the medium was measured with the method of ELISA, and the protein concentration of the cell lysate for each sample was also measured. The ELISA assays were performed with the commercially available ELISA kits (AbFrontier, Millipore) for NGF, BDNF, and GDNF measurement according to the manufacturer's instructions. Briefly, samples were applied onto a 96-well plate precoated with anti-rat NGF, BDNF, or GDNF antibodies and incubated on at 37°C for 90 minutes. After discarding plate content, biotinylated anti-rat NGF, BDNF, or GDNF antibodies were added and incubated at 37°C for 60 minutes. After washing with PBS for four times, the avidin-biotin-peroxidase complex solution was added and incubated at 37°C for 30 minutes. Tetramethylbenzidine solution was added and incubated at 37°C for 15 minutes. The reaction was stopped with 1 M sulfuric acid and absorbance recorded at 450 nm, immediately. The values of standards and samples were corrected by subtracting the absorbance of nonspecific blinding. All samples were measured in triplicate in the same assay to minimize interassay variation.

2.5. Estrogen Receptor Phosphorylation. Astrocytes were seeded onto 12-well plates. When the confluence of cells in the plate reached to 90%, the culture medium was changed to MEM medium without any serum. After serum starvation for at least 5 hours, the cells were treated with drugs at different time points (e.g., 0 to 30 minutes). Then, the cells were harvested and digested with 2 X SDS-PAGE sample buffer (0.125 M Tris-Cl, pH 6.8, 4% SDS, 20% glycerol, 2% 2-mercaptoethanol, and 0.02% bromophenol blue) by shaking for 2 minutes and boiling for 15 minutes. The proteins were subjected to SDS-gel electrophoresis and blotting. The membrane containing the transferred proteins was incubated with antiphospho-ERα-S118 antibody (1 : 2000; Upstate, Lake

Placid, NY) and antitotal ERα antibody (1 : 1000; Upstate) at 4°C for 12 hours. Horseradish-peroxidase- (HRP-) conjugated anti-rabbit secondary antibody (1 : 5000; Invitrogen) was then added to the membranes for 1 hour at room temperature. The secondary antibody, horseradish-peroxidase-(HRP-) conjugated anti-rabbit antibody (1 : 5000; Invitrogen) was then added to the membranes for 1 hour at room temperature. The immunecomplexes were visualized by the enhanced chemiluminescence (ECL) method (GE, Healthcare). The band intensities, recognized by the antibodies in the ECL film, in control and flavonoid-treated samples were run on the same gel and under strictly standardized ECL conditions. The bands were compared on an image analyzer, using in each case a calibration plot constructed from a parallel gel with serial dilution of one of those samples as to ensure the subsaturation of the gel exposure. Total amount of ERα was detected as an internal control.

2.6. Statistical Analysis and Other Assays. The protein concentrations were measured routinely by Bradford's method (Hercules, CA). Statistical analyses were performed using one-way ANOVA followed by Student's t-test. Statistically significant changes were classed as (*) where $P < 0.05$; (**) where $P < 0.01$.

3. Results

3.1. Screening for Flavonoids in Increasing the Expression of Neurotrophic Factors. Rat astrocytes were isolated and cultured. The cells were proliferated in culture for about 3 weeks, which reached maximum cell number under different plating cell numbers (See Supplementary Figure 1 Material available online at http://dx.doi.org/10.1155/2013/127075). The culture showed over 90% identity of astrocyte, that is, the specific staining of GFAP (Supplementary Figure 2). Thirty-three flavonoids from different subclasses were screened for their effects on secretion of neurotrophic factors on cultured astrocytes. These flavonoids are mainly derived from vegetables and Chinese herbal medicines. According to the results of cell viability assay, flavonoids were applied onto the cultures at concentrations of 10 μM, at which the flavonoids induced neither cell proliferation nor cell toxicity. After incubation for 48 hours, the culture medium was harvested to perform the ELISA assay in measuring the concentrations of NGF, GDNF, and BDNF. The results were normalized by protein concentrations of cell lysates from each sample. Estrogen was shown to induce the expression and secretion of neurotrophic factors in cultured hippocampal neuron [21], and therefore 17β-estradiol served as the positive control. From Table 1, several flavonoids showed significant effects in upregulating secretion of NGF, GDNF, and BDNF. Alpinetin, luteolin, calycosin, genistein, and isorhamnetin were revealed in inducing the expression of NGF, GDNF, and BDNF, significantly. On the other hand, the NGF-induced flavonoids was included silybin, calycosin-7-O-glucoside, and fiestin. The GDNF-induced flavonoids were naringin, neohesperidin, apigenin, sulphureting, cardamonin, calycosin-7-O-glucoside, puerarin, galangin, and RNFG. The BDNF-induced flavonoids were very limited (Table 1).

Table 1: The bioactivities of flavonoids in increasing the protein levels of neurotrophic factors.

Flavonoid	NGF	GDNF	BDNF
Flavanones			
Alpinetin	+++	++	+
Hesperidin	—	+	—
Naringenin	—	—	—
Naringin	—	+++	—
Neohesperidin	—	++	—
Flavones			
Apigenin	—	++	—
Baicalein	—	—	—
Luteolin	++++	++++	++
Tangeretin	++	—	—
Wogonin	—	—	—
Aurones			
Sulfuretin	—	++	—
Dihydrochalcones			
Phloretin	—	—	—
Flavonols			
Silybin	++++	—	+
Chalcones			
Cardamonin	+	++	—
Isoflavones			
Calycosin	+++	++++	+++
Calycosin-7-O-glc	+++	++	—
Daidzein	—	—	—
Formononetin	—	—	—
Genistein	++++	++++	++
Genistin	—	—	—
Puerarin	+	+++	—
Flavones			
(−)-Catechin	—	—	+
(−)-Epicatechin	—	—	—
Flavonols			
Fisetin	+++	—	+
Galangin	—	++	—
Hyperin	—	—	—
Icariin	—	—	+
Isorhamnetin	++++	++++	+++
Kaempferol	+	+	+
Quercetin	—	+	—
RNFG	—	++	—
173-estradiol	++++	++++	+++

Percentage of increas + > 100%, ++ > 200%, +++ > 300%, ++++ > 500%. Flavonoids at 10 μM were applied to cultured rat astrocytes and maintained for 48 hours. The protein levels of NGF GDNF and BDNF were measured by ELISA. 17β-Estradiol at 100 nM served as the positive control. Data are Means ± SEM, $n = 3$, each with triplicate samples. The value of SEM is within 5% of the mean, which is not shown for clarity. "+" to "+++" indicate the ranking of the inductive effect on protein amount of neurotrophic factors. "—" indicates no effect, that is, below 10% increase in the tested activities.

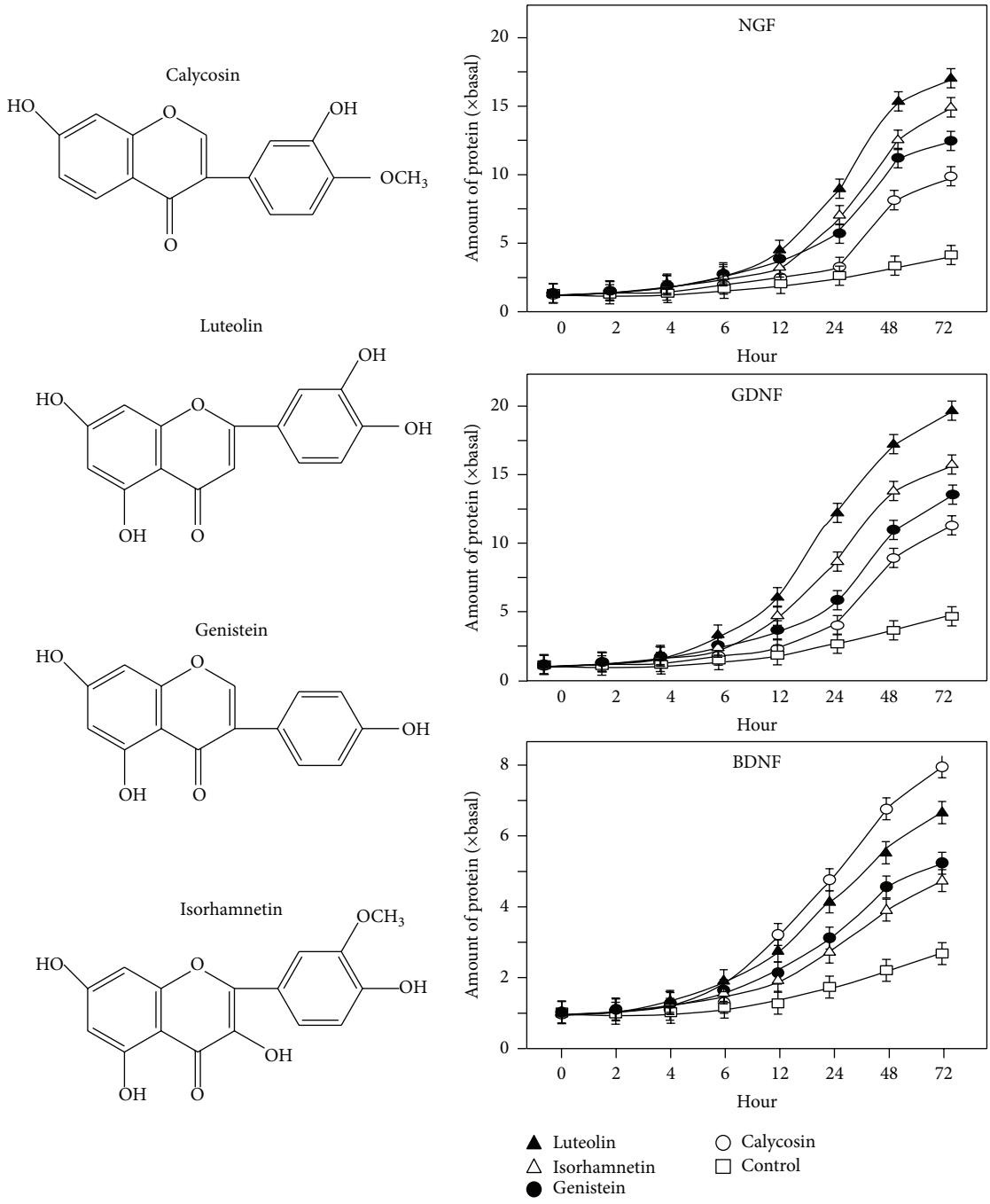

Figure 1: Flavonoids increase the protein expressions of neurotrophic factors in time-dependent manner. (a) The chemical structures of the most effective flavonoids, calycosin, luteolin, genistein, and isorhamnetin, in inducing neurotrophic factors in cultured astrocytes. (b) Calycosin, isorhamnetin, luteolin and genistein at the concentration of 10 μM were applied to cultured astrocytes. Conditional medium was collected at different time points (0–72 hours), and the concentrations of neurotrophic factors were measured by ELISA kits. Values are expressed as the fold of change (× basal) against the control (no treatment at various time points; set as 1) and in Mean ± SEM, $n = 3$.

3.2. Flavonoids Increase the Expression of NGF, BDNF, and GDNF. Among these effective flavonoids, luteolin from Lonicerae Japonicae Flos, isorhamnetin from Ginkgo Folium, genistein from Soybean, and calycosin from Astragali Radix (Figure 1(a)) showed the most promising effects by increasing the secretion of the three neurotrophic factors, which therefore were selected for further elucidation. These flavonoids were applied onto cultured astrocytes for different time points up to 72 hours, and the amount of neurotrophic factors in the conditioned medium was determined by ELISA.

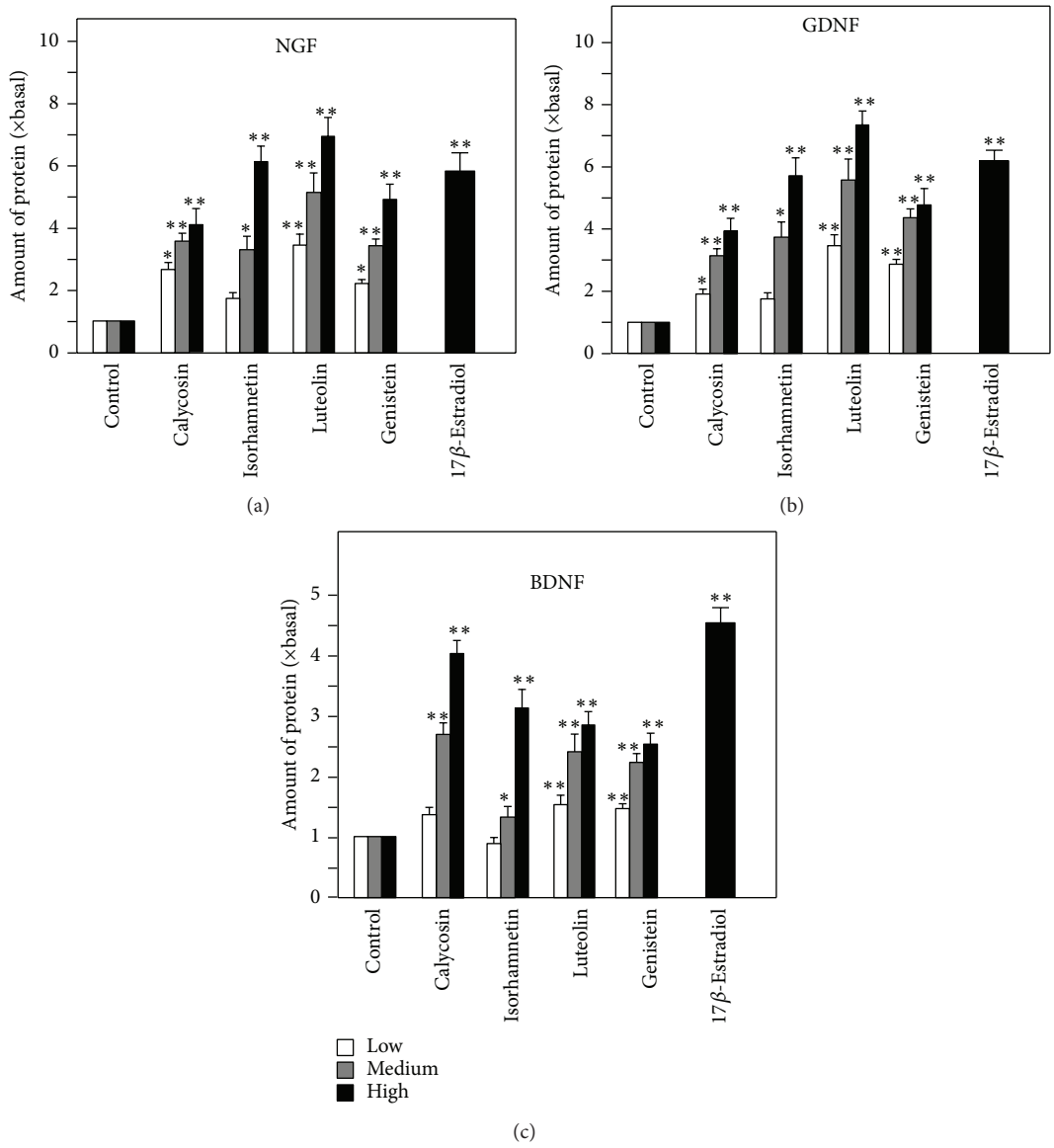

Figure 2: Flavonoids increase the expression of NGF, GDNF, and BDNF in cultured astrocytes in dose-dependent manner. The flavonoids calycosin, isorhamnetin, luteolin, and genistein (1, 3, 10 μM) were applied to cultured astrocytes for 48 hours. 17β-estradiol at 100 nM served as the positive control. The protein levels of NGF, GDNF, and BDNF in the conditional medium were measured by ELISA. Values are expressed as the fold of change (× basal) against the control (no treatment; set as 1) and in Mean ± SEM, $n = 4$, each with triplicate samples. ∗∗ where $P < 0.01$ compared to the control.

The flavonoids induced the amounts of NGF, GDNF and BDNF in the conditioned medium in a time-dependent manner: the increase was significantly at 12 hours after the treatment (Figure 1(b)). The induction was more robust in cases of NGF and GDNF; this induction was higher than that of BDNF by 2 folds. Besides, the flavonoid-induced expression of neurotrophic factors was also in a dose-dependent manner (Figure 2). In most cases, the lowest concentration of flavonoids (i.e., at 1 μM) was able to induce the neurotrophic factor expressions (Figure 2). Here, the induction by estrogen was serving a positive control. The mRNA expressions of NGF, GDNF, and BDNF were revealed in cultured astrocytes under the treatment of different flavonoids, including luteolin, isorhamnetin, genistein, and calycosin. The treatment was at 48 hours, and then the total RNA was subjected to real-time quantitative PCR. Similar to the protein expression, the mRNAs encoding neurotrophic factors were induced by the flavonoids in a dose-dependent manner (Figure 3). The magnitude of induction was very similar in the scenario of protein expression, which suggested the transcriptional regulation of these neurotrophic factors could be a major step in regulation by flavonoids. Among these flavonoids, luteolin at 10 μM showed the most promising effects in increasing the mRNA levels of NGF and GDNF to more than 7 folds,

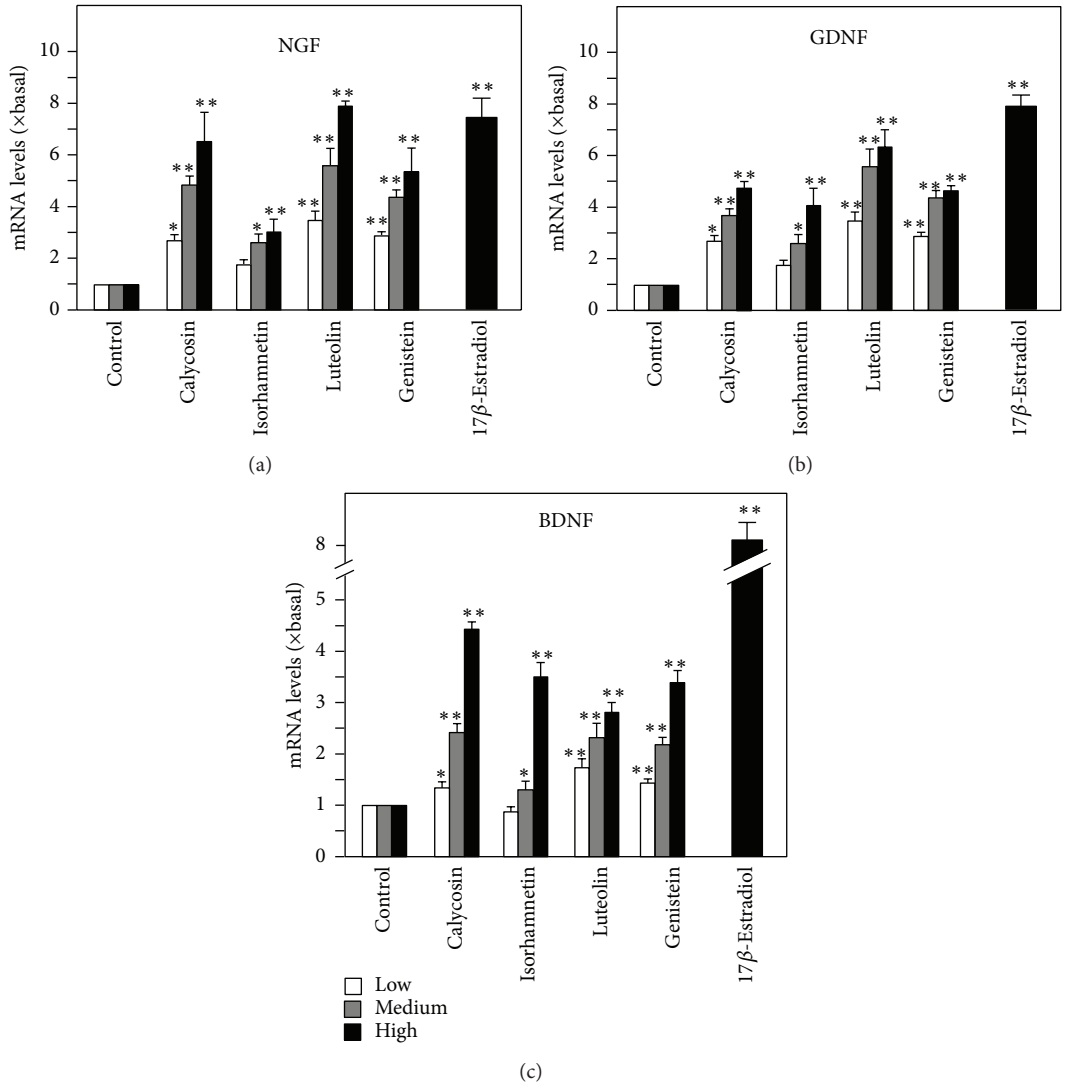

Figure 3: Flavonoids increase the mRNA levels of NGF, GDNF, and BDNF in cultured astrocytes in dose-dependent manner. The flavonoids calycosin, isorhamnetin, luteolin and genistein (1, 3, 10 μM) were applied to cultured astrocytes for 48 hours. 17β-estradiol at 100 nM served as the positive control. The mRNA levels of NGF, GDNF, and BDNF were measured by real-time quantitative PCR. Values are expressed as the fold of change (× Basal) against the control (no treatment; set as 1), and in Mean ± SEM, $n = 4$, each with triplicate samples. ∗∗ where $P < 0.01$ compared to the control.

while calycosin at 10 μM showed most promising effect in increasing the mRNA level of BDNF to more than 4 folds (Figure 3). 17β-Estradiol served as the positive control.

3.3. The Flavonoid-Induced Expression of Neurotrophic Factors Is Mediated by Estrogen Receptor. Since calycosin, isorhamnetin, luteolin, and genistein showed significant effects in modulating mRNA expression and protein secretion of NGF, GDNF, and BDNF, the potential molecular mechanism was elucidated. As mentioned before, estrogen signaling pathway was considered to be closely related to the expression of neurotrophic factors in the brain [21, 22]. The activation of estrogen-mediated transcription requires the phosphorylation of ER, either α or β forms [23]. Different flavonoids, when applied in cultured MCF-7 cells, triggered the estrogenic pathway by phosphorylating ERα at S118 position, as well as the estrogen responsive element [16]. Here, the effects of these flavonoids in activating ERα were firstly determined in astrocytes. The flavonoids were applied onto the cultures at different time points. From Figures 4(a) and 4(b), calycosin, isorhamnetin, luteolin, and genistein induced ERα phosphorylation at S118, significantly. The phosphorylation was observed from 10 minutes after treatment and lasted for at least 30 minutes at maximal phosphorylation (Figures 4(a) and 4(b)). The phosphorylation induced by flavonoids could be fully blocked by the ER antagonist ICI 182, 780 (Figure 4(a)). ICI 182, 780 was used to further investigate the relation between flavonoids induced neurotrophic factors expression and ER-dependent signaling pathway. ICI 182,

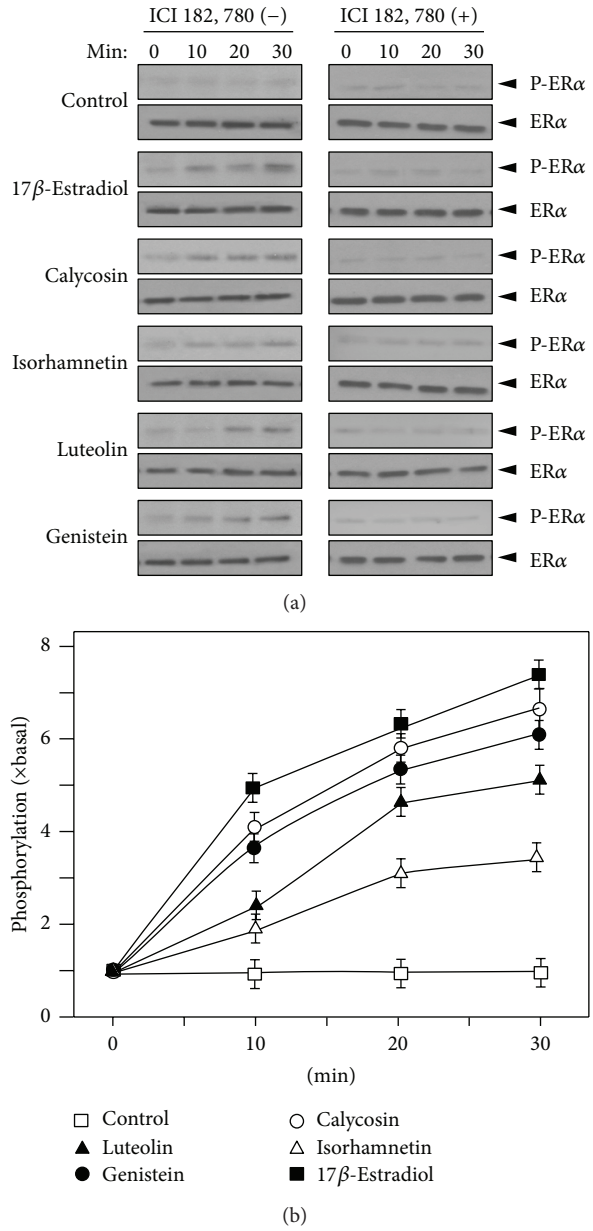

Figure 4: Flavonoids induce the phosphorylation of estrogen receptor. (a) Cultured astrocytes were serum starved for 3 hours with or without the pretreatment of ICI 182, 780 for another 3 hours. Then calycosin, isorhamnetin, luteolin, and genistein at 10 μM were applied onto the cell cultures for a different time. 17β-Estradiol (10 nM) served as the positive control. Total ERα and S118 phosphorylated ERα (both at ~66 kDa) were revealed by using specific antibodies. (b) Quantification plot for the phosphorylation level of ER induced by flavonoids. Data are Means ± SEM, $n = 3$, each with triplicate samples.

780 was applied onto astrocytes 3 hours before the flavonoid treatments, and the mRNA levels of NGF, BDNF, and GDNF were measured. With the pretreatment of ICI 182, 780, the mRNA levels of the neurotrophic factors, increased by calycosin, isorhamnetin, luteolin, and genistein, were blocked close to the basal level. 17β-Estradiol served as the positive control (Figure 5). These results suggested that the activities of calycosin, isorhamnetin, luteolin, and genistein in increasing the expression of NGF, BDNF, and GDNF were achieved through ER-mediated signaling pathway.

4. Discussion

Astrocyte is the most dominant and functional type of neuroglial cell; however, the study about relations between flavonoid and astrocyte is very limited. At the same time, neurotrophic factor has been studied as an important direction to alleviate neurodegenerative disease and depression. So far, most of these works were carried out in animal models [9–11]. Here, the roles of flavonoids in regulating neurotrophic factors were investigated in cultured astrocytes. The effects of calycosin, isorhamnetin, luteolin, and genistein in enhancing neurotrophic factor expressions were closely related to an ER-dependent pathway. Even though there was no direct evidence showing that estrogen could trigger the neurotrophic factor expression in astrocytes; studies had demonstrated that estrogen possessed activities in astrocytes. For example, the expression levels of glutamate transporters were increased by the applied estrogen in cultured astrocytes [24], and estrogen reduced lipopolysaccharide-induced expression of tumor necrosis factor-α and interleukin-18 in midbrain astrocytes [25]. On the other hand, estrogen could modulate the expression of neurotrophic factors in neuronal cells [21, 26, 27], which also enhanced mRNA expression of BDNF by phosphorylating CREB in rat hippocampus [28]. In a study of ER-dependent pathway, the activated ER dimer was shown to bind onto a DNA segment of upstream of BDNF promoter: the binding promoted the mRNA expression of BDNF in hippocampal neuron [29].

Estrogen could be synthesized directly in nervous system [30]; meanwhile, ER (both α and β form) and GPR30 are both widely distributed in the nervous system [31, 32]. Estrogen affects synaptogenesis and morphological plasticity within the brain by enhancing the density of dendritic spines [33, 34] and promoting subsequent synapse formation [35, 36]. In line to this notion, a study showed that ERα played a critical role in estrogen-induced glutamatergic synapse formation, including the expressions of presynaptic vesicular glutamate transporter protein (vGlut1) and postsynaptic NMDA receptor (NR1 subunit) [37]. Flavonoids are well-known phytoestrogens with multiple activities in different systems [38, 39]. Much attention has been focused on the neuronal beneficial effects of flavonoids, including the neuroprotection against neurotoxin stress [16] as well as the promotion of memory and learning and cognitive functions [15]. Previous studies in cultured neurons showed that flavonoids possessed the abilities of antioxidation and inhibiting Aβ-induced cytotoxicity [16, 17]. Many flavonoids showed estrogenic effects by directly inducing the ER phosphorylation [40–43]. Here, the correlation between estrogen signaling pathway and neuronal beneficial effects of flavonoids was innovatively demonstrated. These results explained the mechanism of flavonoids in regulating the expression of neurotrophic factors. Being the very popular phytoestrogen, the properties of flavonoids

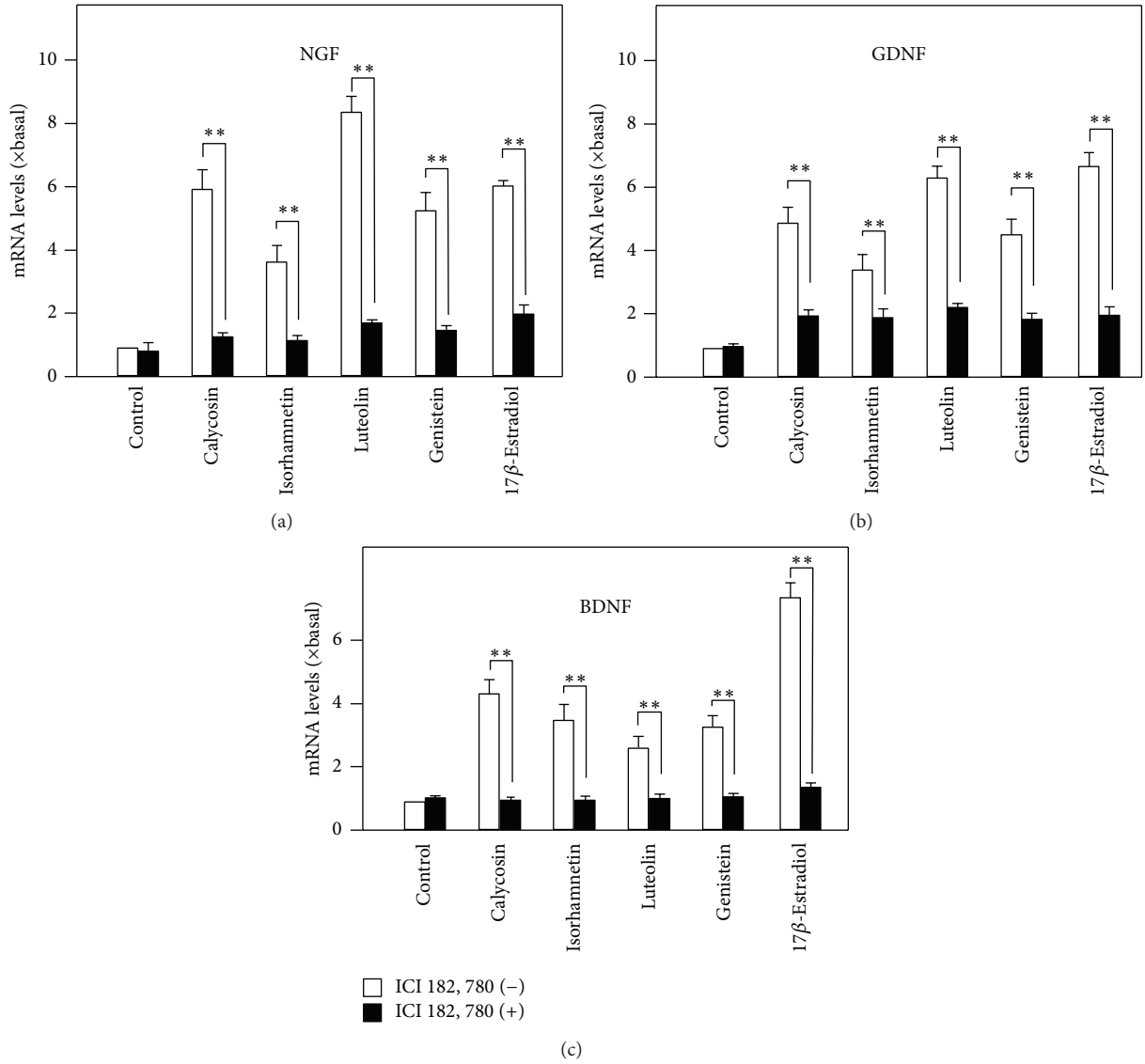

Figure 5: The flavonoid-induced expressions of neurotrophic factors are blocked by inhibitor of estrogen receptor. Cultured astrocytes were serum starved for 3 hours with or without the pretreatment of ICI 182, 780 for another 3 hours, as in Figure 4. Astrocytes were pretreated with ICI 182, 780 (1 μM) for 3 hours and then treated with flavonoids for 48 hours. The mRNA expression levels of neurotrophic factors were analyzed. Values are expressed as the fold of change (× basal) against the control (no treatment; set as 1), and in Mean ± SEM, $n = 4$, ∗∗ where $P < 0.01$.

in the brain health could be the potential candidates for drug development for different types of neurodegenerative diseases.

Conflict of Interests

The authors declare that there is no conflict of interests.

References

[1] J. L. Ridet, S. K. Malhotra, A. Privat, and F. H. Gage, "Reactive astrocytes: cellular and molecular cues to biological function," *Trends in Neurosciences*, vol. 20, no. 12, pp. 570–577, 1997.

[2] J. P. Schwartz and N. Nishiyama, "Neurotrophic factor gene expression in astrocytes during development and following injury," *Brain Research Bulletin*, vol. 35, no. 5-6, pp. 403–407, 1994.

[3] H. Kamiguchi, K. Yoshida, M. Sagoh et al., "Release of ciliary neurotrophic factor from cultured astrocytes and its modulation by cytokines," *Neurochemical Research*, vol. 20, no. 10, pp. 1187–1193, 1995.

[4] K. E. Bowenkamp, A. F. Hoffman, G. A. Gerhardt et al., "Glial cell line-derived neurotrophic factor supports survival of injured midbrain dopaminergic neurons," *Journal of Comparative Neurology*, vol. 355, no. 4, pp. 479–489, 1995.

[5] R. F. Alderson, A. L. Alterman, Y.-A. Barde, and R. M. Lindsay, "Brain-derived neurotrophic factor increases survival

and differentiated functions of rat septal cholinergic neurons in culture," *Neuron*, vol. 5, no. 3, pp. 297–306, 1990.

[6] A. Kruttgen, S. Saxena, M. E. Evangelopoulos, and J. Weis, "Neurotrophins and neurodegenerative diseases: receptors stuck in traffic?" *Journal of Neuropathology and Experimental Neurology*, vol. 62, no. 4, pp. 340–350, 2003.

[7] Y. Dwivedi, A. C. Mondal, H. S. Rizavi, and R. R. Conley, "Suicide brain is associated with decreased expression of neurotrophins," *Biological Psychiatry*, vol. 58, no. 4, pp. 315–324, 2005.

[8] G. A. Higgins and E. J. Mufson, "NGF receptor gene expression is decreased in the nucleus basalis in Alzheimer's disease," *Experimental Neurology*, vol. 106, no. 3, pp. 222–236, 1989.

[9] M. Mogi, A. Togari, T. Kondo et al., "Brain-derived growth factor and nerve growth factor concentrations are decreased in the substantia nigra in Parkinson's disease," *Neuroscience Letters*, vol. 270, no. 1, pp. 45–48, 1999.

[10] M. Narisawa-Saito, K. Wakabayashi, S. Tsuji, H. Takahashi, and H. Nawa, "Regional specificity of alterations in NGF, BDNF and NT-3 levels in Alzheimer's disease," *NeuroReport*, vol. 7, no. 18, pp. 2925–2928, 1996.

[11] R. S. Duman and L. M. Monteggia, "A neurotrophic model for stress-related mood disorders," *Biological Psychiatry*, vol. 59, no. 12, pp. 1116–1127, 2006.

[12] M. C. Bohn, D. A. Kozlowski, and B. Connor, "Glial cell line-derived neurotrophic factor (GDNF) as a defensive molecule for neurodegenerative disease: a tribute to the studies of Antonia Vernadakis on neuronal-glial interactions," *International Journal of Developmental Neuroscience*, vol. 18, no. 7, pp. 679–684, 2000.

[13] F. Sohrabji and D. K. Lewis, "Estrogen-BDNF interactions: implications for neurodegenerative diseases," *Frontiers in Neuroendocrinology*, vol. 27, no. 4, pp. 404–414, 2006.

[14] Q. Li, H. F. Zhao, Z. F. Zhang et al., "Long-term green tea catechin administration prevents spatial learning and memory impairment in senescence-accelerated mouse prone-8 mice by decreasing Aβ1-42 oligomers and upregulating synaptic plasticity-related proteins in the hippocampus," *Neuroscience*, vol. 163, no. 3, pp. 741–749, 2009.

[15] X. Wang, L. Zhang, L. Hua, D. Xing, and L. Du, "Effect of flavonoids in scutellariae radix on depression-like behavior and brain rewards: possible in dopamine system," *Tsinghua Science and Technology*, vol. 15, no. 4, pp. 460–466, 2010.

[16] J. T. T. Zhu, R. C. Y. Choi, G. K. Y. Chu et al., "Flavonoids possess neuroprotective effects on cultured pheochromocytoma PC12 cells: a comparison of different flavonoids in activating estrogenic effect and in preventing β-amyloid-induced cell death," *Journal of Agricultural and Food Chemistry*, vol. 55, no. 6, pp. 2438–2445, 2007.

[17] R. C. Y. Choi, J. T. T. Zhu, K. W. Leung et al., "A flavonol glycoside, isolated from roots of panax notoginseng, reduces amyloid-β-induced neurotoxicity in cultured neurons: signaling transduction and drug development for Alzheimer's disease," *Journal of Alzheimer's Disease*, vol. 19, no. 3, pp. 795–811, 2010.

[18] S. L. Xu, R. C. Y. Choi, K. Y. Zhu et al., "Isorhamnetin, a flavonol aglycone from *Ginkgo biloba* L., induces neuronal differentiation of cultured PC12 cells: potentiating the effect of nerve growth factor," *Evidence-Based Complementary and Alternative Medicine*, vol. 2012, Article ID 278273, 11 pages, 2012.

[19] K. D. McCarthy and J. De Vellis, "Preparation of separate astroglial and oligodendroglial cell cultures from rat cerebral tissue," *Journal of Cell Biology*, vol. 85, no. 3, pp. 890–902, 1980.

[20] H. H. C. Lee, R. C. Y. Choi, A. K. L. Ting et al., "Transcriptional regulation of acetylcholinesterase-associated collagen ColQ: differential expression in fast and slow twitch muscle fibers is driven by distinct promoters," *Journal of Biological Chemistry*, vol. 279, no. 26, pp. 27098–27107, 2004.

[21] N. C. Berchtold, J. P. Kesslak, C. J. Pike, P. A. Adlard, and C. W. Cotman, "Estrogen and exercise interact to regulate brain-derived neurotrophic factor mRNA and protein expression in the hippocampus," *European Journal of Neuroscience*, vol. 14, no. 12, pp. 1992–2002, 2001.

[22] T. Ivanova, M. Karolczak, and C. Beyer, "Estradiol stimulates GDNF expression in developing hypothalamic neurons," *Endocrinology*, vol. 143, no. 8, pp. 3175–3178, 2002.

[23] D. Amantea, R. Russo, G. Bagetta, and M. T. Corasaniti, "From clinical evidence to molecular mechanisms underlying neuroprotection afforded by estrogens," *Pharmacological Research*, vol. 52, no. 2, pp. 119–132, 2005.

[24] J. Pawlak, V. Brito, E. Küppers, and C. Beyer, "Regulation of glutamate transporter GLAST and GLT-1 expression in astrocytes by estrogen," *Molecular Brain Research*, vol. 138, no. 1, pp. 1–7, 2005.

[25] M. Kipp, S. Karakaya, S. Johann, E. Kampmann, J. Mey, and C. Beyer, "Oestrogen and progesterone reduce lipopolysaccharide-induced expression of tumour necrosis factor-α and interleukin-18 in midbrain astrocytes," *Journal of Neuroendocrinology*, vol. 19, no. 10, pp. 819–822, 2007.

[26] H. E. Scharfman and N. J. MacLusky, "Estrogen and brain-derived neurotrophic factor (BDNF) in hippocampus: complexity of steroid hormone-growth factor interactions in the adult CNS," *Frontiers in Neuroendocrinology*, vol. 27, no. 4, pp. 415–435, 2006.

[27] D. T. Solum and R. J. Handa, "Estrogen regulates the development of brain-derived neurotrophic factor mRNA and protein in the rat hippocampus," *Journal of Neuroscience*, vol. 22, no. 7, pp. 2650–2659, 2002.

[28] J. Zhou, H. Zhang, R. S. Cohen, and S. C. Pandey, "Effects of estrogen treatment on expression of brain-derived neurotrophic factor and cAMP response element-binding protein expression and phosphorylation in rat amygdaloid and hippocampal structures," *Neuroendocrinology*, vol. 81, no. 5, pp. 294–310, 2005.

[29] F. Sohrabji, R. C. G. Miranda, and C. D. Toran-Allerand, "Identification of a putative estrogen response element in the gene encoding brain-derived neurotrophic factor," *Proceedings of the National Academy of Sciences of the United States of America*, vol. 92, no. 24, pp. 11110–11114, 1995.

[30] O. Kretz, L. Fester, U. Wehrenberg et al., "Hippocampal synapses depend on hippocampal estrogen synthesis," *Journal of Neuroscience*, vol. 24, no. 26, pp. 5913–5921, 2004.

[31] E. Brailoiu, S. L. Dun, G. C. Brailoiu et al., "Distribution and characterization of estrogen receptor G protein-coupled receptor 30 in the rat central nervous system," *Journal of Endocrinology*, vol. 193, no. 2, pp. 311–321, 2007.

[32] I. Merchenthaler, M. V. Lane, S. Numan, and T. L. Dellovade, "Distribution of estrogen receptor α and β in the mouse central nervous system: in vivo autoradiographic and immunocytochemical analyses," *Journal of Comparative Neurology*, vol. 473, no. 2, pp. 270–291, 2004.

[33] E. Gould, C. S. Woolley, M. Frankfurt, and B. S. McEwen, "Gonadal steroids regulate dendritic spine density in hippocampal pyramidal cells in adulthood," *Journal of Neuroscience*, vol. 10, no. 4, pp. 1286–1291, 1990.

[34] C. S. Woolley and B. S. McEwen, "Roles of estradiol and progesterone in regulation of hippocampal dendritic spine density during the estrous cycle in the rat," *Journal of Comparative Neurology*, vol. 336, no. 2, pp. 293–306, 1993.

[35] C. S. Woolley and B. S. McEwen, "Estradiol mediates fluctuation in hippocampal synapse density during the estrous cycle in the adult rat," *Journal of Neuroscience*, vol. 12, no. 7, pp. 2549–2554, 1992.

[36] C. Leranth, M. Shanabrough, and T. L. Horvath, "Hormonal regulation of hippocampal spine synapse density involves subcortical mediation," *Neuroscience*, vol. 101, no. 2, pp. 349–356, 2000.

[37] K. B. Jelks, R. Wylie, C. L. Floyd, A. K. McAllister, and P. Wise, "Estradiol targets synaptic proteins to induce glutamatergic synapse formation in cultured hippocampal neurons: critical role of estrogen receptor-α," *Journal of Neuroscience*, vol. 27, no. 26, pp. 6903–6913, 2007.

[38] R. J. Miksicek, "Commonly occurring plant flavonoids have estrogenic activity," *Molecular Pharmacology*, vol. 44, no. 1, pp. 37–43, 1993.

[39] A. J. Y. Guo, R. C. Y. Choi, A. W. H. Cheung et al., "Baicalin, a flavone, induces the differentiation of cultured osteoblasts: an action via the Wnt/βcatenin signaling pathway," *Journal of Biological Chemistry*, vol. 286, no. 32, pp. 27882–27893, 2011.

[40] V. Breinholt, A. Hossaini, G. W. Svendsen, C. Brouwer, and S. E. Nielsen, "Estrogenic activity of flavonoids in mice. The importance of estrogen receptor distribution, metabolism and bioavailability," *Food and Chemical Toxicology*, vol. 38, no. 7, pp. 555–564, 2000.

[41] Z. Huang, F. Fang, J. Wang, and C.-W. Wong, "Structural activity relationship of flavonoids with estrogen-related receptor gamma," *FEBS Letters*, vol. 584, no. 1, pp. 22–26, 2010.

[42] F. Virgili, F. Acconcia, R. Ambra, A. Rinna, P. Totta, and M. Marino, "Nutritional flavonoids modulate estrogen receptor α signaling," *IUBMB Life*, vol. 56, no. 3, pp. 145–151, 2004.

[43] M. Wu, S. Zhao, and L. Ren, "Effects of total flavonoids of Epimedium sagittatum on the mRNA expression of the estrogen receptor α and β in hypothalamus and hippocampus in ovariectomized rats," *Journal of Central South University (Medical Sciences)*, vol. 36, no. 1, pp. 15–21, 2011.